

ELECTROMAGNETIC FORMATION FLIGHT DIPOLE SOLUTION PLANNING

by

Samuel Adam Schweighart

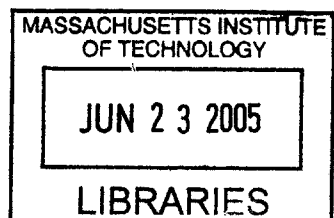
BS in Aeronautical and Astronautical Engineering
University of Illinois, 1999

MS in Aeronautical and Astronautical Engineering
Massachusetts Institute of Technology, 2001

SUBMITTED TO THE DEPARTMENT OF AERONAUTICAL AND ASTRONAUTICAL ENGINEERING
IN PARTIAL FULFILLMENT OF THE REQUIREMENTS
FOR THE DEGREE OF

DOCTOR OF PHILOSOPHY
IN
AERONAUTICAL AND ASTRONAUTICAL ENGINEERING
AT THE
MASSACHUSETTS INSTITUTE OF TECHNOLOGY

JUNE 2005



© 2005 Massachusetts Institute of Technology - All Rights Reserved

Signature of Author:

Samuel Adam Schweighart
Graduate Research Assistant
May 9th, 2005

Certified By:

Dr. Raymond Sedwick
Principal Research Scientist
Thesis Advisor/Committee Member

Certified By:

Dr. David Miller
Associate Professor of Aeronautics and Astronautics
Committee Chairman

Certified By:

Dr. Richard Battin
Professor Emeritus of Aeronautics and Astronautics
Committee Member

Certified By:

Dr. Manuel Martinez-Sanchez
Professor of Aeronautics and Astronautics
Committee Member/Minor Advisor

Certified By:

Dr. Laila Elias
Staff Engineer - NASA JPL
Thesis Reader

Certified By:

Dr. Edmund Kong
Research Scientist
Thesis Reader

Accepted By:

Dr. Jaime Peraire
Professor of Aeronautics and Astronautics
Chair, Committee on Graduate Students

AERO

ELECTROMAGNETIC FORMATION FLIGHT DIPOLE SOLUTION PLANNING

by

Samuel Adam Schweighart

Submitted to the Department of Aeronautical and Astronautical Engineering
on May 9th, 2005 in Partial Fulfillment of the requirements for the degree of
Doctor of Philosophy in Aeronautical and Astronautical Engineering

ABSTRACT

Electromagnetic Formation Flight (EMFF) describes the concept of using electromagnets (coupled with reaction wheels) to provide all of the necessary forces and torques needed to maintain a satellite's relative position and attitude in a formation of satellites. With EMFF, this formation can be controlled without the use of traditional thrusters. This thesis demonstrates the feasibility of the EMFF system. First three different models for the forces and torques produced by the electromagnets are created, and the equations of motion are developed and described. The equations of motion are determined to be polynomial functions of each satellite's magnetic dipole (which is directly related to the current in the electromagnets). Methods for solving the equations of motion are presented along with examples showing that any desired maneuver can be performed as long as the formation's center of mass is not required to change. An effect of Newton's third law causes torques to be applied to the individual vehicles in a direction opposite to the formation's angular acceleration. Reaction wheels are used to absorb the angular momentum. Next, the thesis describes methods for distributing the angular momentum evenly among the satellites. Finally, the additional challenges of operating in low Earth orbit are addressed. These include operating in the Earth's gravitational field (including the J₂ disturbance), and operating in the Earth's magnetic field. The latter is a mixed blessing due to the large disturbance torques produced from the Earth's magnetic field. However, it is shown in this thesis that it is possible to control and utilize these disturbance torques. In fact, the torques from the Earth's magnetic field can be used to remove excess angular momentum built up on the satellite reaction wheels. Overall, this thesis proves that EMFF can be used to control the relative position and attitude of satellites flying in formation.

Thesis Supervisor: Raymond J. Sedwick

Title: Principal Research Scientist

ACKNOWLEDGEMENTS

I'd like to take the time to publicly acknowledge and thank...

God. 'nough said.

Ray, the best damn advisor at MIT.

My committee members, for all the feedback on my thesis.

The EMFF team and the CDIO Class (the EMFForcers), for proving that attraction and repulsion can create shear excitement.

The 4D-artist, for bringing EMFF to the big screen.

The Pit, the Mini-Pit, and the Micro-Pit, where once there were 9, now there are ~~3~~ 2.

MIT-EMS, for providing hours and hours and hours (and hours) of non-engineering work, and for the lights and sirens.

The Rocket Team, for the realization that a huge raging ball of fire can be just as much fun as a working rocket engine.

Krazy Haus, for being absolutely krazy (kind of).

Friends (especially Erica), for proving that nerds really do know how to have fun.

Family, for all the love, and hours of Halo.

And finally...

Stephen Wolfram, for without him, the world would not know Mathematica.

TABLE OF CONTENTS

ABSTRACT.....	3
ACKNOWLEDGEMENTS	5
TABLE OF CONTENTS	7
TABLE OF FIGURES.....	13
CHAPTER 1 INTRODUCTION	19
SECTION 1.1 MOTIVATION	19
SECTION 1.2 OVERVIEW OF THE EMFF CONCEPT.....	20
Section 1.2.1 Electromagnetic Forces and Torques	21
Section 1.2.2 Angular Momentum Management	22
Section 1.2.3 Operation of EMFF in LEO	23
SECTION 1.3 OVERVIEW OF THE EMFF VEHICLE.....	24
Section 1.3.1 The Electromagnets	24
Section 1.3.2 Reaction Wheels.....	25
Section 1.3.3 Solar Arrays.....	25
SECTION 1.4 OVERVIEW OF THE RESEARCH AND THESIS	25
Section 1.4.1 Chapter 2 – Previous Work	25
Section 1.4.2 Chapter 3 – Modeling the Forces and Torques.....	25
Section 1.4.3 Chapter 4 – Solving the Equations of Motion	26
Section 1.4.4 Chapter 5 – Adjusting the Dipole Solution.....	27
Section 1.4.5 Chapter 6 – The Earth’s Gravitational Potential.....	27
Section 1.4.6 Chapter 7 – The Earth’s Magnetic Field.....	27
Section 1.4.7 Chapter 8 – Conclusions.....	28
SECTION 1.5 MATHEMATICA CODE.....	28
CHAPTER 2 PREVIOUS WORK	31
SECTION 2.1 SYSTEM TRADE STUDIES	31
SECTION 2.2 HARDWARE	32
SECTION 2.3 DYNAMICS AND CONTROL.....	32

SECTION 2.4 MAGNETIC DIPOLE TRAJECTORY SOLUTION	34
SECTION 2.5 CONCLUSIONS	34
CHAPTER 3 DERIVING THE FORCES AND TORQUES.....	35
SECTION 3.1 INTRODUCTION	35
Section 3.1.1 Overview	36
SECTION 3.2 DERIVATION OF THE EXACT MODEL	37
Section 3.2.1 The Magnetic Field and the Magnetic Vector Potential	37
Section 3.2.2 The EM Force and Torque	39
SECTION 3.3 DERIVATION OF THE FAR-FIELD MODEL	41
Section 3.3.1 The Magnetic Field and Vector Potential.....	41
Section 3.3.2 The EM Forces and Torques	43
SECTION 3.4 STEERABLE DIPOLE	44
SECTION 3.5 ANGLE REPRESENTATION – FAR-FIELD MODEL.....	45
Section 3.5.1 Two Dimensional Representation	45
Section 3.5.2 Three Dimensional Representation	51
SECTION 3.6 ELECTROSTATICS DUALITY DERIVATION – FAR FIELD MODEL	52
SECTION 3.7 EVALUATION OF THE FAR FIELD MODEL.....	55
SECTION 3.8 DERIVATION OF THE MID-FIELD MODEL.....	56
Section 3.8.1 Overview	56
Section 3.8.2 Derivation.....	57
Section 3.8.3 The Magnetic Vector Potential.....	58
Section 3.8.4 The Magnetic Field	61
Section 3.8.5 The Magnetic Force.....	62
Section 3.8.6 Vector Representation of the Mid-Field	70
SECTION 3.9 COMPARING THE MID-FIELD MODEL	72
SECTION 3.10 CONCLUSION	74
CHAPTER 4 SOLVING THE EQUATIONS OF MOTION	75
SECTION 4.1 OVERVIEW.....	75
SECTION 4.2 RELATIVE MOTION AND DEGREES OF FREEDOM	76

Table of Contents

9

SECTION 4.3 THE FREEDOM OF THE FREE DIPOLE.....	77
Section 4.3.1 The Freedom of the Free Dipole.....	78
SECTION 4.4 SOLVING THE EQUATIONS OF MOTION (TWO SATELLITES)	82
Section 4.4.1 Two Satellites in a Plane	82
Section 4.4.2 Two Satellite's in Three Dimensions	86
Section 4.4.3 Conclusion (2 Satellite Case)	89
SECTION 4.5 SOLVING EQUATIONS OF MOTION (N SATELLITE CASE)	89
Section 4.5.1 Describing the EOM.....	90
SECTION 4.6 DESCRIPTION AND SIMPLIFICATION OF POLYNOMIAL EQUATIONS	91
Section 4.6.1 Degree of a Polynomial System	92
Section 4.6.2 Number of Solutions	93
Section 4.6.3 Solutions at Infinity	93
Section 4.6.4 Reduction of the Solution ³	95
Section 4.6.5 Systematic Reduction of Polynomial Equations ³	96
Section 4.6.6 Application of the Systematic Reduction Method to the EMFF EOM.....	97
Section 4.6.7 Scaling the Equations ³	99
Section 4.6.8 Singular Solutions	103
SECTION 4.7 SOLVING POLYNOMIAL EQUATIONS USING CONTINUATION METHODS.....	106
Section 4.7.1 Introduction.....	106
Section 4.7.2 Overview	107
Section 4.7.3 Solution Paths.....	109
Section 4.7.4 Solutions at Infinity	116
Section 4.7.5 General Solution.....	119
SECTION 4.8 APPLYING THE CONTINUATION METHOD TO AN EMFF SYSTEM.....	121
SECTION 4.9 CONTINUATION WITH RESPECT TO TIME	129
Section 4.9.1 Dealing with Singularities in the Solution Path.....	131
SECTION 4.10 CONCLUSIONS	137
CHAPTER 5 ADJUSTING THE DIPOLE SOLUTION.....	139
SECTION 5.1 DEGREES OF FREEDOM	139
SECTION 5.2 THE APPROACH	140
SECTION 5.3 THE NULLSPACE OF A	141

Section 5.3.1 Changes in Torque.....	142
SECTION 5.4 SPECIFYING THE TORQUE DISTRIBUTION.....	142
Section 5.4.1 Difficulty #1 – Rank Deficiency	143
Section 5.4.2 Difficulty #1 – Rank Deficiency (Continued)	145
Section 5.4.3 Difficulty #2 – Linearizations of Non-Linear Equations	146
Section 5.4.4 Limiting the Step Size	147
Section 5.4.5 Re-Solving the EOM	147
SECTION 5.5 MINIMIZING THE ANGULAR MOMENTUM AT ONE POINT IN TIME	155
Section 5.5.2 Difficulties (Imaginary Paths)	164
Section 5.5.3 Difficulties (Path Smoothness).....	165
SECTION 5.6 ALIGNING THE NULLSPACE	166
Section 5.6.2 Method #1	167
Section 5.6.3 Method #2	169
Section 5.6.4 Method #3	170
SECTION 5.7 MINIMIZING THE ANGULAR MOMENTUM USING ALIGNED NULLSPACES.....	174
Section 5.7.2 Smoothing the Solution	175
Section 5.7.3 Varying the G Matrix	177
SECTION 5.8 MINIMIZING ANGULAR MOMENTUM AT EVERY POINT IN TIME	178
SECTION 5.9 QUADRATIC PROGRAMMING	182
Section 5.9.1 Equality Constrained Quadratic Program.....	182
SECTION 5.10 SOLVING THE INEQUALITY CONSTRAINED QP USING THE ACTIVE SET METHOD	185
Section 5.10.2 Difficulties.....	192
SECTION 5.11 GRADIENT PROJECTION METHOD	193
SECTION 5.12 CONJUGATE GRADIENT METHOD	194
SECTION 5.13 NULLSPACE METHOD	197
SECTION 5.14 RETURN TO GRADIENT PROJECTION METHOD	198
Section 5.14.1 Part 1: Determining the Cauchy Point.....	198
Section 5.14.2 Part 2: Face Search	205
Section 5.14.3 Synopsis	212
SECTION 5.15 APPLICATION TO EMFF	213

Table of Contents

11

Section 5.15.2 Changing the Box Constraints	218
Section 5.15.3 Solutions that Move Into the Imaginary Plane	220
SECTION 5.16 CONCLUSIONS	223
CHAPTER 6 THE EARTH'S GRAVITATIONAL FIELD	227
SECTION 6.1 OPERATING WITHIN THE EARTH'S GRAVITATIONAL FIELD (SPHERICAL EARTH)	227
Section 6.1.1 The CW Equations	227
Section 6.1.2 Free Orbit Ellipse	228
Section 6.1.3 Incorporating the Gravitational Forces into the EOM	229
Section 6.1.4 Stationary Formations Relative to the Rotating Coordinate Frame	230
Section 6.1.5 Stationary Orbits with Respect to an Inertial Frame	239
Section 6.1.6 Rotating Formations	241
Section 6.1.7 Conclusions	243
SECTION 6.2 THE J ₂ GEOPOTENTIAL.....	243
Section 6.2.1 Combating Formation Separation.....	245
Section 6.2.2 Angular Momentum Buildup	245
Section 6.2.3 Conclusions	249
CHAPTER 7 THE EARTH'S MAGNETIC FIELD	251
SECTION 7.1 OPERATING IN THE EARTH'S MAGNETIC FIELD – OVERVIEW	251
SECTION 7.2 MODELING THE EARTH'S MAGNETIC FIELD	251
SECTION 7.3 MAGNITUDE OF THE FORCES AND TORQUES.....	252
Section 7.3.1 The Disturbance Force	252
Section 7.3.2 The Disturbance Torque	255
Section 7.3.3 Conclusions	257
SECTION 7.4 INCORPORATING THE EARTH'S MAGNETIC FIELD INTO THE FORCE EQUATIONS OF MOTION	258
Section 7.4.1 The Earth as Another Dipole	258
Section 7.4.2 The Force on the Formation's Center of Mass	260
Section 7.4.3 The Force on the Formation's Center of Mass (Another Derivation).....	264
Section 7.4.4 Conclusions	268
SECTION 7.5 SETTING THE TORQUE ON ONE SATELLITE	269
Section 7.5.1 Zero-Torque Solutions	270

Section 7.5.2 Zero-Torque Solutions (Non-Zero Magnetic Fields).....	274
Section 7.5.3 Specifying a Non-Zero Torque.....	275
SECTION 7.6 ANGULAR MOMENTUM MANAGEMENT OVERVIEW.....	277
Section 7.6.1 The Obtainable Torques	277
SECTION 7.7 ANGULAR MOMENTUM MANAGEMENT ALGORITHM	278
Section 7.7.1 Overview	278
Section 7.7.2 Normal Mode Overview.....	280
Section 7.7.3 Angular Momentum Reduction Mode Overview	280
Section 7.7.4 Angular Momentum Reduction Method #2 – Specifying the Torque on a Satellite	282
Section 7.7.5 Method #3 - Setting the Dipole to be Perpendicular to the Earth's B Field	288
Section 7.7.6 Conclusions	308
SECTION 7.8 MINIMIZING/SPECIFYING THE TORQUE ON EVERY SATELLITE	309
Section 7.8.1 Minimizing the Torque during the Normal Mode	309
Section 7.8.2 Specifying the Torque to Minimize the Angular Momentum	315
SECTION 7.9 CONCLUSIONS	317
CHAPTER 8 CONCLUSIONS.....	319
SECTION 8.1 SUMMARY AND KEY CONTRIBUTIONS OF THE THESIS	319
SECTION 8.2 FUTURE WORK	322
SECTION 8.3 FINAL COMMENTS	323
REFERENCES.....	325

TABLE OF FIGURES

FIGURE 1-1: EMFF VEHICLE	21
FIGURE 1-2: ATTRACTION, REPULSION, AND SHEAR FORCES	21
FIGURE 3-1: CONCEPTUAL DRAWING OF EMFF VEHICLE	36
FIGURE 3-2: A LOOP OF CURRENT	38
FIGURE 3-3: TWO LOOPS OF CURRENT	40
FIGURE 3-4: ANGLE REPRESENTATION OF TWO DIPOLES IN A PLANE	45
FIGURE 3-5: FORCES AND TORQUES ON TWO DIPOLES	46
FIGURE 3-6: TORQUE ON EACH SATELLITE AS ALPHA IS VARIED	49
FIGURE 3-7: TORQUE RATIO	49
FIGURE 3-8: TORQUES APPLIED TO EACH SATELLITE SATELLITE A -- RED SATELLITE B -- BLACK	50
FIGURE 3-9: TORQUE RATIO	50
FIGURE 3-10: POSSIBLE TORQUE RATIOS AS A FUNCTION OF GAMMA	51
FIGURE 3-11: ANGLE REPRESENTATION OF TWO DIPOLES IN THREE DIMENSIONS	52
FIGURE 3-12: ANGLE DEFINITIONS FOR ELECTROSTATIC DERIVATION	53
FIGURE 3-13: COMPARING THE FORCE FAR-FIELD MODEL AGAINST THE NEAR-FIELD MODEL	55
FIGURE 3-14: COMPARING THE FAR-FIELD MODEL OF THE TORQUE (ON SATELLITE A) AGAINST THE NEAR-FIELD MODEL	56
FIGURE 3-15: VECTOR/ANGLE REPRESENTATION	57
FIGURE 3-16: PLOTS OF DIFFERENT ORDER TAYLOR SERIES EXPANSIONS	59
FIGURE 3-17: VECTOR REPRESENTATION OF THE MAGNETIC FIELD AT A POINT ON A SECOND LOOP	63
FIGURE 3-18: ANGLE REPRESENTATION	63
FIGURE 3-19: ERROR IN THE FAR-FIELD (GREEN) AND THE MID-FIELD FORCE MODEL (RED)	73
FIGURE 3-20: ERROR IN THE FAR-FIELD (GREEN) AND THE MID-FIELD TORQUE MODEL (RED)	73
FIGURE 4-1: 2D ANGLE REPRESENTATION OF TWO DIPOLES	82
FIGURE 4-2: 2D EXAMPLE WITH ROTATING COORDINATE SYSTEM	84
FIGURE 4-3: TWO SATELLITE SPIN-UP EXAMPLE	85
FIGURE 4-4: 3D ANGLE REPRESENTATION OF TWO DIPOLES	86
FIGURE 4-5: 3D EXAMPLE WITH ROTATING COORDINATE SYSTEM	88
FIGURE 4-6: INTERSECTION OF TWO CURVES AT A SINGULARITY	105
FIGURE 4-7: CONDITION OF THE JACOBIAN MATRIX	106
FIGURE 4-8: CONTINUATION PATH FOR EQUATION (4.98)	109
FIGURE 4-9: SOLUTION PATH FOR EQUATION (4.101)	111
FIGURE 4-10: SOLUTION PATH FOR EQUATION (4.106)	114

FIGURE 4-11: SOLUTION PATHS FOR VARYING Q . LEFT -- SMALL Q . RIGHT -- LARGE Q .	115
FIGURE 4-12: EXAMPLE OF PATH JUMPING DUE TO LARGE $\Delta\delta$	116
FIGURE 4-13: POSITION OF SATELLITES	122
FIGURE 4-14: SOLUTION PATH #2 FOR PROJECTED/SCALED VARIABLE M_1	127
FIGURE 4-15: SOLUTION PATH #2 FOR VARIABLE M_1	128
FIGURE 4-16: SOLUTION PATH #8 FOR PROJECTED/SCALED VARIABLE M_1	128
FIGURE 4-17: SOLUTION PATH #8 FOR VARIABLE M_1	129
FIGURE 4-18: REAL SOLUTION PATHS FOR M_1 . FREE DIPOLE MAGNITUDE OF 40,000AM.	133
FIGURE 4-19: MATRIX CONDITION OF THE EOM. FREE DIPOLE MAGNITUDE OF 40,000AM.	134
FIGURE 4-20: SOLUTION PATH/MATRIX CONDITION FOR FREE DIPOLE WITH MAGNITUDE OF 42,000AM.	134
FIGURE 4-21: SOLUTION PATH/MATRIX CONDITION FOR FREE DIPOLE WITH MAGNITUDE OF 43,000AM.	135
FIGURE 4-22: SOLUTION PATH/MATRIX CONDITION FOR FREE DIPOLE WITH MAGNITUDE OF 50,000AM.	135
FIGURE 4-23: SOLUTION PATH/MATRIX CONDITION FOR FREE DIPOLE WITH MAGNITUDE OF 60,000AM.	136
FIGURE 4-24: SOLUTION PATH/MATRIX CONDITION FOR FREE DIPOLE WITH MAGNITUDE OF 200,000AM.	136
FIGURE 5-1: CLOSEST POINT TO A PLANE	145
FIGURE 5-2: MULTIPLE LOCAL MINIMUM	146
FIGURE 5-3: PLOT OF MERIT FUNCTION	153
FIGURE 5-4: ANGULAR MOMENTUM (#1 IS RED, #2 IS BLACK, #3 IS BLUE)	159
FIGURE 5-5: PLOT OF ALPHAS	161
FIGURE 5-6: ANGULAR MOMENTUM PLOT AFTER DIPOLE SOLUTION MODIFICATIONS	163
FIGURE 5-7: DIPOLE SOLUTION PLOT (TOP: ORIGINAL SOLUTION, BOTTOM: MODIFIED SOLUTION)	164
FIGURE 5-8: CHANGE IN DIPOLE SOLUTION DUE TO MODIFICATIONS	164
FIGURE 5-9: ALPHA SOLUTIONS WITH ALIGNED NULLSPACES	174
FIGURE 5-10: CHANGE IN x -COMPONENT OF SATELLITE #1'S DIPOLE WITH ALIGNED NULLSPACES	175
FIGURE 5-11: ADJUSTED ANGULAR MOMENTUM WITH ALIGNED NULLSPACES	175
FIGURE 5-12: ALPHA SOLUTIONS WITH SMOOTHED SOLUTIONS	176
FIGURE 5-13: CHANGE IN x -COMPONENT OF THE DIPOLE SOLUTION	176
FIGURE 5-14: PLOT OF THE FIRST COMPONENT OF THE THREE NULLSPACE VECTORS	177
FIGURE 5-15: INITIAL SOLUTION LYING ON THE BOUNDARY OF THE 2ND INEQUALITY CONSTRAINT	189
FIGURE 5-16: MOVING TO THE MINIMUM SOLUTION	190
FIGURE 5-17: SOLUTION ENCOUNTERING THE 3 RD INEQUALITY CONSTRAINT	191
FIGURE 5-18: SOLUTION ENCOUNTERS THE 1ST INEQUALITY CONSTRAINT	192
FIGURE 5-19: SOLUTION PATH BENDING AT A CONSTRAINT BOUNDARY	193

Table of Figures

15

FIGURE 5-20: PLOT OF THE COST FUNCTION $J(x)$	205
FIGURE 5-21: INITIAL DIPOLE SOLUTION.....	213
FIGURE 5-22: INITIAL ANGULAR MOMENTUM DISTRIBUTION	213
FIGURE 5-23: ALPHA VALUES	215
FIGURE 5-24: UN-SCALED CHANGE IN DIPOLE SOLUTION	215
FIGURE 5-25: SCALED CHANGE IN DIPOLE SOLUTION	216
FIGURE 5-26: RESULTING DIPOLE SOLUTION AFTER ONE ITERATION	216
FIGURE 5-27: RESULTING ANGULAR MOMENTUM DISTRIBUTION AFTER ONE ITERATION.....	216
FIGURE 5-28: FINAL ANGULAR MOMENTUM DISTRIBUTION	217
FIGURE 5-29: FINAL ANGULAR MOMENTUM DISTRIBUTION (ZOOMED IN)	217
FIGURE 5-30: OVERALL CHANGE IN THE DIPOLE SOLUTION	217
FIGURE 5-31: FINAL DIPOLE SOLUTION.....	218
FIGURE 5-32: ALPHA SOLUTIONS WITH VARYING BOX CONSTRAINTS.....	218
FIGURE 5-33: ALPHA SOLUTION WITH BOX CONSTRAINTS LIMITS AT 10,000	219
FIGURE 5-34: RESULTING CHANGE IN DIPOLE SOLUTION.....	219
FIGURE 5-35: FINAL ANGULAR MOMENTUM DISTRIBUTION	220
FIGURE 5-36: FINAL DIPOLE SOLUTION.....	220
FIGURE 5-37: INITIAL DIPOLE SOLUTION.....	221
FIGURE 5-38: INITIAL ANGULAR MOMENTUM DISTRIBUTION	221
FIGURE 5-39: ALPHA SOLUTIONS	221
FIGURE 5-40: INITIAL CHANGE IN DIPOLE SOLUTION	222
FIGURE 5-41: CHANGE IN DIPOLE SOLUTION - SECOND ITERATION.....	222
FIGURE 5-42: FINAL ANGULAR MOMENTUM DISTRIBUTION	222
FIGURE 5-43: FINAL DIPOLE SOLUTION.....	223
FIGURE 6-1: IN-PLANE OFFSET.....	232
FIGURE 6-2: CROSS-TRACK OFFSET	233
FIGURE 6-3: RADIAL OFFSET	235
FIGURE 6-4 SIDE-LOOKING OFFSET.....	236
FIGURE 6-5 FORWARD LOOKING OFFSET	238
FIGURE 6-6 TORQUES APPLIED TO THE SATELLITE.....	248
FIGURE 7-1: COMPARING THE DISTURBANCE FORCE TO THE INTER-SATELLITE FORCES	254
FIGURE 7-2: RATIO BETWEEN THE DISTURBANCE AND THE INTER-SATELLITE FORCES	255
FIGURE 7-3: COMPARING THE DISTURBANCE TORQUES TO THE INTER-SATELLITE TORQUES	256

FIGURE 7-4: CONFIGURATIONS WHERE THE DISTURBANCE AND INTER-SATELLITE TORQUES ARE EQUAL.....	257
FIGURE 7-5: DIPOLE CONFIGURATION FOR EXAMPLE #2.....	273
FIGURE 7-6: ZERO-TORQUE DIPOLE SOLUTIONS X-RED Y-BLACK Z- BLUE	275
FIGURE 7-7: TORQUES ON SATELLITE A X-RED Y-BLACK Z- BLUE.....	275
FIGURE 7-8: DIPOLE STRENGTH ON SATELLITE A AND B X-RED Y-BLACK Z- BLUE	284
FIGURE 7-9: TORQUE ON SATELLITE B AND ON THE EARTH X-RED Y-BLACK Z- BLUE.....	285
FIGURE 7-10:DIPOLE STRENGTH ON SATELLITE A AND B X-RED Y-BLACK Z- BLUE	286
FIGURE 7-11: DIPOLE STRENGTH ON SATELLITE A AND B	290
FIGURE 7-12: TORQUE FROM THE EARTH ON SATELLITE A AND B	290
FIGURE 7-13: INTER-SATELLITE TORQUES	291
FIGURE 7-14: SCHEMATIC OF TWO DIPOLES.....	292
FIGURE 7-15: RESULTING PRODUCT OF DIPOLE STRENGTHS TO SATISFY FORCE EOM.....	293
FIGURE 7-16: REQUIRED STRENGTH ON SATELLITE A'S DIPOLE TO SATISFY FORCE EOM.....	293
FIGURE 7-17: PICTORIAL REPRESENTATION OF THE ANGULAR MOMENTUM VECTOR FOLLOWING THE MAGNETIC FIELD VECTOR	295
FIGURE 7-18: MINIMIZING THE ANGULAR MOMENTUM VECTOR BY WAITING FOR THE MAGNETIC FIELD TO MOVE ..	296
FIGURE 7-19: OVERSHOOTING THE MAGNETIC FIELD	297
FIGURE 7-20: GRAVITATIONAL FORCES ON EACH SATELLITE SATELLITE A – RED SATELLITE B -- BLACK.....	301
FIGURE 7-21 GRAVITATIONAL FORCES ON EACH SATELLITE IN THE ROTATING COORDINATE FRAME SATELLITE A – RED SATELLITE B – BLACK	301
FIGURE 7-22: SATELLITE ANGULAR MOMENTUM OVER ONE ORBIT EXCLUDING THE EARTH'S MAGNETIC FIELD ..	302
FIGURE 7-23: SATELLITE ANGULAR MOMENTUM OVER 20 ORBITAL PERIODS EXCLUDING THE EARTH'S MAGNETIC FIELD	302
FIGURE 7-24: SATELLITE ANGULAR MOMENTUM OVER 20 ORBITAL PERIODS INCLUDING THE EARTH'S MAGNETIC FIELD	302
FIGURE 7-25: SATELLITE ANGULAR MOMENTUM OVER 20 ORBITS INCLUDING THE EARTH'S MAGNETIC FIELD	303
FIGURE 7-26: SATELLITE ANGULAR MOMENTUM MANAGEMENT USING THE ALGORITHM.....	303
FIGURE 7-27: ZOOMED IN PLOT OF ANGULAR MOMENTUM MANAGEMENT	304
FIGURE 7-28: SATELLITE DIPOLE STRENGTH.....	304
FIGURE 7-29: ALGORITHM MODE.....	305
FIGURE 7-30 ANGLE BETWEEN THE SATELLITE ANGULAR MOMENTUM VECTOR AND THE EARTH'S MAGNETIC FIELD (ANGLE IS ONLY SHOWN WHEN THE SATELLITE IS REDUCING ANGULAR MOMENTUM).....	305

Table of Figures

17

FIGURE 7-31: ANGLE BETWEEN THE SATELLITE DIPOLE AND THE VECTOR CONNECTING THE SATELLITES (ANGLE IS ONLY SHOWN WHEN THE SATELLITE IS REDUCING ANGULAR MOMENTUM).....	306
FIGURE 7-32: SATELLITE ANGULAR MOMENTUM OVER 20 ORBITS USING THE ALGORITHM.....	307
FIGURE 7-33: SATELLITE ANGULAR MOMENTUM – INSUFFICIENT MAXIMUM DIPOLE COMPONENT STRENGTH OF 5,500AM.....	308
FIGURE 7-34: ALGORITHM MODE USAGE – INSUFFICIENT DIPOLE COMPONENT STRENGTH	308
FIGURE 7-35: SATELLITE ANGULAR MOMENTUM – MINIMIZE TORQUE IN THE NORMAL MODE.....	314
FIGURE 7-36: MODE DUTY CYCLE – MINIMIZE TORQUE IN THE NORMAL MODE.....	315
FIGURE 7-37: SATELLITE ANGULAR MOMENTUM – FINDING THE TORQUE DISTRIBUTION.....	317

Chapter 1

INTRODUCTION

Section 1.1 Motivation

Over the past several years, there has been a significant amount of research and interest in the formation flight of satellites. Satellite formation flight is the idea of using multiple smaller satellites to accomplish a mission goal. These satellites operate from as close as a few meters to several hundred meters apart.

Satellite formation flight is an attractive option for many reasons. For example, satellite formation flight can be a mission enabler. Space-based telescopes have reached a size limit with the current generation of telescopes. The Hubble and Chandra space telescopes are about the largest satellites that can be launched with today's launch vehicles. When it comes to telescopes, size does matter, not only for the amount of light that is collected, but more importantly the amount of resolution that can be achieved. The resolution is directly dependent on the size of the aperture. The drive for higher and higher resolution has driven telescope designs away from the single aperture to a separated array of telescopes. The images from these telescopes are combined to synthesize an image that has the resolution of an aperture that is equal to the distance that the satellites are separated. These synthetic aperture telescopes, or interferometers, are used today on the ground with the best example being the Very Large Array³⁴ (VLA) in New Mexico.

In order to achieve the high resolution that is possible with synthetic apertures, the individual telescopes must be precisely positioned. Ground based interferometers have the ability to be bolted rigidly to the ground, and thus their spacing is relatively stable. For space-based interferometers, the satellites are floating in space. In order to achieve the desired spacing, the individual satellites will either have to be rigidly connected using some type of expandable structure, or the satellites will have to be flown in formation.

Satellites flying in formation do not come without their difficulties or challenges. They will have to counteract any disturbance force acting on the satellites. The most researched disturbance force is probably the effects of the J_2 geopotential. One aspect of the J_2 disturbance force is that it causes satellites in the formation to drift apart¹⁴.

Counteracting the J_2 disturbance and other disturbance forces (drag, solar pressure, gravity gradients) can be done using traditional thrusters. Over the course of a mission, the ∇V needed to counteract these forces can require a significant amount of propellant. Besides the large propellant load, many formation flight missions such as the interferometer missions described above will have sensitive optics. The propellant used for station-keeping poses a hazard to the optics. The propellant can coat the optics, thus degrading their performance, or depending on the mission, the “hot” propellants can blind the optics since they will also be radiating a significant amount of energy¹³.

Ideally, one would have a means of keeping the satellites in formation that did not require any expendable propellant mass, nor would it coat the optical elements or blind the instruments with ejected propellant. One such idea that would accomplish these goals is Electromagnetic Formation Flight (EMFF).

Section 1.2 Overview of the EMFF Concept

EMFF is the idea of using electromagnets, coupled with reaction wheels, to provide the relative position and attitude control of satellites flying in formation. Figure 1-1 is an artist’s concept of what a satellite using EMFF would look like³⁶.

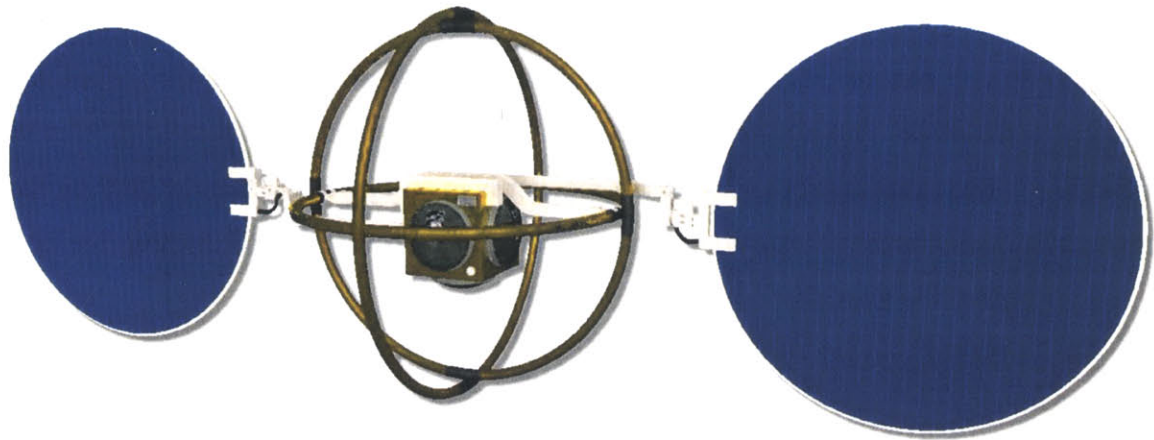


Figure 1-1: EMFF Vehicle

Each vehicle is equipped with three rings of superconducting wire to produce the electromagnetic fields. Solar arrays provide the power to the electromagnets, and reaction wheels are used to maintain the attitude of the vehicle.

Section 1.2.1 Electromagnetic Forces and Torques

Electromagnets can do more than just attract and repel. Schematically shown below is a pair of bar magnets or magnetic dipoles in different orientations.

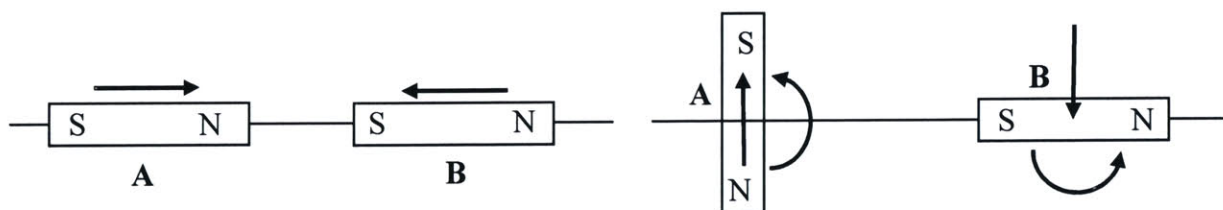


Figure 1-2: Attraction, Repulsion, and Shear Forces

When two electromagnetic dipoles are placed such that their axes are aligned, they either attract or repel along their axes. The left side of Figure 1-2 shows two dipoles with their axes aligned.

The magnets in this orientation will produce an attraction force. If dipole B was flipped, then the magnets would produce a repulsion force.

Shear (off-axis) forces can be produced if the dipoles are placed such that their axes are perpendicular to each other. The right side of Figure 1-2 shows two electromagnetic dipoles in this configuration. The resulting force on the left magnet is in an upwards direction, and on the right magnet it is downwards. These forces are perpendicular to the line connecting the two magnets, and are half of the axial force produced on the left side of Figure 1-2.

With the ability to produce shear forces comes the side-effect of producing torques on the individual dipoles. When shear forces are produced, the satellites begin to rotate about the formation's center of mass. This causes a net gain in angular momentum of the system. However due to Newton's 3rd law, angular momentum must be conserved. Therefore, when shear forces are produced, torques are also produced on the individual satellites that is equal and opposite to the net torque on the satellite formation about the formation's center of mass. The magnetic torques are shown on the right side of Figure 1-2. Both satellites feel a torque in the counter-clockwise direction. (Note that the direction is opposite of the dipole's rotation about the center of mass.) This torque is not the same for both dipoles; the torque on the right dipole is exactly half of that on the left dipole.

If the magnetic dipoles are placed in an orientation other than aligned or perpendicular, they produce a combination of axial and shear forces. Because of this ability to produce axial and shear forces by varying the strength and orientation of the magnetic dipoles, a force in any direction can be produced by the dipoles. The difficulty and focus of this thesis is to take an array of satellites with a desired force profile and determine the strength and orientation of every satellite's magnetic dipole at every instant in time.

Section 1.2.2 Angular Momentum Management

As stated above, when the electromagnets produces shear forces, torques are also produced on the individual satellites. Because satellites typically need to maintain their attitude, reaction

wheels will have to be used to counteract these torques and absorb the angular momentum. This angular momentum is equal and opposite to the angular momentum accumulated by the formation as a whole. For this thesis, it is assumed that the vehicles will be kept inertially fixed, or more specifically, the reaction wheels will absorb all of the torques and angular momentum produced by the electromagnets. Since the orientation of the vehicles is arbitrary and depends on the mission, the thesis does not attempt to keep track of the angular momentum stored in each reaction wheel, but instead keeps track of the overall angular momentum stored in the reaction wheels. Since most satellites contain three orthogonal wheels (plus spares), representing the angular momentum as three orthogonal components is a valid assumption.

While the sum of the angular momentum stored in all of the reaction wheels can't be changed (since it is based on the motion of the formation as a whole), the distribution of the angular momentum on each satellite can be changed. As was shown in the right side of Figure 1-2, the torques produced on each vehicle are not necessarily equal. The distribution depends on the orientation of the dipoles. In fact, with more satellites, the torque distribution can become even more varied. Another aspect of this research will be to determine the orientation and strength of the magnetic dipoles on each satellite so that the torque is more evenly distributed among the satellites over time.

Section 1.2.3 Operation of EMFF in LEO

Finally, satellites using EMFF in LEO must factor in the Earth's magnetic field and the Earth's gravity field including the J_2 disturbance. In order to maintain a formation that is in non-Keplerian orbits, EMFF will have to provide forces to counteract the gravitational forces. Counteracting these forces also produces torques on the satellite formation that must be managed. The effects of the J_2 disturbance cause satellite formations to separate and tumble. EMFF must also be able to counteract these disturbance forces without long term angular momentum gain.

Any time a satellite energizes its electromagnet in LEO, a disturbance force and torque will be produced on it due to the Earth's magnetic field. The disturbance force is typically quite small

and can be neglected. The disturbance torque produced however is not negligible and must be accounted for. Determining the dipole strengths and orientations to allow EMFF to work in LEO is the final aspect of this thesis.

Section 1.3 Overview of the EMFF Vehicle

The EMFF system is composed of three main components: The electromagnets, the reaction wheels, and the solar arrays. Other subsystems including heat exchangers, power electronics, and other support systems are necessary but will not be examined in this thesis.

Section 1.3.1 The Electromagnets

The key component behind EMFF is obviously the electromagnets. The enabling material that made the EMFF coils practical for both lab work and space operations is high-temperature superconducting wire (HTS). This commercially available first generation HTS wire is known as BSCCO-2223. High-temperature refers to the fact the wire becomes superconducting at a critical temperature of 110K or less. At 77K, the HTS wire has the ability to carry over 16,100 A/cm² with zero heat losses³². For space based applications, the wire would need to be maintained at a temperature less than 110K. For some telescope missions, the satellites require low temperatures for the optics, and the satellite is placed behind a sun shield. The EMFF system could reside behind his shield and also be cooled. If such a system was not in place, the heat exchangers or other devices such as cryo-coolers would be used to remove the excess heat from the superconducting wires. Since the wires themselves produce no heat, the heat would be just due to the flux into the system such as solar flux.

The HTS wire is wrapped into three orthogonal rings. These three rings can be visualized in Figure 1-1. The orthogonal rings allow for a magnetic field to be generated in any direction, a feature called a “steerable dipole” which will be discussed in more detail in Chapter 3.

Section 1.3.2 Reaction Wheels

An integral component of EMFF is the reaction wheels. When the EMFF coils are energized, they produce forces and torques on the vehicles. These torques, if left unaccounted for, will cause the vehicles to rotate. Reaction wheels are used to counteract the magnetic torques. Over time, these torques can cause the angular momentum to build up on the reaction wheels. This thesis, specifically Chapter 5, discusses methods for managing the torques and angular momentum build up in the reaction wheels.

Section 1.3.3 Solar Arrays

Power to run the electromagnets is provided by the solar arrays. Since the electromagnets use HTS wire, the power requirements to run the electromagnets are minimal. However, power also may be required to run cryo-coolers to maintain the temperature of the HTS wire.

Section 1.4 Overview of the Research and Thesis

The goal of this thesis is to show that EMFF can be used to control satellites flying in formation. Algorithms for creating valid dipole solutions that manage angular momentum even in the presence of the Earth's magnetic field are presented.

Section 1.4.1 Chapter 2 – Previous Work

In chapter 2, the previous research on EMFF is discussed. Work on EMFF has primarily been done by the MIT SSL and the University of Tokyo. A brief review of the previous work and how it ties into this thesis will be presented.

Section 1.4.2 Chapter 3 – Modeling the Forces and Torques

Chapter 3 will discuss how the EMFF vehicles are modeled. More specifically, three different models are developed: the near-field Model, the mid-field model, and the far-field model. The near-field model models the rings of current as exactly what they are, rings of current. The magnetic forces and torques produced by the rings of current are obtained by a series of double integrations. This provides an accurate, yet unwieldy set of equations of motion. The name

near-field comes from the fact that these equations will work at any separation distance between the vehicles.

The far-field model is a linearized version of the near-field model. Instead of modeling the electromagnets as rings of current, the electromagnets are modeled as a magnetic dipole. By taking a series of first order linearizations, a set of equations that do not contain any integrals can be developed. These equations are linear in the magnetic dipoles and thus each vehicle can be modeled as one large magnetic dipole with three vector components. This model allows for a more straight forward calculation of the magnetic forces and torques. However, due to the linearizations, the model is only valid when the vehicles are separated by at least 6-8 coil radii. The far-field model is used in the remaining chapters as the model for the EMFF vehicles as most missions will fall in this range.

However, if the vehicles are closer than 6-8 coil radii, the mid-field model can be used. The mid-field model uses higher expansions of the Taylor series. It allows for a higher fidelity model than the far-field model, and the magnetic forces and torques can still be calculated without the need for integrals. However, the equations are no longer linear in the magnetic dipole, and thus each vehicle can no longer be considered to have one large steerable dipole. The mid-field model is accurate when the vehicles are separated by 3-4 or more coil radii.

Section 1.4.3 Chapter 4 – Solving the Equations of Motion

Chapter 4 addresses the question of, “Does EMFF have enough control to move the satellites in any way possible?” The chapter will start off with two EMFF vehicles restricted to a plane that rotate about a common CG. The equations of motion are solved and a simple solution is found. More simple examples are performed, each adding slightly more complexity until the n satellite case with an arbitrary trajectory is reached.

The remainder and majority of the chapter are devoted to answering the following question, “Given a set of n satellites and an arbitrary trajectory for each satellite, what is the dipole solution (the current in the wires) needed to achieve the desired trajectory?” This is

accomplished by examining the EOM and recognizing that they are a set of polynomial equations. Descriptions and classifications of large order polynomial equations are presented, and methods for solving these equations are presented. The methods are then adapted for the EMFF EOM, and an EMFF example is performed.

Section 1.4.4 Chapter 5 – Adjusting the Dipole Solution

Chapter 4 creates dipole solutions that are only based off of the magnetic force EOM. Unfortunately due to the number of equations, versus the number of variables (the dipoles), the torque equations of motion cannot be simply included into the EOM. Because the magnetic torque produced by the EMFF coils is not accounted for, the angular momentum stored in the reaction wheels can be unfairly biased to one satellite or another. Chapter 5 discusses methods of adjusting the dipole solution from Chapter 4 into one that produces an acceptable dipole solution.

Section 1.4.5 Chapter 6 – The Earth’s Gravitational Potential

Chapter 6 looks at the gravitational effects of operating in LEO. Due to the Earth’s gravitation potential, forces are required to maintain formation shapes that require satellites to be in non-Keplarian orbits. These forces can include shear forces, and thus torques are applied to the satellite formation. Different formations are evaluated and the torques on the formation are presented. Specifically, Earth pointing, inertially pointing, and rotating formations are investigated. Furthermore, the effects of the J_2 disturbance force are investigated.

Section 1.4.6 Chapter 7 – The Earth’s Magnetic Field

Chapter 7 looks at the effects of operating within the Earth’s magnetic field. The Earth’s magnetic field produces negligible disturbance forces on the formation, however, it produces significant disturbance torques on the formation. These torques are a mixed blessing. Unless they are dealt with, they will cause a significant amount of angular momentum to build on the satellites. At the same time, the Earth’s magnetic field can be used to remove angular momentum from the formation including angular momentum gained from operating in the

Earth's gravitational potential. Finally, the Earth's magnetic field allows for the direct control of the torque on one satellite, thus allowing for the possibility of a zero-torque satellite that needs no reaction wheels.

Section 1.4.7 Chapter 8 – Conclusions

Chapter 8 will conclude the thesis and present the research contributions.

Section 1.5 Mathematica Code

Another deliverable from the research, besides this thesis and other papers, is a series of Mathematica codes. Mathematica (MMA) was chosen as the operating platform due to its ability to handle symbolic equations. The result of the research, besides proving that EMFF is feasible, is an algorithm for creating dipole solutions. This algorithm has been coded and is available for use on future EMFF projects. To ease the learning of the code, I have placed within the thesis short syntax explanations of the MMA code that the section represents. For example, one piece of code finds the minimum of a quadratic program using the active set method. The code written to accomplish this task is called *QPActiveSet[]*. After the section on the Active Set Method, the following text is found:

MATHEMATICA CODE: QPActiveSet [G,d,A₁,b₁,A₂,b₂,x₀]

Description: Solver for the inequality constrained quadratic program.

File: Master EMFF Notebook.nb

Section: QPSolver

Usage: QPActiveSet [G,d,A₁,b₁,A₂,b₂,x₀] = {x_{min} }

G,A₁,A₂ – 2D matrices (See equation (5.109))

d,b₁,b₂ – 1D vectors

x_o – Initial feasible solutions

x_{min} – Minimum solutions

A description of the code, along with which file and section is placed in the text. The usage is also placed in the text. The variables correspond to the equations in the thesis for ease of use.

Available online at <http://ssl.mit.edu/> listed with the digital copy of this thesis is the MMA code that has been written as a companion to this thesis. All of the code mentioned and used is available. The example problems used in the thesis are also available so that anyone interested can more easily understand how the code works and is used.

Chapter 2

PREVIOUS WORK

The idea of using electromagnets to provide the relative positioning control for satellites flying in formation is a relatively new concept. At this time, only two groups have been working and publishing papers on the concept. The two groups are the MIT Space Systems Lab, and the University of Tokyo/ISAS. Their research can be divided into four different categories: system trade studies, hardware, dynamics and control, dipole solution path planning.

Section 2.1 System Trade Studies

System trade studies refer to the analysis of comparing different system architectures or variations in an architecture against a metric or goal. The trade studies on EMFF focus on two questions: Is EMFF comparable to other traditional station keeping systems, and what are the optimal EMFF configurations?

In the reference by Kwon¹⁰, the benefit of EMFF is initially analyzed on simple satellite formations. The effects of varying coil mass, coil mass distribution, number of spacecraft, and other parameters are characterized. The subsystem design and technology levels for the electromagnet coils, thermal systems, structure and power are also presented. Finally, the results of the trade studies are applied to the Terrestrial Planet Finder (TPF) mission. TPF is one of NASA's future telescope missions that calls for multiple spacecraft in formation. One design includes flying five spacecraft in formation. With this mission design, EMFF is compared with traditional propulsion systems including high Isp electric propulsion. According to the research, EMFF is more favorable than Colloids, PPT, or traditional thrusters. EMFF and FEEP thrusters are rated about even when a 5 year mission is proposed, and EMFF is more favorable when a 10 year mission is planned. The end result of this research is that EMFF is a viable system architecture for controlling the relative positions of satellites flying in formation.

The AIAA JSR journal paper by Kong et al.¹³, the thesis by Kong⁸ and the IEEE conference paper by Miller et al.¹⁶ also vary different aspects of the EMFF design in order to obtain an

optimal design that maximizes mission efficiency. These designs are then applied to the NASA TPF mission and compared to more traditional propulsion schemes. Just as with the research by Kwon¹⁰, EMFF is shown to be a viable and desirable option compared to other propulsion schemes.

Section 2.2 Hardware

Research has also been performed on building an EMFF testbed^{9, 10, 12, 35}. At the MIT Space Systems Lab, an EMFF testbed is being built that will allow for the testing of control algorithms. With similarities to SPHERES, another formation flight testbed at the MIT SSL, the EMFF testbed consists of two EMFF vehicles that contain superconducting wire and reaction wheels that are representative of a space-based system. This testbed is currently undergoing continued research and revisions.

Section 2.3 Dynamics and Control

In the series of papers by Kaneda, Hashimoto et al.^{18,19}, EMFF operation in LEO is analyzed. Specifically a formation of two co-planar satellites that maintain an inertially fixed separation direction is analyzed. A simple trade study is performed to show that electromagnets using superconducting wire are able to produce the needed magnetic forces. Initial sizing for the thermal system is also presented without details. Because EMFF satellites operating in LEO will be affected by the Earth's magnetic field, the idea of continuously varying the magnetic field is presented.

The Earth's magnetic field will produce disturbance forces and torques on the satellites when the electromagnets are energized. The disturbance forces are orders of magnitude less than the inter-vehicle forces and are thus neglected in this paper. The disturbance torques are on the same order as the inter-satellite torques, and cannot be neglected. Reaction wheels are used to counteract the disturbance torques acting on the vehicle. Left unattended, the reaction wheels would saturate due to the disturbance torques.

A control scheme is presented to sinusoidally vary the magnitude of magnetic dipoles on the satellites. This would cause the disturbance forces to also vary sinusoidally, thus the angular momentum stored in the wheels would have zero net gain. However, there is no mention of how angular momentum build-up from second-order terms would be handled. A phase-shift controller is designed to provide the relative position control between the satellites. An example is performed, and position errors (both secular and periodic) due to the nature of the controller are presented.

In the thesis by Kong⁸, the controllability of an EMFF system is examined. The author models each vehicle's electromagnetic field as a stationary multi-pole. A controllability analysis is performed to see if the multi-poles have the control authority to counter small perturbations from a nominal position. The result of this analysis shows that an equivalent to the three rings of current used in this thesis has enough control authority to achieve all degrees of translational motion.

In the thesis by Elias⁹, a non-linear model of the spacecraft dynamics is created. The spacecraft bus, reaction wheels, electromagnets, and the coupling between the reaction wheels and the spacecraft are modeled. The electromagnets are modeled using the far-field model described in Chapter 3 of this thesis. The coupling between the reaction wheels and the spacecraft is modeled as a damped spring system. Using Kane's method, a set of non-linear state equations is created.

A nominal trajectory is chosen. In this case, two satellites are rotating about a common center of mass. The radial forces needed to hold the satellites together are produced by the electromagnets. The non-linear equations of motion are linearized about this nominal point, and a stability analysis is performed. The stability analysis shows that there is one unstable pole. A controllability analysis is also performed showing that the system is controllable. Finally a controller is designed and simulations are run using the controller with the linear and non-linear dynamics showing that the system is indeed controllable.

Section 2.4 Magnetic Dipole Trajectory Solution

To date, there has not been any research published that directly address the question of finding dipole solutions over the course of a trajectory profile. (i.e. What are the magnetic strengths and orientations needed to produce the desired forces on each satellite for any desired force profile?)

Research by Kaneda, Hashimoto et al.^{18,19} was focused on presenting a sinusoidal control strategy. While a dipole solution is created for the two satellite example problem, the paper focuses on the control strategy and not the methodology for finding the dipole solution. The paper does not address multiple satellites, arbitrary configurations or angular momentum control beyond the concept of continuously varying the dipole strength in the presence of an external magnetic field.

Other references^{13,15,16,17} provide simple solutions to two satellite configurations or results from multiple satellites in a plane. The research referenced in these papers pertaining to the dipole solution was created by the author of this thesis and was a preliminary stage of the research presented herein.

Section 2.5 Conclusions

Research on EMFF has been fairly limited. To date, published research has primarily focused on trade-studies and control strategies around a nominal trajectory. The trade-studies show that EMFF is a viable and competitive option for satellites flying in formation. The research on the control strategies shows that the relative position and attitude can be controlled by electromagnets and reaction wheels. What is missing from the research are the nominal trajectories around which the controllers are linearized. This thesis will fill in that gap and present a systematic method and algorithms designed to create a nominal trajectory that not only produces a viable dipole solution that provides the desired forces at every instant in time, but will also manage the amount of angular momentum stored in the reaction wheels.

Chapter 3

DERIVING THE FORCES AND TORQUES

Section 3.1 Introduction

Chapter 3 will develop, from first principles, the magnetic fields, forces and torques created by the EMFF system. The exact solution will be developed first, but unfortunately it contains integrals that cannot be solved analytically. Therefore, a Taylor series will be used to develop approximations that can be solved analytically. The first order expansion of the Taylor series will be known as the far-field model. Because of its analytical solution, simplicity and more important linearity, this model is used in the subsequent chapters as the model for the forces and torques.

However, as the name implies, the far-field model is only accurate when the satellites are far apart. Some missions require the satellites to be in fairly close proximity to each other. A mid-field model which takes the next higher order expansion of the Taylor series is also developed herein. This model, while analytic, is more complex than the far-field model and makes solving the EOM significantly harder, but is available for use if necessary.

Section 3.1.1 Overview

The EMFF vehicles are envisioned to have three orthogonal rings of superconducting wire that circumscribe the vehicle. The superconducting wire has the ability to carry high currents with zero resistance and thus zero heating losses. The high current in the coils allows strong electromagnet fields to be produced. These fields interact with the magnetic fields on the other vehicles producing forces and torques. Coupled with reaction wheels, these forces and torques are the basis for attitude and relative position control.

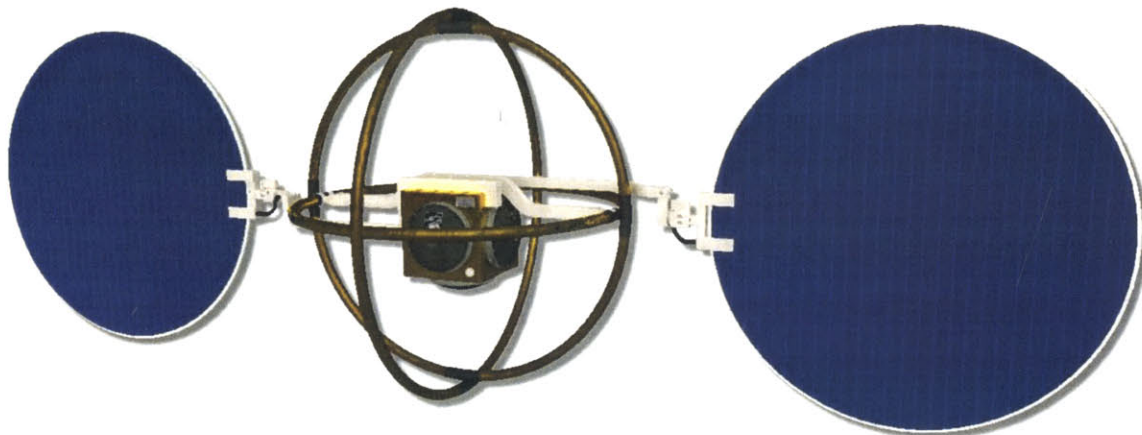


Figure 3-1: Conceptual Drawing of EMFF Vehicle

The forces and torques can be calculated by summing the forces and torques on one ring on a satellite (A) to a ring on another satellite (B). \vec{f}_{ij} is the force on the i^{th} ring on satellite A due to the magnetic field produced by the j^{th} ring on satellite B.

$$\vec{F}_{AB} = \sum_{j=1}^3 \sum_{i=1}^3 \vec{f}_{ij} \quad (3.1)$$

We now begin, starting with first principles to calculate the EM forces and torques.

Section 3.2 Derivation of the Exact Model

Section 3.2.1 The Magnetic Field and the Magnetic Vector Potential

Magnetic monopoles do not exist (except in some theories). Because of this, the divergence of the magnetic field must be zero.

$$\nabla \cdot \vec{B} = 0 \quad (3.2)$$

Since a field is completely defined by its divergence and curl (and since divergence of the electromagnetic field is zero), we can define the electromagnetic field by its curl. The curl is given by Ampere's equation for magnetostatics

$$\nabla \times \vec{B} = \mu_0 \vec{J} \quad (3.3)$$

where \vec{J} is the current density vector, and μ_0 is the permeability of free space. Magnetostatics can be assumed since the magnetic fields and currents will vary slowly over time.

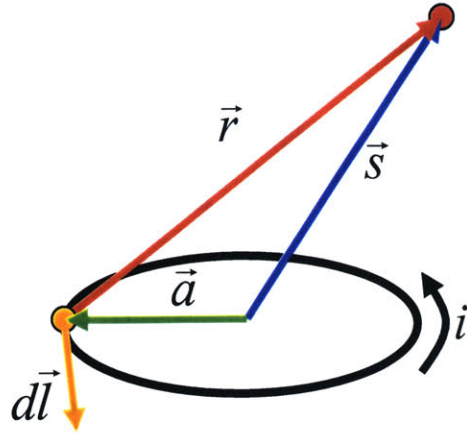
Because the divergence of the magnetic field is zero, we can also write the magnetic field in terms of the curl of a vector potential function.

$$\vec{B} = \nabla \times \vec{A} \quad (3.4)$$

At this point there is some ambiguity in \vec{A} . If we use the Coulomb gauge ($\nabla \cdot \vec{A} = 0$), we can write the vector potential³⁹ as the volume integral of the current density as

$$A(\vec{s}) = \frac{\mu_0}{4\pi} \iiint \frac{J(\vec{\rho})}{|\vec{s} - \vec{\rho}|} d^3 \vec{\rho} \quad (3.5)$$

where ρ is the vector of integration and spans the whole volume.

**Figure 3-2: A Loop of Current**

For a loop of current, as shown in Figure 3-2, the current density is zero everywhere except within the wire. Assuming the wire has no thickness, the equation for the vector potential can be reduced to a path integral around the loop of current.

$$\vec{A}(\vec{s}) = \frac{\mu_0 N i}{4\pi} \oint \frac{1}{|\vec{s} - \vec{a}|} d\vec{l} \quad (3.6)$$

Applying equation (3.4) to equation (3.6) becomes

$$\vec{B}(\vec{s}) = \nabla \times \frac{\mu_0 N i}{4\pi} \oint \frac{1}{|\vec{s} - \vec{a}|} d\vec{l} \quad (3.7)$$

Since the del operation is based on \vec{s} , we can move it inside the integrand. Using the relation³⁹ that

$$\nabla \frac{1}{|\vec{s} - \vec{a}|} = -\frac{\vec{s} - \vec{a}}{|\vec{s} - \vec{a}|^3} \quad (3.8)$$

and other vector identities, equation (3.7) simplifies to

$$\vec{B}(\vec{s}) = \frac{\mu_0 N i}{4\pi} \oint \frac{d\vec{l} \times (\vec{s} - \vec{a})}{|\vec{s} - \vec{a}|^3} \quad (3.9)$$

Re-writing in terms of \vec{r} , we are left with a familiar form of the Biot-Savart law

$$\vec{B}(\vec{r}) = \frac{\mu_0 i}{4\pi} \oint \frac{d\vec{l} \times \hat{r}}{|\vec{r}|^2} \quad (3.10)$$

Solving for the magnetic field, even for a loop of current is not very straightforward. This is due to the difficulty of integrating the magnitude of \vec{r} squared in the denominator. For some special cases, a solution can be found. For example, along the axis, normal to the loop of current, the magnetic field is given by

$$B_{axis} = \frac{\mu_0 Nia^2}{2|\vec{d} - \vec{a}|^3} \quad (3.11)$$

where \vec{d} is the distance along the axis. Off axis, the magnetic field can only be written analytically in terms of elliptical integrals⁴⁰. In polar coordinates $(\hat{r}, \hat{\theta}, \hat{z})$ where \hat{z} is aligned with the axis normal to the loop, the magnetic field is

$$\begin{aligned} \vec{B} = & \frac{i\mu_0}{2\pi a} \frac{1}{\sqrt{(1+\alpha)^2 + \beta^2}} \left(E(n) \frac{1-\alpha^2 - \beta^2}{(1+\alpha)^2 + \beta^2 - 4\alpha} + K(n) \right) \hat{z} + \\ & \frac{i\mu_0}{2\pi a} \frac{\beta}{\alpha \sqrt{(1+\alpha)^2 + \beta^2}} \left(E(n) \frac{1+\alpha^2 + \beta^2}{(1+\alpha)^2 + \beta^2 - 4\alpha} - K(n) \right) \hat{r} \end{aligned} \quad (3.12)$$

where

$$\alpha = \frac{r}{a} \quad \beta = \frac{x}{a} \quad n = \sqrt{\frac{4\alpha}{(1+\alpha)^2 + \beta^2}} \quad (3.13)$$

and $E(n)$ and $K(n)$ are the integrals of the first and second kind respectively and n is the modulus.

Section 3.2.2 The EM Force and Torque

The force on a current element in the presence of a magnetic field is given by

$$d\vec{F}_2 = i_2 d\vec{l}_2 \times \vec{B} \quad (3.14)$$

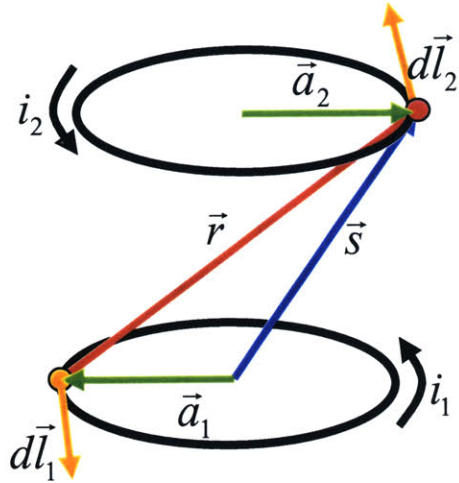


Figure 3-3: Two Loops of Current

Integrating, the force on a second loop of current is given by

$$\vec{F}_2 = i_2 \oint d\vec{l}_2 \times \vec{B} \quad (3.15)$$

Combining equation (3.10) and equation (3.15) results in the force of one loop with respect to another.

$$\vec{F}_2 = \frac{\mu_0 i_1 i_2}{4\pi} \oint \left(\oint \frac{\hat{r} \times d\vec{l}_1}{r^2} \right) \times d\vec{l}_2 \quad (3.16)$$

The torque on a current loop about its center can be found by

$$d\vec{\tau}_2 = \vec{a}_2 \times d\vec{F}_2 \quad (3.17)$$

Substituting

$$\vec{\tau}_2 = \frac{\mu_0 i_1 i_2}{4\pi} \oint \vec{a}_2 \times \left(\left(\oint \frac{\hat{r} \times d\vec{l}_1}{r^2} \right) \times d\vec{l}_2 \right) \quad (3.18)$$

Neither the equation for force nor torque can be solved analytically. A numerical integrator must be employed. This does not allow for an intuitive feel of how the forces and torques relate to the orientation and strength of the coils. More importantly, there is no way to invert the problem and

solve for the orientation and strength of the coils for a given force or torque. To make this problem more tractable, simplifications and linearizations are employed.

Section 3.3 Derivation of the Far-Field Model

Section 3.3.1 The Magnetic Field and Vector Potential

At a sufficient distance away from the coils, the magnetic field created by the coils becomes indistinguishable from a solenoid, or bar magnet. At this distance, all three objects (a coil, a solenoid and a bar magnet) can be represented by a magnetic dipole. A magnetic dipole is an idealization that is similar to an electrostatic dipole. An electrostatic dipole has a positive and negative charge separated by a distance, whereas a magnetic dipole can be thought of as an N pole and an S pole separated by a distance. A bar magnet makes a good visual representation of a magnetic dipole and is used in some of the figures. For a loop of current, one can visualize the bar magnet aligned with the axis of the loop and the N pointing in the direction given by the right-hand rule.

The main difficulty with evaluating the force and torque equations is the presence of the magnitude of r in the denominator. This prevents the integral from being evaluated analytically. Referring to Figure 3-3

$$\vec{r} = \vec{s} - \vec{a} \quad (3.19)$$

At a sufficient distance away from the loop, the size of the loop becomes much smaller than the distance from the loop.

$$|\vec{a}| \ll |\vec{s}| \quad (3.20)$$

We can expand $\frac{1}{|\vec{r}|}$ about $\frac{a}{s} \approx 0$ using a Taylor Series.

$$\frac{1}{|\vec{r}|} = \frac{1}{|\vec{s} - \vec{a}|} = \frac{1}{s} + \frac{\vec{s} \cdot \vec{a}}{s^3} + H.O.T. \quad (3.21)$$

If we substitute equation (3.21) into the equation for the magnetic vector potential, equation (3.5), and observe that the first term in the Taylor series integrates to zero, we have³⁹

$$\vec{A}(\vec{s}) = \frac{\mu_0}{4\pi s^3} \iiint J(\vec{\rho})(\vec{s} \cdot \vec{\rho}) d^3 \vec{\rho} \quad (3.22)$$

Using vector calculus, the integral in equation (3.22) can be written as³⁹

$$\iiint J(\vec{\rho})(\vec{s} \cdot \vec{\rho}) d^3 \vec{\rho} = \vec{\mu} \times \vec{s} \quad (3.23)$$

where

$$\vec{\mu} = \frac{1}{2} \iiint \vec{\rho} \times \vec{J}(\vec{\rho}) d^3 \vec{\rho} \quad (3.24)$$

Substituting, we have the dipole approximation for the magnetic vector potential.

$$\vec{A}(\vec{s}) = \frac{\mu_0}{4\pi} \frac{\vec{\mu} \times \vec{s}}{s^3} \quad (3.25)$$

For a loop of current, the magnetic dipole, equation (3.24), can be written simply as

$$\vec{\mu} = NiA\hat{n} \quad (3.26)$$

where N is the number of turns, i is the current, A is the area enclosed by the loop, and \hat{n} is the vector along the axis of the loop.

The magnetic field can be easily found by substituting equation (3.25) into equation (3.4) resulting in

$$\vec{B}(\vec{s}) = \frac{\mu_0}{4\pi} \left(\frac{3\vec{s}(\vec{\mu} \cdot \vec{s})}{s^5} - \frac{\vec{\mu}}{s^3} \right) \quad (3.27)$$

The magnetic field is now written without integrals and easily evaluated.

Section 3.3.2 The EM Forces and Torques

Without derivation here, the potential energy of a magnetic dipole in a magnetic field is given by³⁹

$$U(\vec{d}) = -\vec{\mu}_2 \cdot \vec{B}_1(\vec{d}) \quad (3.28)$$

where \vec{d} is the vector connecting the center of dipole 1 to dipole 2.

The force on a second dipole is simply derived from the gradient of the potential energy.

$$\vec{F}_2 = -\nabla U = \nabla(\vec{\mu}_2 \cdot \vec{B}_1) \quad (3.29)$$

Evaluating equation (3.29) results in

$$\vec{F}_2 = -\frac{3\mu_0}{4\pi} \left(-\frac{\vec{\mu}_1 \cdot \vec{\mu}_2}{d^5} \vec{d} - \frac{\vec{\mu}_1 \cdot \vec{d}}{d^5} \vec{\mu}_2 - \frac{\vec{\mu}_2 \cdot \vec{d}}{d^5} \vec{\mu}_1 + 5 \frac{(\vec{\mu}_1 \cdot \vec{d})(\vec{\mu}_2 \cdot \vec{d})}{d^7} \vec{d} \right) \quad (3.30)$$

The torque can be calculated by using the fact that a torque applied over a rotation is equal to the change in potential energy.

$$dU = -\vec{\tau} \cdot d\vec{\theta} = -d\vec{\mu} \cdot \vec{B} \quad (3.31)$$

The change in the magnetic dipole due to the rotation is given by

$$d\vec{\mu} = d\vec{\theta} \times \vec{\mu} \quad (3.32)$$

Substituting,

$$\begin{aligned} -\vec{\tau} \cdot d\vec{\theta} &= -(d\vec{\theta} \times \vec{\mu}) \cdot \vec{B} = -(\vec{\mu} \times \vec{B}) \cdot d\vec{\theta} \\ \therefore \vec{\tau}_2 &= \vec{\mu}_2 \times \vec{B}_1 \end{aligned} \quad (3.33)$$

Evaluating equation (3.33) results in

$$\vec{\tau}_2 = \frac{\mu_0}{4\pi} \left(\vec{\mu}_2 \times \left(\frac{3\vec{d}(\vec{\mu}_1 \cdot \vec{d})}{d^5} - \frac{\vec{\mu}_1}{d^3} \right) \right) \quad (3.34)$$

Equations (3.29), and (3.34) are the vector far-field representation of the forces and torques between two dipoles. This model will be used through the rest of this thesis. The forces and torques can be calculated quickly and analytically. More importantly, the equations, while not directly invertible (for more than 2 satellites), can be solved using standard numeric solvers.

Section 3.4 Steerable Dipole

In the introduction, it is stated that the electromagnetic force on a satellite is calculated by summing up the magnetic forces on each ring, and the force on each ring is calculated by summing up the forces that result from each ring on the other vehicle.

$$\vec{F} = \sum_{j=1}^3 \sum_{i=1}^3 \vec{f}_{ij} \quad (3.35)$$

where f is the force on the i^{th} ring due to the magnetic field created by the j^{th} ring on another vehicle. This is still valid, but due to the linearity of the far-field model, it can be simplified.

The far-field force and torque equations are linear functions of the magnetic dipoles. Because of this, the magnetic dipoles from each orthogonal ring can be considered vector components of one large dipole.

$$\vec{\mu} = \sum_{i=1}^3 \vec{\mu}_i \quad (3.36)$$

So instead of having three separate dipoles that are fixed in orientation, there is one “steerable” dipole per vehicle that has the ability to change direction and magnitude. Instead of calculating 9 equations in order to get the total force on one satellite due to another, only one equation is necessary. This simplifies the equations greatly and allows for a more intuitive feel of the dynamics. Unfortunately, this does not work for the mid-field model that is derived later in this chapter.

Section 3.5 Angle Representation – Far-Field Model

Section 3.5.1 Two Dimensional Representation

The equations in the vector form do not give an intuitive feel for the forces and torques. It is more instructive to look at the forces and torques between two dipoles (restricted to a plane) with the coordinate system aligned with the axis connecting the two dipoles.

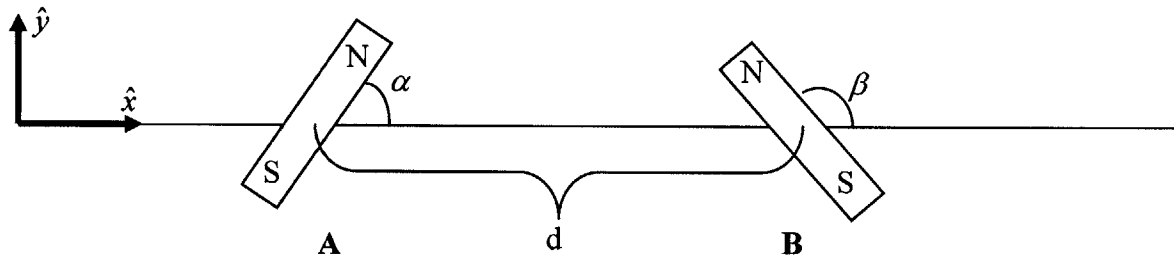


Figure 3-4: Angle Representation of Two Dipoles in a Plane

In the coordinate system described by Figure 3-4, the dipoles are described by

$$\begin{aligned}\vec{\mu}_A &= (\mu_A \cos \alpha) \hat{x} + (\mu_A \sin \alpha) \hat{y} \\ \vec{\mu}_B &= (\mu_B \cos \beta) \hat{x} + (\mu_B \sin \beta) \hat{y} \\ \vec{d}_{AB} &= d \hat{x}\end{aligned}\tag{3.37}$$

Substituting equation (3.37) into equation (3.30) and equation (3.34) results in the angle representations for forces and torques between the two satellites.

$$\begin{aligned}\vec{F}_A &= \frac{3}{4\pi} \frac{\mu_0 \mu_A \mu_B}{d^4} ((2 \cos \alpha \cos \beta - \sin \alpha \sin \beta) \hat{x} - (\cos \alpha \sin \beta + \sin \alpha \cos \beta) \hat{y}) \\ \vec{F}_B &= -\frac{3}{4\pi} \frac{\mu_0 \mu_A \mu_B}{d^4} ((2 \cos \alpha \cos \beta - \sin \alpha \sin \beta) \hat{x} - (\cos \alpha \sin \beta + \sin \alpha \cos \beta) \hat{y}) \\ \vec{\tau}_A &= -\frac{1}{4\pi} \frac{\mu_0 \mu_A \mu_B}{d^3} (2 \sin \alpha \cos \beta + \cos \alpha \sin \beta) \\ \vec{\tau}_B &= -\frac{1}{4\pi} \frac{\mu_0 \mu_A \mu_B}{d^3} (2 \cos \alpha \sin \beta + \sin \alpha \cos \beta)\end{aligned}\tag{3.38}$$

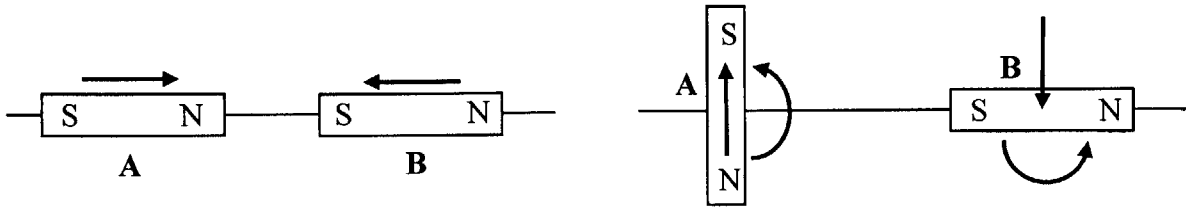


Figure 3-5: Forces and Torques on Two Dipoles

The left side of Figure 3-5 shows two dipoles (shown schematically as bar magnets) with their axis aligned. In this configuration, $\alpha = \beta = 0$. From equation (3.38), the force is only in the radial direction, and as expected the magnets attract. The magnitude of the force between the two magnets is

$$\begin{aligned}\vec{F}_A &= \frac{3\mu_0}{2\pi} \frac{\mu_A \mu_B}{d^4} \hat{x} & \vec{F}_B &= -\frac{3\mu_0}{2\pi} \frac{\mu_A \mu_B}{d^4} \hat{x} \\ \vec{\tau}_A &= 0 & \vec{\tau}_B &= 0\end{aligned}\quad (3.39)$$

When the dipoles are placed in the configuration as shown by the right side of Figure 3-5 ($\alpha = -90^\circ$ and $\beta = 0^\circ$), there are no attraction or repulsion forces created. Instead, “shear” forces are created. The resulting force on the left magnet is in an upwards direction, and on the right magnet it is downwards. These forces are perpendicular to the line connecting the two magnets and are exactly half of the axial forces on the left side of the figure.

$$\begin{aligned}\vec{F}_A &= \frac{3\mu_0}{4\pi} \frac{\mu_A \mu_B}{d^4} \hat{y} & \vec{F}_B &= -\frac{3\mu_0}{4\pi} \frac{\mu_A \mu_B}{d^4} \hat{y}\end{aligned}\quad (3.40)$$

The origin of the shear forces can be visualized by considering the S and N as charges that attract and repel. The S on dipole B will repel the S on dipole A, and attract the N. The axial components cancel out, and the result is a force in the positive \hat{y} direction. The N on dipole B will have the opposite effect on dipole A, except that the forces will be smaller due to the extra distance between the N and dipole A. The net resulting force is in the positive \hat{y} direction.

The dipoles do not have to be in the configuration on the right side of Figure 3-5 to produce pure shear forces. In fact, as will be discussed in Chapter 3, no matter the orientation of dipole A, there is an orientation for dipole B that will produce pure shear forces. (There is also an orientation that will produce pure axial forces).

When shear forces are created, torques are also generated on each dipole. This is due to the conservation of angular momentum. Since there are no external forces and torques, the total angular momentum of the system must remain zero.

$$\frac{-\vec{d}}{2} \times \vec{F}_A + \frac{\vec{d}}{2} \times \vec{F}_B + \vec{\tau}_A + \vec{\tau}_B = 0 \quad (3.41)$$

This can also be visualized by looking at the right side of Figure 3-5. The S on dipole **B** will repel the S on dipole **A**, and attract the N. This causes a counter-clockwise torque on the dipole. The N on dipole **B** has the opposite but smaller effect, but since it is farther away, the net torque will be in the counter-clockwise direction.

From equation (3.38), the torque on dipole **A** and on dipole **B** is

$$\vec{\tau}_A = \frac{\mu_0}{2\pi} \frac{\mu_A \mu_B}{d^3} \hat{z} \quad \vec{\tau}_B = \frac{\mu_0}{4\pi} \frac{\mu_A \mu_B}{d^3} \hat{z} \quad (3.42)$$

It is interesting to note that the torque on dipole **A** is twice that of dipole **B**. The difference in torque is based on the angles of the two dipoles. When pure shear forces are desired, the dipoles can be oriented in such a way that the desired forces are produced and the torque on satellite A can be as little as one half the torque on satellite B, or as much as twice the torque on satellite B. Regardless of how the torques are distributed, the sum of the torques remains constant and satisfies equation (3.41).

The distribution, or ratio, of the torques can be created by dividing the torque equations from equation (3.38).

$$\frac{\tau_A}{\tau_B} = \frac{2 \cos \beta \sin \alpha + \cos \alpha \sin \beta}{\cos \beta \sin \alpha + 2 \cos \alpha \sin \beta} \quad (3.43)$$

This can be simplified to

$$\frac{\tau_A}{\tau_B} = \frac{2 \tan \alpha + \tan \beta}{\tan \alpha + 2 \tan \beta} \quad (3.44)$$

The ratio of torque on satellite A to satellite B just depends on the choice of alpha and beta. However, the inter-satellite forces also depend on alpha and beta and can restrict the torque ratio. For example, assume the satellites are separated by a normalized distance of one, and the force on each satellite is given by

$$\begin{aligned}\vec{F}_A &= 1\hat{y} \\ \vec{F}_B &= -1\hat{y} \\ d_{AB} &= 1\hat{x}\end{aligned} \quad (3.45)$$

From equation (3.41), the sum of the torques on the satellites is

$$\vec{\tau}_A + \vec{\tau}_B = 1 \quad (3.46)$$

Solving the force equations for the relation between alpha and beta produces

$$\begin{aligned}\beta &= \cos^{-1}\left(\frac{\sqrt{2} \sin \alpha}{\sqrt{5+3 \cos 2 \alpha}}\right) \quad \text{for } 0 \leq \alpha \leq \frac{\pi}{2} \\ \beta &= -\cos^{-1}\left(\frac{\sqrt{2} \sin \alpha}{\sqrt{5+3 \cos 2 \alpha}}\right) \quad \text{for } \frac{\pi}{2} \leq \alpha \leq \pi\end{aligned} \quad (3.47)$$

Plotting the torque on each satellite

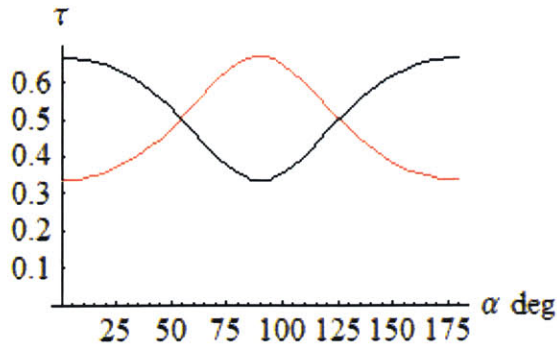


Figure 3-6: Torque on Each Satellite as Alpha is Varied

Satellite A – Red Satellite B – Black

From Figure 3-6, it can be seen that the torque on one satellite is no more than twice the other satellite. The torque ratio is shown in Figure 3-7.

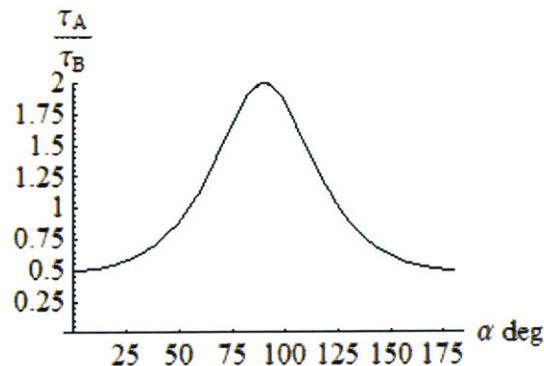


Figure 3-7: Torque Ratio

However, if the desired force direction is changed, then the relationship between alpha and beta changes, and thus the possible torque ratios change. For example, if the inter-satellite forces are

$$\begin{aligned}\vec{F}_A &= \frac{\sqrt{2}}{2} \hat{x} + \frac{\sqrt{2}}{2} \hat{y} \\ \vec{F}_B &= -\frac{\sqrt{2}}{2} \hat{x} - \frac{\sqrt{2}}{2} \hat{y}\end{aligned}\tag{3.48}$$

then the torque on each satellite is given by the following figure.

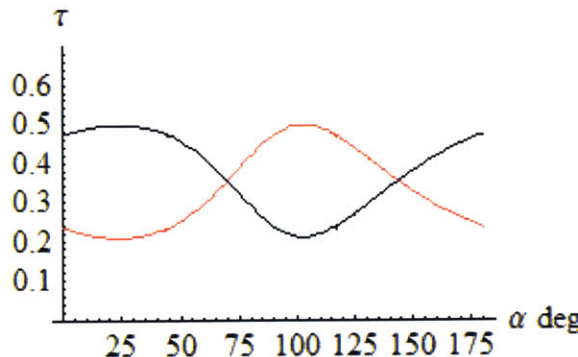


Figure 3-8: Torques Applied to Each Satellite

Satellite A -- Red Satellite B -- Black

The torque ratio is given by

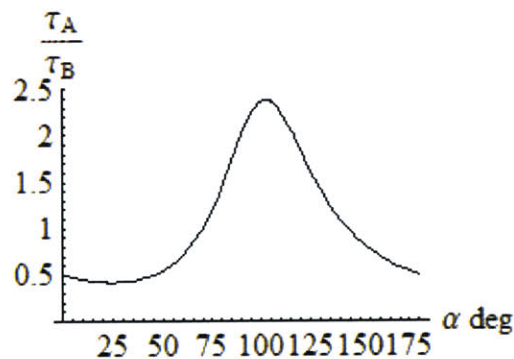


Figure 3-9: Torque Ratio

If the forces are defined by an angle gamma and have an arbitrary magnitude,

$$\begin{aligned}\vec{F}_A &= |\vec{F}|(\cos \gamma \hat{x} + \sin \gamma \hat{y}) \\ \vec{F}_B &= -|\vec{F}|(\cos \gamma \hat{x} + \sin \gamma \hat{y})\end{aligned}\tag{3.49}$$

then the plot showing the possible torque distributions can be created.

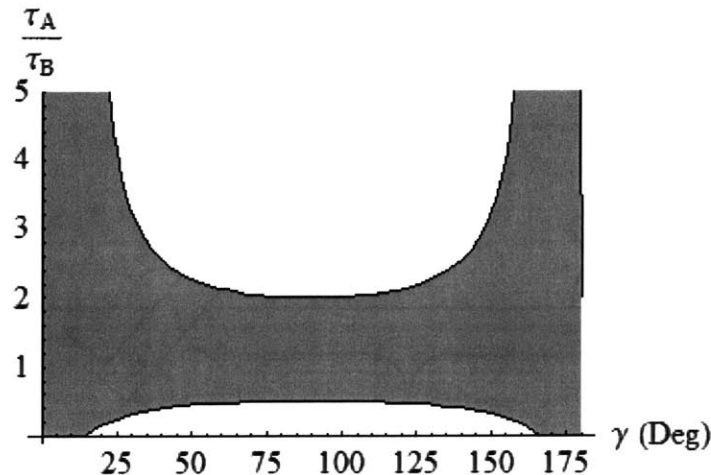


Figure 3-10: Possible Torque Ratios as a Function of Gamma

For gamma less than approximately 14 degrees or greater than 166 degrees, a few things happen. First, any torque ratio can be created. It is also possible to set the torque on a satellite to zero if gamma is within this range. Finally, it is possible to move torque from one satellite to another satellite (since the torque applied to one satellite is in the opposite direction as the other satellite) when the gamma is within the specified range.

Unfortunately these abilities are only available when the desired inter-satellite forces lie within this 28 degree range. Chapter 5 will discuss methods for managing the torque distribution, and Chapter 7 will discuss methods for managing the torque distribution in the presence of the Earth's magnetic field. In fact when operating in the Earth's magnetic field, any torque ratio is possible.

Section 3.5.2 Three Dimensional Representation

Expanding the equations to three dimensions requires the addition of an angle for each dipole. χ and δ are the angles of rotation of the dipole about the \hat{x} vector. Refer to Figure 3-11. The dipole vectors are now represented as

$$\begin{aligned}\vec{\mu}_A &= (\mu_A \cos \alpha) \hat{x} + (\mu_A \sin \alpha \cos \chi) \hat{y} + (\mu_A \sin \alpha \sin \chi) \hat{z} \\ \vec{\mu}_B &= (\mu_B \cos \beta) \hat{x} + (\mu_B \sin \beta \cos \delta) \hat{y} + (\mu_B \sin \beta \sin \delta) \hat{z} \\ \vec{r}_{AB} &= d \hat{x}\end{aligned}\quad (3.50)$$

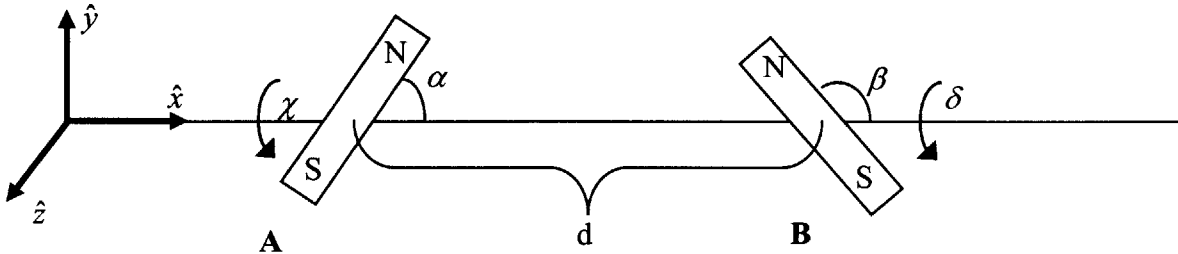


Figure 3-11: Angle Representation of Two Dipoles in Three Dimensions

Substituting equation (3.50) into (3.30) and (3.34) results in the following forces and torques on the left dipole.

$$\begin{aligned}F_x &= \frac{3}{4\pi} \frac{\mu_0 \mu_A \mu_B}{d^4} (2 \cos \alpha \cos \beta - \cos(\delta - \chi) \sin \alpha \sin \beta) \\ F_y &= -\frac{3}{4\pi} \frac{\mu_0 \mu_A \mu_B}{d^4} (\cos \alpha \sin \beta \cos \delta + \sin \alpha \cos \beta \cos \chi) \\ F_z &= -\frac{3}{4\pi} \frac{\mu_0 \mu_A \mu_B}{d^4} (\cos \alpha \sin \beta \sin \delta + \sin \alpha \cos \beta \sin \chi) \\ T_x &= -\frac{1}{4\pi} \frac{\mu_0 \mu_A \mu_B}{d^3} (\sin \alpha \sin \beta \sin(\delta - \chi)) \\ T_y &= \frac{1}{4\pi} \frac{\mu_0 \mu_A \mu_B}{d^3} (\cos \alpha \sin \beta \sin \delta + 2 \sin \alpha \cos \beta \sin \chi) \\ T_z &= -\frac{1}{4\pi} \frac{\mu_0 \mu_A \mu_B}{d^3} (\cos \alpha \sin \beta \cos \delta + 2 \sin \alpha \cos \beta \cos \chi)\end{aligned}\quad (3.51)$$

Section 3.6 Electrostatics Duality Derivation – Far Field Model

Another way to derive the far field model is to invoke the electrostatic/magnetostatic duality theorem. The equations for a magnetic dipole are dual to the equations for an electrostatic dipole.

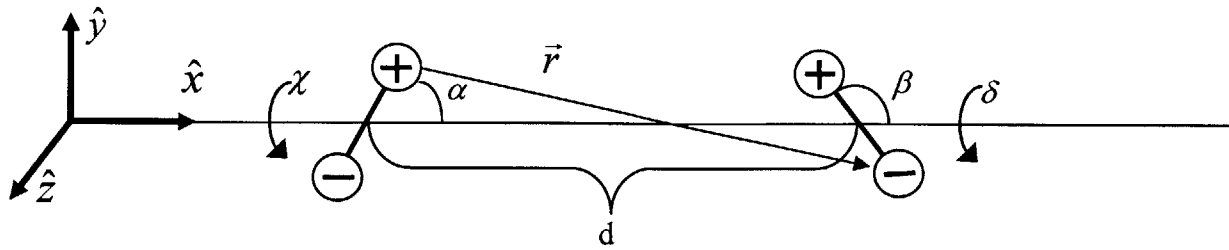


Figure 3-12: Angle definitions for Electrostatic Derivation

The total force on an electrostatic dipole is the sum of the forces between the charges.

$$\vec{F} = \vec{F}_{L^+R^+} + \vec{F}_{L^+R^-} + \vec{F}_{L^-R^+} + \vec{F}_{L^-R^-} \quad (3.52)$$

where L^+ is the positive charge on the left dipole, etc.

The force between two electric charges is given by Coulomb's Law

$$\bar{F} = \frac{kq_1q_2}{r^2} \hat{r} \quad (3.53)$$

where \vec{r} is defined as the vector from one charge to another charge. If we define $\vec{\rho}$ as the location of a charge in space, then \vec{r} is given by

$$\vec{r}_{ji} = \vec{\rho}_i - \vec{\rho}_j \quad (3.54)$$

For example, if the center of the left dipole is considered the origin of the system, the location of the left positive charge is given by

$$\vec{\rho}_{L^+} = \begin{bmatrix} a \cos \alpha \\ a \cos \chi \sin \alpha \\ a \sin \chi \sin \alpha \end{bmatrix} \quad (3.55)$$

and the location of the right negative charge is

$$\vec{\rho}_{R^-} = \begin{bmatrix} -a \cos \beta + d \\ -a \cos \delta \sin \beta \\ -a \sin \delta \sin \beta \end{bmatrix} \quad (3.56)$$

where $2a$ is distance between the positive and negative charge.

The above equations are substituting into equation (3.52). Because $d \gg a$, we can take a Taylor series about $a/d \approx 0$. Ignoring the higher order terms results in

$$\begin{aligned} F_L = & 12k \frac{a^2 q^2}{d^4} (2 \cos \alpha \cos \beta - \cos(\delta - \chi) \sin \alpha \sin \beta) \hat{x} \\ & - 12k \frac{a^2 q^2}{d^4} (\cos \alpha \sin \beta \cos \delta + \sin \alpha \cos \beta \cos \chi) \hat{y} \\ & - 12k \frac{a^2 q^2}{d^4} (\cos \alpha \sin \beta \sin \delta + \sin \alpha \cos \beta \sin \chi) \hat{z} \end{aligned} \quad (3.57)$$

Using the electrostatic/magnetostatic duality principles where

$$\begin{aligned} \varepsilon_0 &\rightarrow \frac{1}{\mu_0} \\ k &\rightarrow \frac{\mu_0}{4\pi} \\ 2(2a)q_i &= \mu_i \end{aligned} \quad (3.58)$$

results in the far-field approximation for electromagnetic dipoles

$$\begin{aligned} F_L = & \frac{3}{4\pi} \frac{\mu_0 \mu_A \mu_B}{d^4} (2 \cos \alpha \cos \beta - \cos(\delta - \chi) \sin \alpha \sin \beta) \hat{x} \\ & - \frac{3}{4\pi} \frac{\mu_0 \mu_A \mu_B}{d^4} (\cos \alpha \sin \beta \cos \delta + \sin \alpha \cos \beta \cos \chi) \hat{y} \\ & - \frac{3}{4\pi} \frac{\mu_0 \mu_A \mu_B}{d^4} (\cos \alpha \sin \beta \sin \delta + \sin \alpha \cos \beta \sin \chi) \hat{z} \end{aligned} \quad (3.59)$$

Equation (3.59) is consistent with equation (3.51). The torques can be found in a similar manner.

Section 3.7 Evaluation of the Far Field Model

The next section compares the far-field model to the exact model for forces and torques. The far-field model is considered valid by picking a tolerance on the percentage error. Typically, we state that a model is valid when the percentage error is less than 10%. Shown below is the percentage error of the far-field model; Figure 3-13 compares the force model with the coils in different orientations, and Figure 3-14 compares the torque model.

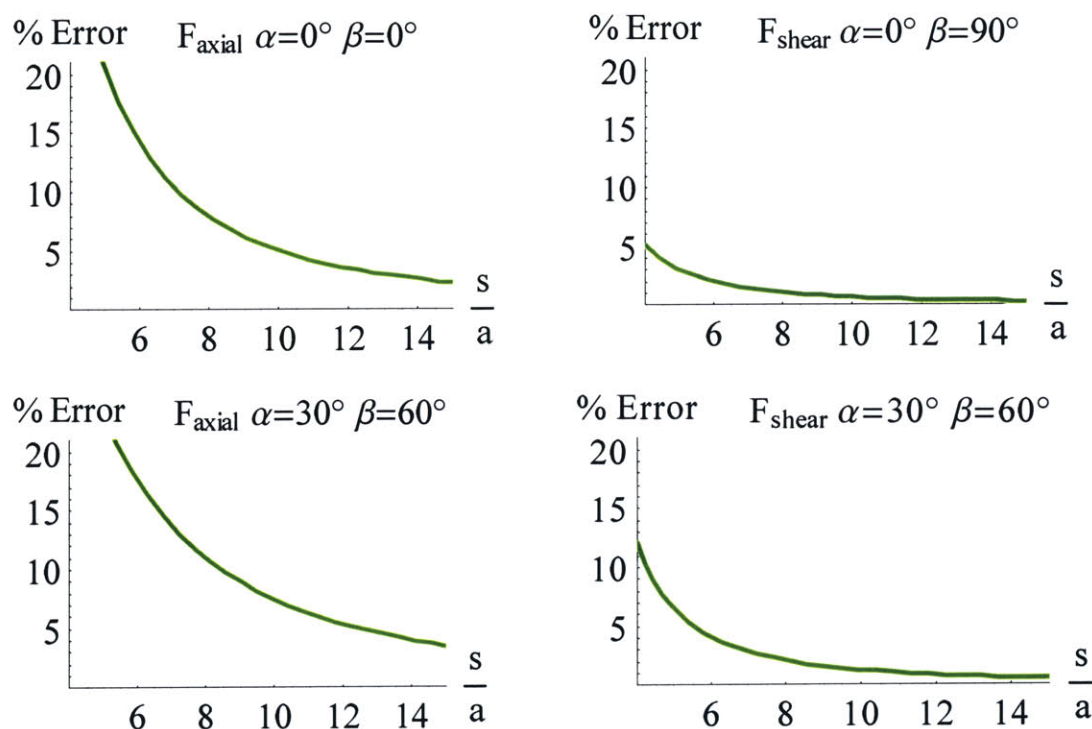


Figure 3-13: Comparing the Force Far-Field Model Against the Near-Field Model

From the figures we can see that the percentage error is dependent on the orientation of the coils. However, to ensure that there is less than 10% error, a good rule of thumb is to have a separation distance of approximately 6-8 coil radii.

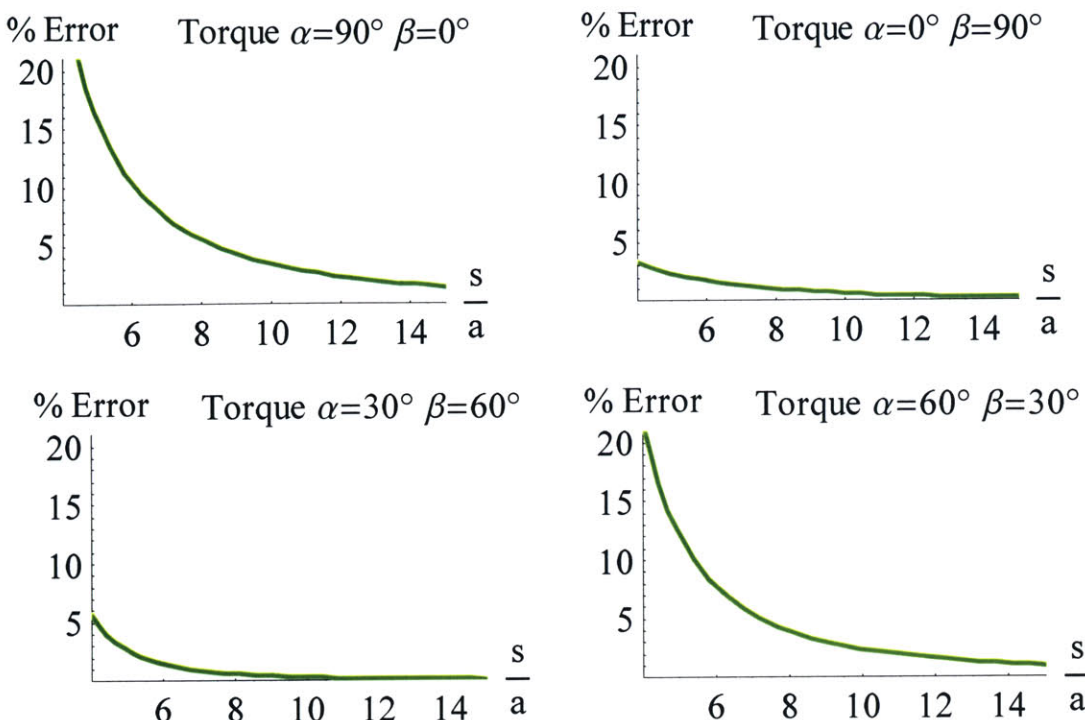


Figure 3-14: Comparing the Far-Field Model of the Torque (on Satellite A) Against the Near-Field Model

Section 3.8 Derivation of the Mid-Field Model

Section 3.8.1 Overview

The following section looks to expand the far-field model. As stated earlier, the far-field model for the forces are not accurate at distances less than about 6-8 coil radii. The goal of this section is to develop a model that more accurately captures the electromagnetic forces and torques at distances as little as a few coil radii.

The difficulty in calculating the exact force lies within integrating the distance r . The far-field model used the 1st order terms in the Taylor expansion to simplify the equations and allow for the integration. The logical step in expanding the fidelity of the model would be to use higher order terms of the Taylor series expansion.

Starting with the magnetic vector potential for a loop of current,

$$\vec{A}(\vec{s}) = \frac{\mu_0 N i}{4\pi} \oint \frac{1}{|\vec{s} - \vec{a}|} d\vec{l} \quad (3.60)$$

If we expand the denominator to the 3rd order term, we have

$$\frac{1}{|\vec{s} - \vec{a}|} = \frac{1}{s} + \frac{\vec{s} \cdot \vec{a}}{s^3} + \left(\frac{3(\vec{s} \cdot \vec{a})^2}{2s^5} - \frac{a^2}{2s^3} \right) + \left(\frac{5(\vec{s} \cdot \vec{a})^3}{2s^7} - \frac{3a^2(\vec{s} \cdot \vec{a})}{2s^5} \right) + H.O.T. \quad (3.61)$$

In the derivation of the far-field model, the 1st order terms were substituted into equation (3.60), and through algebraic manipulations, an expression for the vector potential in terms of the magnetic dipole was obtained. Unfortunately, this process could not be repeated with the higher order terms.

So an alternative approach was tried. The angle representation was examined and the final vector representation of the magnetic force was backed out. The following section works through the derivation.

Section 3.8.2 Derivation

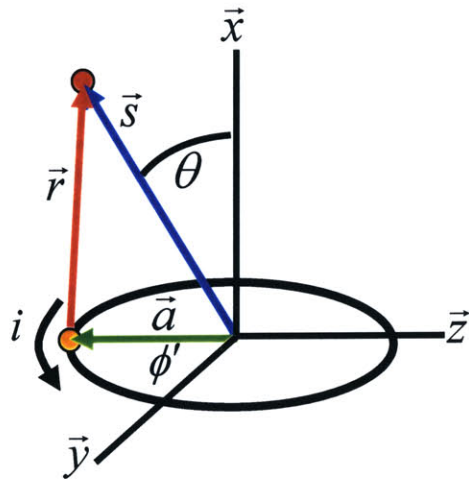


Figure 3-15: Vector/Angle Representation

Looking at Figure 3-15

$$\begin{aligned}\vec{r} &= \vec{s} - \vec{a} \\ \vec{a} &= a(\cos \phi' \hat{y} + \sin \phi' \hat{z}) \\ \vec{s} &= x \hat{x} + y \hat{y} + z \hat{z}\end{aligned}\tag{3.62}$$

then

$$\begin{aligned}\vec{dl} &= a(-\sin \phi' \hat{y} + \cos \phi' \hat{z}) d\phi' \\ |\vec{s} - \vec{a}| &= \sqrt{a^2 + s^2 - 2ya \cos \phi' - 2za \sin \phi'}\end{aligned}\tag{3.63}$$

Section 3.8.3 The Magnetic Vector Potential

Substituting equation (3.63) into equation (3.60), the vector potential is³⁹

$$\vec{A}(x, y, z) = \frac{\mu_0 Nia}{4\pi} \int_0^{2\pi} \frac{-\sin \phi' \hat{y} + \cos \phi' \hat{z}}{\sqrt{a^2 + s^2 - 2ya \cos \phi' - 2za \sin \phi'}} d\phi'\tag{3.64}$$

At this point, the denominator must be simplified in order to perform the integration. A Taylor series is used. It should be noted that expansion of the denominator with Lagrange polynomials can also be used with equivalent results. Since we are assuming that $a \ll s$, we take the Taylor series expansion about $a/s = 0$.

$$\frac{1}{r} = \frac{1}{|\vec{s} - \vec{a}|} = \frac{1}{\sqrt{a^2 + s^2 - 2ya \cos \phi' - 2za \sin \phi'}} = \sum_{k=0}^n T_k\tag{3.65}$$

where

$$\begin{aligned}
 T_0 &= \frac{1}{s} \\
 T_1 &= \frac{a}{s^2} \left(\frac{y \cos \phi' + z \sin \phi'}{s} \right) \\
 T_2 &= \frac{a^2}{s^3} \left(-\frac{1}{2} + \frac{3}{2} \left(\frac{y \cos \phi' + z \sin \phi'}{s} \right)^2 \right) \\
 T_3 &= \frac{a^3}{s^4} \left(-\frac{3}{2} \left(\frac{y \cos \phi' + z \sin \phi'}{s} \right) + \frac{5}{4} \left(\frac{y \cos \phi' + z \sin \phi'}{s} \right)^3 \right) \\
 T_4 &= \frac{a^4}{s^5} \left(\frac{3}{8} - \frac{15}{4} \left(\frac{y \cos \phi' + z \sin \phi'}{s} \right)^2 + \frac{35}{8} \left(\frac{y \cos \phi' + z \sin \phi'}{s} \right)^4 \right)
 \end{aligned} \tag{3.66}$$

Referring back to equation (3.64), the numerator contains only first powers of sine or cosine functions. We can see from inspection that when the even terms of the expansion are incorporated, the total number of sines and cosines in the integrand will be odd (summing the exponents). Because odd numbers of sines and cosines integrate to zero, the even terms of the expansion can be neglected.

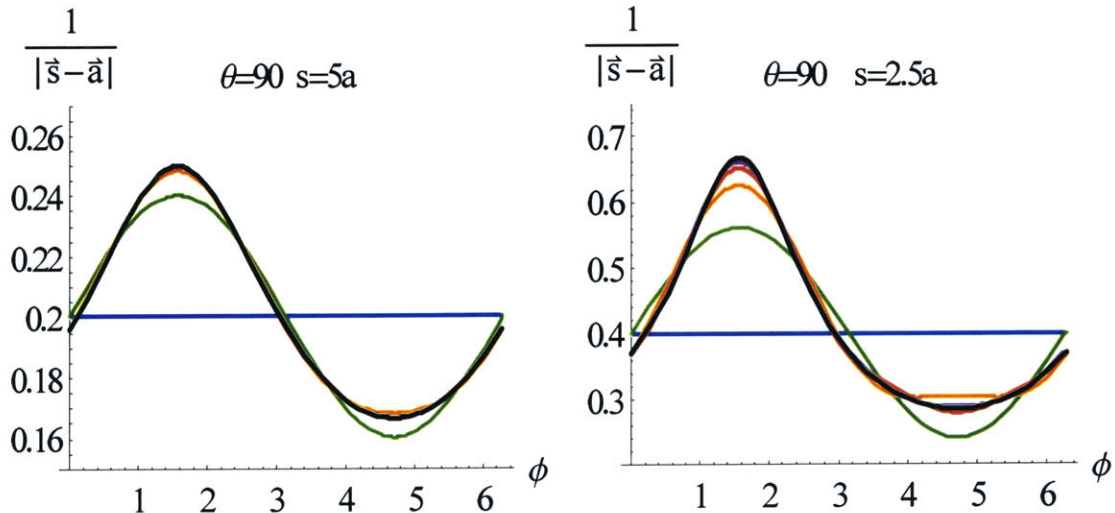


Figure 3-16: Plots of different order Taylor series expansions

Figure 3-16 shows a comparison of the different expansions. In the left graph, $s = 5a$ which is considered not to be in the far-field. Also, $\theta = 90^\circ$ which is the “worst-case” scenario in terms of

error for the approximation. If the graph is not in color, at $\phi \approx 1.5$, the horizontal line (blue) is the 0th order, the line above it is the 1st order (green), the line above that is the 2nd (orange), and the 3rd (Red), 4th (purple), and the exact solution (black) are indistinguishable above that. The 1st order solution is the far-field solution, and while not extreme, there is some error in the approximation. The 3rd order solution which will be used for the mid-field model is nearly indistinguishable from the exact solution. The plot on the right shows a separation distance of 2.5 coil radii. Once again if the graph is not in color, at $\phi \approx 1.5$ the horizontal line (blue) is the 0th order, the top line is the exact solution (black) and in between are the 1st, 2nd, 3rd and 4th order solutions. At this separation distance, the far-field solution begins to have some significant errors. The third order solution, while errors are now visible, still provides a decent representation of the exact solution.

We can now evaluate equation (3.64) using the Taylor series expansions of (3.65).

$$\vec{A}(x, y, z) \approx \frac{\mu_0 Ni a}{4\pi} \sum_{k=0}^n \int_0^{2\pi} T_k(-\sin \phi' \hat{y} + \cos \phi' \hat{z}) d\phi' = \sum_{k=0}^n \vec{A}_k \quad (3.67)$$

where

$$\begin{aligned} \vec{A}_0 &= \vec{0} \\ \vec{A}_1 &= \frac{a^2}{s^3} \frac{Ni\mu_0 z}{4} \hat{y} + \frac{a^2}{s^3} \frac{Ni\mu_0 y}{4} \hat{z} \\ \vec{A}_2 &= \vec{0} \\ \vec{A}_3 &= \frac{a^4}{s^7} \frac{Ni\mu_0 z}{4} \frac{3}{8} (-5x^2 + s^2) \hat{y} + \frac{a^4}{s^7} \frac{Ni\mu_0 y}{4} \frac{3}{8} (-5x^2 + s^2) \hat{z} \\ \vec{A}_4 &= \vec{0} \end{aligned} \quad (3.68)$$

The even terms are zero because, as stated above, the even components of the expansion integrate to zero. The first order expansion (\vec{A}_1) can be verified as the far field model.

Due to the symmetry of the vector field about the \hat{x} axis, we can rewrite the magnetic vector potential more simply in the (r, ϕ, θ) spherical coordinate system.

$$\vec{A}(r, \theta) = \frac{\mu_0 N a}{4\pi} \int_0^{2\pi} \frac{\sin \phi' \hat{\phi}}{\sqrt{a^2 + s^2 - 2as \sin \theta \sin \phi'}} d\phi' \quad (3.69)$$

The Taylor series expansion of the denominator, r , becomes

$$\begin{aligned} T_0 &= \frac{1}{s} \\ T_1 &= \frac{a}{s^2} \sin \theta \sin \phi' \\ T_2 &= \frac{a^2}{s^3} \left(-\frac{1}{2} + \frac{3}{2} \sin \theta \sin \phi' \right) \\ T_3 &= \frac{a^3}{s^4} \left(-\frac{3}{2} \sin \theta \sin \phi' + \frac{5}{2} (\sin \theta \sin \phi')^3 \right) \\ T_4 &= \frac{a^4}{s^5} \left(\frac{3}{8} - \frac{15}{4} (\sin \theta \sin \phi')^2 + \frac{35}{8} (\sin \theta \sin \phi')^4 \right) \end{aligned} \quad (3.70)$$

Evaluating equation (3.69), using the Taylor series expansion results in

$$\begin{aligned} \vec{A}_0 &= \vec{0} \\ \vec{A}_1 &= \frac{a^2}{s^2} \frac{N i \mu_0 \sin \theta}{4} \hat{\phi} \\ \vec{A}_2 &= \vec{0} \\ \vec{A}_3 &= \frac{a^4}{s^4} \frac{N i \mu_0 \sin \theta}{4} \left(-\frac{3}{2} + \frac{15}{8} \sin^2 \theta \right) \hat{\phi} \\ \vec{A}_4 &= \vec{0} \end{aligned} \quad (3.71)$$

Section 3.8.4 The Magnetic Field

The magnetic field can be calculated by taking the curl of the magnetic vector potential that resulted from using the Taylor series expansion

$$\vec{B}_n = \nabla \times \vec{A}_n \quad (3.72)$$

or the curl of the exact formula for the vector potential can be used. In this case, a Taylor series expansion of the denominator is again used yielding equivalent results.

$$\vec{B}(x, y, z) = \frac{\mu_0 Nia}{4\pi} \int_0^{2\pi} \frac{(a - y \cos \phi - z \sin \phi) \hat{x} + x \cos \phi \hat{y} + x \sin \phi' \hat{z}}{\left(\sqrt{a^2 + s^2 - 2ya \cos \phi' - 2za \sin \phi'} \right)^3} d\phi'$$

$$\vec{B}(r, \theta) = \frac{\mu_0 Nia}{4\pi} \int_0^{2\pi} \frac{a \cos \theta \hat{r} + (r \sin \phi' - a \sin \theta) \hat{\theta}}{\sqrt{a^2 + s^2 - 2as \sin \theta \sin \phi'}} d\phi'$$
(3.73)

If we define

$$\vec{B}(x, y, z) = \sum_{k=0}^n \vec{B}_k$$
(3.74)

Evaluating equation (3.72), (taking the curl of equation (3.68)) results in the following equations for the magnetic field.

$$\begin{aligned} \vec{B}_0 &= \vec{0} \\ \vec{B}_1 &= \frac{\mu_0 Nia^2}{4s^5} ((3x^2 - s^2) \hat{x} + 3xy \hat{y} + 3xz \hat{z}) \\ \vec{B}_2 &= \vec{0} \\ \vec{B}_3 &= \frac{3}{32} \frac{\mu_0 Nia^4}{s^9} ((-5x^2(7x^2 - 6s^2) + 3s^4) \hat{x} + 5xy(3s^2 - 7x^2) \hat{y} + 5xz(3s^2 - 7x^2) \hat{z}) \\ \vec{B}_4 &= \vec{0} \end{aligned}$$
(3.75)

In spherical coordinates

$$\begin{aligned} \vec{B}_0 &= \vec{0} \\ \vec{B}_1 &= \frac{\mu_0 Nia^2}{2s^3} (\cos \theta \hat{r} + \frac{1}{2} \sin \theta \hat{\theta}) \\ \vec{B}_2 &= \vec{0} \\ \vec{B}_3 &= \frac{3}{8} \frac{\mu_0 Nia^4}{s^5} \left(\cos \theta (5 \sin^2 \theta - 2) \hat{r} - \frac{3}{8} \sin \theta (3 + 5 \cos(2\theta)) \hat{\theta} \right) \end{aligned}$$
(3.76)

Section 3.8.5 The Magnetic Force

The force between the two coils is given by

$$\vec{F}_B = i_B \oint d\vec{l}_B \times \vec{B} \quad (3.77)$$

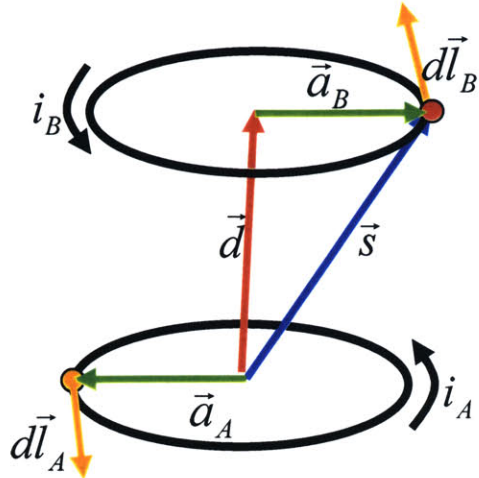


Figure 3-17: Vector Representation of the Magnetic Field at a Point on a Second Loop

Looking at Figure 3-17, we currently have the ability to calculate the magnetic field at a point (\vec{s}) on the 2nd loop due to the first loop. In order to calculate the total force, we must integrate the B field along this 2nd loop.

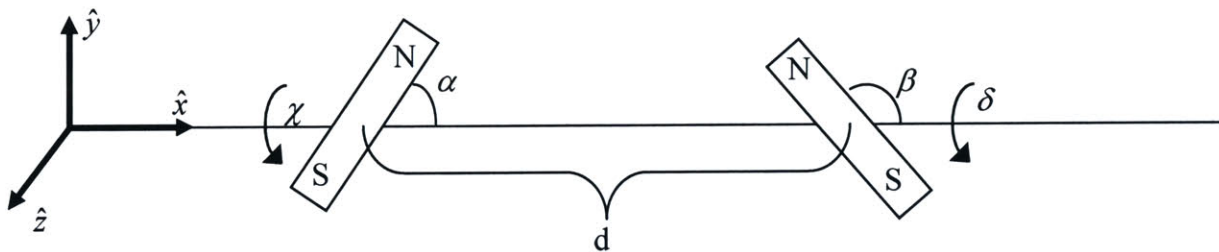


Figure 3-18: Angle Representation

In order to more easily calculate the integral, a change in coordinate system is used. Using the $(\alpha, \beta, \chi, \delta)$ representation of two dipoles separated by a distance d , we can convert the equation for the magnetic field. Figure 3-18 shows the definition of the angles. I apologize for switching from a loop representation to a bar-magnet representation of the dipoles, but the bar magnet

representation is best for showing the angles $(\alpha, \beta, \chi, \delta)$. Remember, the bar magnet aligns with the axis of the loop and follows the right hand rule.

Up to this point in the derivation, the coordinate system was aligned with the axis of the 1st dipole. Keeping the coordinate system fixed and freeing the dipole to rotate with angles (α, χ) , a point in the new coordinate system can be converted to the original coordinate system by a series of cosine rotation matrices.

$$\vec{s} = (x, y, z)^T = \begin{bmatrix} \cos \alpha & \sin \alpha & 0 \\ -\sin \alpha & \cos \alpha & 0 \\ 0 & 0 & 1 \end{bmatrix} \cdot \begin{bmatrix} 1 & 0 & 0 \\ 0 & \cos \chi & \sin \chi \\ 0 & -\sin \chi & \cos \chi \end{bmatrix} \cdot (X', Y', Z')^T \quad (3.78)$$

The second loop can be defined in this new coordinate system in a similar manner. Allowing γ to be the clock angle of the loop, and using (β, δ) to define the orientation of the loop, the position in the new coordinate system can be written as

$$(X', Y', Z')^T = (d, 0, 0)^T + \begin{bmatrix} 1 & 0 & 0 \\ 0 & \cos \delta & -\sin \delta \\ 0 & \sin \delta & \cos \delta \end{bmatrix} \cdot \begin{bmatrix} \cos \beta & -\sin \beta & 0 \\ \sin \beta & \cos \beta & 0 \\ 0 & 0 & 1 \end{bmatrix} \cdot (0, a_B \cos \gamma, a_B \sin \gamma)^T \quad (3.79)$$

Equation (3.79) and (3.78) can be substituted into the equation for the magnetic field and expressions for the magnetic field in terms of $(d, \alpha, \chi, \beta, \delta, \gamma, a_A, a_B)$. This new expression for magnetic field is not displayed here because of its size. In fact, if the first order representation of the magnetic field is expanded, there are 66 terms (in the \hat{X} component of the magnetic field). In the third order expansion, there are 7038 terms. An example of one of these terms is

$$\vec{B} = \frac{i_A \mu_0}{\left(\sqrt{a_B^2 + d^2 - 2a_B d \cos \gamma \sin \beta} \right)^9} \left(\dots + \frac{a_A^2 a_B^2 d^4 \cos^3 \alpha \cos^2 \beta \cos^2 \gamma \cos^2 \delta \cos^2 \chi}{4} + \dots \right) \quad (3.80)$$

Referring to equation (3.77), in order to calculate the force, each term will be crossed with the vector $d\vec{l}$ and integrated. The expression for the $d\vec{l}$ can be simply calculated by

$$d\vec{l}_B = \frac{d}{d\gamma} (X', Y', Z') \quad (3.81)$$

where (X', Y', Z') is defined in equation (3.79). After taking the cross-product, there are 76 terms in the first order expansion and 25,216 terms in the 3rd order expansion.

In order to perform the integration, the radical in the denominator of equation (3.80) must be simplified. It can be seen by inspection that this is the variable s .

$$s = |\vec{d} - \vec{a}_B| = \sqrt{a_B^2 + d^2 - 2a_B d \cos \gamma \sin \beta} \quad (3.82)$$

The variable s is in a very similar form to r in equation (3.69). The expression for s will be simplified with a Taylor series expansion just as r was. The only difference is that r was not raised to any power. In this case, depending on whether the 1st or 3rd order expansion was used for calculating r , s is raised to the 5th or 9th power respectively.

Before sending the expression for the cross-product of the magnetic field to the integrator, it is informative to look at the integrand. Once again there are over 25,000 terms in the 3rd order expansion. We can group each term by the ratio of (a/d) where a represents both (a_A, a_B) . Since we are still assuming that $a \ll d$, terms with higher powers of (a/d) can be neglected. The third order expansion has terms of $(a/d)^3$ to $(a/d)^{12}$.

If we define

$$\vec{F}_B = i_B \int_0^{2\pi} (d\vec{l}_B \times \vec{B}) d\gamma = i_B \int_0^{2\pi} \left(\sum_{k=0}^9 \vec{f}'_k \right) d\gamma \quad (3.83)$$

in the \hat{X} direction alone there are

$$\begin{aligned}
 f_0 &\rightarrow 8\left(\frac{a}{d}\right)^3 \text{ terms} \\
 f_1 &\rightarrow 50\left(\frac{a}{d}\right)^4 \text{ terms} \\
 f_2 &\rightarrow 210\left(\frac{a}{d}\right)^5 \text{ terms} \\
 f_3 &\rightarrow 446\left(\frac{a}{d}\right)^6 \text{ terms}
 \end{aligned} \tag{3.84}$$

After integration, many of the terms cancel out. Looking at the lowest order terms, we find that terms with odd powers of (a/d) all integrate to zero.

$$\begin{aligned}
 f_0 &= 0 \\
 f_1 &\rightarrow 3\left(\frac{a}{d}\right)^4 \text{ terms} \\
 f_2 &= 0 \\
 f_3 &\rightarrow 15\left(\frac{a}{d}\right)^6 \text{ terms}
 \end{aligned} \tag{3.85}$$

Since we are considering $a \ll d$, we will neglect the higher order terms. Essentially, we are performing yet another Taylor series about $(a/d) = 0$. $(a/d)^4$ is defined as the 1st order term and $(a/d)^6$ as the 3rd order term.

At this point we should recap the simplifications so far. In this derivation, there have been three simplifications. The first is in the calculation of r . The second was in the calculation of s . Finally, there is a third simplification of F . At each simplification, there is the ability to expand the model to any degree of fidelity. How do the varying degrees of fidelity at each point in the derivation interact?

It's best to look at the last simplification first. If you only want to expand the final solution to the first order, terms with $(a/d)^4$, then you only need to carry out the expansions of r and s to the 1st order. Expanding r and s to higher order does not affect the final solution any. Likewise, if you want the expansion of the final solution to the third order, terms with $(a/d)^6$, then you only need to take the expansions of r and s to the third order. Anything more is just a waste, and anything less will produce errors. From here on, we will define a first order expansion as having taken the first order terms in all three simplifications. A third order expansion refers to taking the third order terms in all three simplifications, etc.

The first order expansion recaptures the far-field model, see equation (3.51), and the third order expansion captures the mid-field model. Note that the equations below have been derived for the force on the 2nd loop.

Defining the force on the second dipole due to the first as

$$\bar{F}_n \approx \sum_{k=0}^n \bar{f}_k \quad (3.86)$$

where \bar{f}_k is the k th order expansion, then

$$\begin{aligned}
f_1 &= \frac{3}{4} \frac{\mu_0 \pi i_1 a_1^2 b_2 a_2^2}{d^4} \left(-2 \cos[\alpha] \cos[\beta] - \cos[\delta - \chi] \sin[\alpha] \sin[\beta] \right) \hat{X} + \\
&\quad (\cos[\alpha] \sin[\beta] \cos[\delta] + \sin[\alpha] \cos[\beta] \cos[\chi]) \hat{Y} + \\
&\quad (\cos[\alpha] \sin[\beta] \sin[\delta] + \sin[\alpha] \cos[\beta] \sin[\chi]) \hat{Z}; \\
f_3 &= \frac{1}{256 d^6} (15 a_1^2 a_2^2 i_1 i_2 \pi \mu_0 (40 a_1^2 \cos[\alpha]^3 \cos[\beta] + 4 \cos[\alpha] \cos[\beta] \\
&\quad (-9 a_1^2 - 4 a_2^2 + 15 a_1^2 \cos[2\alpha] + 20 a_2^2 \cos[2\beta]) - 90 a_1^2 \cos[\alpha]^2 \cos[\delta - \chi] \sin[\alpha] \sin[\beta] - \\
&\quad 3(-3 a_1^2 + 12 a_2^2 + 5 a_1^2 \cos[2\alpha] + 20 a_2^2 \cos[2\beta]) \cos[\delta - \chi] \sin[\alpha] \sin[\beta])) \hat{X} + \\
&- \frac{1}{512 d^6} (15 a_1^2 a_2^2 i_1 i_2 \pi \mu_0 (4 a_2^2 \cos[\beta]^3 (3 \cos[2\delta - \chi] + 10 \cos[\chi]) \sin[\alpha] + \\
&\quad 3 \cos[\beta] (20 a_1^2 \cos[2\alpha - \chi] + 10 a_2^2 \cos[2\beta - \chi] - 10 a_2^2 \cos[2\delta - \chi] + \\
&\quad 3 a_2^2 \cos[2\beta + 2\delta - \chi] + 24 a_1^2 \cos[\chi] - 12 a_2^2 \cos[\chi] + \\
&\quad 20 a_1^2 \cos[2\alpha + \chi] + 10 a_2^2 \cos[2\beta + \chi] + 3 a_2^2 \cos[2\beta - 2\delta + \chi]) \sin[\alpha] + \\
&\quad 180 a_2^2 \cos[\alpha] \cos[\beta]^2 \cos[\delta] \sin[\beta] + \cos[\alpha] (40 a_1^2 \cos[2\alpha - \delta] + 15 a_2^2 \cos[2\beta - \delta] - \\
&\quad 16 a_1^2 \cos[\delta] - 18 a_2^2 \cos[\delta] + 40 a_1^2 \cos[2\alpha + \delta] + 15 a_2^2 \cos[2\beta + \delta] - \\
&\quad 24 a_1^2 \cos[\delta - 2\chi] + 12 a_1^2 \cos[2\alpha + \delta - 2\chi] + 12 a_1^2 \cos[2\alpha - \delta + 2\chi]) \sin[\beta])) \hat{Y} + \\
&\frac{1}{128 d^6} (15 a_1^2 a_2^2 i_1 i_2 \pi \mu_0 (\cos[\beta] \sin[\alpha] (15 a_1^2 \sin[2\alpha - \chi] + 10 a_2^2 \sin[2\beta - \chi] + \\
&\quad 6 a_2^2 \sin[2\delta - \chi] - 3 a_2^2 \sin[2\beta + 2\delta - \chi] - 18 a_1^2 \sin[\chi] + 4 a_2^2 \sin[\chi] - \\
&\quad 15 a_1^2 \sin[2\alpha + \chi] - 10 a_2^2 \sin[2\beta + \chi] + 3 a_2^2 \sin[2\beta - 2\delta + \chi]) + \cos[\alpha] \sin[\beta] \\
&\quad (10 a_1^2 \sin[2\alpha - \delta] + 15 a_2^2 \sin[2\beta - \delta] + 4 a_1^2 \sin[\delta] - 18 a_2^2 \sin[\delta] - 10 a_1^2 \sin[2\alpha + \delta] - \\
&\quad 15 a_2^2 \sin[2\beta + \delta] - 6 a_1^2 \sin[\delta - 2\chi] + 3 a_1^2 \sin[2\alpha + \delta - 2\chi] - 3 a_1^2 \sin[2\alpha - \delta + 2\chi])) \hat{Z}
\end{aligned}$$

Equation (3.87)

The derivation for the mid-field model of the torque is the same as that for the force.

$$\vec{\tau} = i_B \oint \vec{a}_B \times (d\vec{l}_B \times \vec{B}) \quad (3.88)$$

The integrand will have more terms due to the extra cross-product. In the \hat{X} direction alone there are 34,944 terms. After integrating we are left with

$$\begin{aligned}
 t_0 &\rightarrow 0 \left(\frac{a}{d} \right)^2 \text{ terms} \\
 t_1 &\rightarrow 4 \left(\frac{a}{d} \right)^3 \text{ terms} \\
 t_2 &\rightarrow 0 \left(\frac{a}{d} \right)^4 \text{ terms} \\
 t_3 &\rightarrow 112 \left(\frac{a}{d} \right)^5 \text{ terms}
 \end{aligned} \tag{3.89}$$

Performing the final simplification, and defining

$$\vec{\tau}_n \approx \sum_{k=0}^n \vec{t}_k \tag{3.90}$$

the far and mid-field models for torque are

$$\begin{aligned}
 \vec{t}_1 &= \frac{a1^2 a2^2 i1 i2 \pi \mu_0 \sin[\alpha] \sin[\beta] \sin[\delta - \chi]}{4 d^3} \hat{X}, \\
 &\frac{a1^2 a2^2 i1 i2 \pi \mu_0 (2 \cos[\alpha] \sin[\beta] \sin[\delta] + \cos[\beta] \sin[\alpha] \sin[\chi])}{4 d^3} \hat{Y}, \\
 &- \frac{a1^2 a2^2 i1 i2 \pi \mu_0 (\cos[\beta] \cos[\chi] \sin[\alpha] + 2 \cos[\alpha] \cos[\delta] \sin[\beta])}{4 d^3} \hat{Z} \\
 \vec{t}_3 &= - \frac{9 a1^2 a2^2 i1 i2 \pi \mu_0 (3(a1^2 + a2^2) + 5 a1^2 \cos[2\alpha] + 5 a2^2 \cos[2\beta]) \sin[\alpha] \sin[\beta] \sin[\delta - \chi]}{64 d^5} \hat{X}, \\
 &\frac{1}{128 d^5} (3 a1^2 a2^2 i1 i2 \pi \mu_0 (-8 \cos[\alpha] (-a1^2 + 9 a2^2 + 5 a1^2 \cos[2\alpha] + 15 a2^2 \cos[2\beta]) \sin[\beta] \sin[\delta] + \\
 &\quad 3 \cos[\beta] \sin[\alpha] (5 a1^2 \sin[2\alpha - \chi] + 10 a2^2 \sin[2\beta - \chi] + 10 a2^2 \sin[2\delta - \chi] - 5 a2^2 \sin[2\beta + 2\delta - \chi] - \\
 &\quad 6 a1^2 \sin[\chi] + 4 a2^2 \sin[\chi] - 5 a1^2 \sin[2\alpha + \chi] - 10 a2^2 \sin[2\beta + \chi] + 5 a2^2 \sin[2\beta - 2\delta + \chi])) \hat{Y}, \\
 &\frac{1}{512 d^5} (3 a1^2 a2^2 i1 i2 \pi \mu_0 (60 a2^2 \cos[\beta]^3 (\cos[2\delta - \chi] + 2 \cos[\chi]) \sin[\alpha] + \\
 &\quad 3 \cos[\beta] (20 a1^2 \cos[2\alpha - \chi] + 30 a2^2 \cos[2\beta - \chi] - 50 a2^2 \cos[2\delta - \chi] + \\
 &\quad 15 a2^2 \cos[2\beta + 2\delta - \chi] + 24 a1^2 \cos[\chi] - 36 a2^2 \cos[\chi] + 20 a1^2 \cos[2\alpha + \chi] + \\
 &\quad 30 a2^2 \cos[2\beta + \chi] + 15 a2^2 \cos[2\beta - 2\delta + \chi]) \sin[\alpha] + 720 a2^2 \cos[\alpha] \cos[\beta]^2 \cos[\delta] \sin[\beta] + \\
 &\quad 8 \cos[\alpha] (-4 a1^2 - 9 a2^2 + 20 a1^2 \cos[2\alpha] + 15 a2^2 \cos[2\beta]) \cos[\delta] \sin[\beta])) \hat{Z}
 \end{aligned} \tag{3.91}$$

Equation (3.91)

Section 3.8.6 Vector Representation of the Mid-Field

Equation (3.87) and (3.91), while correctly representing the mid-field model, are not useful when calculating the force between more than two satellites. Since the coordinate system is defined as the vector between two satellites, it becomes a hassle to change coordinate systems every time the force or torque between two satellites needs to be calculated. What is desired is a vector representation of the forces, similar to the representation of the far-field in equation (3.30). Therefore, the next and final step in this derivation is to convert equation (3.87) and (3.91) into a vector representation.

To create the vector representation, we expand the equations to contain terms with sines and cosines of single angles, (no sums of angles or double angles). This allows us to more readily match up the terms with vectors. One exception is $\cos(\delta - \chi)$ since it is readily created using vectors. For example the x component of the force has the following terms.

$$\left(\begin{array}{c} \cos[\alpha] \cos[\beta] \\ \cos[\alpha]^3 \cos[\beta] \\ \cos[\alpha] \cos[\beta]^3 \\ \cos[\alpha] \cos[\beta] \sin[\alpha]^2 \\ \cos[\delta - \chi] \sin[\alpha] \sin[\beta] \\ \cos[\alpha]^2 \cos[\delta - \chi] \sin[\alpha] \sin[\beta] \\ \cos[\beta]^2 \cos[\delta - \chi] \sin[\alpha] \sin[\beta] \\ \cos[\delta - \chi] \sin[\alpha]^3 \sin[\beta] \\ \cos[\alpha] \cos[\beta] \sin[\beta]^2 \\ \cos[\delta - \chi] \sin[\alpha] \sin[\beta]^3 \end{array} \right) \quad (3.92)$$

The next step is to create each one of these terms using vector representations. The following vectors are available

$$(\vec{\mu}_A, \vec{\mu}_B, \vec{r}) \quad (3.93)$$

along with the cross-product and the dot-product operations. Using multiple combinations of these terms every term in the force and torque function can be created. For example to create

$$\begin{aligned}
 \cos \alpha &\sim \vec{\mu}_A \cdot \vec{r} \\
 \cos \beta &\sim \vec{\mu}_B \cdot \vec{r} \\
 \sin^2 \alpha &\sim (1 - (\vec{\mu}_A \cdot \vec{r})^2) \\
 \cos(\delta - \chi) \sin \alpha \sin \beta &\sim \vec{\mu}_A \cdot \vec{\mu}_B - (\vec{\mu}_A \cdot \vec{r})(\vec{\mu}_B \cdot \vec{r})
 \end{aligned} \tag{3.94}$$

Without going into further details, the following vector representation for the mid-field force and torque models were (with much difficulty) created.

$$\begin{aligned}
 \vec{F}_3 = & \frac{15}{32} \frac{\mu_0}{r^6 \pi} \left(-24(a_A^2 + a_B^2) \frac{(\vec{\mu}_A \cdot \vec{r})(\vec{\mu}_B \cdot \vec{r})\vec{r}}{r^3} \right. \\
 & + 63 \frac{a_A^2(\vec{\mu}_A \cdot \vec{r})^3(\vec{\mu}_B \cdot \vec{r})\vec{r}}{\mu_A^2 r^5} + 63 \frac{a_B^2(\vec{\mu}_A \cdot \vec{r})(\vec{\mu}_B \cdot \vec{r})^3\vec{r}}{\mu_B^2 r^5} \\
 & + 3(2a_A^2 + a_B^2) \frac{(\vec{\mu}_A \cdot \vec{r})\vec{\mu}_B}{r} + 3(a_A^2 + 2a_B^2) \frac{(\vec{\mu}_B \cdot \vec{r})\vec{\mu}_A}{r} \\
 & - 10 \frac{a_A^2(\vec{\mu}_A \cdot \vec{r})^3\vec{\mu}_B}{\mu_A^2 r^3} - 10 \frac{a_B^2(\vec{\mu}_B \cdot \vec{r})^3\vec{\mu}_A}{\mu_B^2 r^3} \\
 & - 18 \frac{a_A^2(\vec{\mu}_A \cdot \vec{r})^2(\vec{\mu}_B \cdot \vec{r})\vec{\mu}_A}{\mu_A^2 r^3} - 18 \frac{a_B^2(\vec{\mu}_A \cdot \vec{r})(\vec{\mu}_B \cdot \vec{r})^2\vec{\mu}_B}{\mu_B^2 r^3} \\
 & + 3(a_A^2 + a_B^2) \frac{(\vec{\mu}_A \cdot \vec{\mu}_B)\vec{r}}{r} \\
 & - 18 \frac{a_A^2(\vec{\mu}_A \cdot \vec{r})^2(\vec{\mu}_A \cdot \vec{\mu}_B)\vec{r}}{\mu_A^2 r^3} - 18 \frac{a_B^2(\vec{\mu}_B \cdot \vec{r})^2(\vec{\mu}_A \cdot \vec{\mu}_B)\vec{r}}{\mu_B^2 r^3} \\
 & + 3 \frac{a_A^2(\vec{r} \cdot (\vec{\mu}_A \times \vec{\mu}_B))(\vec{\mu}_A \cdot \vec{r})(\vec{\mu}_A \times \vec{r})}{\mu_A^2 r^3} + 3 \frac{a_B^2(\vec{r} \cdot (\vec{\mu}_B \times \vec{\mu}_A))(\vec{\mu}_B \cdot \vec{r})(\vec{\mu}_B \times \vec{r})}{\mu_B^2 r^3} \\
 & \left. + 3 \frac{a_A^2(\vec{\mu}_A \cdot \vec{\mu}_B)(\vec{\mu}_A \cdot \vec{r})\vec{\mu}_A}{\mu_A^2 r} + 3 \frac{a_B^2(\vec{\mu}_A \cdot \vec{\mu}_B)(\vec{\mu}_B \cdot \vec{r})\vec{\mu}_B}{\mu_B^2 r} \right) \tag{3.95}
 \end{aligned}$$

The torque vector representation is

$$\begin{aligned}
\vec{\tau}_3 = & \frac{3\mu_0}{32r^5\pi} \left(12(a_A^2 + a_B^2) \frac{(\vec{\mu}_A \cdot \vec{r})(\vec{\mu}_B \times \vec{r})}{r^2} \right. \\
& + 3(a_A^2 + 6a_B^2) \frac{(\vec{\mu}_B \cdot \vec{r})(\vec{\mu}_A \times \vec{r})}{r^2} - 30 \frac{a_B^2 (\vec{\mu}_B \cdot \vec{r})^2 (\vec{\mu}_A \times \vec{\mu}_B)}{\mu_B^2 r^2} \\
& + 20 \frac{a_A^2 (\vec{\mu}_A \cdot \vec{r})^2 (\vec{\mu}_A \times \vec{\mu}_B)}{\mu_A^2 r^2} - 105 \frac{a_B^2 (\vec{\mu}_A \cdot \vec{r})^2 (\vec{\mu}_B \times \vec{r})}{\mu_B^2 r^4} \\
& - 35 \frac{a_A^2 (\vec{\mu}_A \cdot \vec{r})^2 (\vec{\mu}_B \cdot \vec{r})(\vec{\mu}_A \times \vec{r})}{\mu_A^2 r^4} + 15 \frac{a_B^2 (\vec{r} \cdot (\vec{\mu}_A \times \vec{\mu}_B))(\vec{\mu}_B \cdot \vec{r}) \vec{\mu}_B}{\mu_B^2 r^2} \\
& - 35 \frac{a_A^2 (\vec{r} \cdot (\vec{\mu}_A \times \vec{\mu}_B))(\vec{\mu}_A \cdot \vec{r})^2 \vec{r}}{\mu_A^2 r^4} + 15 \frac{a_B^2 (\vec{\mu}_A \cdot \vec{\mu}_B)(\vec{\mu}_B \cdot \vec{r})(\vec{\mu}_B \times \vec{r})}{\mu_B^2 r^2} \\
& \left. + 3(a_A^2 + a_B^2) \frac{(\vec{r} \cdot (\vec{\mu}_A \times \vec{\mu}_B)) \vec{r}}{r^2} \right) \quad (3.96)
\end{aligned}$$

It should be noted that the full mid-field model includes the addition of the terms from the far-field model. Please refer to equation (3.90) and equation (3.86).

Section 3.9 Comparing the mid-field model

This section compares the mid-field model against the exact solution (which was calculated numerically). The far-field model is also plotted for reference. As stated earlier, the model is considered valid if the errors are less than approximately 10%. For the far-field this was about 6-8 coil radii. For the mid-field, the model is valid up to around 3-4 coil radii. The mid-field model cuts the minimum separation distance in half.

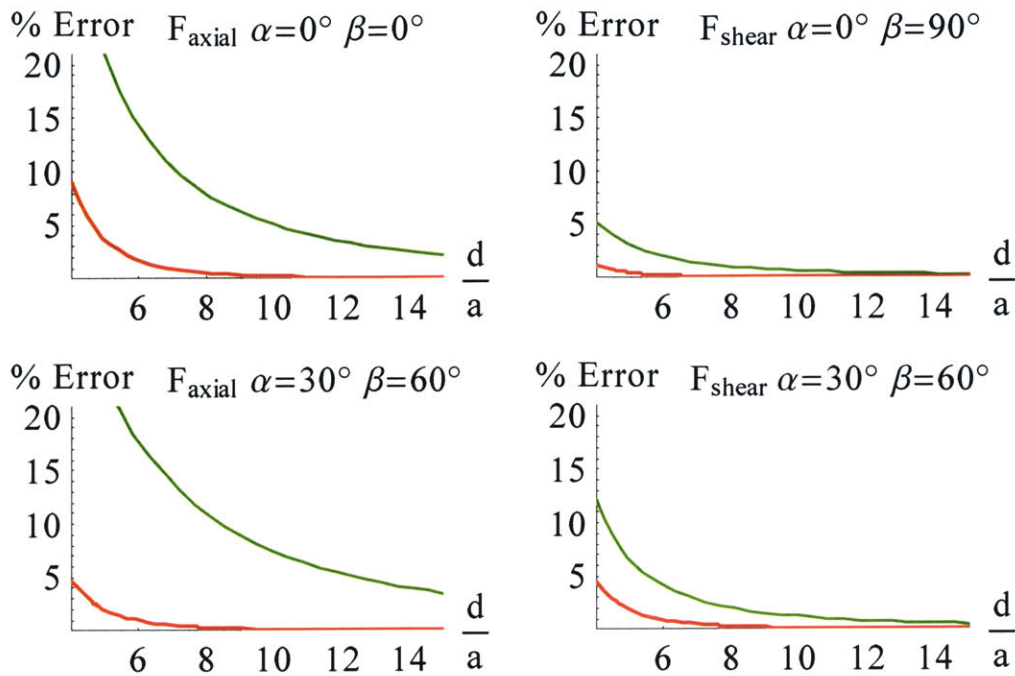


Figure 3-19: Error in the Far-Field (green) and the Mid-Field Force Model (red)

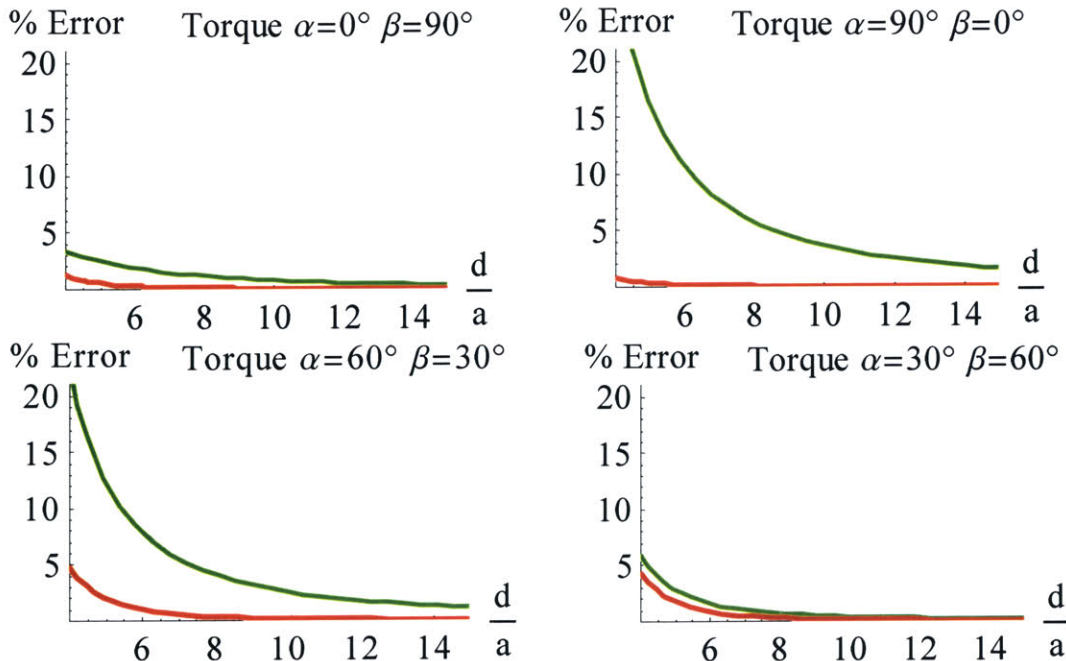


Figure 3-20: Error in the Far-Field (green) and the Mid-Field Torque Model (red)

Section 3.10 Conclusion

In this chapter four important equations were developed. A force and torque equation in the far-field and a force and torque equation in the mid-field, equation (3.30), (3.34), (3.95), and (3.96) respectively. These equations are analytic and do not require numeric integration to solve. The only drawback is that the equations breakdown as the separation distance between the vehicles gets smaller.

Chapter 4

SOLVING THE EQUATIONS OF MOTION

Section 4.1 Overview

At every instant in time, EMFF must provide a specific force for each satellite in the formation. In order to accomplish this goal, every magnetic dipole in the formation must have the proper strength and direction. This chapter will discuss methods of accomplishing this task. Given a desired force profile or distribution on each satellite at different points in time, along with their position, and the strength and direction of the free dipole, this chapter will show how to determine the remaining magnetic dipoles.

More concisely, this chapter will discuss methods of solving the following system of equations:

$$\begin{aligned}\vec{F}_1(\vec{r}_1, \vec{r}_2, \dots, \vec{r}_n, \vec{\mu}_1, \vec{\mu}_2, \dots, \vec{\mu}_n) - \vec{f}_1 &= \vec{0} \\ \vec{F}_2(\vec{r}_1, \vec{r}_2, \dots, \vec{r}_n, \vec{\mu}_1, \vec{\mu}_2, \dots, \vec{\mu}_n) - \vec{f}_2 &= \vec{0} \\ &\vdots \\ \vec{F}_n(\vec{r}_1, \vec{r}_2, \dots, \vec{r}_n, \vec{\mu}_1, \vec{\mu}_2, \dots, \vec{\mu}_n) - \vec{f}_n &= \vec{0}\end{aligned}\tag{4.1}$$

where \vec{F}_j is the overall magnetic force on a satellite and \vec{f}_j is the desired force on a satellite.

In chapter 3, we showed that the far-field approximation of the magnetic force on one satellite (A) due to a second satellite (B) is given by :

$$\vec{F}_{AB} = \vec{\mu}_A \cdot \nabla \vec{B}_B = \frac{3\mu_0}{4\pi} \left(-\frac{\vec{\mu}_1 \cdot \vec{\mu}_2}{r_{AB}^5} \vec{r}_{AB} - \frac{\vec{\mu}_1 \cdot \vec{r}_{AB}}{r_{AB}^5} \vec{\mu}_2 - \frac{\vec{\mu}_2 \cdot \vec{r}_{AB}}{r_{AB}^5} \vec{\mu}_1 + 5 \frac{(\vec{\mu}_1 \cdot \vec{r}_{AB})(\vec{\mu}_2 \cdot \vec{r}_{AB})}{r_{AB}^7} \vec{r}_{AB} \right)\tag{4.2}$$

where $\vec{\mu}_A$ is the magnetic dipole of satellite A, $\vec{\mu}_B$ is the magnetic dipole of satellite B, \vec{r}_{AB} is the position vector between the two satellites, and $\mu_0 = 4\pi * 10^{-7} \text{ NA}^{-2}$. In formations of more than one satellite, the total magnetic force on the satellite is given as the sum of the magnetic forces due to every other satellite in the formation.

$$\vec{F}_j = \sum_{\substack{i=A,B,C\dots \\ i \neq j}} \vec{F}_{ji} \quad (4.3)$$

Section 4.2 Relative Motion and Degrees of Freedom

An electromagnetic force is generated by two or more dipoles “pushing” or interacting with each other. In this chapter we are assuming that the dipoles only interact with the magnetic fields generated by other satellites. (Chapter 6 discusses EMFF in the presence of an external magnetic field.) Because the magnetic forces are only generated by satellites pushing and pulling on each other, we are bound by Newton’s third law; each generated force is matched by one that is equal and opposite, and thus EMFF cannot change the formation center of mass. Algebraically this is represented by:

$$\sum_{j=1}^n f_j = 0 \quad (4.4)$$

Because of this relationship, the equations in (4.1) are dependent and thus can be arbitrarily reduced to $(n - 1)$ independent vector equations without loss of generality.

$$\begin{aligned} \vec{F}_1(\vec{r}_1, \vec{r}_2, \dots, \vec{r}_n, \vec{\mu}_1, \vec{\mu}_2, \dots, \vec{\mu}_n) - \vec{f}_1 &= \vec{0} \\ \vec{F}_2(\vec{r}_1, \vec{r}_2, \dots, \vec{r}_n, \vec{\mu}_1, \vec{\mu}_2, \dots, \vec{\mu}_n) - \vec{f}_2 &= \vec{0} \\ &\vdots \\ \vec{F}_{n-1}(\vec{r}_1, \vec{r}_2, \dots, \vec{r}_n, \vec{\mu}_1, \vec{\mu}_2, \dots, \vec{\mu}_n) - \vec{f}_{n-1} &= \vec{0} \end{aligned} \quad (4.5)$$

Doing a quick count of equations and variables, we see that there are n vector variables (the magnetic dipoles on each satellite) and $(n - 1)$ vector equations. Essentially there is a ‘free’ dipole vector that may be chosen at random. The ability to choose a dipole at will is an enabling component of EMFF. Actually any three dipole components can be chosen at will, or three other constraint equations can be applied.

$$\begin{aligned}
 \vec{F}_1(\vec{r}_1, \vec{r}_2, \dots, \vec{r}_n, \vec{\mu}_1, \vec{\mu}_2, \dots, \vec{\mu}_n) - \vec{f}_1 &= \vec{0} \\
 \vec{F}_2(\vec{r}_1, \vec{r}_2, \dots, \vec{r}_n, \vec{\mu}_1, \vec{\mu}_2, \dots, \vec{\mu}_n) - \vec{f}_2 &= \vec{0} \\
 \vdots & \\
 \vec{F}_{n-1}(\vec{r}_1, \vec{r}_2, \dots, \vec{r}_n, \vec{\mu}_1, \vec{\mu}_2, \dots, \vec{\mu}_n) - \vec{f}_{n-1} &= \vec{0} \\
 \vec{g}(\vec{\mu}_1, \vec{\mu}_2, \dots, \vec{\mu}_n, \dots) &= \vec{0}
 \end{aligned} \tag{4.6}$$

For example, we could control the magnetic torque on a satellite, or select the free dipole in such a way that we minimize the total dipole strength of the formation. Finally, another constraint equation could be added that, when satisfied, minimizes a parameter.

For the rest of this chapter and analysis, the free dipole will be chosen at random with the only requirement that it is non-zero. For consistency, the free dipole will always be $\vec{\mu}_1$, but any dipole could just as easily be chosen. The remainder of this chapter will analyze equation (4.5) and discuss methods of solving.

Section 4.3 The Freedom of the Free Dipole

Once again, the object of this chapter is to describe methods of finding the correct dipole strengths and directions to produce a specified force on each satellite. This is accomplished by solving the equations of motion described in equation (4.5). Before the equations of motion can be solved, the three extra degrees of control (the free dipole) must be specified, or three constraint equations must be added so that there is an equal number of equations and variables.

The extra degrees of control are the vector components of the magnetic dipoles. We basically have the freedom to arbitrarily choose the extra degrees of control, but there are some degenerate choices that will not allow for any real solutions to the equations of motion. For example, if the three degrees of control are the three dipole components of one satellite, then if the three components of the dipole are set to zero, there is no way for a force to be produced on that satellite and the equations of motion fail to solve for any real solutions.

The same restrictions on choosing the constraint equations also exist. For example, consider the 2D example of two satellites in a plane. (There are only two free degrees of control since we are working in a plane.) If we choose to constrain the magnitude of the overall dipole strength of each satellite, and constrain their magnitude to be small, there is no way to orient the spacecraft to achieve a comparatively large force.

Currently, the most intuitive and versatile way of defining the three extra degrees of control is to allow the three vector components of one satellite's dipole to be the free degrees of control. Essentially, one satellite's dipole can be chosen at will, and will be referred to as the "free dipole". The next section will look at the freedom of choosing the free dipole and derive choices that should be avoided.

Section 4.3.1 The Freedom of the Free Dipole

The magnetic force on a vehicle is created when it generates a magnetic dipole in the presence of an external magnetic field. This external magnetic field is created by the other spacecraft in the formation. Let's look at the simple case of two satellites in a plane.

Section 4.3.1.1 Two satellites in 2D

Let's take two satellites A and B. Satellite A will be the free dipole. The question is, no matter how the free dipole is chosen, can one always generate an arbitrary force profile on the satellites? From equation (3.29) the force on satellite B due to satellite A is given by

$$\vec{F}_B = \nabla \vec{B}_A \bullet \vec{\mu}_B \quad (4.7)$$

where \vec{B}_A is the magnetic field produced by satellite A at satellite B's position. As long as $\nabla \vec{B}_A$ is full rank, then any desired force (\vec{F}_B) can be created. In other words given \vec{F}_B and $\nabla \vec{B}_A$, there always exists a $\vec{\mu}_B$ to satisfy equation (4.7) as long as $\nabla \vec{B}_A$ is full rank. How do we guarantee that $\nabla \vec{B}_A$ is full rank?

If $\nabla \vec{B}_A$ is rank deficient then the matrix is singular, and the determinant is zero. Assume that satellite A is located at the origin of our coordinate system. The gradient of the magnetic field at a point $(d,0)$ is

$$\nabla \vec{B}_A = \frac{3\mu_0}{4\pi d^4} \begin{pmatrix} -2\mu_{Ax} & \mu_{Ay} \\ \mu_{Ay} & \mu_{Ax} \end{pmatrix} \quad (4.8)$$

The determinant is

$$|\nabla \vec{B}_A| = -\frac{9\mu_0^2}{16\pi^2 d^8} (2\mu_{Ax}^2 + \mu_{Ay}^2) \quad (4.9)$$

The only way for the determinant to be zero is if both components of the magnetic dipole on satellite A are zero. This was the trivial case described in the introduction where the dipole components were all set to zero and no magnetic field was generated.

The dipole on satellite A can also be represented as a magnitude and an angle. See Figure 4.1.

$$\vec{\mu}_A = (\mu_A \cos \alpha) \hat{x} + (\mu_A \sin \alpha) \hat{y} \quad (4.10)$$

The gradient is

$$\nabla \vec{B}_A = \frac{3\mu_A \mu_0}{4\pi d^4} \begin{pmatrix} -2 \cos \alpha & \sin \alpha \\ \sin \alpha & \cos \alpha \end{pmatrix} \quad (4.11)$$

and the determinant is

$$|\nabla \vec{B}_A| = -\frac{9\mu_0^2}{32d^8 \pi^2} \mu_A^2 (3 + \cos(2\alpha)) \quad (4.12)$$

Once again, the only way for the determinant to become zero is if the magnitude of the dipole is also zero.

Therefore when restricted to a plane, we can choose the free dipole in **any** non-zero configuration and still be able to produce any desired magnetic force. Put in other words, we can choose the free dipole in any non-zero way and still solve equation (4.7).

Section 4.3.1.2 Two satellites in 3D

The same argument can be expanded to three dimensions. If satellite A's dipole is defined as

$$\vec{\mu}_A = \mu_{Ax}\hat{x} + \mu_{Ay}\hat{y} + \mu_{Az}\hat{z} \quad (4.13)$$

then the gradient of the magnetic field at satellite B's position is

$$\nabla \vec{B}_A = \frac{3\mu_0}{4d^4\pi} \begin{pmatrix} -2\mu_x & \mu_y & \mu_z \\ \mu_y & \mu_x & 0 \\ \mu_z & 0 & \mu_x \end{pmatrix} \quad (4.14)$$

The determinant of the gradient is

$$|\nabla \vec{B}_A| = -\frac{27\mu_0^3}{64d^{12}\pi^3} \mu_x(2\mu_x^2 + \mu_y^2 + \mu_z^2) \quad (4.15)$$

Aside from the trivial solution where the magnitude of the dipole is zero, there is another way to make the determinant of the gradient of the magnetic field zero. If the x component of the magnetic dipole is zero, the determinant is zero.

When the dipole on satellite A is represented in angle form (refer to Figure 4-4),

$$\vec{\mu}_A = (\mu_A \cos \alpha)\hat{x} + (\mu_A \sin \alpha \cos \chi)\hat{y} + (\mu_A \sin \alpha \sin \chi)\hat{z} \quad (4.16)$$

the gradient is

$$\nabla \vec{B}_A = \frac{3\mu_0\mu_A}{4d^4\pi} \begin{pmatrix} -2\cos \alpha & \sin \alpha \cos \chi & \sin \alpha \sin \chi \\ \sin \alpha \cos \chi & \cos \alpha & 0 \\ \sin \alpha \sin \chi & 0 & \cos \alpha \end{pmatrix} \quad (4.17)$$

and the determinant is

$$|\nabla \vec{B}_A| = -\frac{27\mu_0^3\mu_A^3}{128d^{12}\pi^3} \cos \alpha (3 + 2\cos(2\alpha)) \quad (4.18)$$

The determinant is zero when

$$\alpha = \pm \frac{\pi}{2} \quad (4.19)$$

When the dipole on satellite A is aligned such that it points perpendicular to the line that connects the two satellites, the gradient of the magnetic field is not full rank at satellite B's location. Because the force on satellite B is

$$\vec{F}_B = \nabla \vec{B}_A \bullet \vec{\mu}_B \quad (4.20)$$

if the gradient is not full rank, then no matter what $\vec{\mu}_B$ is, there are certain force directions that cannot be generated. The null space of the transpose of the gradient, or the left nullspace, gives the basis of the space that cannot be achieved. Since our matrix is symmetric, the transpose can be dropped. In component form and angle form respectively, the null space of the gradient is

$$\begin{aligned} \text{NullSpace}(\nabla \vec{B}_A) &= -\mu_z \hat{y} + \mu_y \hat{z} \\ \text{NullSpace}(\nabla \vec{B}_A) &= -\sin \chi \hat{y} + \cos \chi \hat{z} \end{aligned} \quad (4.21)$$

Essentially, when the dipole of satellite A points perpendicular to the line that connects the two satellites, the force on satellite B can have no component out of the plane that contains satellite A's dipole and the line connecting the two satellites. This is why in 2D there are no restrictions since all forces are by definition constrained to a plane.

Section 4.3.1.3 Multiple Spacecraft

When there are multiple spacecraft in the formation, the force on the satellite is given by

$$\vec{F}_B = (\nabla \vec{B}_A + \nabla \vec{B}_C + \nabla \vec{B}_D + \dots) \bullet \vec{\mu}_B \quad (4.22)$$

To ensure that any force can be generated, the sum of matrices in the parenthesis must be full rank. To be rank deficient, either all the matrices must have the same null space, or have a relationship that when summed, vectors in the basis are canceled out. Neither case is very probable since all the dipoles would have to be aligned in a very specific way.

Section 4.4 Solving the Equations of Motion (Two Satellites)**Section 4.4.1 Two Satellites in a Plane**

Before looking at the n satellite case, it is helpful to look at the simplified case of two satellites (A and B) in a plane. In this example we have chosen satellite A (left satellite) as the free dipole.

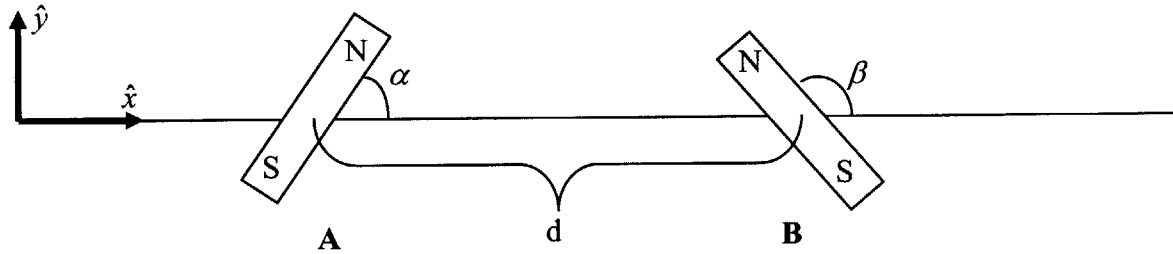


Figure 4-1: 2D Angle Representation of Two Dipoles

The EOM to solve is

$$\vec{F}_A(\vec{r}_A, \vec{r}_B, \vec{\mu}_A, \vec{\mu}_B) - \vec{f}_A = 0 \quad (4.23)$$

The magnetic dipoles are represented as bar magnets. In order to get a better intuitive feel, a ‘polar’ coordinate system is used where each dipole is defined by a magnitude and an angle from the \hat{x} axis.

$$\begin{aligned} \vec{\mu}_A &= (\mu_A \cos \alpha) \hat{x} + (\mu_A \sin \alpha) \hat{y} \\ \vec{\mu}_B &= (\mu_B \cos \beta) \hat{x} + (\mu_B \sin \beta) \hat{y} \\ \vec{r}_{AB} &= d \hat{x} \end{aligned} \quad (4.24)$$

Substituting equation (4.24) into equation (4.2) we are left with

$$\vec{F}_A = \frac{3}{4\pi} \frac{\mu_0 \mu_A \mu_B}{d^4} ((2 \cos \alpha \cos \beta - \sin \alpha \sin \beta) \hat{x} - (\cos \alpha \sin \beta + \sin \alpha \cos \beta) \hat{y}) \quad (4.25)$$

and the EOM (in component form) are now

$$\begin{aligned} \frac{3}{4\pi} \frac{\mu_0 \mu_A \mu_B}{d^4} (2 \cos \alpha \cos \beta - \sin \alpha \sin \beta) - f_{Ax} &= 0 \\ -\frac{3}{4\pi} \frac{\mu_0 \mu_A \mu_B}{d^4} (\cos \alpha \sin \beta + \sin \alpha \cos \beta) - f_{Ay} &= 0 \end{aligned} \quad (4.26)$$

These equations can be explicitly solved for $\vec{\mu}_B$. (Remember $\vec{\mu}_A$ is the free dipole and can be chosen at will. For simplicity, we can set $\alpha = 0^\circ$ and leave μ_A as a parameter.) Solving for μ_B, β , we get

$$\begin{aligned} \mu_B \mu_A &= \frac{2\pi}{3\mu_0} d^4 \sqrt{f_{Ax}^2 + 4f_{Ay}^2} \\ \beta &= -\text{sign}(f_{Ay}) \cos^{-1} \left(\frac{f_{Ax}}{\sqrt{f_{Ax}^2 + 4f_{Ay}^2}} \right) \end{aligned} \quad (4.27)$$

Equation (4.27) gives us the ability to directly calculate the magnetic dipole strength and direction for each satellite in the formation for any forcing profile. It should be noted that there is only one unique solution to this problem.

Example # 1 2D Example Formation

A good demonstrative example of using equation (4.27) is calculating the required magnetic dipole configuration to have two satellites, initially at rest, end up spinning about their overall center of mass. To simplify things, we make a small change in coordinate systems and allow the coordinate system to rotate with the formation.

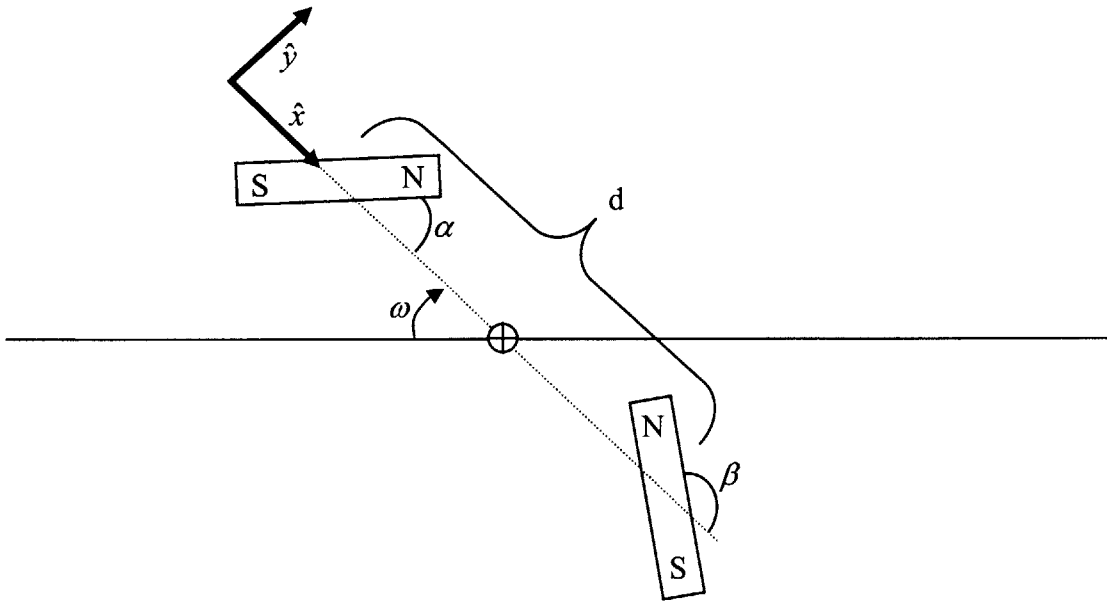


Figure 4-2: 2D Example with Rotating Coordinate System

The force in the \hat{x} direction is required to counteract the centrifugal acceleration due to the formation spinning. The force in the \hat{y} direction causes the formation to increase or decrease in angular rate. Once again, for simplicity the free dipole $\vec{\mu}_A$ will be chosen so that $\alpha = 0$. The required forces are

$$\begin{aligned} f_{Ax} &= m \omega^2 \frac{d}{2} \\ f_{Ay} &= m \dot{\omega} \frac{d}{2} \end{aligned} \tag{4.28}$$

where ω is the angular velocity of the formation.

Inserting equation (4.28) into equation (4.27), the following result is obtained

$$\begin{aligned} \mu_A \mu_B &= \frac{\pi}{3} \frac{m d^5 \sqrt{4\dot{\omega}^2 + \omega^4}}{\mu_0} \\ \beta &= -\text{sign}(\dot{\omega}) \cos^{-1} \left(\frac{\omega^2}{\sqrt{4\dot{\omega}^2 + \omega^4}} \right) \end{aligned} \tag{4.29}$$

Some insight that can be gained from (4.29) is that the product of the dipole strength is a function of d^5 . d^4 is due to the fact that the magnetic force falls off with this scaling, and the other d is due to the increase with distance in the required centripetal force.

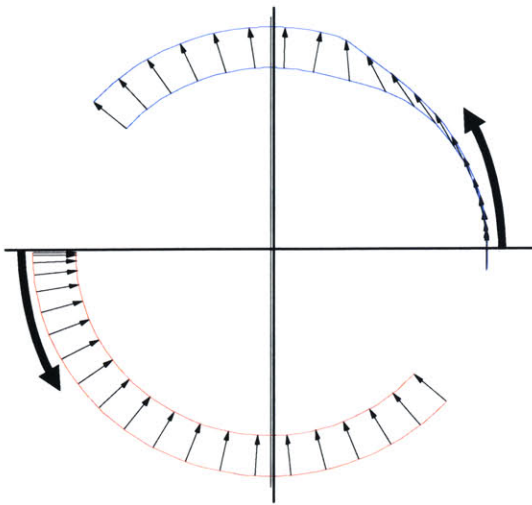


Figure 4-3: Two Satellite Spin-Up Example

Using equation (4.29), a simulation of two satellites “spinning up” was created and is shown in Figure 4-3. The arrows point in the direction of the magnetic dipole. Magnetic strength is not indicated.

Initially the satellites are at rest ($\omega = 0$) on the \hat{x} axis. Satellite A starts with $\alpha = 0^\circ$, and from equation (4.29) $\beta = 90^\circ$. As the formation begins to spin-up, the dipole on satellite B is rotated in order to provide a centrifugal force and hold the formation together. At the end of the spin-up phase ($\dot{\omega} = 0$) the dipoles are aligned radially, and only provide a centripetal force.

Section 4.4.2 Two Satellite's in Three Dimensions

For completeness, equation (4.25) is now calculated for 3D. Once again the dipoles are represented by bar magnets.

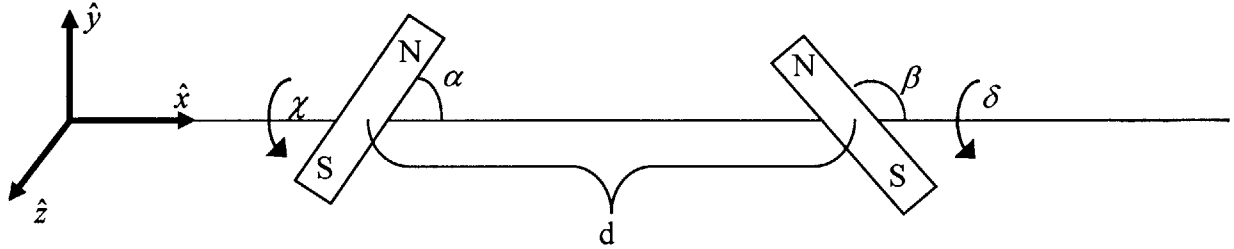


Figure 4-4: 3D Angle Representation of Two Dipoles

Angles χ and δ represent the rotation of the dipole about the \hat{x} axis of the dipoles on satellite A and B respectively. Equation (4.24) now becomes

$$\begin{aligned}\vec{\mu}_A &= (\mu_A \cos \alpha) \hat{x} + (\mu_A \sin \alpha \cos \chi) \hat{y} + (\mu_A \sin \alpha \sin \chi) \hat{z} \\ \vec{\mu}_B &= (\mu_B \cos \beta) \hat{x} + (\mu_B \sin \beta \cos \delta) \hat{y} + (\mu_B \sin \beta \sin \delta) \hat{z} \\ \vec{r}_{AB} &= d \hat{x}\end{aligned}\quad (4.30)$$

and equation (4.25) becomes

$$\begin{aligned}\vec{F}_A = \frac{3}{4\pi} \frac{\mu_0 \mu_A \mu_B}{d^4} & ((2 \cos \alpha \cos \beta - \cos(\delta - \chi) \sin \alpha \sin \beta) \hat{x} \\ & - (\cos \alpha \sin \beta \cos \delta + \sin \alpha \cos \beta \cos \chi) \hat{y} \\ & - (\cos \alpha \sin \beta \sin \delta + \sin \alpha \cos \beta \sin \chi) \hat{z})\end{aligned}\quad (4.31)$$

Just as in the 2D case, we can set one dipole at will and solve for the magnetic moment of the second dipole. The EOM are

$$\begin{aligned} \frac{3}{4\pi} \frac{\mu_0 \mu_A \mu_B}{d^4} (2 \cos \alpha \cos \beta - \cos(\delta - \chi) \sin \alpha \sin \beta) - f_{Ax} &= 0 \\ -\frac{3}{4\pi} \frac{\mu_0 \mu_A \mu_B}{d^4} (\cos \alpha \sin \beta \cos \delta + \sin \alpha \cos \beta \cos \chi) - f_{Ay} &= 0 \quad (4.32) \\ -\frac{3}{4\pi} \frac{\mu_0 \mu_A \mu_B}{d^4} (\cos \alpha \sin \beta \sin \delta + \sin \alpha \cos \beta \sin \chi) - f_{Az} &= 0 \end{aligned}$$

Setting the free dipole to $\alpha = 0^\circ$, avoids having a rank deficient gradient at satellite B's location. Solving for the magnitude and direction of satellite B results in

$$\begin{aligned} \mu_B &= \frac{2\pi}{3\mu_0} \frac{d^4}{\mu_A} \sqrt{f_{Ax}^2 + 4(f_{Ay}^2 + f_{Az}^2)} \\ \beta &= \cos^{-1} \left(\frac{f_{Ax}}{\sqrt{f_{Ax}^2 + 4(f_{Ay}^2 + f_{Az}^2)}} \right) \\ \delta &= \cos^{-1} \left(\frac{f_{Ay}}{\sqrt{(f_{Ay}^2 + f_{Az}^2)}} \right) \quad (4.33) \end{aligned}$$

Example # 2 3D Example

For this example, there will be two satellites rotating about their center of mass in a plane at an angular rate of ω_z . The plane of rotation will also rotate at a rate of ω_y . See Figure 4-5.

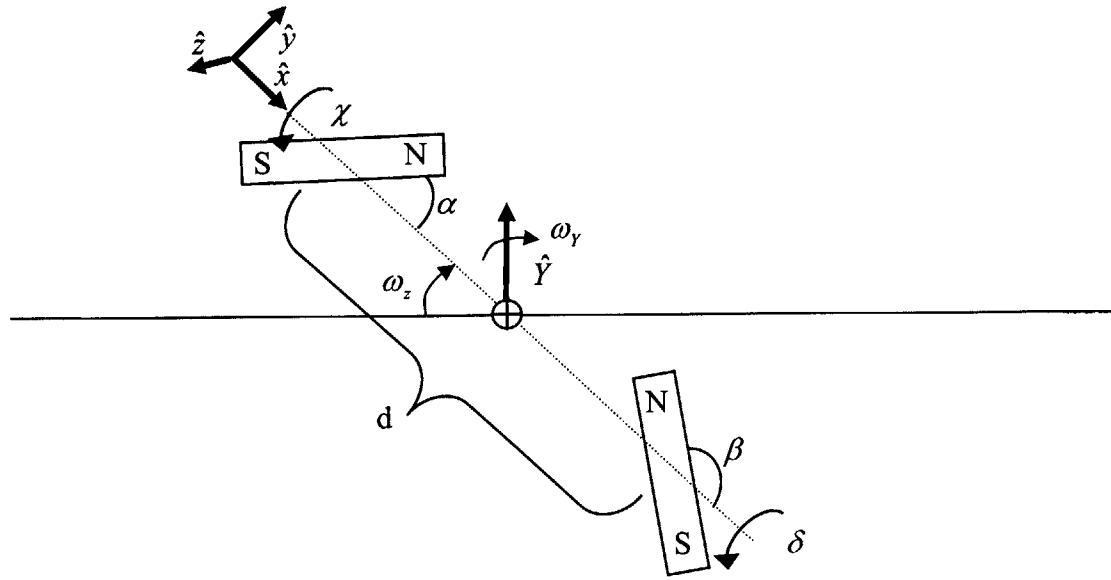


Figure 4-5: 3D Example with Rotating Coordinate System

For simplicity, the coordinate system (x, y, z) will rotate with the formation, with the x direction aligned with the axis connecting the two satellites, the z direction is normal to the plane of rotation, and the y direction completes the orthogonal triad. In the local (x, y, z) coordinate system, the forces are

$$\begin{aligned} f_{Ax} &= \frac{md}{2} \omega_z^2 \\ f_{Ay} &= 0 \\ f_{Az} &= \frac{md}{2} \omega_y \omega_z \cos(t \omega_z) \end{aligned} \tag{4.34}$$

Substituting equation (4.34) into equation (4.33) results in the solution for the dipole on satellite B.

$$\begin{aligned}\mu_B &= \frac{m\pi}{3\mu_0} \frac{\omega_z d^5}{\mu_A} \sqrt{\omega_z^2 + 4(\omega_Y^2 \cos(t\omega_z))} \\ \beta &= -\cos^{-1} \left(\frac{\omega_z}{\sqrt{\omega_z^2 + 4(\omega_Y^2 \cos(t\omega_z))}} \right) \\ \delta &= \frac{\pi}{2}\end{aligned}\quad (4.35)$$

Section 4.4.3 Conclusion (2 Satellite Case)

In this section, explicit solutions for the required magnetic dipole strengths and orientations were derived given a free dipole orientation. Any maneuver or force profile can be substituted into equation (4.33) to produce the required dipole solution. With two satellites, there is only one solution. In the next section, there will be multiple solutions, but they cannot be analytically solved as with the two satellite case.

Section 4.5 Solving Equations of Motion (N Satellite Case)

In the previous section, dipole strengths and angles were used to calculate the resulting magnetic forces. This convention of representing the dipoles as strengths and angles does not lend itself well to $n > 2$ satellites, because the coordinate system was selected to align with the \vec{r}_{AB} vector. Unless all the satellites are collinear, the magnetic forces will lie in different coordinate systems. This is less than ideal for any type of programming and solution determination. To remedy this problem, Cartesian dipole components will be used with a Cartesian coordinate system that remains inertially fixed. We will use the vector representation of the magnetic force, equation (4.2), to calculate the resulting forces. The equation is reproduced here for convenience

$$\vec{F}_{AB} = \frac{3\mu_0}{4\pi} \left(-\frac{\vec{\mu}_1 \cdot \vec{\mu}_2}{r_{AB}^5} \vec{r}_{AB} - \frac{\vec{\mu}_1 \cdot \vec{r}_{AB}}{r_{AB}^5} \vec{\mu}_2 - \frac{\vec{\mu}_2 \cdot \vec{r}_{AB}}{r_{AB}^5} \vec{\mu}_1 + 5 \frac{(\vec{\mu}_1 \cdot \vec{r}_{AB})(\vec{\mu}_2 \cdot \vec{r}_{AB})}{r_{AB}^7} \vec{r}_{AB} \right) \quad (4.36)$$

Section 4.5.1 Describing the EOM

Looking back again at equation (4.5) and (4.3)

$$\begin{aligned}\vec{F}_1(\vec{r}_1, \vec{r}_2, \dots, \vec{r}_n, \vec{\mu}_1, \vec{\mu}_2, \dots, \vec{\mu}_n) - \vec{f}_1 &= \vec{0} \\ \vec{F}_2(\vec{r}_1, \vec{r}_2, \dots, \vec{r}_n, \vec{\mu}_1, \vec{\mu}_2, \dots, \vec{\mu}_n) - \vec{f}_2 &= \vec{0} \\ \vdots \\ \vec{F}_{n-1}(\vec{r}_1, \vec{r}_2, \dots, \vec{r}_n, \vec{\mu}_1, \vec{\mu}_2, \dots, \vec{\mu}_n) - \vec{f}_{n-1} &= \vec{0}\end{aligned}$$

where

$$\vec{F}_j = \sum_{\substack{i=A,B,C\dots \\ i \neq j}} \vec{F}_{ji} \quad (4.37)$$

It can be seen that we are solving a system of equations where each equation is simply the total magnetic force on a specific satellite. The total magnetic force is just the sum of the magnetic forces generated between one satellite and every other satellite in the formation.

If we re-write equation(4.37), and consolidate the constants into the parameter C, we are left with

$$\vec{F}_j = \left\{ \begin{array}{l} \sum_{\substack{i=1 \\ i \neq j}}^n \sum_{k=x,y,z} \sum_{l=x,y,z} C_{ijkl1} \mu_{ik} \mu_{jl} \\ \sum_{\substack{i=1 \\ i \neq j}}^n \sum_{k=x,y,z} \sum_{l=x,y,z} C_{ijkl2} \mu_{ik} \mu_{jl} \\ \sum_{\substack{i=1 \\ i \neq j}}^n \sum_{k=x,y,z} \sum_{l=x,y,z} C_{ijkl3} \mu_{ik} \mu_{jl} \end{array} \right\} \quad (4.38)$$

where μ_{1x} is the x component of $\vec{\mu}_1$

Up until now we have used $\vec{\mu}_i$ to designate the magnetic dipole vector. When describing and solving the equations, it is more convenient to express the vectors as their components $\mu_{1x}, \mu_{1y}, \mu_{1z}$. However, it can become cumbersome and confusing to write the components with the “ Ix, Iy ” subscript. For simplicity, I instead choose to use

$$\{\mu_{1x}, \mu_{1y}, \mu_{1z}, \mu_{2x}, \mu_{2y}, \mu_{2z}, \dots, \mu_{nx}, \mu_{ny}, \mu_{nz}\} = \{m_1, m_2, m_3, m_4, m_5, m_6, \dots, m_{3n-2}, m_{3n-1}, m_{3n}\} \quad (4.39)$$

The same convention carries for \vec{F} and \vec{f} . (m_1, \dots, m_{3n} is an ordered list of all components of the dipoles and F_1, \dots, F_{3n} and f_1, \dots, f_{3n} are similarly ordered lists of the force components of the satellites.)

$$\begin{aligned} F_1(\vec{r}_1, \vec{r}_2, \dots, \vec{r}_n, m_1, m_2, \dots, m_{3n}) - f_1 &= 0 \\ F_2(\vec{r}_1, \vec{r}_2, \dots, \vec{r}_n, m_1, m_2, \dots, m_{3n}) - f_2 &= 0 \\ &\vdots \\ F_{3n-3}(\vec{r}_1, \vec{r}_2, \dots, \vec{r}_n, m_1, m_2, \dots, m_{3n}) - f_{3n-3} &= 0 \end{aligned} \quad (4.40)$$

Instead of there being $n-1$ vector equations, there are now $3(n-1)$ scalar equations.

Expanding out equation (4.40) and consolidating all constants we are left with

$$\begin{aligned} F_1 \sim F_2 \sim F_3 &= m_1(Cm_4 + Cm_5 + Cm_6 + Cm_7 + \dots + Cm_n) + \\ &\quad m_2(Cm_4 + Cm_5 + Cm_6 + Cm_7 + \dots + Cm_n) + \\ &\quad m_3(Cm_4 + Cm_5 + Cm_6 + Cm_7 + \dots + Cm_n) \\ F_4 \sim F_5 \sim F_6 &= m_4(Cm_1 + Cm_2 + Cm_3 + Cm_7 + \dots + Cm_n) + \\ &\quad m_5(Cm_1 + Cm_2 + Cm_3 + Cm_7 + \dots + Cm_n) + \\ &\quad m_6(Cm_1 + Cm_2 + Cm_3 + Cm_7 + \dots + Cm_n) \end{aligned} \quad (4.41)$$

where each C is a different constant, and $F_1 \sim F_2 \sim F_3$ means that the equations have the same form, just different C s.

From equation (4.41) it can be seen that we are essentially trying to solve a system of non-linear polynomial equations. In fact, the system is more specialized in that it can be described as a multivariate bilinear system of polynomial equations.

Section 4.6 Description and Simplification of Polynomial Equations

Solving systems of polynomial equations has been the focus of vast amounts of research that is active to this day. The ability to quickly solve large systems of polynomial equations has

applications in computer graphics, kinematics, and chemical equilibrium equations to name a few.

Section 4.6.1 Degree of a Polynomial System

The degree of a polynomial system is a good indicator of the complexity of the system. Much the same as the degree of a univariate polynomial equation gives the anticipated difficulty in finding a solution, the degree of a system of polynomial equations gives an indication of the difficulty in solving the system.

The degree of a polynomial system is given by³

$$d = \prod_{j=1}^n d_j \quad (4.42)$$

where d_j is the maximum degree of the monomials in each equation. For example consider the following system of two equations.

$$\begin{aligned} x^2 + yz + y^3 &\rightarrow d_1 = 3 \\ x^2yz + yz + y^3 &\rightarrow d_2 = 4 \\ d = d_1 d_2 &= 12 \end{aligned} \quad (4.43)$$

Looking now at the EOM for EMFF, from (4.41) we can see that for EMFF systems

$$d_j \leq 2 \quad (4.44)$$

If we define $\vec{\mu}_1$ as the free dipole (m_1, m_2, m_3 are constants), then the degree of F_1, F_2, F_3 is 1, and the remaining F have degree 2.

$$\begin{aligned} d_1 &= d_2 = d_3 = 1 \\ d_4 &= d_5 = \dots = d_{3n-3} = 2 \end{aligned} \quad (4.45)$$

If we assume a system of equations in the form of (4.40), where the last vector equation is removed, the overall degree of the system is

$$d = 2^{3(n-2)} \quad (4.46)$$

Very quickly we can see that the complexity of the system increases exponentially for each satellite added to the formation.

Section 4.6.2 Number of Solutions

The number of solutions for a system of n polynomial equations of n variables is given by Benzout Theorem.³ Each system of polynomial equations has a degree d as defined in equation (4.42). The Benzout Theorem states that if there are a finite number of non-infinite solutions and a finite number of solutions at infinity, then there are exactly d solutions (including solutions at infinity) including multiplicities.

Section 4.6.3 Solutions at Infinity

When solving systems of polynomial equations, if the system is not fully reduced, solutions at infinity can be present. Examine the following standard bivariate polynomial equation³

$$F(x, y) = ax^2 + bxy + cy^2 + dx + ey + f = 0 \quad (4.47)$$

if we let $x = rx$ and $y = ry$

$$F(rx, ry) = ar^2x^2 + br^2xy + cr^2y^2 + drx + ery + f = 0 \quad (4.48)$$

Dividing through by r^2

$$\frac{F(rx, ry)}{r^2} = (ax^2 + bxy + cy^2) + \frac{1}{r}(dx + ey) + \frac{1}{r^2}f = 0 \quad (4.49)$$

as r goes to infinity we are left with the “homogenous” component of F .

$$F_H(x, y) = (ax^2 + bxy + cy^2) = 0 \quad (4.50)$$

Any non-zero solutions x and y of (4.50) are considered “solutions at infinity” of (4.47). Also, any multiple of a solution at infinity is also a solution at infinity. (If x and y are a solution to (4.50), so is sx and sy).³

A systematic method of finding the solutions at infinity is to define F_i^H to be the “homogeneous” component of F_i . F_i^H can be found by

$$F_j^H(m_1, m_2, \dots, m_{3n}) = r^{d_j} F_j\left(\frac{m_1}{r}, \frac{m_2}{r}, \dots, \frac{m_{3n}}{r}\right) \text{ with } r = 0 \quad (4.51)$$

Solving for $\tilde{F}^H = 0$ will produce the solutions at infinity.

Section 4.6.3.1 Example 1 (Degree of Polynomial Systems/Solutions at Infinity)

A simple example of Benzout’s theorem and solutions at infinity is given by the following bivariate polynomial system

$$\begin{aligned} x^3 + x^2 + xy^2 + y^3 + 1 &= 0 \\ x^3 + xy^2 + y^3 &= 0 \end{aligned} \quad (4.52)$$

The degree of this system is $d = 9$. From Benzout’s theorem, there are exactly 9 solutions. Inputting equation (4.52) into a numeric equation solver only produces the following 6 solutions.

$$\begin{aligned} (\pm i, -0.79552 \pm 0.232786i) \\ (x, y) = (\pm i, \mp 1.46557i) \\ (\pm i, 0.79552 \pm 0.232786i) \end{aligned} \quad (4.53)$$

The remaining three solutions must lie at infinity. To determine the solutions at infinity, the homogenous system of equations is formed by removing lower degree terms. The resulting equations are

$$\begin{aligned} x^3 + xy^2 + y^3 &= 0 \\ x^3 + xy^2 + y^3 &= 0 \end{aligned} \quad (4.54)$$

These equations need not be identical, but are in this example to allow for a simple reduction step to be done in the next section. Solving equation (4.54) results in the following solutions at infinity.

$$\begin{aligned}y &= -1.46557x \\y &= (0.232786 \pm 0.792552i)x\end{aligned}\tag{4.55}$$

Adopting the convention of assigning the first term to have a value of 1, with the note that any multiple of the solution is also a solution at infinity, we are left with the following three solutions at infinity.

$$(x, y) = \begin{cases} (1, -1.46557) \\ (1, 0.232786 \pm 0.792552i) \end{cases}\tag{4.56}$$

Section 4.6.4 Reduction of the Solution³

Reduction is the simplification of the equations of motion with the goal of reducing the complexity and removal of redundant terms and variables. For a system of polynomial equations, one goal is to reduce the degree of the system. For example, let

$$\begin{aligned}G_1(\vec{x}) + G_2(\vec{x}) &= 0 \\G_2(\vec{x}) &= 0\end{aligned}\tag{4.57}$$

where the degree of G_1 is d_1 and the degree of G_2 is d_2 . If $d_2 > d_1$, then the total degree of the system is $d = d_2 * d_2$. Reducing the system, by subtracting the second equation from the first results in

$$\begin{aligned}G_1(\vec{x}) &= 0 \\G_2(\vec{x}) &= 0\end{aligned}\tag{4.58}$$

The degree of this system is now only $d = d_1 * d_2$. The system has $(d_2 - d_1)d_2$ fewer solutions, even though the equations of motion are algebraically the same. The solutions that are removed are solutions at infinity, and therefore reduction does not reduce the number of finite solutions.

Example # 3 Example 1 Continued

Continuing with our example system of polynomial equations, we know that the equations have the possibility of being reduced since there are solutions at infinity. Equation (4.52) can be reduced to the following system of equations

$$\begin{aligned}x^2 + 1 &= 0 \\x^3 + xy^2 + y^3 &= 0\end{aligned}\tag{4.59}$$

The degree of this system is now only 6. Solving this system, we find that we have the same finite solutions as the original system. This is expected as reducing the system does not change the finite solutions to the system. Since the degree of the system is only 6, and we have 6 finite solutions we know that they system is completely reduced, generic, and has no solutions at infinity. For completeness, we will attempt to find the solutions at infinity. Creating the homogenous system from the reduced set of equations we have

$$\begin{aligned}x^2 &= 0 \\x^3 + xy^2 + y^3 &= 0\end{aligned}\tag{4.60}$$

The only solution is $(x, y) = (0, 0)$. Since there are no non-zero solutions, there are no solutions at infinity.

Section 4.6.5 Systematic Reduction of Polynomial Equations³

A systematic way of reducing the system is similar to row reduction for linear systems. A matrix with the coefficients of each monomial is created. Each monomial is associated with a column of matrix. The columns should be ordered with higher terms to the left so that when the matrix is reduced, the number of higher order terms is reduced. A Gaussian elimination is preformed on the matrix. The reduced matrix is then converted back into equational form, hopefully with a smaller degree. This is probably better illustrated with an example. Let's begin with a system of polynomial equations of degree 9.

$$\begin{aligned} F_1(x, y) &= y^3 - 4x^3 + 3y + 3xy^2 + 2x^2 + 1 = 0 \\ F_2(x, y) &= 2y^3 - 8x^3 + 6xy^2 + y + 2 = 0 \end{aligned} \quad (4.61)$$

Place the coefficients into the matrix as shown.

$$\begin{array}{ccccccc} & y^3 & xy^2 & x^3 & x^2 & y & 1 \\ F_1 & \rightarrow & \begin{pmatrix} 1 & 3 & -4 & 2 & 3 & 1 \end{pmatrix} \\ F_2 & \rightarrow & \begin{pmatrix} 2 & 6 & -8 & 0 & 1 & 2 \end{pmatrix} \end{array} \quad (4.62)$$

Gaussian elimination is used to place the matrix into reduced row echelon form.

$$\begin{array}{ccccccc} & y^3 & xy^2 & x^3 & x^2 & y & 1 \\ F_1 & \rightarrow & \begin{pmatrix} 1 & 3 & -4 & 0 & 0.5 & 1 \end{pmatrix} \\ F_2 & \rightarrow & \begin{pmatrix} 0 & 0 & 0 & 1 & 1.25 & 0 \end{pmatrix} \end{array} \quad (4.63)$$

Looking at the resulting reduced matrix, zeros appeared in the columns for all the degree 3 terms in the second row. The second equation is now only degree 2. The resulting reduced equations are

$$\begin{aligned} F_1^R(x, y) &= y^3 + 3xy^2 - 4x^3 + 0.5y + 1 = 0 \\ F_2^R(x, y) &= x^2 + 1.25y = 0 \end{aligned} \quad (4.64)$$

This reduced system has degree 6. The missing solutions all lay at infinity.

Section 4.6.6 Application of the Systematic Reduction Method to the EMFF EOM

Earlier, we discussed the fact that the equations of motion (4.1) are dependent. In other words they are not sufficiently reduced. We reduced the equations by stating that the sum of the forces is zero, and thus we removed three of the equations. As stated earlier, we should choose to remove equations with a higher degree (Those that didn't directly contain the free dipole).

The reduction method described above can be used to systematically accomplish the same goal. For this example, we assume that there are four satellites, and that the free dipole is on satellite 1. We order the columns of the reduction matrix such that the terms containing the dipole on

satellite 1 are in the right most columns. The constants are entered into the matrix. For simplification, C_i is a 3×9 matrix of coefficients relating the components of one magnetic dipole to another as indicated by $\vec{\mu}_i \vec{\mu}_j$ at the top of the column.

$$\begin{array}{l} \vec{F}_1 \rightarrow \begin{pmatrix} \vec{\mu}_3 \vec{\mu}_4 & \vec{\mu}_2 \vec{\mu}_4 & \vec{\mu}_2 \vec{\mu}_3 & \vec{\mu}_1 \vec{\mu}_4 & \vec{\mu}_1 \vec{\mu}_3 & \vec{\mu}_1 \vec{\mu}_2 \\ 0 & 0 & 0 & C_4 & C_5 & C_6 \end{pmatrix} \\ \vec{F}_2 \rightarrow \begin{pmatrix} 0 & C_2 & C_3 & 0 & 0 & -C_6 \\ 0 & C_2 & C_3 & 0 & 0 & -C_6 \end{pmatrix} \\ \vec{F}_3 \rightarrow \begin{pmatrix} C_1 & 0 & -C_3 & 0 & -C_5 & 0 \\ C_1 & 0 & -C_3 & 0 & -C_5 & 0 \end{pmatrix} \\ \vec{F}_4 \rightarrow \begin{pmatrix} -C_1 & -C_2 & 0 & -C_4 & 0 & 0 \end{pmatrix} \end{array} \quad (4.65)$$

Performing the reduction we are left with the following matrix.

$$\begin{array}{l} \vec{F}_1 \rightarrow \begin{pmatrix} \vec{\mu}_3 \vec{\mu}_4 & \vec{\mu}_2 \vec{\mu}_4 & \vec{\mu}_2 \vec{\mu}_3 & \vec{\mu}_1 \vec{\mu}_4 & \vec{\mu}_1 \vec{\mu}_3 & \vec{\mu}_1 \vec{\mu}_2 \\ C_1 & 0 & -C_3 & 0 & -C_5 & 0 \end{pmatrix} \\ \vec{F}_2 \rightarrow \begin{pmatrix} 0 & C_2 & C_3 & 0 & 0 & -C_6 \\ 0 & C_2 & C_3 & 0 & 0 & -C_6 \end{pmatrix} \\ \vec{F}_3 \rightarrow \begin{pmatrix} 0 & 0 & 0 & C_4 & C_5 & C_6 \\ 0 & 0 & 0 & 0 & 0 & 0 \end{pmatrix} \\ \vec{F}_4 \rightarrow \begin{pmatrix} 0 & 0 & 0 & 0 & 0 & 0 \end{pmatrix} \end{array} \quad (4.66)$$

As expected, the number of equations has been reduced by 3. Also, because the three right columns only have degree 1, we have also ensured that one of the vector equations, \vec{F}_3 , is of degree 1.

MATHEMATICA CODE: ReduceEquations[equation,<variables>]

File: Master EMFF Notebook.nb

Section: Continuation Notebook

Usage: ReduceEquations[equations,<variables>]={reduced_equations}

equations – A list of equations. (See equation (4.61))

The equation can either be a function (no equal sign) or an equation (with an equal sign).

There can be no other variables in the equation.

<variables> -- An optional list of variables.

The default is $\{x[1], x[2], \dots, x[n]\}$.

reduced_equations – A list of reduced equations.

The equations are either functions or equations depending on the input form.

Section 4.6.7 Scaling the Equations³

Scaling refers to the changing of variables and equations themselves so that the variables, and constants are of similar order of magnitude. If there are varying orders of magnitude in the equations, numeric solvers can have significant errors. Scaling doesn't affect the final solution of the problem, it is just a change of variable before the solution step, and then a change of variables back to the original.

Example # 4 Scaling Introduction³

One aspect of scaling is the scaling of the equation as a whole so that the constants in front of the variables are centered around unity. For example:

$$2*10^{10}x^2 + 3*10^{10}x + 10^{10} = 0 \quad (4.67)$$

It makes much more sense to multiply both sides of the equation by 10^{-10} , and instead solve the following equation.

$$2x^2 + 3x + 1 = 0 \quad (4.68)$$

The other aspect of scaling is to scale the individual variables within the equation. For example:

$$2*10^{10}x + 3*10^{-10}y + 3 = 0 \quad (4.69)$$

we could make a change of variables with

$$\begin{aligned} x' &= 10^{10}x \\ y' &= 10^{-10}y \end{aligned} \quad (4.70)$$

and instead solve the following equation.

$$2x' + 3y' + 3 = 0 \quad (4.71)$$

x and y are recovered by solving the inverse of equation (4.70).

Section 4.6.7.2 Systematic Approach

The following approach is based off of Morgan³, and has been implemented in Mathematica. Assume that we have a set of equations based on the variables x_k .

$$\vec{f}_j(x_1, \dots, x_n) = 0 \quad (4.72)$$

The first step is to make a change of variables with

$$x_k = 10^{s_k} z_k \quad (4.73)$$

where s is a vector of scaling values. Each equation is also scaled by

$$10^{v_j} f_j(\vec{x}) = 0 \quad (4.74)$$

Therefore we are now solving the following equation

$$\begin{aligned} 10^{v_i} f_i(10^{s_1} z_1, \dots, 10^{s_k} z_k) &= 0 \\ f'_i(z_1, \dots, z_k) &= 0 \end{aligned} \quad (4.75)$$

If each term in the unscaled equation is given by

$$a_{ij} x_1^{d_{1ij}} x_2^{d_{2ij}} \dots x_n^{d_{nij}} \quad (4.76)$$

where a_{ij} is the coefficient of the i th term in the j th equation, and $d_{l_{ij}}$ is the degree of each variable in that term, then the scaled term is given by

$$10^{v_j} a_{ij} (10^{s_1} z_1)^{d_{1ij}} (10^{s_2} z_2)^{d_{2ij}} \dots (10^{s_n} z_n)^{d_{nij}} \quad (4.77)$$

which can be written more succinctly as

$$\exp_{10}(v_j + \sum_{k=1}^n s_k d_{kij}) a_{ij} \prod_{k=1}^n z_k^{d_{kij}} \quad (4.78)$$

The goal is to now pick the values for s and v so that the scaled EOM is numerically well behaved. Once the new equations have been solved, we can obtain the initial solutions by applying the scaling used in equation (4.73).

To find the appropriate scaling values, a least squares method is used. We want to minimize the deviation from unity of the constants in front of the variables, and we want to minimize the difference between the constants. To accomplish the first task, we notice that if each term as in equation (4.78) is written of the form

$$10^{c_{ij}} z_1 z_2 \dots z_n \quad (4.79)$$

where

$$c_{ij} = v_j + \sum_{k=1}^n s_k d_{kij} + \log_{10}(|a_{ij}|) \quad (4.80)$$

then to minimize the deviations from unity, we must just minimize

$$J_1 = \sum_{j=1}^n \sum_{i=1}^{l_j} c_{ij}^2 \quad (4.81)$$

where l_j is the number of terms in equation j .

To minimize the variation in the constants, we minimize the square of the differences between the constants in each equation. This is accomplished by minimizing

$$J_2 = \sum_{j=1}^n \sum_{1 \leq i \leq m \leq l_j} b_{ijm}^2 \quad (4.82)$$

where l_j is the number of terms in equation j . b_{ijm} can be written as

$$b_{ijm} = c_{ij} - c_{mj} \quad (4.83)$$

In order to have one objective function, the two objective functions are combined.

$$J \equiv J_1 + J_2 \quad (4.84)$$

which is just a quadratic function in v and s and can be solved in a straightforward manner.

MATHEMATICA CODE: `ScaleEquation[equations, <variables>]`

File: `Master EMFF Notebook.nb`

Section: `Continuation Notebook`

Usage: `ScaleEquation[equations, <variables>] = {scaled_equation, variable_gains}`

equations – A list of equations. (See equation (4.72))

The equation can either be a function (no equal sign) or an equation (with an equal sign).

The number of equations must equal the number of variables

There can be no other variables in the equation

<variables> -- An optional list of variables

The default is {x[1],x[2],...,x[n]}

scaled_equations – A list of scaled equations. (See equation (4.75))

The equations are either functions or equations depending on the input form.

variable_gains – A list of gains. (See equation (4.73)).

The unscaled values can be obtained by multiplying the scaled solution by $10^{\text{variable_gains}}$.

Section 4.6.8 Singular Solutions

Section 4.6.8.1 Single Variable Equations

For single variable equations, a solution is said to be singular when the equation and the derivative of the equation are both equal to zero. m is a singular point if

$$\begin{aligned} F(m) &= 0 \\ \frac{dF(m)}{dm} &= 0 \end{aligned} \tag{4.85}$$

Example # 5 Singularity Example

For example if

$$\begin{aligned} g(x) &= x^2 - 2x + 1 \\ \frac{dg(x)}{dx} &= 2x - 2 \end{aligned} \tag{4.86}$$

then $x=1$ is a singular solution to the problem. At this point, the solution has multiplicity of two because there are essentially two merged solutions at $x=1$. This can be seen if we vary the parameters of the equation slightly. If

$$\begin{aligned} x^2 - 1.99x + 1 = 0 &\longrightarrow x = (0.995 + 0.0999i, 0.995 - 0.0999i) \\ x^2 - 2x + 1 = 0 &\longrightarrow x = (1, 1) \\ x^2 - 2.01x + 1 = 0 &\longrightarrow x = (1.11, 0.905) \end{aligned} \tag{4.87}$$

Because of this, we can say that the solution transitions from imaginary to real at the singularity. This concept is useful later in this chapter.

Section 4.6.8.2 Multiple Variables

If there is more than one variable and more than one equation, then the requirement for a point to be singular is that the equation and the determinant of the Jacobian must be zero. The Jacobian is defined by

$$J(m_1, m_2, \dots, m_n) = \begin{pmatrix} \frac{\partial F_1}{\partial m_1} & \frac{\partial F_1}{\partial m_2} & \dots & \frac{\partial F_1}{\partial m_n} \\ \frac{\partial F_2}{\partial m_1} & \frac{\partial F_2}{\partial m_2} & & \vdots \\ \vdots & & \ddots & \\ \frac{\partial F_n}{\partial m_1} & \dots & & \frac{\partial F_n}{\partial m_n} \end{pmatrix} \quad (4.88)$$

If we represent the polynomials as geometric curves or shapes, a singular solution is one where the tangents to the curves coincide. In other words the curves are barely touching but do not completely intersect. It also marks the region where a solution transitions from being real to imaginary. A solution is singular iff it has a multiplicity of two or more.

For example

$$\begin{aligned} -x^4 + 2x^2 - y &= 0 \\ x^2 + (y - c)^2 - 1 &= 0 \end{aligned} \quad (4.89)$$

when $c = 1.05$ there are four real solutions with the associated determinant of the Jacobian

$$\begin{aligned} (x, y) &= (\pm 0.185, 0.0672) & \det(J) &= \mp 1.034 \\ (x, y) &= (\pm 0.999, 0.998) & \det(J) &= \pm 1.997 \end{aligned} \quad (4.90)$$

when $c = 1$, the solutions ‘merge’ together at the origin and the solution $(0, 0)$ has multiplicity 2.

The determinant of the jacobian is also zero at this point. With $c < 1$, the solutions and the Jacobian become imaginary.

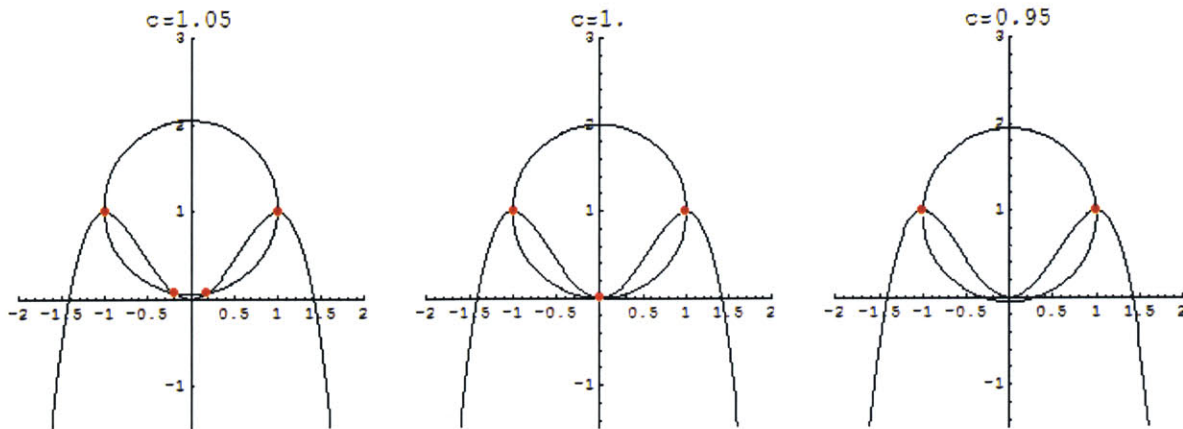


Figure 4-6: Intersection of Two Curves at a Singularity

We can see when a solution is approaching a singularity (when varying c) by tracking the Jacobian determinant. If the determinant approaches zero, then we know that the solution is becoming singular. However, this method is dependent on the scaling of the matrix. Instead of using the determinant to determine how close to singularity the matrix is, we can use the matrix condition where the norm is any matrix norm.

$$C(J) \equiv \|J\| \|J^{-1}\| \quad (4.91)$$

One simple and efficient method of determining the condition of the matrix is to use the singular value decomposition (SVD) of the matrix.

$$J = UDV^{-1} \quad (4.92)$$

where D is a diagonal matrix. The condition matrix is

$$C(J) \equiv \frac{\max D_i}{\min D_i} \quad (4.93)$$

Now when there is a singular solution, the condition matrix is equal to infinity. The condition matrix is useful because it always produces a real number and is unaffected by scaling. Continuing our example we see that the condition of the matrix for the solutions that are singular

at $c=1$, approaches infinity at that point while the condition of the other solutions remain around 2.

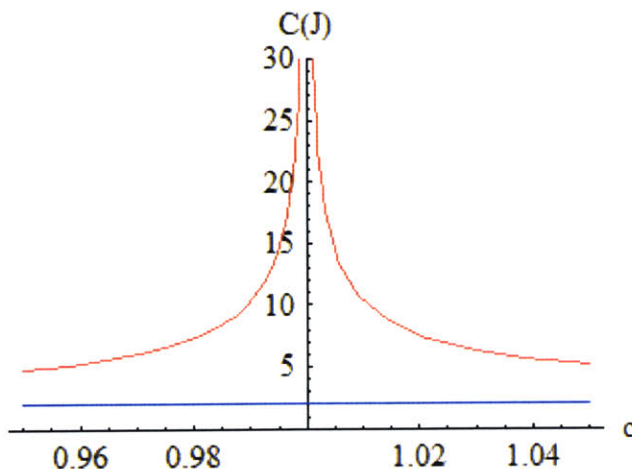


Figure 4-7: Condition of the Jacobian Matrix

MATHEMATICA CODE: `MatrixCondition [matrix]`

Description: Determine the condition of a matrix.

File: Master EMFF Notebook.nb

Section: Initialization Code

Usage: `MC[matrix] = condition`

matrix – A numerical square matrix.

condition – A scalar representing the condition of the matrix. See equation (4.93)

Section 4.7 Solving Polynomial Equations Using Continuation Methods

Section 4.7.1 Introduction

Newton's Method is designed to find a local solution to a system of non-linear equations given an initial guess. As long as the initial guess is sufficiently close to the final solution, then Newton's Method will typically converge to the solution. However, from Bezout's theorem, we

know that there are multiple solutions to the system of equations. Some solutions may be more “desirable” than other solutions. Using Newton’s method, one would have to randomly search out the space in the hopes of finding each solution. Due to solutions at infinity and singularities, one would never know if all possible solutions had been found. What is discussed next is a systematic method for finding all solutions to polynomial equations.

The continuation method (A.K.A. homotopy) is explained very well in Morgan’s book³, “Solving Polynomial Systems Using Continuation for Engineering and Scientific Problems”. The following section will briefly review continuation methods, since the background is helpful to explain the modifications used in solving the EMFF EOM.

Section 4.7.2 Overview

Continuation methods use the idea of taking an equation that is difficult to solve and changing it to a simple equation to solve. This new equation is then slowly (discretely) changed back to the original equation. At each step of converting the new equation to the original equation, the equation is re-solved using Newton’s Method. Since at each step, the equation is very similar to the previous step, the solutions are also very close to the previous step. This situation is perfect for Newton’s Method since the solutions at the previous step are used as the initial guess. Eventually, the equation begins to resemble the initial equation we were trying to solve, and we have the solutions to the initial equation.

Example # 6 Continuation Method

Probably the best way to explain continuation methods is to provide an example. Starting with a simple quadratic equation

$$x^2 + 3x - 3 = 0 \quad (4.94)$$

The equation has two real solutions

$$\begin{aligned} x &= -3.79129 \\ x &= 0.791288 \end{aligned} \quad (4.95)$$

While equation (4.94) can be solved using the quadratic formula, we instead use the continuation method and assume that equation (4.94) is not easily solvable.

The first step is to reduce the equation into a more simple equation.

$$x^2 - 3 = 0 \quad (4.96)$$

which can be directly solved.

$$x = \pm\sqrt{3} \quad (4.97)$$

We must now create an equation that will slowly change from the simple equation (4.96), to the initial equation (4.94). This is accomplished by the introduction of the parameter δ and the equation

$$x^2 + 3\delta x - 3 = 0 \quad (4.98)$$

When $\delta = 0$, equation (4.98) is equal to equation (4.96). When $\delta = 1$, equation (4.98) is equivalent to equation (4.94). The next step is to slowly vary δ from 0 to 1 and solve for x at each step by using Newton's Method. The following table shows the progression of the solutions as δ varies from 0 to 1 at a step of 0.1.

Table 1: Solutions to Equation (4.98)

δ	x_1	x_2
0	1.7321	-1.7321
0.1	1.5885	-1.8885
0.2	1.4578	-2.0528
0.3	1.3396	-2.2396
0.4	1.2330	-2.4330
0.5	1.1375	-2.6375
0.6	1.0519	-2.8519
0.7	0.9755	-3.0755
0.8	0.9071	-3.3075
0.9	0.8460	-3.5460
1.0	0.7913	-3.7913

When $\delta = 1$, we have recovered the original solutions to (4.94).

This can also be seen graphically in Figure 4-8 where the solution paths from the simplified equations to the original equations are shown.

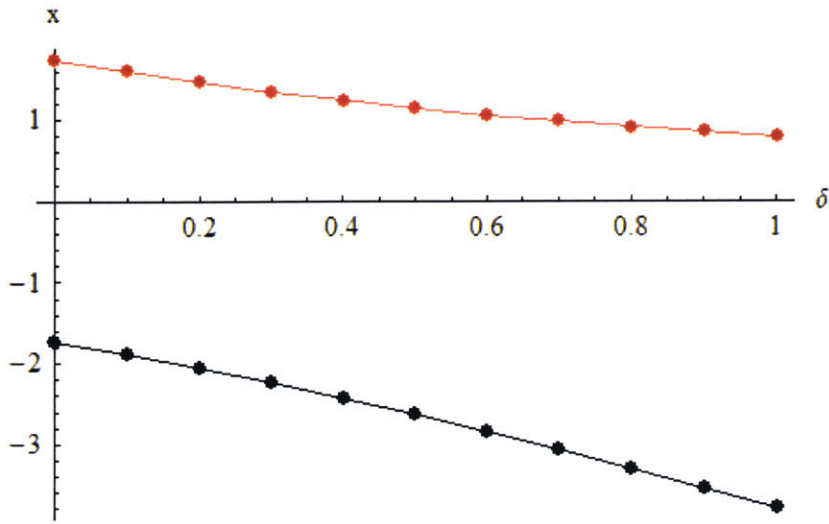


Figure 4-8: Continuation Path for Equation (4.98)

This was a simple example to the continuation method. Before describing the general method and how it is applied to the EMFF EOM, it is instructive to go over the pitfalls and difficulties that the general method must overcome.

Section 4.7.3 Solution Paths

It is helpful to graphically represent the solutions to the equations as δ varies. The solutions, except for the single variable, real solution case, have a dimension that is greater than one, and is difficult to represent graphically. Whether or not the paths cross and remain bounded is important.

Example # 7 Path Crossing

In the previous example, the two solutions were never equal at any δ . Their paths did not cross. However, let's try another innocent looking quadratic equation.

$$x^2 + 5x + 4 = 0 \quad (4.99)$$

The equation has solutions of

$$x = \{-1, -4\} \quad (4.100)$$

The continuation equation is

$$x^2 + \delta(5x) + 4 = 0 \quad (4.101)$$

The running solution is

Table 2: Solution to Equation (4.101)

δ	x_1	x_2
0	$2i$	$-2i$
0.1	$-0.25+1.984i$	$-0.25-1.984i$
0.2	$-0.5+1.936i$	$-0.5-1.936i$
0.3	$-0.75+1.854i$	$-0.75-1.854i$
0.4	$-1+1.732i$	$-1-1.732i$
0.5	$-1.25+1.561i$	$-1.25-1.561i$
0.6	$-1.5+1.323i$	$-1.5-1.323i$
0.7	$-1.75+0.968i$	$-1.75-0.968i$
0.8	-2	-2
0.9	-1.219	-1.219
1.0	-1	-1

At $\delta = 0.8$, the solution paths cross. Having solution paths cross is a problem for two reasons. First, at $\delta = 0.8 + \Delta\delta$, Newton's method is seeded with the same initial conditions for both paths $x(0.8) = -2$. Because Newton's method is seeded with the same initial conditions, it will produce the same results. One of the solution paths after the intersection will be lost.

Second, when the solution paths cross, they are crossing at a singular solution to the continuation equation. Newton's Method does not guarantee quadratic convergence at singular points, and in general does not behave well. Since we are using real coefficients, it should be noted that when a singular point is reached, (except for very specific cases), the solution passes from the real to the

complex plane, and vice versa. The converse is also true, if a solution path switches from a real to a complex solution or vice versa, then it must happen through a singular point.

Since we are only looking at solutions of one variable, we can actually plot the solution path. The following plot is the solution path in the complex plane.

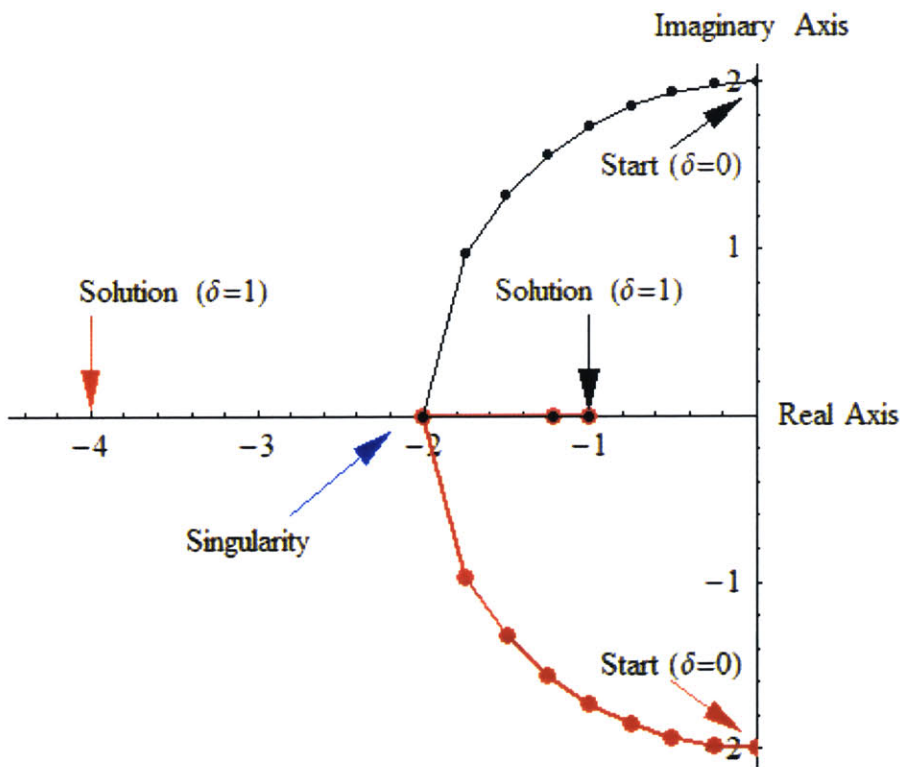


Figure 4-9: Solution Path for Equation (4.101)

From the graph, we can see that the two paths intersect at the singularity. At that time, Newton's method doesn't have two distinct starting points, and both solutions end up on the same path.

Section 4.7.3.2 Independence and Singularities

One method of dealing with singular points is to choose a continuation equation that does not contain any singularities (except at $\delta=1$ if the solution to the original equation contains

singularities). An equation of one variable has a singularity when it and the first derivative are equal to zero. For a quadratic continuation equation in the form of

$$x^2 + \delta bx + c = 0 \quad (4.102)$$

the first derivative is

$$2x + \delta b = 0 \quad (4.103)$$

Solving both equations for δ

$$\begin{aligned} \delta &= \pm \frac{2\sqrt{c}}{b} \\ x &= \mp \sqrt{c} \end{aligned} \quad (4.104)$$

Since we constrain $0 \leq \delta \leq 1$, for both the equation and the first derivative to be zero at some point, the following condition must hold.

$$0 \leq \left| \frac{2\sqrt{c}}{b} \right| < 1 \quad (4.105)$$

Note, singularities are allowed at $\delta = 1$ since the continuation method cannot remove singularities in the final equation. When the above condition is true, then the solutions paths cross.

To remove this problem, we can instead try a different continuation equation.

$$x^2 + \delta bx + \delta c - (1-\delta)q^2 = 0 \quad (4.106)$$

with a first derivative of

$$2x + \delta b = 0 \quad (4.107)$$

There is a singular point when

$$-q^2(1-\delta) + c\delta - \frac{b^2\delta^2}{4} = 0 \quad (4.108)$$

Since equation (4.108) is quadratic in δ , we know that there are two possible δ s that satisfy the equations. All we must do is find q such that equation (4.108) is not satisfied for $0 \leq \delta < 1$. If we know b and c , it is straightforward to find an appropriate q . However, it is possible to find a generic q that almost always prevents equation (4.108) from being satisfied when $0 \leq \delta < 1$. If we make q an imaginary number, then the δ that satisfies (4.108) will also be an imaginary number unless q,a,b are in a very specific relationship. As long as we pick q randomly, the chances that q,a,b are in the required specific relation is quite small, and thus equation (4.108) cannot be generally satisfied with a real δ .

Another way of looking at this is to fix δ at some point between zero and one. Since we have already chosen the other constants we have two equations ((4.106) and (4.107)) of one variable that must be identically satisfied. The only way this could happen is if the equations were dependent on each other. However, we have chosen q independently from the other constants. Therefore unless we choose the unique number out of an infinite set of numbers, the equations will not identically solve, and there will be no singular point.

For a more thorough explanation, the reader is referred to Morgan's book³.

Continuing with our previous example, let's randomly pick a value for q .

$$q = .15235 + 1.98546i \quad (4.109)$$

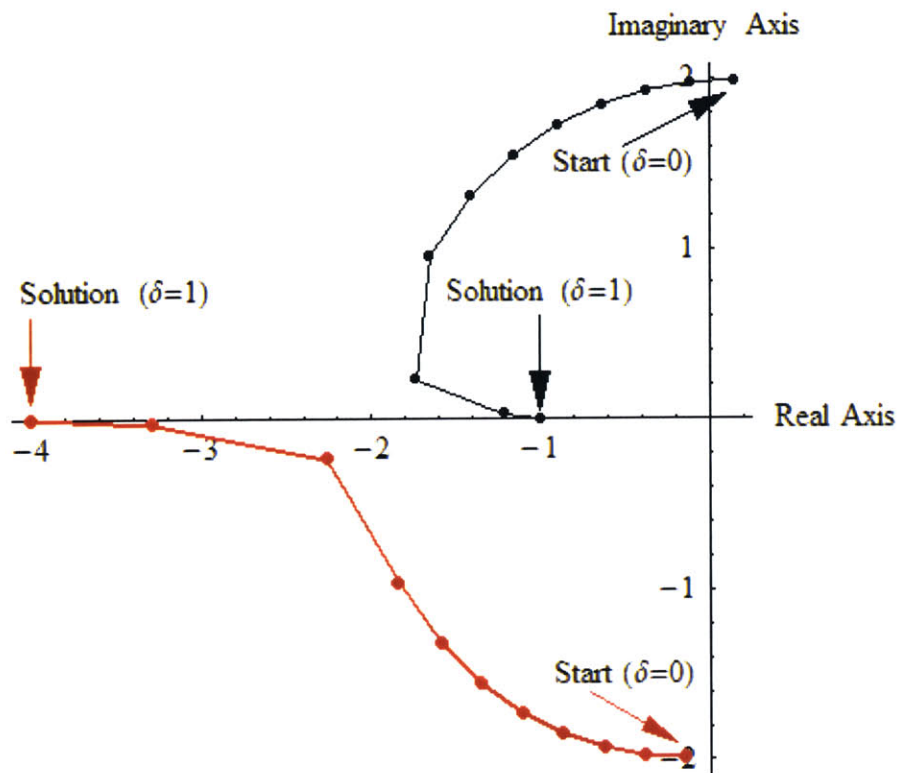


Figure 4-10: Solution Path for Equation (4.106)

As we can see from the plot, the solution paths do not intersect and both solutions are found. This is a good place to point out that the size of q has an influence on the path shape. If q is very small, then the equations can be nearly dependent, and the solutions pass near each other but don't cross. If the paths come too close together, the solution from Newton's method can jump from one path to another. The plot on the left of Figure 4-11 shows that the solutions come very close to each other near the old singular point. If we make q too large (as seen on the plot on the right side of Figure 4-11), then the initial solutions are very far away from the final solutions. The solution must change significantly as δ varies from zero to one. This also can cause problems since if the jump from one step to the next is too large, the solution can also jump paths.

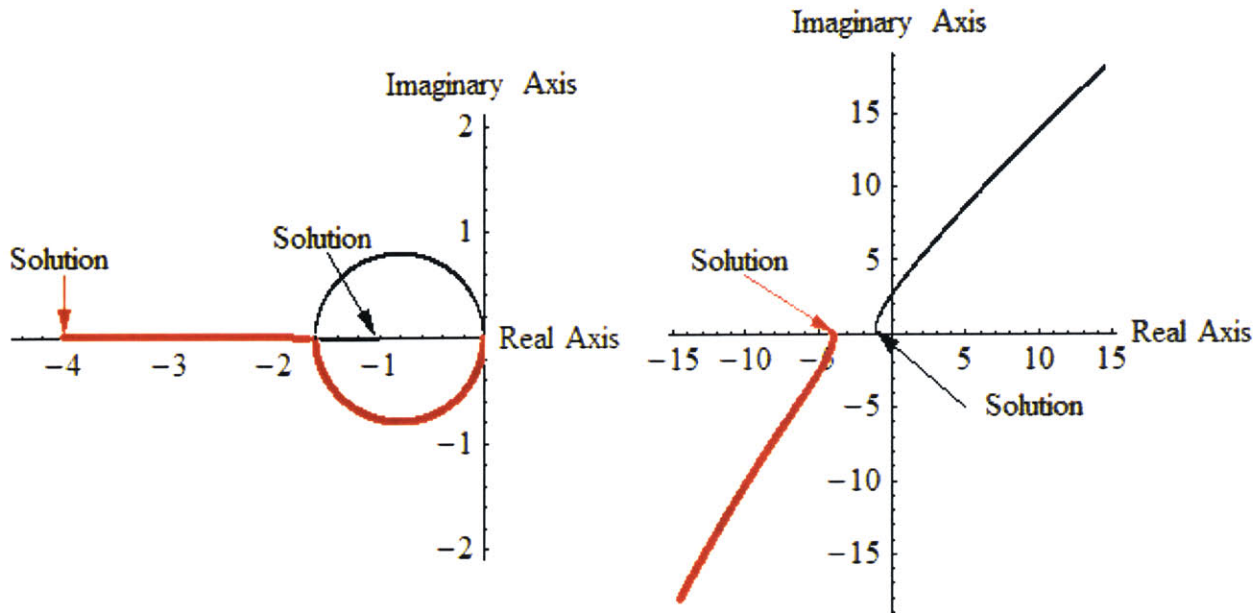


Figure 4-11: Solution Paths for varying q . Left -- Small q . Right -- Large q .

From these examples, a good rule of thumb is to choose q to be of the same order as the constants in the equations. As long as we have appropriately scaled the equations (as described in the previous sections), the constants should be close to unity. Therefore, the magnitude of q should be close to unity.

Example # 8 Path Jumping

As long as the initial guess is sufficiently close to the solution, Newton's method will find the solution. Problems arise when two different paths have similar solutions. If there are two solutions near each other, and the guess isn't sufficiently close, Newton's method could just as easily find one or the other solution. In the continuation method, this is called path crossing. If $\Delta\delta$ is not sufficiently small, then the next solution can be far away from the initial guess. If there is another path nearby, Newton's method may find the wrong solution. If we re-run the

scenario in Figure 4-10, with $\Delta\delta = 0.125$, then the red solution path jumps to the black solution path. To avoid this problem, the $\Delta\delta$ must be kept sufficiently small.

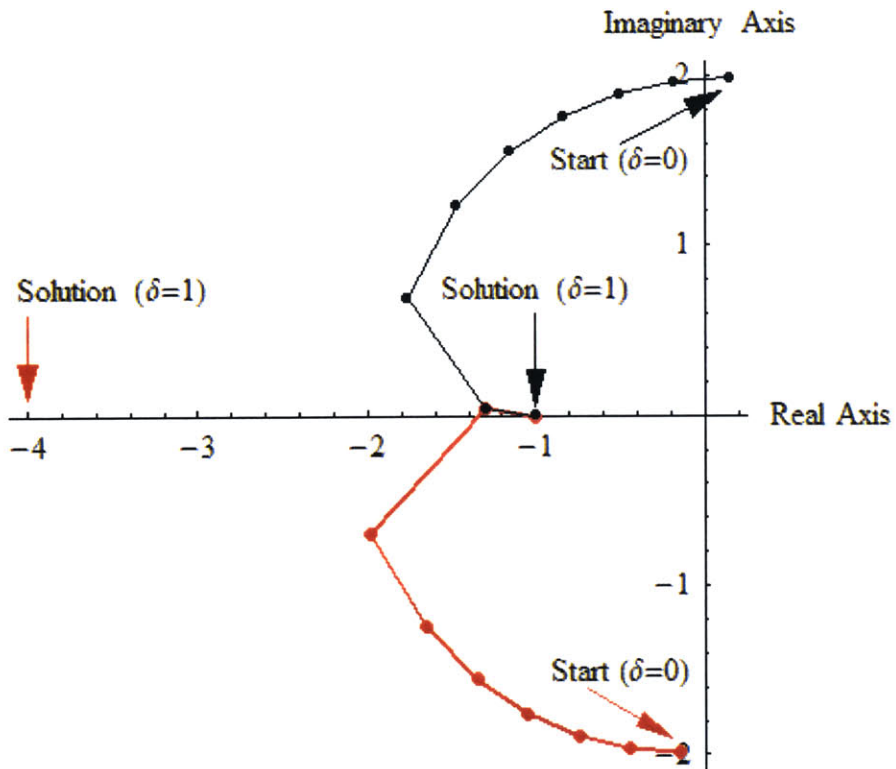


Figure 4-12: Example of Path Jumping Due to Large $\Delta\delta$

Section 4.7.4 Solutions at Infinity

The final obstacle to overcome is “solutions at infinity”. Even though we may have attempted to reduce the system as much as possible, we may not have completely done so. Therefore, there may be some solutions that remain at infinity. If a system has n solutions, (some of which lie at infinity), and we start with n finite points, some paths must diverge to infinity.

Diverging solutions are a problem because the numeric solvers can get bogged down chasing after these solutions as they increase to infinity. Unfortunately we cannot tell a priori which

solutions are bound for infinity. We could select bounds on the solution and terminate it if it crosses the bound, but it is difficult to know where to set the bounds

The preferred method of dealing with solutions at infinity is to use a projective representation of the EOM. This is essentially a change of basis. We can change the basis in such a way that all of the solutions remain bounded. Once the solutions have been found, we simply change back to the original basis.

The explanation and proof of projective representations are given in chapter 3 of Morgan's book. Below is the method that has been implemented using this reference.

If the initial set of equations we are trying to solve is

$$\vec{F}_j(m_1, \dots, m_n) = 0 \quad (4.110)$$

the first step is a change of variables.

$$m_i \rightarrow \frac{y_i}{y_{n+1}} \quad (4.111)$$

such that we define a new function \hat{F}

$$\hat{F}_j(y_1, y_2, \dots, y_{n+1}) = y_{n+1}^{d_j} F_j\left(\frac{y_1}{y_{n+1}}, \frac{y_2}{y_{n+1}}, \dots, \frac{y_n}{y_{n+1}}\right) \quad (4.112)$$

where d_j is the degree of the equation. \hat{F}_j is simply the original equation with an added variable multiplied onto each term so that each term has the same degree as the original equation. For example if

$$F_1(\vec{m}) = 3m_1^2 m_2^2 + m_3^2 + m_1 m_3^2 \quad (4.113)$$

which has degree 4, then

$$\hat{F}_1(\vec{y}) = 3y_1^2 y_2^2 + y_3^2 y_4^2 + y_1 y_3^2 y_4 \quad (4.114)$$

It should be noted that solutions to

$$\hat{F}(y_1, y_2, \dots, y_n, 0) = 0 \quad (4.115)$$

produce the solutions at infinity for \vec{F} since equation (4.115) produces the homogenous equations of \vec{F} . Please refer to equation (4.51).

We now define

$$\begin{aligned} L(\vec{y}) &= a_1x_1 + a_2x_2 + \dots + a_nx_n + a_{n+1} \\ l(\vec{y}) &= a_1x_1 + a_2x_2 + \dots + a_nx_n \end{aligned} \quad (4.116)$$

where the constants a_j are real or complex numbers chosen at random, and $a_{n+1} \neq 0$. The projective representation of \vec{F} is given as

$$\hat{F}^{L,j}(y_1, \dots, y_{j-1}, L(\vec{y}), y_j, \dots, y_n) = 0 \quad (4.117)$$

The purpose of all of this is that if we choose the coefficients of $L(\vec{y})$ at random, then the solutions to $\hat{F}^{L,j} = 0$ will not have any solutions at infinity. Therefore, we just need to solve equation (4.117), and then change variables back to regain the original solution. Specifically, solutions to

$$\hat{F}^{L,n+1}(\vec{y}) = \hat{F}^{L,j}(y_1, \dots, y_n, L(\vec{y})) = 0 \quad (4.118)$$

can be converted to solutions of $\vec{F}(\vec{m})$ by

$$\vec{m}_j = \frac{\vec{y}_j}{l(\vec{y}_j)} \quad (4.119)$$

where j is the solution number, and not the vector component of m or y .

Solutions at infinity are recovered when $l(\vec{y}) = 0$. In this case the solution at infinity is given by convention as

$$m_i = \frac{y_i}{y_1} \quad (4.120)$$

To recap, some solutions of \vec{F} may lie at infinity. These solutions are problematic to the numeric solver since the solution grows without bound. To avoid this situation, \vec{F} is changed into \hat{F} through a change of basis. Random constants are chosen, and $L(x)$ and $l(x)$ are created. $\hat{F}^{L,n+1}$ has no solutions at infinity, and can be solved using the numeric solver. These solutions are mapped exactly back to solutions to the original equation by dividing by $l(\vec{y})$.

Section 4.7.5 General Solution

Having discussed all of the troubles and pitfalls that can happen when trying to find the solutions to a set of polynomial equations (such as the EMFF EOM), we finally have all the pieces to develop a method to solve the EOM.

Starting off with the problem statement, our goal is to solve the following equation.

$$\vec{f}(\vec{m}) = 0 \quad (4.121)$$

where each component of f is a polynomial equation in the variables m . The number of equations is the same as the number of variables.

Before we attempt to solve the equation, we must reduce and scale them. Since we can't guarantee that we have completely reduced the equations, we must also use the projective representation to account for solutions at infinity.

$$\vec{f}(\vec{m}) = 0 \xrightarrow{\text{Reduce}} \vec{f}'(\vec{m}) = 0 \xrightarrow{\text{Scale}} \vec{f}''(\vec{m}'') = 0 \xrightarrow{\text{Projection}} \vec{f}'''(\vec{m}''') = 0 \quad (4.122)$$

For simplicity and to avoid carrying triple primes, let

$$\vec{F}(\vec{x}) \equiv \vec{f}'''(\vec{m}''') \quad (4.123)$$

Because the form and degree of the equations vary, we need a continuation equation that will handle all the different types³. The following continuation equation essentially starts with a completely different equation at $\delta = 0$. Each individual equation in $\vec{g}(\vec{x})$ has the same degree as the associated equation in $\vec{F}(\vec{x})$.

$$\vec{h}(\vec{x}, \delta) \equiv (1 - \delta)\vec{g}(\vec{x}) + \delta\vec{F}(\vec{x}) = 0 \quad (4.124)$$

Because we don't want to allow solution paths to cross, we must add randomness (independence) to the continuation equation. This can be accomplished by the choice of $\vec{g}(\vec{x})$. Let \vec{p} and \vec{q} be vectors of random complex numbers with magnitude near one.

$$g_j(\vec{x}) = p_j^{d_j} x_j^{d_j} - q_j^{d_j} \quad (4.125)$$

where d_j is the degree of the j^{th} equation. The initial solutions, $\vec{h}(\vec{x}, 0) = 0$ are given by

$$\vec{x}|_{\delta=0} = (u(d_1, k_1) \frac{q_1}{p_1}, u(d_2, k_2) \frac{q_2}{p_2}, \dots, u(d_n, k_n) \frac{q_n}{p_n})$$

where $1 \leq k_i \leq d_i, \dots, 1 \leq k_n \leq d_n$
and $k_i \in \text{Integer}$

(4.126)

The function u is defined by

$$u(d, k) = \cos \frac{2\pi k}{d} + i \sin \frac{2\pi k}{d} = e^{i \frac{2\pi k}{d}} \quad (4.127)$$

The final step is to step each initial solution as δ varies from 0 to 1. Once all solutions have been found, they must be changed back to the original basis, and then the values must be rescaled.

The result is all possible solutions (real, imaginary, and infinite) have been systematically found.

MATHEMATICA CODE: CM [equations,<variables>]

Description: Continuation Method

File: Master EMFF Notebook.nb

Section: Continuation Code

Usage: CM[equations,<variables>] = solutions

equations – A list of equations. The number of equations must equal the number of variables.

<variables> -- An optional list of variables.

The default is $\{x[1], x[2], \dots, x[n]\}$.

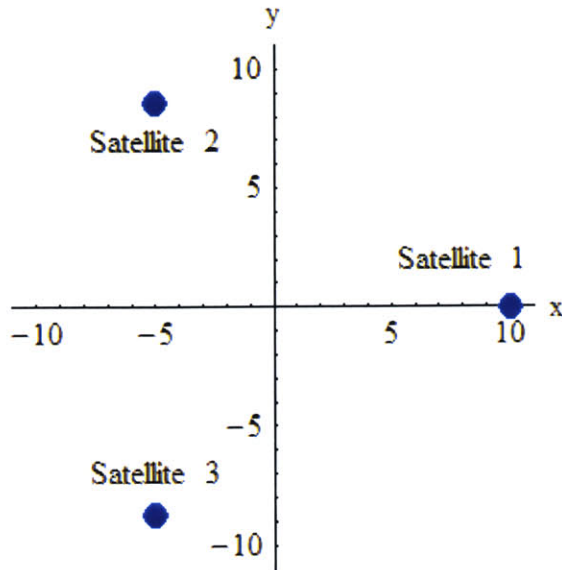
solutions – A matrix of solutions with the following indices [time, solution #, dipole #]

Section 4.8 Applying the Continuation Method to an EMFF System.

This section will apply the continuation methods from the above sections to an EMFF example. At a specific point in time, we are given the desired forces to be applied on each satellite. The free dipole has not been assigned and we will choose it at will. Using the Benzout theorem, we know that for two satellites, there will be only one solution and the use of the continuation method is fairly pointless since we can easily use Newton's Method to seek out the one real solution to the problem. Therefore for our example, we will use three satellites in three dimensions. This will provide eight solutions. See equation (4.42).

The parameters of the example problem are the following: There are three satellites in an equilateral triangle configuration with center of mass corresponding to the origin of an inertial frame. Each satellite is 10m from the center of mass. There are no outside forces or fields present. The plane in which the satellites initially reside is the x - y plane. Each satellite has a mass of 250 kg. Their positions are given by

$$\begin{aligned}\vec{r}_1 &= [10, 0, 0]^T \\ \vec{r}_2 &= [-5, 8.66025, 0]^T \\ \vec{r}_3 &= [-5, -8.66025, 0]^T\end{aligned}\tag{4.128}$$

**Figure 4-13: Position of Satellites**

At a specific point in time, we want the following forces applied to the satellites.

$$\begin{aligned}\vec{f}_1 &= [-30.46, 0, 7.62] \text{mN} \\ \vec{f}_2 &= [15.23, -26.79, -3.81] \text{mN} \\ \vec{f}_3 &= [15.23, 26.79, -3.81] \text{mN}\end{aligned}\tag{4.129}$$

It should be noted that the sum of the desired forces is equal to zero as required. Since the free dipole can be chosen at will, it was selected to be on satellite 1.

$$\begin{aligned}\vec{\mu}_1 &= [0, 40000, 0]^T \text{Am} \\ \vec{\mu}_2 &= [m_1, m_2, m_3]^T \\ \vec{\mu}_3 &= [m_4, m_5, m_6]^T\end{aligned}\tag{4.130}$$

Substituting equations (4.128) through (4.130) into equation (4.1) results in the following nine equations of motion

$$\begin{aligned}
 & -1.83333e-7 m_1 + 2.88675e-8 m_2 + 3.33333e-12 m_2 m_4 + 3.33333e-12 m_1 m_5 - 0.0152309 = 0 \\
 & 2.88675e-8 m_1 + 1.16666e-7 m_2 + 3.33333e-12 m_1 m_4 - 6.66666e-12 m_2 m_5 \dots \\
 & \quad + 3.33333e-12 m_3 m_6 + 0.0267928 = 0 \\
 & 6.66666e-8 m_3 + 3.33333e-12 m_3 m_5 + 3.33333e-12 m_2 m_6 + 0.00380772 = 0 \\
 & 1.83333e-7 m_4 - 3.33333e-12 m_2 m_4 + 2.88675e-8 m_5 - 3.33333e-12 m_1 m_5 - 0.0152309 = 0 \\
 & 2.88675e-8 m_4 - 3.33333e-12 m_1 m_4 - 1.16666e-7 m_5 + 6.66666e-12 m_2 m_5 \dots \quad (4.131) \\
 & \quad - 3.33333e-12 m_3 m_6 - 0.0267928 = 0 \\
 & -6.66666e-8 m_6 - 3.33333e-12 m_3 m_5 - 3.33333e-12 m_2 m_6 + 0.00380772 = 0 \\
 & 1.83333e-7 m_1 - 2.88675e-8 m_2 - 1.83333e-7 m_4 - 2.88675e-8 m_5 + 0.0304617 = 0 \\
 & -2.88675e-8 m_1 - 1.16666e-7 m_2 - 2.88675e-8 m_4 + 1.16666e-7 m_5 = 0 \\
 & -6.66666e-8 m_3 + 6.66666e-8 m_6 - 0.00761544 = 0
 \end{aligned}$$

Because the sum of the forces is constrained to be zero, we know that three of the equations are dependent and can be simply removed. From inspection, the first six equations have degree two, while the last three equations of motion have degree one. In order to reduce the overall degree of the system, it would be smart to remove the equations that have degree two. This way the overall degree will be eight.

However, to demonstrate the reduction step, all nine equations of motion will remain in place. We can also see that we could easily scale each equation by 10^8 , but will once again allow the algorithms to do the work and the equations will be rescaled in the scaling step.

After running the *ReduceEquation[]* function on the equations of motion in equation (4.131), we are left with the following reduced equations of motion.

$$\begin{aligned}
 & 8660.25m_1 + 35000m_2 + m_1 m_4 - 2m_2 m_5 + m_3 m_6 + 8.03785e9 = 0 \\
 & 20000m_3 + m_3 m_5 + m_2 m_6 + 1.14232e9 = 0 \\
 & -55000 m_1 + 8660.25 m_2 + m_2 m_4 + m_1 m_5 - 4.56926e9 = 0 \\
 & \quad -m_3 + m_6 - 114232. = 0 \quad (4.132) \\
 & -0.476314m_1 - 0.925m_2 + m_5 + 39571.0 = 0 \\
 & -0.925m_1 + 0.303109m_2 + m_4 - 159924. = 0
 \end{aligned}$$

As we can see, the algorithm, reduced what was initially a system of nine equations with a total degree of 64, to a system of six equations with a total degree of only 8. We now run the *ScaleEquation[]* routine on the reduced system of equations.

$$\begin{aligned}
 0.279516m'_1 + 1.00487m'_2 + 1.24091m'_1m'_4 - 1.49933m'_2m'_5 + 0.907924m'_3m'_6 + 2.10764 &= 0 \\
 0.857617m'_3 + 1.11967m'_3m'_5 + 1.94412m'_2m'_6 + 0.535662 &= 0 \\
 -2.04576m'_1 + 0.286541m'_2 + 1.27210m'_2m'_4 + 0.971225m'_1m'_5 - 1.38076 &= 0 \\
 -1.24575m'_3 + 0.515832m'_6 - 1.55618 &= 0 \tag{4.133} \\
 -1.17802m'_1 - 2.035m'_2 + 0.524647m'_5 + 0.795089 &= 0 \\
 -1.63995m'_1 + 0.478026m'_2 + 0.553777m'_4 - 2.30347 &= 0
 \end{aligned}$$

The scaling gains for each variable are

$$\vec{s} = \begin{bmatrix} 5.09022 \\ 5.03938 \\ 4.96116 \\ 4.58487 \\ 4.41683 \\ 4.57823 \end{bmatrix} \tag{4.134}$$

After this, we have reduced and conditioned the equations of motion on which to use the continuation solver. Setting up the solver, we need to pick random constants. As stated earlier, we want p , q and a to have a magnitude near unity. Also q is allowed to be either real or complex. For this example, q was chosen to be real. The random number generator produced the following values for equation (4.125) and (4.116)

$$\bar{p} = \begin{bmatrix} 1.15401 + 1.00508i \\ 1.19348 + 1.04615i \\ 1.04282 + 1.14291i \\ 1.14017 + 1.02323i \\ 1.19478 + 1.12771i \\ 1.08507 + 1.13666i \end{bmatrix}, \quad \bar{q} = \begin{bmatrix} 0.864487 \\ 0.837416 \\ 0.975093 \\ 0.969640 \\ 0.899466 \\ 0.891435 \end{bmatrix}, \quad \bar{a} = \begin{bmatrix} 1.22727 \\ 0.760458 \\ 0.989790 \\ 1.47949 \\ 1.01317 \\ 1.04592 \\ 1.28896 \end{bmatrix} \tag{4.135}$$

We must now use the projection method, so that the equation has no solutions at infinity. This is accomplished by forming L and l from equation (4.116), and then \hat{F} from equation (4.118). Because the equation for \hat{F} is fairly long, it has not been included herein, but it can be found in the Mathematica code in the examples section.

The next step is to create the “simple” equations, g , that the continuation solver starts with initially. See equation (4.125).

$$\vec{g}(\vec{x}) = \begin{bmatrix} -0.747338 + (0.321569 + 2.31974i)x_1^2 \\ -0.701265 + (0.329952 + 2.49712i)x_2^2 \\ -0.950807 - (0.218769 - 2.38369i)x_3^2 \\ -0.969640 + (1.14017 + 1.02323i)x_4 \\ -0.899466 + (1.19478 + 1.12771i)x_5 \\ -0.891435 + (1.08507 + 1.13666i)x_6 \end{bmatrix} = 0 \quad (4.136)$$

The initial solutions can be determined from equation (4.126), and are made from all possible (8) combinations of the following vector below.

$$\vec{x}|_{\delta=0} = \begin{bmatrix} \pm 0.425987 \mp 0.371009i \\ \pm 0.396787 \mp 0.347807i \\ \pm 0.424799 \mp 0.465571i \\ 0.471053 - 0.422741i \\ 0.398139 - 0.375789i \\ 0.391705 - 0.410330i \end{bmatrix} \quad (4.137)$$

The next step is to create the continuation equation (4.124), and begin solving. In this example, the value used was $\Delta\delta = 0.002$. Once again, for brevity, all 8 solutions to the continuation equation are not shown. They can be found in the Mathematica code in the Examples section. Once all 8 solutions have been found, we must change back to the original basis using equation (4.119).

$$\vec{l}(\vec{x}_j) = \begin{bmatrix} -0.354591 - 0.168556i \\ -4.99701 \\ 3.10786 \\ 0 \\ -0.303596 \\ -0.155297 \\ 0 \\ -0.354591 + 0.168556i \end{bmatrix} \quad (4.138)$$

where \vec{l} is a list of scalars, (one scalar for each solution). From equation (4.138), we see that there are two solutions at infinity since \vec{l} is zero for solution 4 and 7. The next step is to re-scale the variables. See equation (4.73). The final eight solutions are the columns of the following matrix.

$$\begin{bmatrix} \vec{m}_A, \dots, \vec{m}_H \end{bmatrix} = \left[\begin{array}{cccc|ccccc} -80646.3 - 5379.09i & -136724. & -84652.1 & 1 & -84652.1 & -14540. & 1 & -80646.3 + 5379.09i \\ 15440.2 - 34161.8i & 62401.8 & -10000 & -0.247436 & -10000 & 32169.1 & -0.247436 & 15440.2 + 34161.8i \\ -57115.8 + 0i & -72187.3 & -117725. & 1.05946i & 3493.14 & -42044.2 & -1.05946i & -57115.8 \\ 80646.3 + 5379.09i & 14540.0 & 84652.1 & 1 & 84652.1 & 136724. & 1 & 80646.3 - 5379.09i \\ 15440.2 - 34161.8i & 32169.1 & -10000 & 0.247436 & -10000 & 62401.8 & 0.247436 & 15440.2 + 34161.8i \\ 57115.8 + 0i & 42044.2 & -3493.14 & 1.05946i & 117725. & 72187.3 & 1.05946i & 57115.8 \end{array} \right] \quad (4.139)$$

From this, we can see that there are two infinite solutions (#4 & #7), two complex solutions (#1 & #8), and four real solutions. Since we are working with real solutions, we see that there are *four* viable solutions; four different ways of arranging the dipoles to produce the desired force profile we specified in equation (4.129).

It is informative to look at the solution paths of the variables. The following path is the 2nd solution for m_1 . Remember, we are solving the reduced/scaled/projected equation, so constants and the solution are of order unity. Starting off at $0.425987 - 0.371009i$, the path wonders fairly smoothly until it ends up on the real axis at the end.

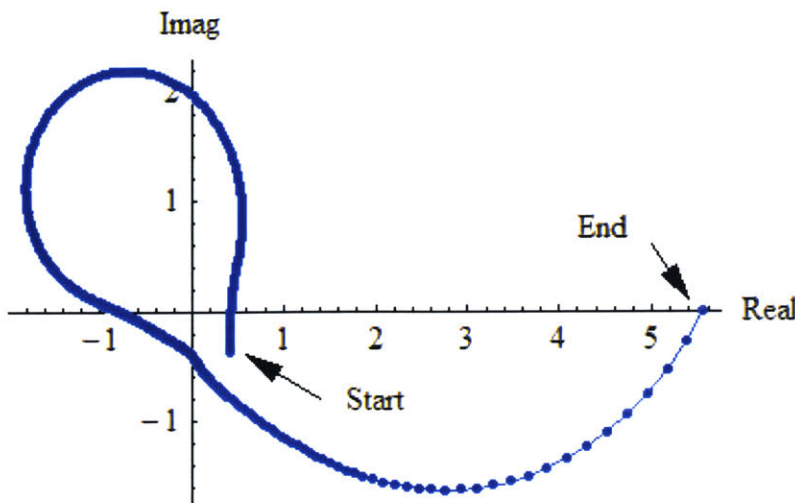


Figure 4-14: Solution Path #2 for Projected/Scaled Variable m_1

Early in the solution path, the solution varies slowly. This is desirable since each successive solution is near the last, and the probability of path jumping is reduced. Towards the end of the solution path however, the spacing is increased. While the spacing between the points is not so large as to instigate path jumping, it should be noted that the change in δ between points is already very small at 0.002. If the spacing was larger, δ would have to be reduced even further.

One explanation why a solution path would tend to jump right at the end of the solution can be seen with the following equation.

$$\delta 0.1x_1 + (1 - \delta)100x_2 \quad (4.140)$$

Remember δ is the variable that changes the continuation equation from the very simple equation to the one we are trying to solve. If the constants are not balanced, then the switch from one solution to the other doesn't happen smoothly. In the above example, the constants are equal when $\delta = 0.999$. It is for this reason that we scale the equations, and choose p and q close to unity in an attempt to minimize this phenomenon.

If we rescale the solutions, we can see the path that the actual variable would take.

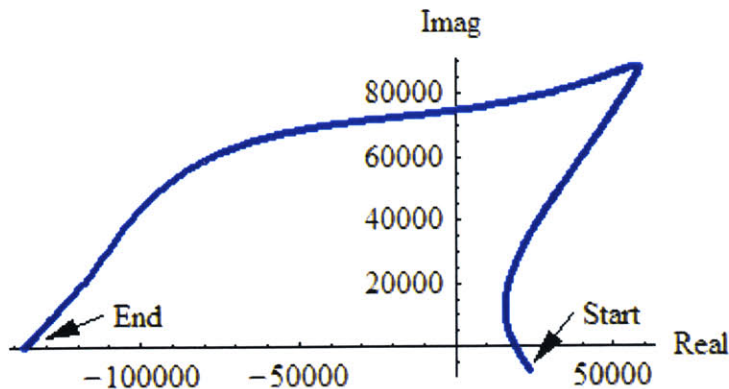


Figure 4-15: Solution Path #2 for Variable m_1

Another solution path shown below is for the 8th solution of m_1 . In this path, the solution has a much larger excursion from the origin midway through the solution path. Also, the same section has large jumps in the solution. Here the jumps are fairly significant, but luckily no path jumping took place. If it did, we would have to re-run the code with a smaller $\Delta\delta$.

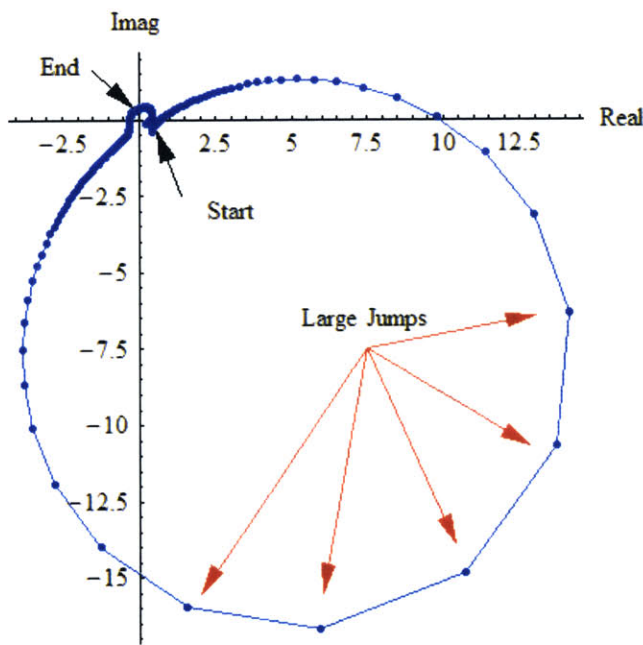


Figure 4-16: Solution Path #8 for Projected/Scaled Variable m_1

If we re-scale the solution path we have the following solution plot.

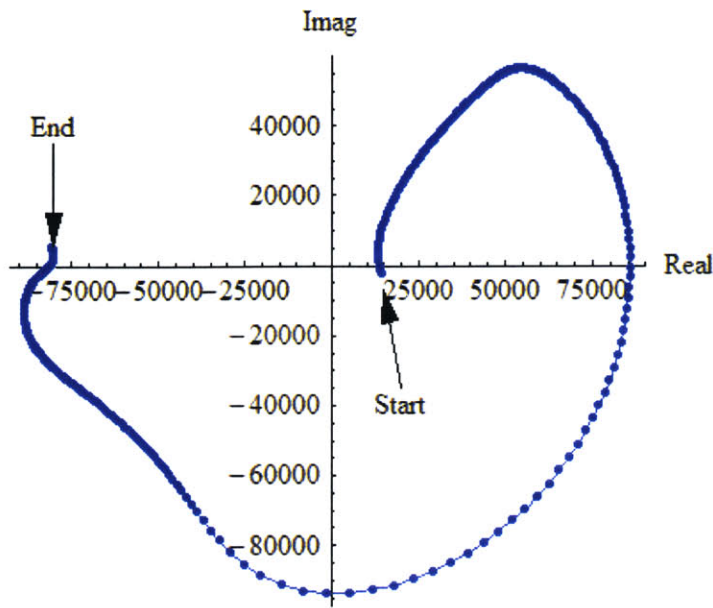


Figure 4-17: Solution Path #8 for Variable m_1

From these plots, we see that it is important to select a $\Delta\delta$ that is small enough to prevent path jumping. Ideally we would have a solver that varies $\Delta\delta$ dynamically to prevent large changes in the solution while at the same time, keeping the change in $\Delta\delta$ from being prohibitively small (large delta when the solution doesn't change much and small delta when the solution is varying quickly). We could find the change in solution based on the change in delta by taking the derivative of the EOM with respect to delta. A larger derivative would result in a smaller delta. This method has been implemented with some success.

Section 4.9 Continuation with Respect to Time

Having successfully found every solution at one point in time, our focus now turns to finding the dipole solution at other points in time. Specifically, the dipole solution $\vec{m}(t)$, from an initial time to a final time is found.

$$\vec{F}(\vec{m}(t), t) - \vec{f}(t) = 0 \quad \forall t \in [t_0, t_1, \dots, t_f] \quad (4.141)$$

Because we are using numeric solvers, there is no way to find a continuous solution, so we will have to find the dipole solution at the discrete points in time and interpolate solutions in-between.

One way of finding the solution at every point in time is to repeat the continuation method at each point. While this would work, it would be time consuming and neglect important information already gathered, specifically the solution at the previous time step. Since we can make Δt be relatively small, we can infer that $\Delta \vec{m}$ will also be small; the solutions at one point in time, will be very near the previous time point.

$$\vec{m}(t_k) - \vec{m}(t_{k-1}) \rightarrow 0 \text{ as } t_k - t_{k-1} \rightarrow 0 \quad (4.142)$$

Newton's method could just use the old solution to seed the numeric solver. Essentially what we are doing is creating a continuation equation that instead of varying in δ now varies in t .

While this seems very straightforward, we can use the knowledge about continuation equations to see the pitfalls we will encounter. In the continuation method we used a specific continuation equation that included **independent** constants so that there would not be any singularities in the continuation method. Remember at singularities solution paths cross and cause trouble for Newton's method. Our continuation equation no longer has those independent equations, and the solutions paths will cross when the equations become singular.

Another difficulty is that we scaled and reduced the equations based on the constants. These constants are based on the geometry of the formation. Now the geometry of the formation is changing. We could re-scale the equation initially, but if the geometry changes significantly, the scaling could be useless. Re-scaling at every point in time could be prohibitive in terms of processing.

One could imagine that the geometry could become such that the equations would reduce in degree. (For example if the satellites moved in such a way that they became co-planar or co-linear). If this is the case, a solution could move to infinity, or move from infinity if the

satellites moved into a more complex geometry. Since these are the actual solutions, we cannot use projective representations to get around solutions at infinity.

Section 4.9.1 Dealing with Singularities in the Solution Path

As stated above, because the continuation equation does not contain independent constants, it is very possible that the solution has singular points at some point in time. Since a singularity usually only happens at distinct points in time, and we are only solving at distinct points in time, it is possible that the singularity may also lie between the two distinct points in time we are solving. Even though we don't solve for the singularity, it will still cause difficulty for the continuation solver. Since we are working with real coefficients, every time a solution passes into the complex plane, there is a singularity. And since complex solutions must have their complex conjugate present, there must be two solution paths that intersect at the singularity point. So even though we aren't sampling at the singularity, the paths will be close together and path jumping can easily and often occur.

One method around this problem is to detect the singularity, and at the next time step, re-solve for all of the points using the original continuation method. Essentially, start over. However, because two of the solutions are very close to each other path crossing can easily still happen as $\delta \rightarrow 1$.

Another more efficient, albeit less elegant solution, is to first detect for path jumping; are there two distinct solutions after the singularity? If so, then we need not do anything. If there is path jumping, and both solutions are the same then we must determine if the solution went from real to imaginary or imaginary to real. If the solution is imaginary after the singularity then the solution to our problem is easy. We can easily recover the second solution since it is just the complex conjugate of the first solution.

If the solution is real on the other side of the singularity, it is less straightforward to find the second solution. Since Newton's Method finds the closest solution to the initial guess, all one has to do is seed Newton's Method appropriately. We know the solution must lie near the

singularity, so if we seed Newton's Method with random small deviations from the singular point, chances are we will recover the solution after only a few attempts.

If all else fails, one could move away from the singularity a few time steps, re-solve for every solution point and work backwards to the singularity.

The above method has been implemented in the continuation code with respect to time called `CMTIME[]`.

MATHEMATICA CODE: `CMTIME[equations,<variables>]`

Description: Determine the condition of a matrix.

File: Master EMFF Notebook.nb

Section: Continuation Code

Usage: `CMTIME[equations,<variables>]=solutions`

equations – A list of equations. The number of equations must equal the number of variables.

<variables> -- An optional list of variables.

The default is `{x[1],x[2],...,x[n]}`.

solutions – A matrix of solutions with the following indices [time, solution #, dipole #]

Example # 9 Continuing the Current Example

Let's expand on our current example. The satellites will start in the previous configuration. Let's assume that the satellites are already initially rotating in their plane with an angular velocity of one revolution every thirty minutes. Let's also assume that the plane that the satellites are in also rotates about the x axis at a rate of one revolution every four hours. One could imagine this is a formation of satellites acting as an interferometer. The satellites rotate in their physical plane to fill the uv plane. The rotation about the x axis can be thought of as a re-pointing maneuver.

The free dipole in this example will be chosen such that it always points in the plane of the satellites and is normal to the line that connects it and the center of mass of the formation. Initially the free dipole has a magnitude of 40,000Am, but we will vary that later on in the example.

Conveniently, the solution for the previous example is the initial solution for this example. Thus we already have the initial solutions to input into the solver. Running the **CMTTime[]** MMA code produces the following results.

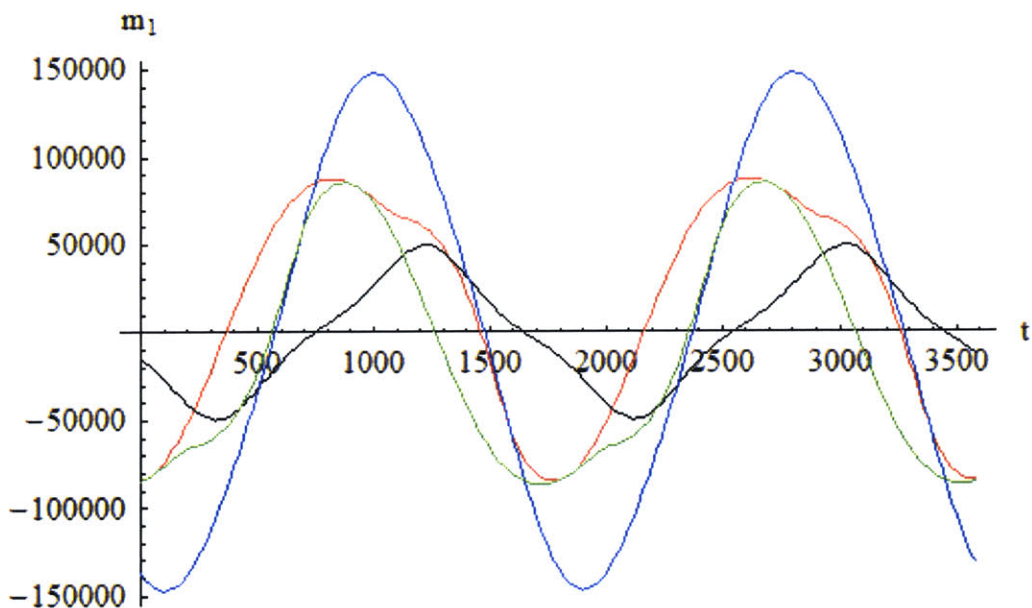


Figure 4-18: Real Solution Paths for m_1 . Free Dipole Magnitude of 40,000Am.

The above plot shows the real solutions to m_1 (the x component of the magnetic dipole on satellite 1). As we can see, all four solution paths behave very well. There appears to be no singularities or path jumpings. While some of the paths in this plot do cross, it's the n dimensional paths that must cross for a true path crossing to take place, so they must cross in all of the variables. We can tell that no paths cross because there are no singularity points where the real solutions disappear or where real solutions appear. We can also look at the matrix condition

of the Jacobin of the equations and see that all are well behaved indicating that there are no singularity points.

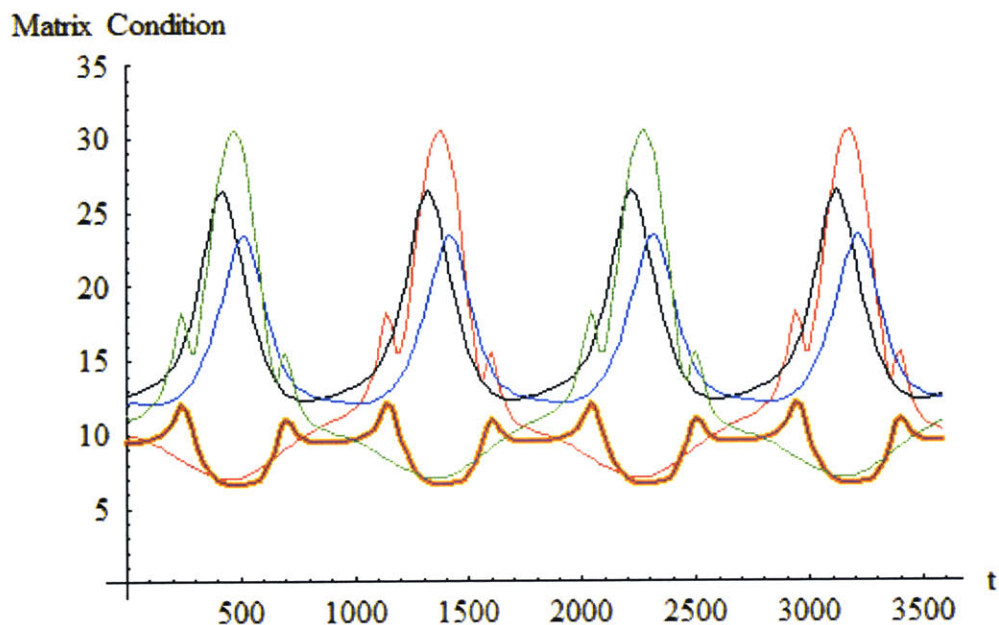


Figure 4-19: Matrix Condition of the EOM. Free Dipole Magnitude of 40,000Am.

Our free dipole has a magnitude of 40,000Am, and the magnitude of m_1 ranges from 50,000 to 150,000. It makes sense to try to balance out the magnitudes and increase the magnitude of our free dipole. The following plot has the magnitude of the free dipole at 42,000Am.

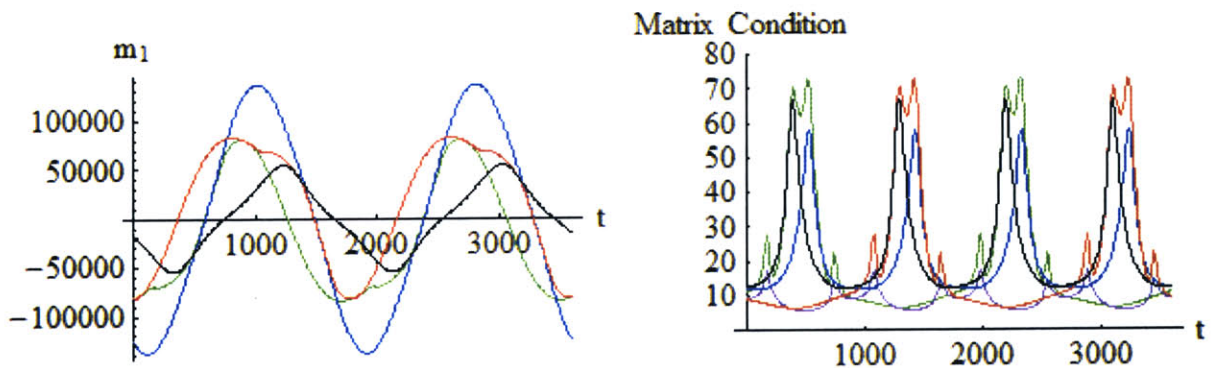


Figure 4-20: Solution Path/Matrix Condition for Free Dipole with Magnitude of 42,000Am.

In this plot, the solution path still remains continuous, but the condition of the EOM is deteriorating. There are points where the matrix condition is increasing. It should be noted that the points always increase in pairs. This is due to the fact at a singularity the matrix condition is infinite, and two paths must cross. Therefore two path's matrix condition must reach infinity at the same time.

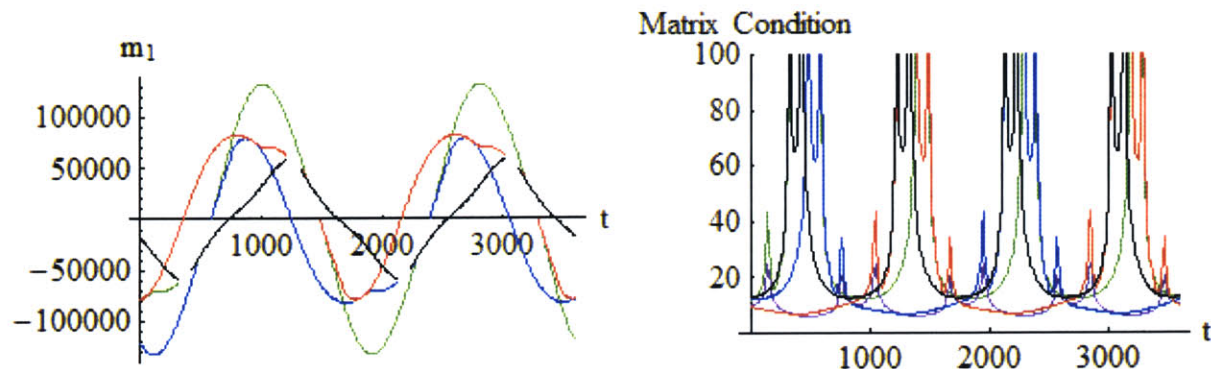


Figure 4-21: Solution Path/Matrix Condition for Free Dipole with Magnitude of 43,000Am.

As we continue to increase the free dipole to 43,000Am, we see that the solution paths are no longer continuous. We see breaks or gaps in the solution paths. Where the paths meet are the singular points, and when they disappear, the solutions are imaginary. It is also interesting to note that there are always at least two real solutions to the problem. We continue by increasing the dipole strength now to 50,000Am. In this plot, the regions of imaginary values have increased in length.

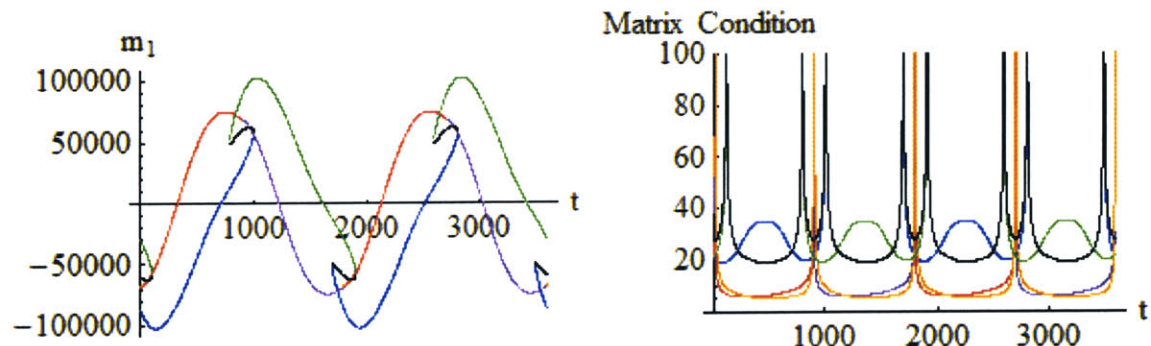


Figure 4-22: Solution Path/Matrix Condition for Free Dipole with Magnitude of 50,000Am.

Continuing to increase the dipole strength to 60,000Am we see the solutions become continuous again, but this time there are only two real solutions.

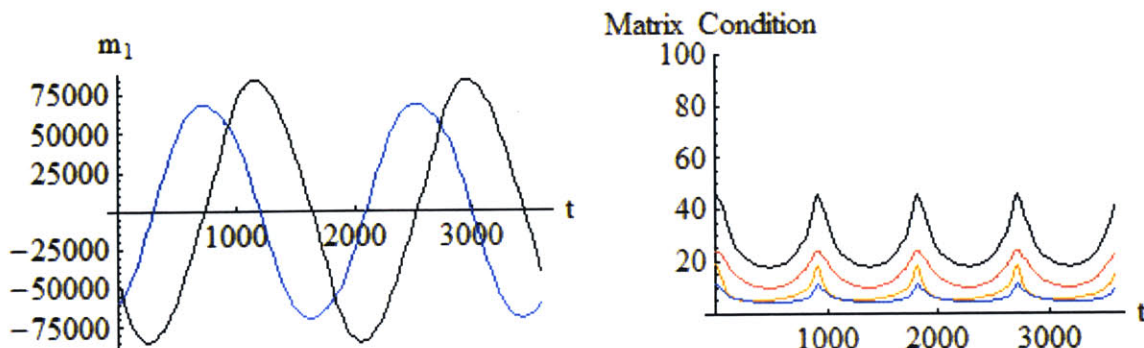


Figure 4-23: Solution Path/Matrix Condition for Free Dipole with Magnitude of 60,000Am.

As we vary the free dipole, different paths will become real, or imaginary, or both. If we imagine the equations as surfaces and the solutions the intersection of the surfaces, the disappearing and re-appearing of solutions is due to the surfaces that once intersect, no longer intersect each other, much like the curves in Figure 4-6. Finally, we include the results with the free dipole at 200,000Am. This plot is included because it shows that you can have continuous paths and at the same time have paths that jump in and out of the complex plane.

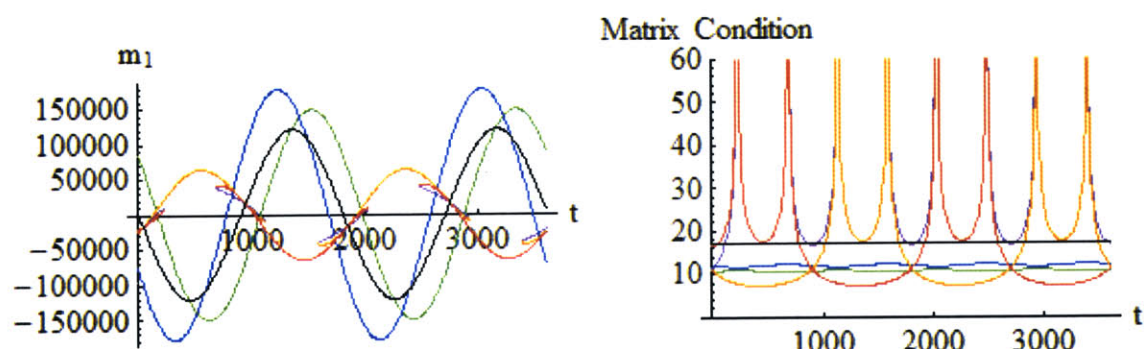


Figure 4-24: Solution Path/Matrix Condition for Free Dipole with Magnitude of 200,000Am.

Section 4.10 Conclusions

In this chapter, we first looked at the form of the EOM and realized that not all of the EOM were independent. We also realized that the EOM were a system of bivariate polynomial equations. This allowed the use of algorithms specifically designed to solve polynomial equations to be used on the EMFF equations. It also allowed insight to be gained on the solution paths and difficulties to anticipate when solving the EOM. Newton's method is well suited for finding solutions to the EOM, but the continuation method is best when all of the solutions are necessary. After finding the solutions at one point in time, the continuation method was expanded to solve for all points in time. Some added techniques were needed, but in the end a method of finding all the solution paths was achieved.

This chapter looked solely at the force EOM, and didn't incorporate the torque EOM. The next chapter will look at the torque distribution that is created by using dipole solutions generated from this chapter. Because of the presence of the free dipole, these solutions can be changed and manipulated in a way that preserves the force distribution created in this chapter, and at the same time, produce a favorable torque distribution.

Chapter 5

ADJUSTING THE DIPOLE SOLUTION

In chapter 4, a time varying force profile or distribution was provided for each satellite in the formation. From this force profile, a solution was created that provides the correct magnetic dipole orientation and strength for each satellite at every point in time. This magnetic dipole solution was dependent on the selection of a “free dipole”. Because the free dipole could be selected in an infinite number of ways, there are an infinite number of dipole solutions. The previous chapter didn’t provide a method of selecting this free dipole, but focused solely on providing a dipole distribution given the free dipole.

This chapter will exploit the free dipole and extra degrees of freedom to improve on the dipole solution. More specifically, this chapter will vary the dipole solution in order to achieve a favorable torque distribution and angular momentum distribution.

Section 5.1 Degrees of Freedom

A viable dipole solution produces the desired force distribution at every point in time. However, different viable dipole solutions produce different torque distribution on each satellite even though they produce the same force distribution. Ideally, the EOM could be solved to find a dipole solution that produces the desired torque distribution as well as the desired force distribution at every point in time. However, a quick accounting of variables and equations shows that this is not always feasible.

From Chapter 4, each vehicle has three degrees of control (the vector components of the magnetic dipoles). Since there are N vehicles, there are $3N$ dipole components. These are the free variables, and the equations of motion are solved for these variables. There are $3N$ translational degrees of freedom, but the center of mass of the formation cannot be changed. This forces three of the translational EOM to be linearly dependent, and thus there are $(3N-3)$ independent equations of motion. There are also $3N$ rotational degrees of freedom. The angular momentum of the system must also be conserved since there are no outside forces or torques. Therefore there

are $(3N-3)$ linearly independent torque equations of motion. Putting them together, there are $(6N-6)$ equations of motion and $3N$ variables.

With two satellites, there is the same number of equations as variables. In this case, both the torque and force equations of motion can be solved concurrently. Notice that there is no longer a free dipole; the equations require the ability to set both satellites' dipole strength and direction in order to be able to produce the desired force and torque distribution. It should be noted that due to the non-linearity of the EOM, even though a solution is guaranteed to exist, it could be imaginary. (Refer to the discussion in Section 3.5.)

When there are more than two satellites, there are more equations of motion than free variables. This prevents the direct (analytic or numeric) solving of the EOM to produce the desired torque and force distributions. In this chapter, the requirement that the desired forces are produced at every instant in time is continued to be placed on the dipole solution. Therefore, the force EOMs are always incorporated as a constraint. Because of this hard constraint, the constraints on the torques must be relaxed and instead the *best possible* torque distribution will be the goal.

This chapter discusses methods to produce the desired force distributions along with torque distributions that provide acceptable torques and angular momentum distribution.

Section 5.2 The Approach

There are three extra degrees of freedom or three ways to change the dipole distribution. As stated earlier, at every point in time a desired force distribution that the dipole solution **must always** produce is given. Therefore, any changes made to the dipole distribution, $\Delta\vec{\mu}$, must not have any effect on the force distribution.

$$\text{Find } \Delta\mu(t) \text{ such that } \vec{\Delta F}(t) = 0 \quad (5.1)$$

This quickly leads to a solution method. Given an initial dipole solution, changes to the dipole solution that do not change the force distribution can be made. These solutions are chosen such that they make favorable changes to the torque distribution or another metric.

If the changes in the dipole solution are restricted to be small, the magnetic force equations of motion can be linearized with respect to small changes in the magnetic dipoles. This matrix is defined here as A .

$$A(t) = \frac{\partial \vec{F}(t)}{\partial \vec{\mu}} \quad (5.2)$$

This allows for the easy calculation of the change in force due to the change in the magnetic dipoles.

$$\Delta \vec{F}(t) = A(t) \cdot \Delta \vec{\mu}(t) \quad (5.3)$$

As stated above, there must not be a change in force, $\Delta \vec{F} = 0$, therefore

$$0 = A(t) \cdot \Delta \vec{\mu}(t) \quad (5.4)$$

From equation (5.4), $\Delta \mu$ must lie in the nullspace of A .

Section 5.3 The Nullspace of A

The matrix A is mxn where m is the number of independent force EOM (3N-3), and n is the number of variables (3N). Therefore the nullspace of A has a dimension of three. The nullspace can therefore be spanned by three independent vectors. Typically the vectors are given as orthonormal, but any combination of linearly independent vectors that spans the space is acceptable. These vectors will be represented by

$$\text{NullSpace}(A(t)) = N(A) = [\vec{n}_A(t) \quad \vec{n}_B(t) \quad \vec{n}_C(t)] \quad (5.5)$$

The change in the dipole solution that satisfies equation (5.4) can be now written as

$$\Delta \vec{\mu}(t) = N(A(t)) \bullet \begin{bmatrix} \alpha_A(t) \\ \alpha_B(t) \\ \alpha_C(t) \end{bmatrix} = \alpha_A(t) \vec{n}_A(t) + \alpha_B(t) \vec{n}_B(t) + \alpha_C(t) \vec{n}_C(t) \quad (5.6)$$

The α 's are scalars that can be picked at will so long as the magnitude of $\Delta\vec{\mu}$ does not violate the linearity of the equations of motion. Equation (5.6) shows that the free dipole can be changed in three different ways without changing the force distribution. The ability to change the dipole in more than one way is an enabling attribute.

To the initial dipole solution, the results of equation (5.6) are added to produce the new dipole solution. Because of the constraint (5.1), the resulting magnetic forces produced do not change.

Section 5.3.1 Changes in Torque

If the goal is to apply this method in order to affect the torque distribution, then it is useful to know how the changes in the dipole distribution will affect the torque distribution. This can be easily accomplished by linearizing the torque equations.

$$B(t) = \frac{\partial \vec{\tau}(t)}{\partial \vec{\mu}} \quad (5.7)$$

The change in torque due to the change in the dipole solution is given by

$$\Delta \vec{\tau}(t) = B(t) \cdot \Delta \vec{\mu}(t) \quad (5.8)$$

Since $\Delta \vec{\mu}$ is restricted to satisfy (5.4) and defined by (5.6), the change in torques can be written as

$$\Delta \vec{\tau}(t) = B(t) \cdot (\alpha_A(t) \vec{n}_A(t) + \alpha_B(t) \vec{n}_B(t) + \alpha_C(t) \vec{n}_C(t)) \quad (5.9)$$

Section 5.4 Specifying the Torque Distribution

The logical first step is to attempt to specify the desired torque distribution at one point in time $\vec{\tau}_{des}$. Given the desired torque distribution, can the above method be used to create the desired change in the torque distribution?

$$\Delta \vec{\tau}(t_i) = \vec{\tau}_{des}(t_i) - \vec{\tau}(t_i) \quad (5.10)$$

There are inherent restrictions on the torque distribution that can be specified. Since the forces remain fixed even when the dipole solution changes, the overall system torque must also remain unchanged. (This is simply the conservation of angular momentum.) Therefore, the sum of the torques applied to each satellite must remain unchanged.

$$\sum_{j=1}^n \vec{\tau}_{des,j} = \sum_{i=1}^n \vec{\tau}_j(t_i) \quad \text{or} \quad \sum_{i=1}^n \Delta \vec{\tau}_i = 0 \quad (5.11)$$

The correct alphas that produce the desired change in torque in equation (5.9) must be found. Equation (5.9) can be written as

$$\Delta \vec{\tau}(t_i) = [B(t_i) \bullet \vec{n}_A(t_i) \mid B(t_i) \bullet \vec{n}_B(t_i) \mid B(t_i) \bullet \vec{n}_C(t_i)] \cdot \begin{bmatrix} \alpha_A(t_i) \\ \alpha_B(t_i) \\ \alpha_C(t_i) \end{bmatrix} \quad (5.12)$$

OR

$$\Delta \vec{\tau}(t_i) = C(t_i) \bullet \vec{\alpha}(t_i) \quad (5.13)$$

$$C(t_i) \equiv \begin{bmatrix} B(t_i) \bullet \vec{n}_1(t_i) \\ B(t_i) \bullet \vec{n}_2(t_i) \\ B(t_i) \bullet \vec{n}_3(t_i) \end{bmatrix}_{3N \times 3}^T \quad \vec{\alpha}(t_i) \equiv \begin{bmatrix} \alpha_A(t_i) \\ \alpha_B(t_i) \\ \alpha_C(t_i) \end{bmatrix}_{3 \times 1} \quad (5.14)$$

Section 5.4.1 Difficulty #1 – Rank Deficiency

C is a $3N \times 3$ matrix and $\vec{\alpha}$ is a 3×1 vector. Since C only has 3 columns, unless $\Delta \tau$ happens to be in the basis spanned by the column vectors of C , there is no solution to equation (5.13).

Example # 1 Rank Deficiency

This can be visualized by the following example. Imagine \mathbb{R}^3 space and a C with a rank of only 2.

$$\vec{\tau}_{des} = \begin{bmatrix} 1 \\ 5 \\ 10 \end{bmatrix} \quad \vec{\tau}_0 = \begin{bmatrix} 4 \\ 2 \\ 0 \end{bmatrix} \quad C = \begin{bmatrix} 1 & 1 \\ 0 & -1 \\ 1 & 0 \end{bmatrix} \quad (5.15)$$

The change in torque $\Delta\tau$ is a linear combination of the columns of C . Because C is rank deficient (with a rank of two), the solutions are restricted to lie in a plane. If the desired solution also happens to lie in that plane, then a solution can be found. But if the desired solution is not in the plane, then the best that can be done is to get as close as possible. The minimum distance between the point in the plane and the desired point is given as

$$\min |\vec{\tau}_{des} - (C \bullet \vec{\alpha} + \vec{\tau}_0)| \quad (5.16)$$

This point is where the normal to the plane intersects the desired point. Solving equation (5.16), the torque that is closest to the desired torque is

$$\vec{\tau}_{min} = (C \bullet \vec{\alpha}_{min} + \vec{\tau}_0) = \begin{bmatrix} \frac{13}{3} \\ \frac{25}{3} \\ \frac{20}{3} \end{bmatrix} \quad (5.17)$$

This can be shown graphically in the following figure where the blue plane is the possible solution space, and the red dot is the desired solution

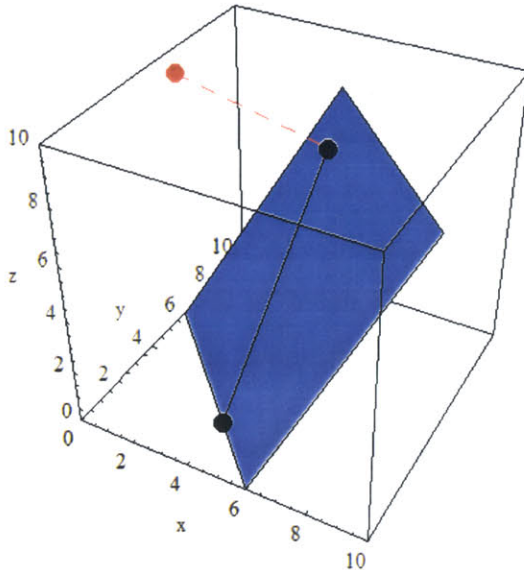


Figure 5-1: Closest Point to a Plane

Section 5.4.2 Difficulty #1 – Rank Deficiency (Continued)

Referring back to the equation (5.14), C is $3N \times 3$. Therefore, C has a rank of 3, or is rank deficient by $3N-3$. However, due to the conservation of angular momentum, 3 of the rows of C are linear dependent. Essentially, the change in C matrix does not allow for an overall system change in torque. Therefore the left nullspace of C will always contain the following vectors

$$NullSpace(C^T) = \begin{bmatrix} 1 & 0 & 0 \\ 0 & 1 & 0 \\ 0 & 0 & 1 \\ \hline 1 & 0 & 0 \\ 0 & 1 & 0 \\ 0 & 0 & 1 \\ \hline 1 & 0 & 0 \\ 0 & 1 & 0 \\ 0 & 0 & 1 \\ \hline \vdots & \vdots & \vdots \end{bmatrix}_{3N \times (3N-3)} \quad (5.18)$$

However, from equation (5.11), we restrict the change in torques to prevent any change in the overall system angular momentum, and thus we can ignore that part of the basis.

In other words, $\Delta\tau$ has no component in the space spanned by the three vectors listed in equation (5.18). The columns of C does not span that space, but neither does $\Delta\tau$. Therefore C is only rank deficient by $3N-6$. For two satellites ($N=2$), C is NOT rank deficient, and thus we can solve for both the force and torques at stated in the introduction. If there are more than 2 satellites, chances are the desired torque distribution cannot be achieved since C is rank deficient.

Section 5.4.3 Difficulty #2 – Linearizations of Non-Linear Equations

Besides being rank deficient, there is another difficulty that must be overcome. Because the matrices are linearizations of the actual surfaces, they are planar approximations to curved surfaces. If the current solution is far away from the final solution, small steps must be made, and the matrices will have to be re-linearized at each step. More importantly however, because of the non-linearity of the surfaces, there may be more than one *local* minimum to equation (5.16).

Looking again at an example in \mathbb{R}^3 space with a rank deficient C , the following figure shows how there can be multiple solutions that are local minima to equation (5.16).

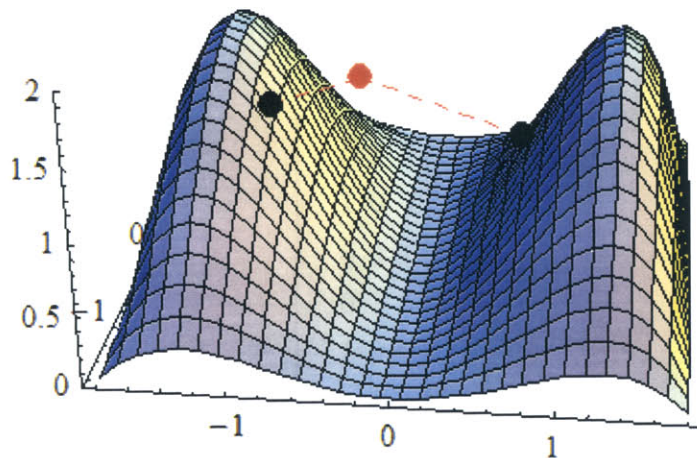


Figure 5-2: Multiple Local Minimum

The red dot is the desired torque solution. However, since C is rank deficient, that point cannot be achieved. (The point does not lie on the surface). Minimizing the distance from the surface to the point, multiple local minima are found.

Finding the global minimum (as opposed to the local minimum) can be very difficult. Luckily for EMFF, the EOM are polynomial and some minimization methods claim to be able to find the global minimum. Unfortunately the EOM can be quite large and attempts to use MMA's built-in global minimization programs have yielded mixed results. For very simplified versions of the equations of motion the minimum would be found, but with the full equations the solution would take an extremely large amount of time, or would find an infeasible solution.

Typically, I have just used the linearized equations with a fixed step length, and re-linearized at each step. This is done with an assortment of starting values in an attempt to find the global minimum. Example # 2 below gives an example of this.

Section 5.4.4 Limiting the Step Size

Because linearized equations of motion are being used, it is important to stay within the linearization range. This can be accomplished by limiting the values of $\Delta\mu_i$.

$$\Delta\vec{\mu}_{\text{limited}} = \frac{\Delta\vec{\mu}}{\max(l, |\Delta\vec{\mu}|)} l \quad (5.19)$$

where l is the maximum length of the $\Delta\vec{\mu}$. l can be set by trial and error, but is typically set to be less than 10% of the magnitude of $\Delta\mu$. Chapter 8 gives an example of using the Active Set Method described later in Section 5.10 to incorporate the limit to he change in the magnetic dipoles into the minimization routine. This method is incorporated into the MMA code. The examples in this chapter will use equation (5.19).

Section 5.4.5 Re-Solving the EOM

Once the dipole solution has been changed, the equations of motion need to be resolved using the non-linear equations of motion to remove the linearization errors. Since there are 3N-3 EOM,

and $3N$ variables, 3 of the variables must be fixed so that there is an equal number of variables and equations. This can be accomplished by choosing one of the magnetic dipoles as the free dipole, fixing its values and solving for the remaining dipoles.

Example # 2 Minimizing the Torque at One Point in Time

Continuing the EMFF example in Chapter 4, the system torque produced at the initial time step is given by

$$\sum_i \tau_i(0) = [0, 0.114232, 0]^T \text{ Nm} \quad (5.20)$$

Because of the conservation of angular momentum we cannot change the system torque. Our desired torque in this example will be for the torque to be evenly distributed between the three satellites.

$$\begin{aligned} \vec{\tau}_{1des}(0) &= [0, 0.0380772, 0]^T \text{ Nm} \\ \vec{\tau}_{2des}(0) &= [0, 0.0380772, 0]^T \text{ Nm} \\ \vec{\tau}_{3des}(0) &= [0, 0.0380772, 0]^T \text{ Nm} \end{aligned} \quad (5.21)$$

Because the method described above only finds local minima, the minimization routine will have to be run with many different initial dipole solutions. Starting with an initial dipole solution and torque distribution of

$$\bar{\mu} = \begin{bmatrix} \vec{\mu}_1 \\ \vec{\mu}_2 \\ \vec{\mu}_3 \end{bmatrix} = \begin{bmatrix} 24368.2 \\ -4940.32 \\ \underline{33077.4} \\ -19595.0 \\ -235288. \\ \underline{-61127.2} \\ 21954.5 \\ -14891.2 \\ 694.971 \end{bmatrix} \text{ Am}^2 \quad \vec{\tau} = \begin{bmatrix} -0.079919 \\ 0.155791 \\ \underline{0.0821449} \\ 0.0821037 \\ -0.0302917 \\ \underline{0.0902781} \\ -0.00218463 \\ -0.0112678 \\ -0.172423 \end{bmatrix} \text{ Nm} \quad (5.22)$$

This gives a cost function of

$$|\vec{\tau}_{des} - \vec{\tau}(\mu_{ini})| = 0.280582 \quad (5.23)$$

The next step is to create the A and B matrices of equations (5.2) and (5.7). Because both are 9x9 matrices, they are not shown here but can be found in the examples notebook. The next step is to find the nullspace of A .

$$NullSpace(A) = \begin{bmatrix} -0.325339 & 0.291975 & -0.195016 \\ 0.409275 & 0.678460 & -0.139062 \\ 0.378943 & -0.461845 & -0.350432 \\ -0.605391 & -0.193367 & -0.130528 \\ -0.311926 & 0.259942 & -0.145208 \\ -0.216495 & 0.242407 & -0.540079 \\ -0.166004 & -0.204105 & -0.0239466 \\ 0.096395 & 0.0774525 & 0.115399 \\ -0.18851 & 0.172519 & 0.690021 \end{bmatrix} \quad (5.24)$$

As expected the nullspace of A has dimension of 3 due to the three free variables. The C matrix can also be calculated.

$$C = 10^{-7} \begin{bmatrix} -4.44581 & 2.76461 & 2.75694 \\ 2.12112 & -8.33587 & -6.63882 \\ -2.47391 & -11.6643 & 2.76782 \\ 0.621055 & -0.401644 & -8.21867 \\ -2.07788 & -0.412709 & -1.62661 \\ 9.43152 & -0.538113 & 5.19327 \\ 3.82475 & -2.36296 & 5.46173 \\ -0.0432401 & 8.74858 & 8.26543 \\ 6.95761 & 12.2025 & -7.96108 \end{bmatrix} \quad (5.25)$$

Minimizing equation (5.16), there is a minimum value of

$$\vec{\alpha} = \begin{bmatrix} 341127. \\ -397494. \\ -49966.2 \end{bmatrix} \quad (5.26)$$

which when substituted into equation (5.6) produces the following changes in magnetic dipole strength.

$$\Delta\vec{\mu} = \begin{bmatrix} 68186.1 \\ 19247.3 \\ \underline{22632.0} \\ 45193.3 \\ 452666. \text{ Am}^2 \\ \underline{249183.} \\ 41953.0 \\ -22713.7 \\ -4024.74 \end{bmatrix} \quad (5.27)$$

Substituting into equation (5.16), the new cost value is

$$|\bar{\tau}_{des} - (C \bullet \vec{\alpha} + \bar{\tau}(\vec{\mu}_{ini}))| = 0.107674 \quad (5.28)$$

Unfortunately the $\Delta\mu$ is very large, and will violate the linearity of the system. Therefore the change in dipole solution must be limited. This is accomplished by using equation (5.19) and limiting $\Delta\vec{\mu}$. In the MMA code, the magnitude of the allowable change is dynamic. If the resoving of the dipole produces a cost value that is worse than the previous step, then the step value is too large, and is cut in half. This way, the minimum can be quickly found and at the same time the exact solution can be found without “jumping” around the solution because the step size is too large. In this example, our first limit is

$$|\Delta\vec{\mu}| \leq 2500 \text{ Am}^2 \quad (5.29)$$

The new $\Delta\vec{\mu}$ is

$$\Delta \vec{\mu} = \begin{bmatrix} 323.968 \\ 91.4484 \\ \underline{107.530} \\ 214.723 \\ 2150.72 \\ \underline{1183.92} \\ 199.328 \\ -107.918 \\ -19.1224 \end{bmatrix} \text{ Am}^2 \quad (5.30)$$

This gives us the following dipole distribution

$$\bar{\mu}_{lin} = \begin{bmatrix} 24692.2 \\ -4848.87 \\ \underline{33185.0} \\ -19380.3 \\ -233138. \\ \underline{-59943.3} \\ 22153.8 \\ -14999.2 \\ 675.849 \end{bmatrix} \text{ Am}^2 \quad (5.31)$$

This dipole solution is based on the linear matrix A and therefore has some errors. The next step is to re-solve the non-linear EOM. Three dipole components must be chosen to remain fixed, and the EOM are solved using Newton's method with equation (5.31) as the initial guess. Choosing the first satellite as the free dipole and fixing its dipole, the final dipole solution is given as

$$\vec{\mu}_{fin} = \begin{bmatrix} 24692.2 \\ -4848.87 \\ \underline{33185.0} \\ -19378.5 \\ -233149. \\ -\underline{59962.6} \\ 22154.3 \\ -14999.2 \\ 676.479 \end{bmatrix} \text{ Am}^2 \quad (5.32)$$

with the final cost value of

$$|\vec{\tau}_{des} - \vec{\tau}(\vec{\mu}_{fin})| = 0.279445 \quad (5.33)$$

This process is repeated many times until a minimum value is obtained. For this initial $\vec{\mu}$, the final minimum is at

$$\mu_{min} = \begin{bmatrix} 80006.9 \\ 32012.8 \\ \underline{17106.8} \\ 14206.4 \\ -73595.1 \\ \underline{-19424.1} \\ 42231.5 \\ -21783.7 \\ 23920.6 \end{bmatrix} \quad \tau_{min} = \begin{bmatrix} -0.0226059 \\ 0.0523072 \\ \underline{0.00784043} \\ -0.0000209231 \\ 0.00516442 \\ \underline{-0.0195826} \\ 0.0226268 \\ 0.0567599 \\ 0.0117421 \end{bmatrix} \quad |\vec{\tau}_{des} - \vec{\tau}_{min}| = 0.0569264 \quad (5.34)$$

The desired torque distribution was not achieved, but the final solution was close to the desired torque distribution. If a different initial dipole distribution was initially used, chances are a different local minimum that may be closer or farther away from the desired torque distribution will be found.

The following plots show the results of trying several hundred different initial dipole solutions. Because the vector $\vec{\mu}$ has nine dimensions, it is somewhat tricky to show the results. The plots here show

$$(x, y, z) = (|\vec{\tau}_{1des} - \vec{\tau}_{1min}|, |\vec{\tau}_{2des} - \vec{\tau}_{2min}|, |\vec{\tau}_{3des} - \vec{\tau}_{3min}|) \quad (5.35)$$

since the following function is being minimized.

$$|\vec{\tau}_{des} - \vec{\tau}| \text{ where } \vec{\tau} = \begin{bmatrix} \vec{\tau}_1 \\ \vec{\tau}_2 \\ \vec{\tau}_3 \end{bmatrix}_{9 \times 1} \quad (5.36)$$

Our goal is represented by the red point at the origin. The blue dots represent the initial torque distribution. The black dots represent the local minimum torque distribution. The green dots represent the solution when it changes from real to imaginary during the minimization process.

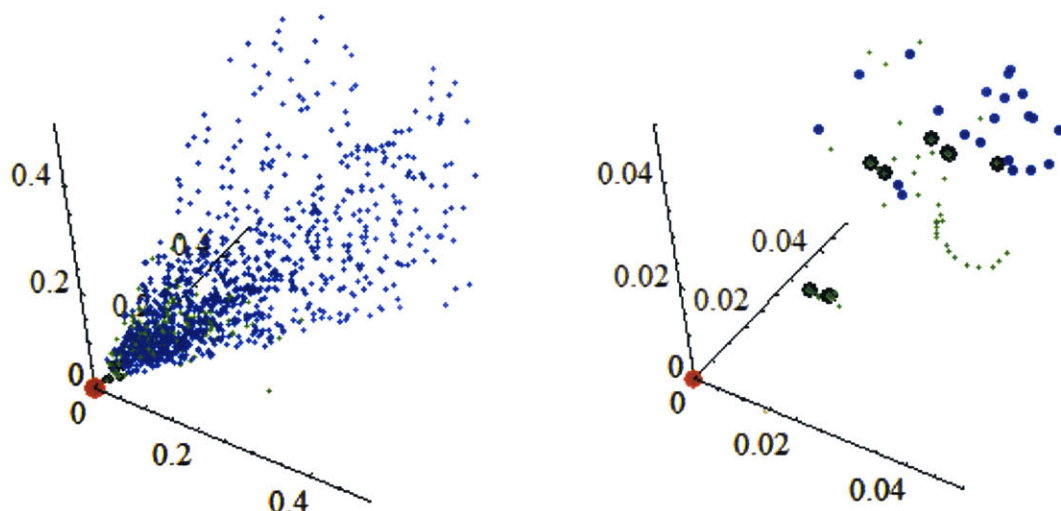


Figure 5-3: Plot of Merit Function

The plot on the left shows the initial blue points. As expected the points are randomly distributed, but the black points are much closer to the origin. Zooming into the origin, (the right plot), there are seven distinct solutions. To actually arrive at those solutions, the fidelity of the

MMA minimization routine had to be increased. Otherwise there was enough numerical error that the points looked more like families of solutions. However, when the fidelity was increased, all the solutions merged into 14 separate solutions. Seven of the solutions are unique, and the other seven solutions are just the negative of the first seven. (Remember, you can take the negative of the dipole solution and the forces and torques all remain unchanged). The dipole solutions are given as columns of the following matrix along with their associated torques.

$$\mu_{\min} = \pm \begin{bmatrix} -80007.1 & -80007.1 & -69441.5 & -69441.5 & -51028.3 & -51028.3 & 0 \\ 32010.6 & -32010.6 & -1421.14 & 1421.14 & -24759.2 & 24759.2 & 65380.0 \\ -17082.8 & -17082.8 & 2748.15 & 2748.15 & -47799. & -47799. & 0 \\ -42229.8 & -14206.7 & -41630.5 & -41598.0 & -4814.87 & -53635.1 & -55079.6 \\ -21779.5 & 73593.7 & 18316.1 & 36908.2 & -11716.0 & 47804.5 & -27004.6 \\ -23951.3 & 19438.7 & -107189. & 62637.2 & 108087. & -43150.2 & -34943.9 \\ -14206.7 & -42229.8 & -41598.0 & -41630.5 & -53635.1 & -4814.87 & 55079.6 \\ -73593.7 & 21779.5 & -36908.2 & -18316.1 & -47804.5 & 11730.8 & -27004.6 \\ 19438.7 & -23951.3 & 62637.2 & -107189. & -43150.2 & 108076. & 34943.9 \end{bmatrix} \quad (5.37)$$

$$\tau_{\min} = \begin{bmatrix} 0.0225864 & -0.0225864 & -0.00146655 & 0.00146655 & -0.0137092 & 0.0137092 & 0 \\ 0.0522688 & 0.0522688 & 0.0502429 & 0.0502429 & 0.0465642 & 0.0465642 & 0 \\ -0.00783925 & 0.00783925 & -0.0110755 & 0.0110755 & -0.00948416 & 0.00948416 & 0 \\ -0.0226394 & -0.000053 & 0.0114969 & 0.0100304 & 0.0276099 & 0.0139007 & -0.0291524 \\ 0.0568026 & 0.00516011 & 0.0370553 & 0.0269333 & 0.0542172 & 0.0134502 & 0.0571158 \\ -0.0117353 & -0.0195746 & 0.00186666 & -0.00920882 & 0.00710673 & -0.00237743 & 0.00181188 \\ 0.000053 & 0.0226394 & -0.0100304 & -0.0114969 & -0.0139007 & -0.0276099 & 0.0291524 \\ 0.00516011 & 0.0568026 & 0.0269333 & 0.0370553 & 0.0134502 & 0.0542172 & 0.0571158 \\ 0.0195746 & 0.0117353 & 0.00920882 & -0.00186666 & 0.00237743 & -0.00710673 & -0.00181188 \end{bmatrix}$$

(5.38)

In terms of our metric, there are the following minimum values

$$[\vec{\tau}_{ides} - \vec{\tau}_{imin}, \dots] = \begin{bmatrix} 0.05693 \\ 0.05693 \\ 0.02682 \\ 0.02682 \\ 0.04721 \\ 0.04721 \\ 0.06231 \end{bmatrix}^T \quad (5.39)$$

Therefore, the global minimum, and the closest solution to the desired torque distribution is solution #3 and #4.

MATHEMATICA CODE: Minimize $\tau [tdes, tini, mini, range]$

Description: Minimize the torque distribution at one point in time.

File: Master EMFF Notebook.nb

Section: Adjust Dipole Solution

Usage: MinimizeTorque [tdes, tint, mini, range]

tdes – Desired torque distribution

tini – Initial torque distribution

mini – Initial dipole solution

range – Initial dipole limits

Section 5.5 Minimizing the Angular Momentum at One Point in Time

The amount of angular momentum stored by the reaction wheels due to the torques applied by the EMFF system is a concern. Assuming discrete points in time, the angular momentum at time t_k can be calculated by summing the torques applied at the previous time steps.

$$\vec{h}(t_k) = \sum_{i=0}^k \vec{\tau}(t_i) \Delta t \quad (5.40)$$

Our goal is to now change the magnetic dipole solution $\Delta\mu$, such that the angular momentum at a specific point in time has a favorable distribution. This is accomplished without changing the force distribution by using the nullspace method in the previous section.

The desired change in angular momentum distribution is defined by

$$\Delta\vec{h}_{des} = \vec{h}_{des}(t_k) - \vec{h}(t_k) \quad (5.41)$$

Assuming no external magnetic field, the system angular momentum must remain constant. Therefore when choosing the desired angular momentum distribution, it must be chosen such that the system angular momentum is conserved.

$$\sum_{i=1}^N \vec{h}_i(t_k)_{des} = \sum_{i=1}^N \vec{h}_i(t_k) \quad (5.42)$$

The desired change can be created by

$$\Delta\vec{h}(t_k)_{des} = \sum_{i=0}^k \Delta\vec{\tau}(t_i) \Delta t \quad (5.43)$$

$\Delta\vec{\tau}(t_i)$ is defined by equation (5.13). Equation (5.43) can be re-written as

$$\Delta\vec{h}_{des} = \Delta t C \cdot \vec{\alpha} \quad (5.44)$$

$$C \equiv \begin{bmatrix} B(t_1) \cdot \vec{n}_A(t_1) \\ B(t_1) \cdot \vec{n}_B(t_1) \\ B(t_1) \cdot \vec{n}_C(t_1) \\ B(t_2) \cdot \vec{n}_A(t_2) \\ B(t_2) \cdot \vec{n}_B(t_2) \\ B(t_2) \cdot \vec{n}_C(t_2) \\ \vdots \end{bmatrix}^T \quad \vec{\alpha} \equiv \begin{bmatrix} \alpha_A(t_1) \\ \alpha_B(t_1) \\ \alpha_C(t_1) \\ \alpha_A(t_2) \\ \alpha_B(t_2) \\ \alpha_C(t_2) \\ \vdots \end{bmatrix} \quad (5.45)$$

The matrix C has a dimension of $3N \times 3k$, where k is the index of the point in time that is to be minimized, and is assumed to be much larger than N . We can also reasonably assume that due to the large number of column vectors, that the column space of C is fully spanned.

However, as with C in the previous section, three of the rows of matrix C are always linearly dependent, and thus C will have at most a rank of $3N-3$. This is due to the fact that the system angular momentum cannot change. Because of this, the left nullspace of C will always at least span the following basis.

$$NullSpace(C^T) = \begin{bmatrix} 1 & 0 & 0 \\ 0 & 1 & 0 \\ 0 & 0 & 1 \\ \hline 1 & 0 & 0 \\ 0 & 1 & 0 \\ 0 & 0 & 1 \\ \hline 1 & 0 & 0 \\ 0 & 1 & 0 \\ 0 & 0 & 1 \\ \hline \vdots & \vdots & \vdots \end{bmatrix} \quad (5.46)$$

Equation (5.46) is simply saying that the sum of the x, y and z components of the angular momentum vector must remain unchanged. Fortunately, the desired angular momentum is restricted in this way also. Therefore, even though C is not full column rank, (the rank of C is $3N-3$), we know that the desired angular momentum vector is in the space spanned by the columns of C . Therefore, there is always a solution of alpha's to solve equation (5.44).

Typically, $k > N$. Therefore, there will be many different possible solutions for the alpha vector. Because of this, a way must be determined to select the alphas. One option is to minimize the alphas.

$$\min |\vec{\alpha}|^2 \text{ such that } \Delta \vec{h}_{des} = \Delta t C \cdot \vec{\alpha} \quad (5.47)$$

Since equation (5.13) shows that the magnitude of the change in torques is related to the magnitude of the alphas, if the alphas are minimized, the changes in torques are minimized. This is desirable since large changes in alphas can cause the solution to be less smooth. Also, since the equations are linearized, large changes in the alphas will cause a breakdown in the linearizations.

Looking more closely at equation (5.47), there is a quadratic cost function and a linear constraint. This is the basic problem of quadratic programming with equality constraints.

$$\begin{aligned} & \min_{\vec{x}} \frac{1}{2} \vec{x}^T G \vec{x} + \vec{x}^T \vec{d} \\ & \text{subject to } A \vec{x} = \vec{b} \end{aligned} \quad (5.48)$$

Equation (5.48) can be simply solved by solving the following linear equation where \vec{x}_{\min} is the desired solution and $\vec{\lambda}$ are the Legendre constants.

$$\begin{bmatrix} G & -A^T \\ A & 0 \end{bmatrix} \begin{bmatrix} \vec{x}_{\min} \\ \vec{\lambda} \end{bmatrix} = \begin{bmatrix} -\vec{d} \\ \vec{b} \end{bmatrix} \quad (5.49)$$

Equation (5.49) can be solved using any commercially available linear solver. For EMFF applications, we can substitute our variables into equation (5.48) and (5.49) with

$$\begin{aligned} G &= I_{3k \times 3k} \\ \vec{d} &= \vec{0}_{3k \times 1} \\ A &= \Delta t C \\ \vec{b} &= \Delta \vec{h} \\ \vec{x} &= \vec{\alpha} \end{aligned} \quad (5.50)$$

From equation (5.50), we see that the matrix in (5.49) is very sparse. This information is useful when deciding how to solve equation (5.49). Mathematica and other software have special and fast algorithms to solve sparse linear algebra equations.

Example # 3 Minimizing the Angular Momentum at One Point in Time

Let's continue with the example problem from the previous chapter where the free dipole has a strength of 40,000Am. For this example, the angular momentum at time t_k will be reduced.

$$t_k = 3600 \text{ sec} \quad \text{where } k = 360 \quad (5.51)$$

and

$$\Delta t = 10 \text{ sec} \quad (5.52)$$

Remember, from equation (4.137) there are four real solutions. For this example, I picked the third solution (the third column of the matrix). The dipole solution is the red solution in Figure 4-18.

The following array of plots shows the angular momentum distribution for each satellite. Satellite 1 is shown in red, satellite 2 is in black, and satellite 3 is in blue. Time t_k is located at the end of the plot.

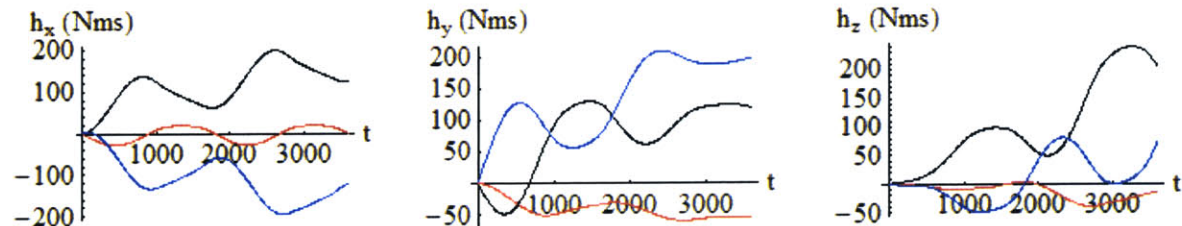


Figure 5-4: Angular Momentum (#1 is Red, #2 is Black, #3 is Blue)

At time t_{360} the angular momentum distribution is

$$\vec{h}(t_{360}) = \begin{bmatrix} \vec{h}_1(3600) \\ \vec{h}_2(3600) \\ \vec{h}_3(3600) \end{bmatrix} = \begin{bmatrix} 0 \\ -54.9811 \\ -15.7728 \\ \hline 123.027 \\ 119.75 \\ \hline 205.495 \\ -123.027 \\ 197.601 \\ \hline 71.5057 \end{bmatrix} \text{ N-m-s} \quad (5.53)$$

From equation (5.53) and Figure 5-4, it can be seen that the angular momentum distribution is not distributed evenly. The goal is to make the angular momentum distribution equal on each satellite at time t_{360} .

$$\vec{h}(t_{360})_{des} = \frac{1}{N} \sum_{i=1}^N \vec{h}_i(t_{360}) = \begin{bmatrix} 0 \\ 87.4567 \\ 87.0759 \end{bmatrix} \text{ N-m-s} \quad (5.54)$$

When attempting to minimize the torques at one point in time, the C matrix was 9 X 3 and had a rank of only 3. Now the C matrix has a dimension of 9 X 1080 and a rank of 6. Performing the left nullspace operation on the C matrix results in

$$NullSpace(C^T) = \begin{bmatrix} 0.00104005 & 0.552234 & -0.168433 \\ -0.189689 & 0.15941 & 0.521479 \\ 0.545298 & 0.0543994 & 0.181724 \\ \hline 0.00104005 & 0.552234 & -0.168433 \\ -0.189689 & 0.15941 & 0.521479 \\ 0.545298 & 0.0543994 & 0.181724 \\ \hline 0.00104005 & 0.552234 & -0.168433 \\ -0.189689 & 0.15941 & 0.521479 \\ 0.545298 & 0.0543994 & 0.181724 \end{bmatrix} \quad (5.55)$$

This can be simply converted using column reduction to

$$NullSpace(C^T) = \begin{bmatrix} 1 & 0 & 0 \\ 0 & 1 & 0 \\ 0 & 0 & 1 \\ \hline 1 & 0 & 0 \\ 0 & 1 & 0 \\ 0 & 0 & 1 \\ \hline 1 & 0 & 0 \\ 0 & 1 & 0 \\ 0 & 0 & 1 \end{bmatrix} \quad (5.56)$$

This is the left null space that was expected. Due to the EOM, angular momentum must be conserved, and this is represented in the left nullspace of C . Because the columns of C and the possible torque distributions span the same space, the alphas that will solve equation (5.44) can be found. However, the alphas are also being minimized. Using equation (5.49) and (5.50) the minimum alphas are found.

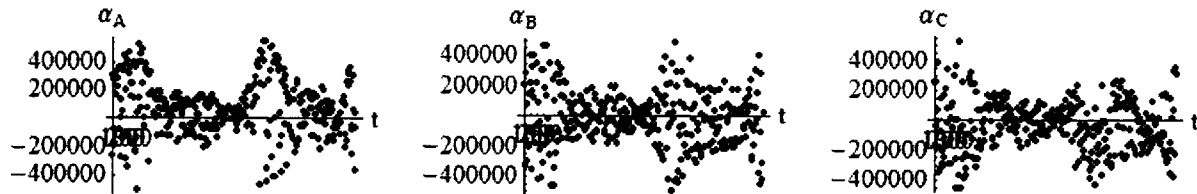
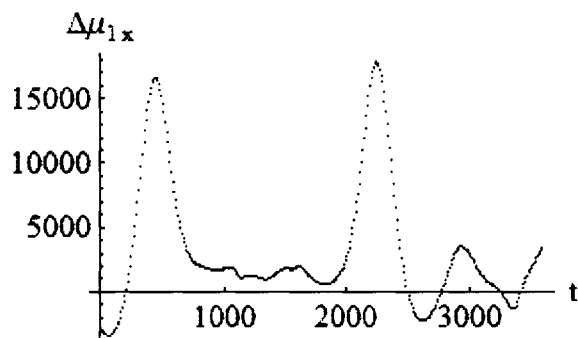


Figure 5-5: Plot of Alphas

These alphas appear to be scattered randomly. However, the geometry of the formation and the dipole solutions do not change significantly from one time step to the next. Therefore the nullspace does not significantly change from one time step to the next. In fact the *basis* of the nullspace does not significantly change from one time step to the next, but from the MMA software, the vectors returned from the `NullSpace[]` command point in a random direction within the basis. Remember, that a linear combination of the vectors that span a basis also span the

basis and are just as valid of a representation. At different points in time MMA is outputting different combinations of those vectors. (This can be visualized by imagining a typical x - y plane. The plane can be spanned by *any* set of two non-collinear vectors residing in the plane, not just the typical x - y axis.)

Even though the alphas appear to be random, they produce a smooth change in μ . The following plot shows the change in the x component of Satellite 1's dipole.



From the plot, the dipoles must change a significant amount to accomplish the goal. Large changes can violate the linearizations and therefore the size of the change in dipole strength must be restricted. If the maximum change in a dipole component is limited to 5000Am, and $\Delta\vec{\mu}$ is scaled accordingly, the angular momentum at time t_k is

$$\vec{h}(t_{360}) = \begin{bmatrix} -0.0459132 \\ -32.6518 \\ 0.419317 \\ \hline 104.721 \\ 114.782 \\ 186.614 \\ \hline -104.675 \\ 180.24 \\ 74.1947 \end{bmatrix} \text{ N-m-s} \quad (5.57)$$

This is an improvement of about 18%. Taking the new linearized values for the dipole solution at each point in time, the non-linear dipole solution are re-solved using the force EOM. Because just the force EOM are being used, there is a free dipole that must be fixed. In this example, the first dipole is chosen to be the free dipole. The EOM of motion are solved, and the non-linear solutions to the force EOM are found. Because small steps are being taken, the non-linear solution will be similar to the linearized solutions. Therefore, the torque distribution should not significantly change and the desired changes in the angular momentum vector will not be lost.

At the next iteration step, the A , B , and C matrices are all re-calculated and the alphas are found again. For this example, it took about eight iterative steps to converge on the solution. A plot of the final angular momentum is shown below. The goal of setting the angular momentum on each satellite equal at time $t_{360} = 3600s$ was reached. Compare this plot to Figure 5-4.

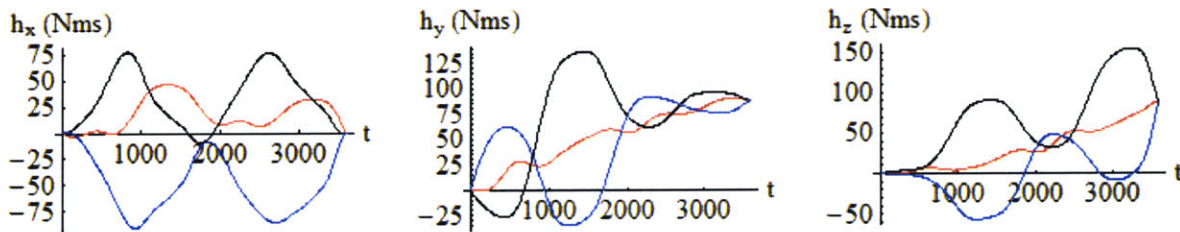


Figure 5-6: Angular Momentum Plot after Dipole Solution Modifications

The angular momentum at $t_{360} = 3600s$

$$\vec{h}(t_{360}) = \begin{bmatrix} 0 \\ 87.4567 \\ 87.0759 \\ \hline 0 \\ 87.4567 \\ 87.0759 \\ \hline 0 \\ 87.4567 \\ 87.0759 \end{bmatrix} \text{ N-m-s} \quad (5.58)$$

Shown below are the initial and final dipole solutions for each satellite.

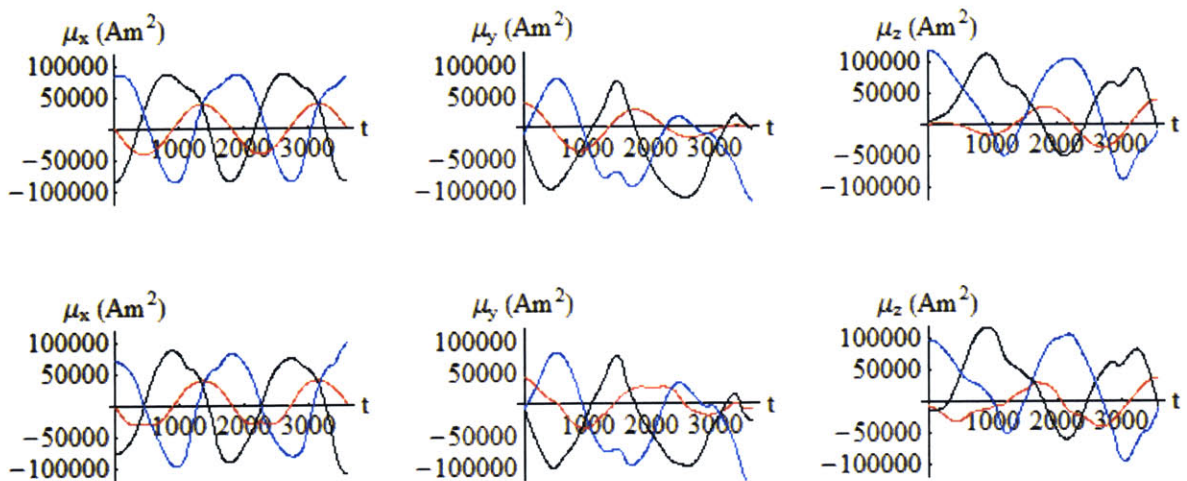


Figure 5-7: Dipole Solution Plot (Top: Original Solution, Bottom: Modified Solution)

From these plots it can be seen that the dipole solution did not change a lot, and remains smoothly varying over time. Plotting the overall change in the magnetic dipole moment results in

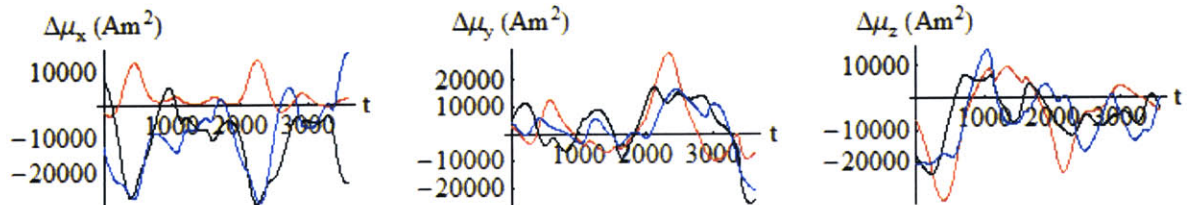


Figure 5-8: Change in Dipole Solution due to Modifications

Section 5.5.2 Difficulties (Imaginary Paths)

If one satellite is considered the free dipole, then equation (5.6) can be thought of as specifying how to change the free dipole to accomplish a goal. The remaining information on the changes of the other satellites' dipoles can be thought of as merely linear predictions for the solution that the EOM of motion will determine.

From chapter 4, changing the free dipole can cause some solution paths to become imaginary. This can also happen here since we are in effect just changing the free dipole. If imaginary solutions do appear in the solution path, one could attempt to “push through” the imaginary section in hope that the solution returns to a smooth real path. This has its difficulties though because the torques and angular momentum also become imaginary. One could also not apply the changes to the dipole solutions at the points in time where the dipole solution would become imaginary. This has the downfall of creating solutions with discrete jumps. Typically it is easier to attempt a new starting dipole solution. A good rule of thumb is that dipole solutions that are close to the desired solution do not become imaginary as easily simply because they don’t change that much.

Section 5.5.3 Difficulties (Path Smoothness)

Above, the change in dipole strength was minimized by minimizing the alphas. More specifically, the sum of the square of the alphas was minimized. This had an effect of not only minimizing the magnitude of the dipole change, but also making the dipole change smooth.

For example, if at one point in time the desired change in angular momentum, thus torque, aligns perfectly with the null space, then a change would only be applied at that one point in time. However that change would be extremely large. Also the points to either side of it will have a similar basis for the nullspace. By minimizing the sum of the squares, the solution tends to distribute the changes evenly to all the points in time, thus smoothing out and distributing the change in dipole strength.

This method of minimizing the alphas is fairly effective at keeping the change in the dipole solution small, and the final dipole solution relatively smooth. However, instead of penalizing the magnitude of the alphas, the *change* in alphas could be penalized. Since the change in basis for the nullspace from one point in time to the next is small, a penalty function could be assigned to the difference in alphas from one point in time to the next. This would minimize the change in dipole strength from one point in time to the next resulting in smooth solutions.

However, the vectors in the nullspace are not necessarily aligned. Therefore minimizing the change in alphas does not correspond to minimizing the change in the dipole solution. If instead the vectors in the nullspace were aligned, then minimizing the change in alpha would in fact minimize the change in dipole solutions. The next section will discuss how to align the nullspace, and then how to apply the above method.

Section 5.6 Aligning the nullspace

When calculating the nullspace at two different points in time separated by a small Δt , the differences in the basis of the nullspaces will be very small. However due to the large size and complexity of A , the MMA code *Nullspace[]*, gives widely different results for the individual vectors in (5.5). The space spanned by the two different nullspaces are still very similar, however the vectors themselves have just been rotated. This section describes how to rotate the vectors so that they are aligned.

Example # 4 Nullspace Alignment

This is more easily explained by a 3D example. Let

$$A(t_1) = \begin{bmatrix} 1 \\ 0 \\ 0.001 \end{bmatrix}^T \quad (5.59)$$

The nullspace of A is

$$\text{NullSpace}[A(t_1)] = \begin{bmatrix} 0 & -0.001 \\ 1 & 0 \\ 0 & 1 \end{bmatrix} \quad (5.60)$$

At a later time t_2 ,

$$A(t_2) = \begin{bmatrix} 1 \\ 0 \\ 0 \end{bmatrix}^T \quad (5.61)$$

The nullspace could be written as

$$\text{NullSpace}[A(t_2)] = \begin{bmatrix} 0 & 0 \\ 1 & 0 \\ 0 & 1 \end{bmatrix} \quad (5.62)$$

And so the change in nullspace vectors from one point in time to the other is very small. However, the nullspace of $A(t_2)$ could just as easily be written as

$$\text{NullSpace}[A(t_2)] = \begin{bmatrix} 0 & 0 \\ \frac{1}{\sqrt{2}} & -\frac{1}{\sqrt{2}} \\ \frac{1}{\sqrt{2}} & \frac{1}{\sqrt{2}} \end{bmatrix} \quad (5.63)$$

In this case, even though the bases for both nullspaces (5.63) and (5.60) are very similar, they have widely different vector representations. Since the goal is to provide a smooth transition between steps, the nullspaces must be aligned. This can be simply accomplished with the following methods.

Section 5.6.2 Method #1

Here is a good point to introduce some notation to make life simpler.

$$N_1 = [\vec{n}_{1A}, \vec{n}_{1B}, \vec{n}_{1C}] \equiv \text{NullSpace}(A(t_1)) \quad (5.64)$$

The vectors in the nullspace are labeled n , and the vectors can be combined as column vectors into a matrix labeled N . The vectors in the nullspace are assumed to be orthonormal.

As stated earlier, the goal is to align the nullspaces, or essentially minimize the angle between the vectors in the nullspace.

$$\min \left(\cos^{-1} \vec{n}_{1i} \cdot \vec{n}_{2i} \right) \quad (5.65)$$

The dot product of the two vectors could instead be maximized. An equivalent metric is to minimize the distance between the two vectors (since the vectors have the same length of 1).

$$\min \sum_{i=1}^3 |\vec{n}_{2i} - \vec{n}_{1i}|^2 \quad (5.66)$$

The goal is to align the vectors in the nullspace N_2 with the vectors in the nullspace N_1 .

The nullspace can be spanned by any linear combination of the vectors in the nullspace. One solution (and the first one attempted) is to determine the correct linear combination of the null space vectors that align with the nullspace vectors at the previous time step. Representing the new nullspace with the “prime” designation, results in

$$\begin{aligned}\vec{n}'_{2A} &\equiv R_{AA} \vec{n}_{2A} + R_{BA} \vec{n}_{2B} + R_{CA} \vec{n}_{2C} \\ \vec{n}'_{2B} &\equiv R_{AB} \vec{n}_{2A} + R_{BB} \vec{n}_{2B} + R_{CB} \vec{n}_{2C} \\ \vec{n}'_{2C} &\equiv R_{AC} \vec{n}_{2A} + R_{BC} \vec{n}_{2B} + R_{CC} \vec{n}_{2C}\end{aligned}\quad (5.67)$$

Which can be written more succinctly as

$$N'_2 = N_2 \cdot R \quad (5.68)$$

where

$$R \equiv \begin{bmatrix} R_{AA} & R_{AB} & R_{AC} \\ R_{BA} & R_{BB} & R_{BC} \\ R_{CA} & R_{CB} & R_{CC} \end{bmatrix}_{3 \times 3} \quad (5.69)$$

where R is a 3X3 matrix. Writing out the objective function in terms of linear combination of the nullspace, results in

$$\min \sum_{i=A,B,C} |\vec{n}_{1i} - (R_{Ai} \vec{n}_{2A} + R_{Bi} \vec{n}_{2B} + R_{Ci} \vec{n}_{2C})|^2 \quad (5.70)$$

The resulting rotated nullspace is required to remain orthonormal. Therefore a constraint on the selection of R is placed such that the columns are orthonormal.

$$\begin{aligned}\vec{R}_A \cdot \vec{R}_B &= \vec{R}_A \cdot \vec{R}_C = \vec{R}_B \cdot \vec{R}_C = 0 \\ |\vec{R}_A| &= |\vec{R}_B| = |\vec{R}_C| = 1\end{aligned}\quad (5.71)$$

There are nine variables and six constraint equations which leave three free variables which can be thought of as three rotational angles.

Equation (5.70) with constraints in (5.71) can be solved fairly straightforwardly using commercial software because equation (5.70) is a second order polynomial equation with second order constraints. In MMA, the command **Minimize[]** is used and solves in about 0.8 seconds on my computer (Toshiba laptop, P4, 2.8 Ghz).

Section 5.6.3 Method #2

Because equation (5.70) is quadratic, it lends itself to the possibility of being written in matrix form and possibly solved in a more straightforward way. Expanding out equation (5.70), it can be seen (if you squint really hard) that equation (5.70) can be written in the form

$$\min\left(\frac{1}{2} \vec{r}^T G \vec{r} + \vec{r}^T \vec{d}\right) \quad (5.72)$$

where

$$\begin{aligned}\vec{r}_{9 \times 1} &= [R_{AA} \ R_{BA} \ R_{CA} \ R_{AB} \ R_{BB} \ R_{CB} \ R_{AC} \ R_{BC} \ R_{CC}]^T \\ G_{9 \times 9} &= 2 \begin{bmatrix} \vec{N}_2^T \vec{N}_2 & 0 & 0 \\ 0 & \vec{N}_2^T \vec{N}_2 & 0 \\ 0 & 0 & \vec{N}_2^T \vec{N}_2 \end{bmatrix} \\ \vec{d}_{9 \times 1} &= -2 [\vec{N}_{1A}^T \vec{N}_2 \ \vec{N}_{1B}^T \vec{N}_2 \ \vec{N}_{1C}^T \vec{N}_2]^T\end{aligned}\quad (5.73)$$

The constraints are unfortunately quadratic also.

$$\vec{r}^T P_i \vec{r} = q_i \quad (5.74)$$

where

$$\begin{aligned}
 P_1 &= \frac{1}{2} \begin{bmatrix} 0 & I_{3 \times 3} & 0 \\ I_{3 \times 3} & 0 & 0 \\ 0 & 0 & 0 \end{bmatrix} & P_2 &= \frac{1}{2} \begin{bmatrix} 0 & 0 & I_{3 \times 3} \\ 0 & 0 & 0 \\ I_{3 \times 3} & 0 & 0 \end{bmatrix} & P_3 &= \frac{1}{2} \begin{bmatrix} 0 & 0 & 0 \\ 0 & 0 & I_{3 \times 3} \\ 0 & I_{3 \times 3} & 0 \end{bmatrix} \\
 P_4 &= \begin{bmatrix} I_{3 \times 3} & 0 & 0 \\ 0 & 0 & 0 \\ 0 & 0 & 0 \end{bmatrix} & P_5 &= \begin{bmatrix} 0 & 0 & 0 \\ 0 & I_{3 \times 3} & 0 \\ 0 & 0 & 0 \end{bmatrix} & P_6 &= \begin{bmatrix} 0 & 0 & 0 \\ 0 & 0 & 0 \\ 0 & 0 & I_{3 \times 3} \end{bmatrix} \\
 \vec{q} &= [0, 0, 0, 1, 1, 1]^T
 \end{aligned} \tag{5.75}$$

If the constraints were linear, a method such as quadratic programming could be used, but since they are quadratic, no method is instantly apparent.

Section 5.6.4 Method #3

Since the vectors in both nullspaces are orthonormal, there must be a rotation matrix that rotates one nullspace to the other. But since the vectors don't exactly align, the rotation matrix would rotate one nullspace so that it is as closely aligned as possible to the other. In fact the R matrix in equation (5.69) can be thought of a rotation matrix. Even though the space has a dimension of \mathbb{R}^{3N} , the rotation is being done within a space of only \mathbb{R}^3 . R can be thought of as a rotation matrix within the Nullspace.

A dual problem is to determine the rotation matrix of a solid body from a set of measurements from multiple points on the body at an initial point in time, and set of measurements at a final point in time. From these measurements, a rotation matrix and center of rotation can be found. Because the measurements are real data, there are some inherent errors. Because of this, the method uses a least squares approach. This works well for our uses since the two nullspaces don't completely align. A least squares approach can be used to align them as closely as possible. The best method was found in the reference by Kwon²⁴. For simplicity, the center of rotation will be taken at the origin. This provides no loss of generality for our use.

The problem statement for the dual problem can be represented by the following equations where $\vec{x}_i(t_1)$ is the set of points on the rigid body at time t_1 . n is the number of points sampled. For our application, $n = 3$ (The dimensions of the nullspace).

$$\vec{x}_i(t_2) = R \cdot \vec{x}_i(t_1) \quad \forall i = 1, 2, \dots, n \quad (5.76)$$

or written with simplified notation as

$$\vec{x}_{2i} = R \cdot \vec{x}_{1i} \quad \forall i = 1, 2, \dots, n \quad (5.77)$$

Typically the points are actual data and have some inherent errors. The rotation matrices are found by using a least squares approach.

$$\min \sum_{i=1}^n \left| \vec{x}_{2i} - R \cdot \vec{x}_{1i} \right|^2 \quad (5.78)$$

This is equivalent²⁴ to

$$\max \frac{1}{n} \sum_{i=1}^n \vec{x}_{2i}^T \cdot R \cdot \vec{x}_{1i} = \max \left(\text{tr}(R^T \frac{1}{n} \sum_{i=1}^n \vec{x}_{2i} \cdot \vec{x}_{1i}^T) \right) \quad (5.79)$$

The correlation matrix c is defined as

$$c = \frac{1}{n} \sum_{i=1}^n \vec{x}_{2i} \cdot \vec{x}_{1i}^T \quad (5.80)$$

This simplifies our objective to

$$\max \text{tr}(R^T c) \quad (5.81)$$

Given c , the R that maximizes the above function must be found. This can be easily accomplished using the singular value decomposition theorem. Decomposing the matrix c ,

$$c = u w v^T \quad (5.82)$$

The objective is re-written as

$$\max \text{tr}(R^T uwv^T) = \max \text{tr}(v^T R^T uw) = \max \text{tr}(fw) \quad (5.83)$$

where $f \equiv v^T R^T u$

Since the matrix w is diagonal, only the diagonal components of f contribute to the maximization step. Also, f must be orthonormal since all three matrices composing f are orthonormal. Therefore, the objective is maximized when f is the identity matrix!

Therefore the rotation matrix can be simply solved for.

$$v^T R^T u = I \rightarrow R = uv^T \quad (5.84)$$

According to the reference²⁴, the matrix R can have a determinant of -1, and in this case the reflection of the desired rotation matrix has been found. This ambiguity can be solved by

$$R = u \begin{bmatrix} 1 & 0 & 0 \\ 0 & 1 & 0 \\ 0 & 0 & |uv^T| \end{bmatrix} v^T \quad (5.85)$$

The size of the rotation matrix is based on the size of the space being considered. For example, if one is working in an \mathbb{R}^3 space, the rotation vector is 3X3. However, an \mathbb{R}^{3N} space is currently required. The R matrix should therefore be $3N \times 3N$. This would provide $9N^2$ unknowns, but only $9N$ data points are being supplied. Therefore the R matrix does not have nearly enough information to be accurate. Specifically, there is no information to restrict the R matrix to the space spanned by the nullspace.

Since the nullspace has a dimension of three, one can imagine that we are rotating within an \mathbb{R}^3 space. If so, can a 3X3 rotation matrix be found using the above method? The answer is yes, and in fact this was already done in the above section (Method #1) where R was as 3X3 matrix that contained the linear combination information. Can this new method determine the 3X3 R matrix? Yes, with a few variations.

Another way of looking at this method is instead of thinking of the nullspace as 3 vectors of length $3N$, imagine the nullspace as $3N$ vectors of length 3. Let us define the transpose of the nullspace vector as

$$Y \equiv N^T \quad (5.86)$$

with

$$\vec{y}_{li} \equiv i^{th} \text{ row of } N_1 \quad (5.87)$$

Equation (5.77) is now simply written as

$$Y_2 = R \bullet Y_1 \quad (5.88)$$

The correlation matrix c is now

$$c = \frac{1}{3N} \sum_{i=1}^{3N} \vec{y}_{2i} \bullet \vec{y}_{li}^T = \frac{1}{3N} Y_2^T \bullet Y_1 \quad (5.89)$$

R can be found in the same way as in equation (5.82) and (5.85). R is now 3×3 as desired. This method works as long as the vectors in Y are orthonormal. While not proven herein, the results exactly match the solutions given by the first method!

Substituting in for the nullspace vectors

$$N_2 = N_1 R^T \quad (5.90)$$

where

$$c = \frac{1}{3N} N_2^T \bullet N_1 = u w v^T \quad (5.91)$$

$$R = u v^T \quad (5.92)$$

The new aligned nullspace is thus defined by

$$N'_2 = N_2 R \quad (5.93)$$

This method of rotating the nullspace is extremely fast since the SVD of the matrix c is a very fast process. On my computer this process completes in less than 0.001 seconds which is a significant improvement over the 0.8 seconds for the previous method. This is important since the alignment must happen for every step in time.

Section 5.7 Minimizing the Angular Momentum using Aligned Nullspaces

Aligning the vectors in the nullspace doesn't change the basis or the magnitude of the vectors in the nullspace. Therefore, one wouldn't expect that the resulting solution will change significantly, and as the following example shows, it doesn't. The next section will utilize the aligned nullspaces.

Example # 5 Continuing Example #4 with an Aligned Nullspace

Re-running the previous example but this time using the new aligned nullspace vectors, we find that the alphas vary smoothly as predicted earlier.

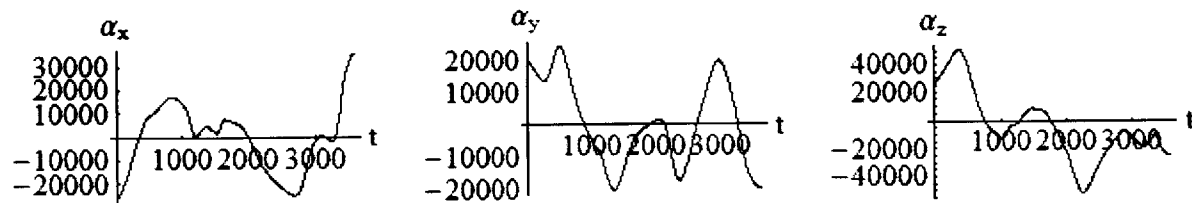


Figure 5-9: Alpha Solutions with Aligned Nullspaces

The resulting change in dipole solution and angular momentum is nearly identical to the previous solution in Figure 5-5.

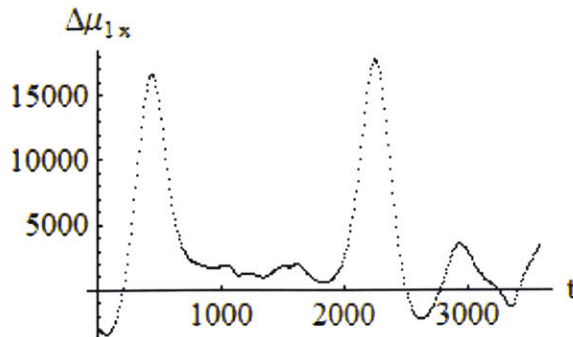


Figure 5-10: Change in x-Component of Satellite #1's Dipole with Aligned Nullspaces

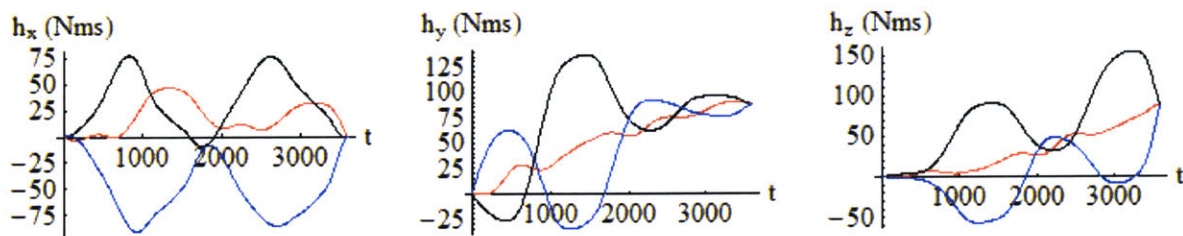


Figure 5-11: Adjusted Angular Momentum with Aligned Nullspaces

Section 5.7.2 Smoothing the Solution

Now that the nullspaces are aligned, instead of just minimizing the magnitude of the alphas, the change in alpha between one time step and the next can be minimized in the hope of smoothing the change in dipole solution.

$$\min \sum_{i=1}^k (a_A(t_i) - a_A(t_{i-1}))^2 + (a_B(t_i) - a_B(t_{i-1}))^2 + (a_C(t_i) - a_C(t_{i-1}))^2 \quad (5.94)$$

Because equation (5.94) is a quadratic equation, the same form as equation (5.48) can be used except that now the matrix G has changed into

$$G_2 = \begin{bmatrix} 1 & 0 & 0 & -1 & 0 & 0 \\ 0 & 1 & 0 & 0 & -1 & 0 \\ 0 & 0 & 1 & 0 & 0 & -1 \\ -1 & 0 & 0 & 2 & 0 & 0 \\ 0 & -1 & 0 & 0 & 2 & 0 \\ 0 & 0 & -1 & 0 & 0 & 2 \\ \vdots & & & & & \end{bmatrix} \quad (5.95)$$

where there are 2s on the diagonal (except for the first and last three rows where there are ones on the diagonal), and there are minus ones on the off diagonals.

Example # 6 Continuing Example #5 with the “Smoothing” G.

Solving equation (5.49) produces the following alpha values

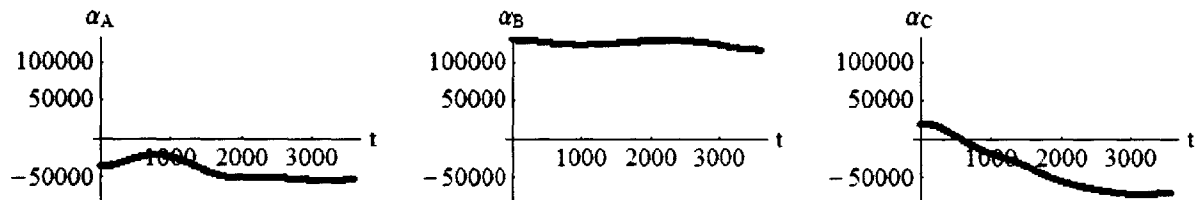


Figure 5-12: Alpha Solutions with Smoothed Solutions

This produces a change in the x component of the dipole solutions of

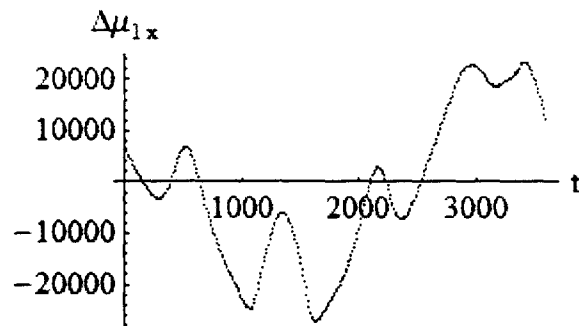


Figure 5-13: Change in x-Component of the Dipole Solution

This solution, while slightly smoother than the dipole solution in Figure 5-10, is not as smooth as the alpha values in Figure 5-12. This is due to the fact that the nullspace has significant variation in it. The following figure looks at the x component of the first satellite in the nullspace,

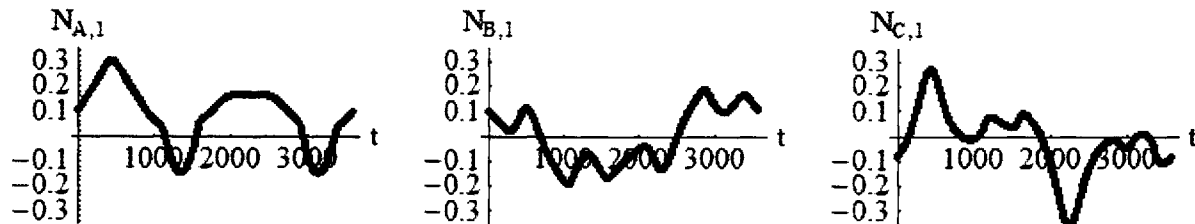


Figure 5-14: Plot of the First Component of the three Nullspace Vectors

From the above figure, it can be seen that the variation in the dipole solution now comes from the variation in the nullspace and not the variation in alpha. This represents the smoothest solution one can achieve due to the fact that the nullspace is dependent on the geometry of the formation and the current dipole solution which are set.

Section 5.7.3 Varying the G Matrix

From Figure 5-12 it can be seen that the variation in alpha is much less than previous. However, the magnitude of the solutions is very large, especially for α_B . Typically when using the G matrix in equation (5.95), the solution is very large. This is somewhat intuitive. If the minimum solutions are already found using equation (5.50), then any other solution will have larger values. Therefore the smooth solution will have larger values than the minimum solutions. Ideally a solution that is both a minimum and smooth would be found, but instead a compromise can be reached. The methods are combined using

$$G = cG_1 + (1-c)G_2 \quad (5.96)$$

where c is a weighting factor.

$$\begin{aligned} & \min_{\vec{x}} \frac{1}{2} \vec{x}^T c G_1 \vec{x} + \frac{1}{2} \vec{x}^T (c-1) G_2 \vec{x} + \vec{x}^T \vec{d} \\ & \text{subject to } A\vec{x} = \vec{b} \end{aligned} \quad (5.97)$$

Section 5.8 Minimizing Angular Momentum at Every Point in Time

Instead of minimizing the angular momentum (or some other objective function) at one instant in time, why not try to minimize a quantity across the whole span in time? The objective function would be to minimize the sum of the square of the angular momentum at every point in time.

$$\min_{\vec{\mu}} \sum_{i=1}^k \sum_{j=1}^N \sum_{l=x,y,z} \left(h_{jl}(t_i) \right)^2 \quad (5.98)$$

where $\vec{h}_{2x}(t_3)$ would refer to the x component of the angular momentum vector of satellite 2 at time t_3 , N is the number of satellites, and k is the index of the final time step. Essentially, equation (5.98) is the sum of the squares of the angular momentum components on each satellite at every point in time. Since

$$\vec{h}_j(t_i) = \Delta t \sum_{l=1}^i \vec{\tau}_j(t_l) \quad (5.99)$$

our new objective function is

$$\min_{\vec{\mu}} \sum_{i=1}^k \sum_{j=1}^N \sum_{m=1}^i \sum_{l=x,y,z} \Delta t \left(\vec{\tau}_{j,l}(t_m) \right)^2 \quad (5.100)$$

In the previous section the alphas were minimized while using the constraints to move a torque or angular momentum vector to the desired value. In this case, the alphas will still be solved for, but instead an attempt to minimize the angular momentum distribution every point in time will be made.

Our objective function is still a quadratic function and can be written in the form of

$$\begin{aligned} \min_{\vec{x}} & \frac{1}{2} \vec{x}^T G \vec{x} + \vec{x}^T \vec{d} \\ \text{subject to } & A \vec{x} = \vec{b} \end{aligned} \quad (5.101)$$

The difficulty now lies in converting equation (5.100) into the form of (5.101).

The sum of the squares of the angular momentum at time t_k is given by

$$\begin{aligned} \sum_{i=1}^N |\vec{h}_i(t_k)|^2 &= \sum_{i=1}^N (h_{ix}(t_k) + \Delta t (\Delta\tau_{ix}(t_1) + \Delta\tau_{ix}(t_2) + \Delta\tau_{ix}(t_3) \dots))^2 + \\ &\quad \sum_{i=1}^N (h_{iy}(t_k) + \Delta t (\Delta\tau_{iy}(t_1) + \Delta\tau_{iy}(t_2) + \Delta\tau_{iy}(t_3) \dots))^2 \\ &\quad \sum_{i=1}^N (h_{iz}(t_k) + \Delta t (\Delta\tau_{iz}(t_1) + \Delta\tau_{iz}(t_2) + \Delta\tau_{iz}(t_3) \dots))^2 \end{aligned} \quad (5.102)$$

Let

$$\Delta \vec{\tau} = \vec{T}_A \alpha_A + \vec{T}_B \alpha_B + \vec{T}_C \alpha_C \quad (5.103)$$

where

$$\vec{T}_i \equiv B \bullet \vec{n}_i \quad (5.104)$$

and

$$C = \begin{bmatrix} B(t_1) \bullet \vec{n}_A(t_1) \\ B(t_1) \bullet \vec{n}_B(t_1) \\ B(t_1) \bullet \vec{n}_C(t_1) \\ \hline B(t_2) \bullet \vec{n}_A(t_2) \\ B(t_2) \bullet \vec{n}_B(t_2) \\ B(t_2) \bullet \vec{n}_C(t_2) \\ \hline B(t_3) \bullet \vec{n}_A(t_3) \\ B(t_3) \bullet \vec{n}_B(t_3) \\ B(t_3) \bullet \vec{n}_C(t_3) \\ \vdots \end{bmatrix}_{3N \times 3k} \quad \vec{T} = \begin{bmatrix} \vec{T}_A(t_1) \\ \vec{T}_B(t_1) \\ \vec{T}_C(t_1) \\ \hline \vec{T}_A(t_2) \\ \vec{T}_B(t_2) \\ \vec{T}_C(t_2) \\ \hline \vec{T}_A(t_3) \\ \vec{T}_B(t_3) \\ \vec{T}_C(t_3) \\ \vdots \end{bmatrix}_{3N \times 3k}^T \quad \vec{\alpha} = \begin{bmatrix} \alpha_A(t_1) \\ \alpha_B(t_1) \\ \alpha_C(t_1) \\ \hline \alpha_A(t_2) \\ \alpha_B(t_2) \\ \alpha_C(t_2) \\ \hline \alpha_A(t_3) \\ \alpha_B(t_3) \\ \alpha_C(t_3) \\ \vdots \end{bmatrix}_{3k \times 1} \quad (5.105)$$

Rewriting equation (5.102)

$$\begin{aligned} \sum_{i=1}^N |\vec{h}_i(t_k)|^2 &= \sum_{i=1}^N (h_{ix}(t_k) + \Delta t \sum_{i=1}^k (T_{Ax}(t_i)\alpha_A(t_i) + T_{Bx}(t_i)\alpha_B(t_i) + T_{Cx}(t_i)\alpha_C(t_i))) + \\ &\quad \sum_{i=1}^N (h_{iy}(t_k) + \Delta t \sum_{i=1}^k (T_{Ay}(t_i)\alpha_A(t_i) + T_{By}(t_i)\alpha_B(t_i) + T_{Cy}(t_i)\alpha_C(t_i)))^2 \quad (5.106) \\ &\quad \sum_{i=1}^N (h_{iz}(t_k) + \Delta t \sum_{i=1}^k (T_{Az}(t_i)\alpha_A(t_i) + T_{Bz}(t_i)\alpha_B(t_i) + T_{Cz}(t_i)\alpha_C(t_i)))^2 \end{aligned}$$

From equation (5.106), the sum of the squares of the angular momentum components at time t_k is given by

$$\sum_{i=1}^N |\vec{h}_i(t_k)|^2 = \Delta t^2 \vec{\alpha}^T C^T C \vec{\alpha} + 2\Delta t \vec{h}(t_k)^T C \vec{\alpha} + \vec{h}(t_k)^T \vec{h}(t_k) \quad (5.107)$$

At time t_{k-1} , the angular momentum components are only dependent on the torques that happen on or before t_{k-1}

$$\begin{aligned} \sum_{i=1}^N |\vec{h}_i(t_{k-1})|^2 &= \sum_{i=1}^N (h_{ix}(t_{k-1}) + \Delta t \sum_{i=1}^{k-1} (T_{Ax}(t_i)\alpha_A(t_i) + T_{Bx}(t_i)\alpha_B(t_i) + T_{Cx}(t_i)\alpha_C(t_i))) + \\ &\quad \sum_{i=1}^N (h_{iy}(t_{k-1}) + \Delta t \sum_{i=1}^{k-1} (T_{Ay}(t_i)\alpha_A(t_i) + T_{By}(t_i)\alpha_B(t_i) + T_{Cy}(t_i)\alpha_C(t_i)))^2 \quad (5.108) \\ &\quad \sum_{i=1}^N (h_{iz}(t_{k-1}) + \Delta t \sum_{i=1}^{k-1} (T_{Az}(t_i)\alpha_A(t_i) + T_{Bz}(t_i)\alpha_B(t_i) + T_{Cz}(t_i)\alpha_C(t_i)))^2 \end{aligned}$$

Defining C' such that the torques are zero after time j

$$C^j = \begin{bmatrix} \vec{T}_A(t_1) \\ \vec{T}_B(t_1) \\ \vec{T}_C(t_1) \\ \vdots \\ \vec{T}_A(t_j) \\ \vec{T}_B(t_j) \\ \vec{T}_C(t_j) \\ \vec{0} \\ \vdots \\ \vec{0} \end{bmatrix}_{3N \times 3k} \quad (5.109)$$

equation (5.98) can be re-written as

$$\min_{\vec{\alpha}} \sum_{j=1}^k \Delta t^2 \vec{\alpha}^T C^{jT} C^j \vec{\alpha} + 2\Delta t \vec{h}(t_j)^T C^j \vec{\alpha} + \vec{h}(t_j)^T \vec{h}(t_j) \quad (5.110)$$

Since the last term in equation (5.110) is a constant, it can be dropped from the equation. Also everything is multiplied by a constant (one half) and the final minimization equation is

$$\min_{\vec{\alpha}} \sum_{j=1}^k \frac{\Delta t^2}{2} \vec{\alpha}^T C^{jT} C^j \vec{\alpha} + \Delta t \vec{h}(t_j)^T C^j \vec{\alpha} \quad (5.111)$$

Equation (5.111) is in the same form as (5.101) with

$$G = \Delta t^2 \sum_{j=1}^k C^{jT} C^j \quad (5.112)$$

$$\vec{d} = \Delta t \sum_{j=1}^k \vec{h}(t_j)^T C^j$$

The matrix G , which in the previous section was very sparse, is now fully dense and large. Substituting equation (5.112) into (5.101), yields a very large and complex quadratic equation to minimize, but with no constraints. As will be shown later, when the alphas are not restrained,

the solution can produce large values for alpha. The next section will discuss methods for solving the class of equations represented in equation (5.101) called quadratic programming.

Section 5.9 Quadratic Programming

Quadratic programming is an optimization problem that attempts to find a solution to the following general problem.

$$\begin{aligned} & \min_{\vec{x}} \frac{1}{2} \vec{x}^T G \vec{x} + \vec{x}^T \vec{d} \\ & \text{subject to } A_1 \vec{x} = \vec{b}_1 \\ & \quad A_2 \vec{x} \geq \vec{b}_2 \end{aligned} \tag{5.113}$$

G is required to be a symmetric matrix. Essentially, a quadratic program attempts to minimize a quadratic function with linear equality and inequality constraints. If G is positive definite, then equation (5.113) is called a convex quadratic program and allows for a better behaved solution. (EMFF produces a positive definite G).

There is much research on quadratic programming^{4,25,26,27,28,29}, however the best reference found was by Nocedel and Wright⁴ where much of the following section on quadratic programming was based.

Section 5.9.1 Equality Constrained Quadratic Program

The first step in understanding quadratic programming is looking at the equality constrained quadratic program.

$$\begin{aligned} & \min_{\vec{x}} \frac{1}{2} \vec{x}^T G \vec{x} + \vec{x}^T \vec{d} \\ & \text{subject to } A_1 \vec{x} = \vec{b}_1 \end{aligned} \tag{5.114}$$

where G is $n \times n$, d is $n \times 1$, A is $m \times n$, and b is $m \times 1$. A is assumed to be full row rank, and $m \leq n$.

Using Lagrange multipliers, the stationary points are given as the solution to the following matrix equation.

$$\begin{bmatrix} G & -A^T \\ A & 0 \end{bmatrix} \begin{bmatrix} \vec{x}_{\min} \\ \vec{\lambda} \end{bmatrix} = \begin{bmatrix} -\vec{d} \\ \vec{b} \end{bmatrix} \quad (5.115)$$

Equation (5.115) gives the first-order solutions. According to the proof in the reference⁴, a unique solution to (5.115) is guaranteed if A has full row rank and $Z^T G Z$ is positive definite. The columns of the Z matrix are the nullspace of A . Essentially, for there to be a guaranteed unique solution to (5.115), G must be positive definite. However, if A constrains the negative semi-definite aspects of G , then there can still be a unique solution if $Z^T G Z$ is positive definite. This seemingly academic exception will come in useful later.

Typically equation (5.115) is re-written into the following form which is essentially just a change of coordinates.

$$\begin{bmatrix} G & A^T \\ A & 0 \end{bmatrix} \begin{bmatrix} -\vec{p} \\ \vec{\lambda} \end{bmatrix} = \begin{bmatrix} \vec{g} \\ \vec{c} \end{bmatrix}$$

where

$$\begin{aligned} \vec{c} &\equiv A\vec{x}_0 - \vec{b} \\ \vec{g} &\equiv \vec{d} + G\vec{x}_0 \\ \vec{p} &\equiv \vec{x}_{\min} - \vec{x}_0 \end{aligned} \quad (5.116)$$

The form of equation (5.116) allows for an iterative approach to the quadratic program in that it gives the solution as a step from an initial value. It also allows for the matrix to be symmetric which is useful for solving the equation. The solutions to both equations satisfy the KKT conditions. (The KKT conditions are a set of conditions that must be satisfied for the solution to be a minimum.) The matrix

$$K = \begin{bmatrix} G & A^T \\ A & 0 \end{bmatrix} \quad (5.117)$$

is typically called the KKT matrix. The K matrix is symmetric, but it is indefinite. It has n positive eigenvalues, and m negative eigenvalues. Solving (5.116) for small systems is fairly straightforward. One could use matrix inversion, LU decomposition, or other similar methods.

For large systems other methods are generally available including³⁰: symmetric indefinite factorization, Choleski decomposition, range-space methods, null-space methods, and conjugacy methods. However, Choleski decomposition (which allows the matrix to be decomposed into two symmetric upper and lower triangle matrices) cannot be used to solve the KKT matrix since it is not semi-positive definite. MMA uses a routine called LAPACK for dense matrices³⁰.

If K is sparse, then other solution opportunities exist. MMA uses the Krylov method for sparse matrices including the conjugate gradient method for symmetric positive definite systems and BiCGSTAB for all other sparse matrices. These methods are significantly faster than their dense matrix counterparts.

The code written for this thesis that will solve equation (111) is called *QPLinSolve[]*. It is well suited when attempting to minimize the torque at one point in time, Section 5.4, or attempting to minimize the angular momentum at one point in time, Section 5.5, because these matrices are very sparse.

QPLinSolve[] is not very fast for large dense systems. If you are just trying to solve (111) once, then *QPLinSolve[]* will work fine. However, if solving (111) is part of an iterative step, then using *QPLinSolve[]* may be too time intensive.

MATHEMATICA CODE: *QPLinSolve [G,d]*, *QPLinSolve [G,d,A,b]*

Description: *Solver for equality constrained Quadratic Program for small or sparse K .*

File: *Master EMFF Notebook.nb*

Section: *QPSolver*

Usage: *QPLinSolve [G,d]*, *QPLinSolve [G,d,A,b] = {x_{min}, λ}*

G,A – 2D matrices (See equation (5.114))

$d, b - 1D \text{ vectors}$

$x_{\min} - \text{Minimum solutions}$

$\lambda - \text{Lagrange variables}$

Section 5.10 Solving the Inequality Constrained QP using the Active Set Method

The next challenge is to account for the inequality constraints. In the literature there are three main types of solutions to the inequality constrained QP: Active Set Methods-ASM (good for small to medium size problems), Gradient Projection Methods-GPM (which is a variant of the active set method and useful when the inequality constraints are just bounded constraints), and Interior-Point Methods- IPM (which are good for large convex QP). For this thesis and EMFF, the ASM and GPM method are used. The IPM would work since EMFF produces a convex QP, but since the AS and GP methods worked well, the IPM was not investigated.

$$\begin{aligned} & \min_{\vec{x}} \frac{1}{2} \vec{x}^T G \vec{x} + \vec{x}^T \vec{d} \\ & \text{subject to } a_i^T \vec{x} = \vec{b}_i \quad i \in E \\ & \quad a_j^T \vec{x} \geq \vec{b}_j \quad j \in I \end{aligned} \tag{5.118}$$

The active set method is an iterative search method. At each iterative step, \vec{x} moves closer to the minimum value. The active set requires and produces a feasible solution (one that satisfies the constraints in (5.118)) at every time step.

The solution method is this⁴. An initial feasible solution is chosen that satisfies all the constraints of (5.118).

$$\begin{aligned} & \vec{x}_0 \text{ such that } a_i^T \vec{x} = \vec{b}_i \quad i \in E \\ & \quad a_j^T \vec{x} \geq \vec{b}_j \quad j \in I \end{aligned} \tag{5.119}$$

If the solution lies on the boundary of an inequality constraint, then the inequality constraint is considered active since it is actively restricting the solution. A set of active inequality constraints is maintained, and inequality constraints that are in the active set (A) are treated as

equality constraints. These active constraints are ‘locked in’ and an attempt is made to minimize the following equation.

$$\begin{aligned} & \min_{\vec{x}} \frac{1}{2} \vec{x}^T G \vec{x} + \vec{x}^T \vec{d} \\ & \text{subject to } \vec{a}_i^T \vec{x} = \vec{b}_i \quad i \in E \cup A \end{aligned} \quad (5.120)$$

Since the inequality constraints that are not in the active set are already satisfied and are not impacting the solution, they are temporarily omitted. Equation (5.120) is now solved using the KKT matrix defined in equation (5.116). This gives a solution direction and length \vec{p} to the minimum solution of (5.120) which will be called \vec{x}_1 since it is the solution to the first iterative step.

$$\vec{x}_1 = \vec{p}_1 + \vec{x}_0 \quad (5.121)$$

This change in the solution will satisfy the equality constraints of (5.118) and the inequality constraints that are in the active set. However, this new solution may violate the inequality constraints that are not in the active set. Therefore, we must check to see if any inequality constraints are violated. If so, then we must find the first inequality constraint boundary that is crossed by moving along a path \vec{p} from \vec{x}_0 .

$$\vec{x}_1 = \alpha_1 \vec{p}_1 + \vec{x}_0 \quad (5.122)$$

We can find the location of the first boundary crossing by the following formula⁴

$$\alpha_k = \min(1, \min_{i \in E \cup A, \vec{a}_i^T \vec{p}_k < 0} \frac{\vec{b}_i - \vec{a}_i^T \vec{x}_k}{\vec{a}_i^T \vec{p}_k}) \quad (5.123)$$

If $\alpha_1 = 1$, then no boundary was reached and the full step can be taken. If $\alpha_1 < 1$, then an inequality boundary was reached. The first boundary that was reached is now included into the active set, and \vec{x}_1 is calculated from equation (5.122). The process is now repeated by solving (5.120) with the new expanded active set until a minimum value is reached (no boundary is reached). This can be verified easily by checking that

$$\vec{p} = 0 \quad (5.124)$$

Once a minimum point is reached, then we must check to see if we can relax an inequality constraint in the active set that will further minimize the solution. This is accomplished by looking at the λ 's corresponding to the inequality constraints. (The Lagrange multipliers are the sensitivities of the corresponding constraints.) If the Lagrange multiplier is negative, then a better solution can be reached if that constraint is removed from the active set. If there are multiple negative Lagrange values, then the most negative Lagrange value is removed from the active set.

Equation (5.120) is now re-solved with this reduced active set until a new minimum is found. Once the new minimum is found, the Lagrange values associated with the inequality constraints in the active set are again checked for negative values. If there are negative values, the inequality constraint with the most negative Lagrange value is removed from the active set and the process is repeated. If all the values are non-negative then the final minimal solution is found.

MATHEMATICA CODE: `QPActiveSet [G,d,A1,b1,A2,b2,x0]`

Description: *Solver for the inequality constrained Quadratic Program.*

File: *Master EMFF Notebook.nb*

Section: *QPSolver*

Usage: `QPActiveSet [G,d,A1,b1,A2,b2,x0] = {xmin }`

G,A₁,A₂ – 2D matrices (See equation (5.113))

d,b₁,b₂ – 1D vectors

x₀ – Initial feasible solutions

x_{min} – Minimum solutions

Example # 7 Active Set Method

The following is a simple example problem. We are trying to solve (5.118) with

$$G = \begin{bmatrix} 10 & -2 & 0 & 0 & 0 \\ -2 & 2 & 1 & 0 & 0 \\ 0 & 1 & 1 & 0 & 0 \\ 0 & 0 & 0 & 4 & 0 \\ 0 & 0 & 0 & 0 & 1 \end{bmatrix} \quad \vec{d} = \begin{bmatrix} 2 \\ 4 \\ -6 \\ 3 \\ 5 \end{bmatrix} \quad A = \begin{bmatrix} 1 & 1 & 1 & 1 & 1 \\ 1 & 0 & 0 & 0 & 1 \\ 2 & 3 & -1 & -3 & 1 \\ 1 & 2 & 4 & 5 & 1 \\ 1 & 4 & 3 & 2 & 1 \\ 2 & 3 & -1 & -1 & 1 \end{bmatrix} \quad \vec{b} = \begin{bmatrix} 3 \\ 4 \\ 5 \\ .4 \\ -20 \\ 4 \end{bmatrix} \quad (5.125)$$

$$[1, 2, 3] \in E$$

$$[4, 5, 6] \in I$$

$$[5] \in A$$

The first three rows of A are equality constraints, and the last three are inequality constraints. We will start with the assumption that the fifth row of A is in the active set. Our initial solution is

$$x_0 = \begin{bmatrix} 4 \\ -19 \\ -60 \\ 40 \\ 0 \end{bmatrix} \quad (5.126)$$

The first step is to verify that our initial solution is a feasible solution (satisfies the constraints).

$$\begin{array}{ll} A\vec{x}_0 & \vec{b} \\ \begin{bmatrix} 3 \\ 4 \\ 5 \\ 2 \\ -20 \\ 85 \end{bmatrix} & = \begin{bmatrix} 3 \\ 4 \\ 5 \\ .4 \\ -20 \\ 4 \end{bmatrix} \end{array} \quad (5.127)$$

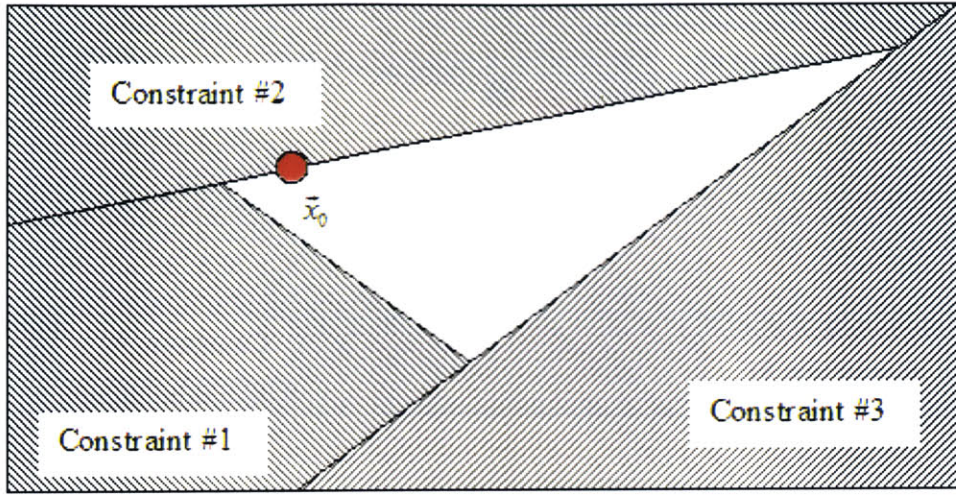


Figure 5-15: Initial Solution lying on the Boundary of the 2nd Inequality Constraint

The next step is to solve the equality constrained QP using the equality constraints and the inequality constraint in the active set (2^{nd} inequality constraint). This produces

$$\vec{p}_1 = [8.03448, -4.01724, 8.03448, -4.01724, -8.03448]^T \quad (5.128)$$

The α values are calculated next.

$$\alpha = [-.398283 \ 0 \ 10.0815]^T \quad (5.129)$$

The first alpha value is negative which means that we are moving away from the boundary of inequality constraint #1. The second alpha is zero since we are already on the boundary (the value is actually undefined since the numerator and denominator are both zero). Finally the third alpha is greater than one, meaning that we encounter the minimum value before we encounter the 3^{rd} inequality constraint. Since we did not encounter any boundary we will take the full step of $\alpha = 1$.

$$\vec{x}_1 = \vec{x}_0 + 1 \vec{p}_1 = [12.03 \ 14.98 \ -51.96 \ 35.98 \ -8.034]^T \quad (5.130)$$

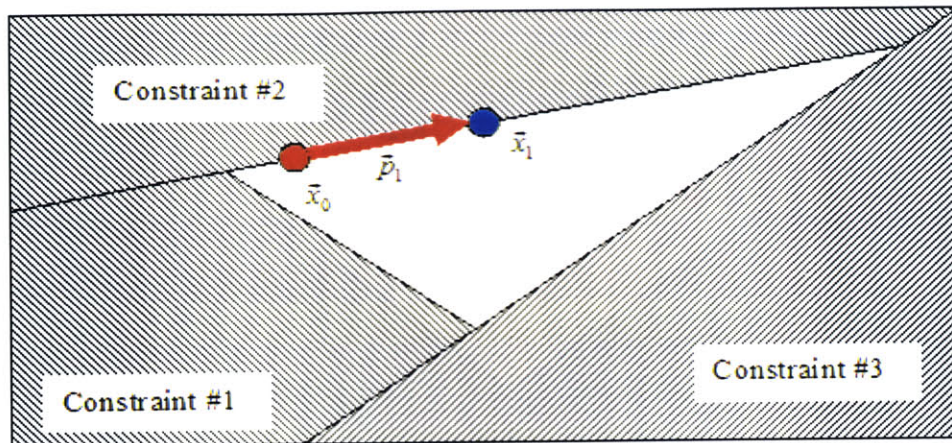


Figure 5-16: Moving to the Minimum Solution

Since we took a full step, we know that we are at the minimum value for this set of equality and active constraints. The next step is to see if we should relax the inequality constraint in the active set. This is done by finding the Lagrange values for the constraint at x_1 .

$$\begin{aligned}\vec{p}_2 &= [0 \ 0 \ 0 \ 0 \ 0]^T \\ \vec{\lambda}_2 &= [1195 \ -912.4 \ 95.41 \ -380.8]\end{aligned}\tag{5.131}$$

The Lagrange values correspond to the first three equality constraints and then inequality constraint #2 which is in the active set. The last Lagrange value which corresponds to the inequality constraint in the active set is negative indicating that a more minimum value can be obtained by relaxing the constraint and removing it from the active set. We now look for the minimum value with an empty active set.

$$\begin{aligned}\vec{p}_3 &= [-11.50 \ -16.49 \ -51.97 \ 35.98 \ -8.035]^T \\ \alpha_3 &= [0.9767 \ 0 \ 0.9421]\end{aligned}\tag{5.132}$$

This time the boundary from the inequality constraint #1 and #3 are reached by the solution before the minimum value. Boundary #3 is reached first.

Using the 3rd alpha, we get the following solution.

$$\vec{x}_3 = [1.198 \ -0.5495 \ 0.04951 \ -0.5 \ 2.802]^T \quad (5.133)$$

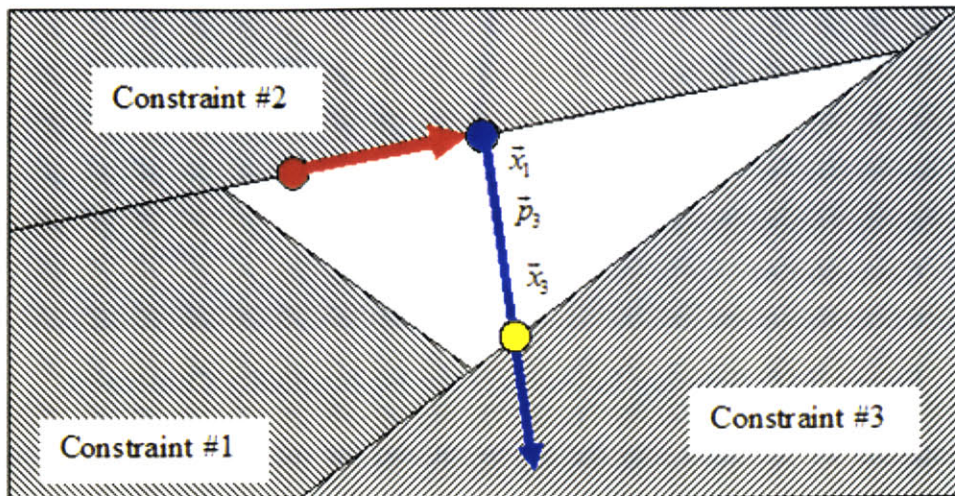


Figure 5-17: Solution Encountering the 3rd Inequality Constraint

Because the 3rd inequality constraint was reached, it is added into the active set and we now resolve for the next solution point.

$$\begin{aligned}\vec{p}_4 &= [-0.4571 \ 0.1142 \ -0.1143 \ 0 \ 0.4571]^T \\ \alpha_4 &= [0.8708 \ -183.3 \ 0] \\ \vec{x}_4 &= [0.8 \ -0.45 \ -0.05 \ -0.5 \ 3.2]\end{aligned} \quad (5.134)$$

Once again we run into the first constraint and must use the first alpha when calculating the fourth solution.

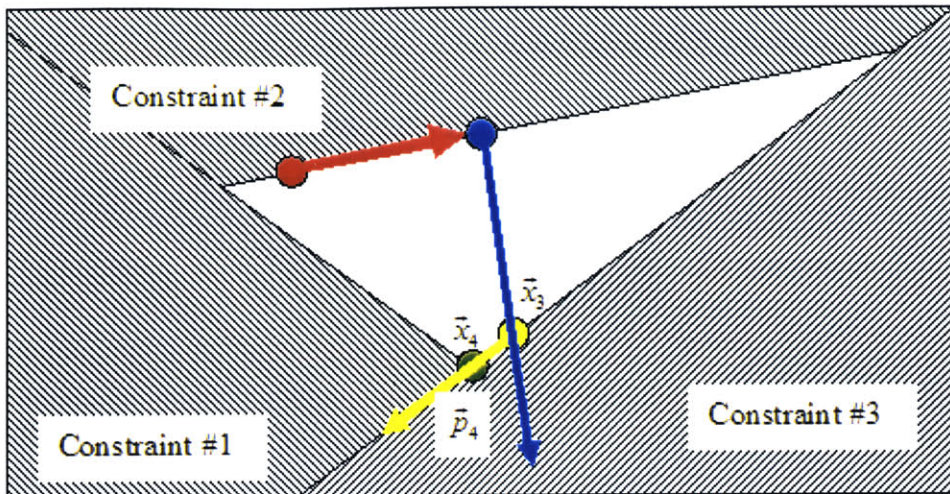


Figure 5-18: Solution Encounters the 1st Inequality Constraint

Inequality constraint #1 is added into the active set and the minimum solution using the new active set is found yet again resulting in

$$\begin{aligned}\vec{p}_5 &= [0 \ 0 \ 0 \ 0 \ 0]^T \\ \lambda_5 &= [-9.5 \ 13.58 \ -3.038 \ 1.425 \ 5.738]\end{aligned}\tag{5.135}$$

The last two Lagrange values correspond to the active constraints. Since both are positive, we know that we are at the constrained minimum and have our final solution of x_4 . This solution is verified using MMA's *Minimize[]* command.

Section 5.10.2 Difficulties

From this example, we had to solve an equality constrained quadratic program five separate times. If G and A are large, then the equality constrained quadratic program will have to be solved a prohibitively large number of times. Especially since only one constraint is added or removed from the active set at each iterative step. For EMFF which has hundreds to thousands of data points, the active set method is not very practical especially since constraints can become active and inactive multiple times in the solution process.

Section 5.11 Gradient Projection Method

An alternative to the active set method is the gradient projection method. This method allows for multiple changes to the active set at each iterative step. The downfall is that the constraints must be simplified to be bounded constraints. (Reference 4 states that other more complex linear constraints can be used with a severe increase of complexity.)

$$\begin{aligned} & \min_{\vec{x}} \frac{1}{2} \vec{x}^T G \vec{x} + \vec{x}^T \vec{d} \\ & \text{subject to } l_i \leq x_i \leq u_i \end{aligned} \quad (5.136)$$

The gradient projection method is a two-step iterative process. In the first step, the steepest descent method is used. Once a path direction has been chosen, the solution moves along this path until a minimum value is reached or a boundary condition is reached. If a minimum is reached, the next step of the iteration process is begun. If a boundary has been reached, then the component of the solution associated with the boundary is fixed at the boundary, and the solution continues along this new path along the boundary until the next boundary or minimum is reached. This is shown graphically in the following figure.

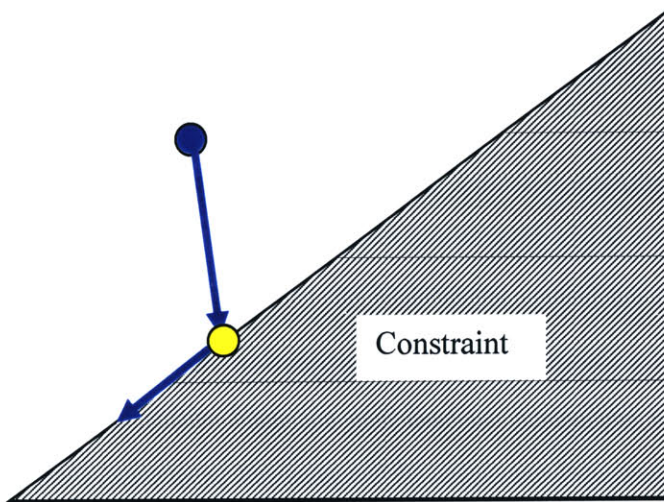


Figure 5-19: Solution Path Bending at a Constraint Boundary

Once a minimum point has been found, \vec{x}_c , (called the Cauchy Point), the constraints that are active at the Cauchy point become the active set. The second step is to now solve the following quadratic program.

$$\begin{aligned} \min_{\vec{x}} J(\vec{x}) &= \frac{1}{2} \vec{x}^T G \vec{x} + \vec{x}^T \vec{d} \\ \text{subject to } x_i &= x_i^c \quad i \in A \\ l_i &\leq x_i \leq u_i \quad i \notin A \end{aligned} \tag{5.137}$$

Now this problem can be just as difficult to solve as the original problem⁴. Luckily, for global convergence, all that is necessary is to find an approximate solution x^+ such that $J(x_{\min}) \leq J(x^+) \leq J(x^c)$. Reference 4 recommends using the nullspace method to reduce the problem since the box bounding constraints are well suited for creating the nullspace matrix. (See below). A variant of conjugate gradient method is then used to solve the reduced minimization problem. But since the conjugate gradient method requires positive semi-definite G , and does not incorporate constraints, a variation of the method is used that stops the method from finding the minimum value if a constraint is reached. By stopping the conjugate gradient method early, we are not finding the absolute minimum of (5.137), but that's acceptable since we are just trying to improve on the solution, not necessarily finding the minimum of this iteration step.

Once the approximate solution is found, the iterative process is repeated and a new Cauchy point is found. Since the active set is determined every time by the location of the Cauchy point, there is no explicit step where inequality constraints are removed from the active set.

Before going into details about the gradient projection method, I will describe the conjugate gradient method and the nullspace method that are used within the gradient projection method. After which the description and examples of the gradient projection method will resume.

Section 5.12 Conjugate Gradient Method

The conjugate gradient method is an iterative solver for the following linear problem

$$G\vec{x} = -\vec{d} \quad (5.138)$$

where G is $n \times n$ and symmetric positive definite. Equation (5.138) can be re-written as a minimization problem where the solution x is a minimum of

$$\min_{\vec{x}} \frac{1}{2} \vec{x}^T G \vec{x} + \vec{d}^T \vec{x} \quad (5.139)$$

The property and key to conjugate gradient methods is the creation of a set of linear independent vectors \vec{p}_i with the property of

$$[\vec{p}_0, \vec{p}_1, \dots, \vec{p}_n] \mid \vec{p}_i^T G \vec{p}_j = 0 \quad \forall i \neq j \quad (5.140)$$

The residual is defined to be

$$\vec{r}(\vec{x}) = G\vec{x} + \vec{d} \quad (5.141)$$

Using the conjugate vectors we can minimize (5.139), (solve (5.138), or force the residual (5.141) to be zero) in n steps! The idea is to move the solution in the direction of each of the conjugate vectors with a step size that minimizes (5.139). Once the solution has moved along each vector once, the minimum is reached. This method, called the conjugate direction method, is given by the following sequence where

$$\begin{aligned} \vec{x}_{k+1} &= \vec{x}_k + \alpha_k \vec{p}_k \\ \alpha_k &= -\frac{\vec{r}_k^T \vec{p}_k}{\vec{p}_k^T G \vec{p}_k} \end{aligned} \quad (5.142)$$

Essentially, alpha is just the step length needed to find the minimum along the path \vec{p}_i . After moving along all of the conjugate vectors, the minimum solution is reached. The proof and a good visual explanation of this method is given on page 103-105 of reference 4. The difficulty with the conjugate direction method is that it requires the creation of the conjugate vectors. For small systems these can be created using the eigenvectors, however, that becomes difficult for large systems.

The solution is to use the conjugate gradient method which has the property of automatically producing a new conjugate direction at each iterative step. In this way, one does not need to know or store all of the conjugate vectors *a priori*. The conjugate vector at each step is just a linear combination of the steepest descent direction and the previous conjugate vector.

$$\vec{p}_k = -\vec{r}_k + \beta_k \vec{p}_{k-1} \quad (5.143)$$

β_k is chosen so that the conjugate vector is in fact conjugate to the previous vector.

$$\beta_k = -\frac{\vec{r}_k^T G \vec{p}_{k-1}}{\vec{p}_{k-1}^T G \vec{p}_k} \quad (5.144)$$

With some simplifications, this leads to the following algorithm (Reference 4, page 111).

$$\begin{aligned} \alpha_k &= \frac{\vec{r}_k \vec{r}_k^T}{\vec{p}_k^T G \vec{p}_k} \\ \vec{x}_{k+1} &= \vec{x}_k + \alpha_k \vec{p}_k \\ \vec{r}_{k+1} &= \vec{r}_k + \alpha_k G \vec{p}_k \\ \beta_{k+1} &= \frac{\vec{r}_{k+1}^T \vec{r}_{k+1}}{\vec{r}_k^T \vec{r}_k} \\ \vec{p}_{k+1} &= -\vec{r}_{k+1} + \beta_{k+1} \vec{p}_k \end{aligned} \quad (5.145)$$

where

$$\begin{aligned} \vec{r}_0 &= G \vec{x}_0 + \vec{d} \\ \vec{p}_0 &= -\vec{r}_0 \end{aligned}$$

This algorithm is implemented in the MMA code written for this thesis with the only change being that the matrix $A\vec{p}_k$ is calculated and stored so that it does not need to be calculated twice per iteration step. Morgan⁴ discusses the speed at which the method converges. The method will converge within n solutions where n is the dimensions of \vec{p} , but can converge to sufficient accuracy faster, especially if the eigenvalues are favorable distributed.

MATHEMATICA CODE: QPConGrad [G,d,x0]

Description: Solver for non-constrained Quadratic Program.

QPConGrad [G,d,A,b,x₀] is available, but should be used with caution. Since the K matrix is not positive definite, the solution has a decent chance of not being a minimum.

File: Master EMFF Notebook.nb

Section: QPSolver

Usage: QPConGrad [G,d,x₀] = {x_{min}}

G – 2D matrix

d – 1D vector

x_{min} – Minimum solution

Section 5.13 Nullspace Method

The nullspace method is a method of solving the KKT equation (5.116). It requires that A is full row rank, and that $Z^T G Z$ is positive definite. (G can be singular). Z is defined as the nullspace of A . Y is the basis spanned by A , and the matrix $[Y|Z]$ is non-singular. \vec{p} can be divided into two parts⁴.

$$\vec{p} = Y\vec{p}_y + Z\vec{p}_z \quad (5.146)$$

$Y\vec{p}_y$ is the particular solution to the constraints, and $Z\vec{p}_z$ is the movement along the constraints. If we substitute (5.146) into (5.116) we have the following two equations

$$\begin{aligned} AY\vec{p}_y &= -\vec{c} \\ -GY\vec{p}_y - GZ\vec{p}_z + A^T \tilde{\lambda} &= \vec{g} \end{aligned} \quad (5.147)$$

The first equation can be directly solved for \vec{p}_y . The second equation can be multiplied by Z to get

$$(Z^T G Z) \vec{p}_z = -(Z^T G Y \vec{p}_y + Z^T \vec{g}) \quad (5.148)$$

Equation (5.148) can be solved to obtain \vec{p}_z . We can then use (5.146) to obtain the final solution. The nullspace method is useful when the number of degrees of freedom is small, and thus $Z^T G Z$ is small and positive definite. This allows for special solvers such as Cholesky. (Remember K was not positive definite and thus could not be as easily solved.) The difficulty lies in determining the Z matrix.

Section 5.14 Return to Gradient Projection Method.

Having described the main components of the solution, the followings section will describe the algorithm in detail. The problem to solve is given again.

$$\begin{aligned} \min_{\vec{x}} J(\vec{x}) &= \frac{1}{2} \vec{x}^T G \vec{x} + \vec{x}^T \vec{d} \\ \text{subject to } l_i &\leq x_i \leq u_i \end{aligned} \quad (5.149)$$

Section 5.14.1 Part 1: Determining the Cauchy Point

The first step in the gradient projection method is to find the Cauchy point by moving along the steepest descent path and then bending the trajectory along the constraint when a constraint was encountered. The path of \vec{x} towards the Cauchy point is defined as⁴

$$\begin{aligned} \vec{x}(t) &= P(\vec{x}(0) - t \vec{g}, \vec{l}, \vec{u}) \\ P(\vec{x}, \vec{l}, \vec{u}) &= \begin{cases} l_i & \text{if } x_i < l_i \\ x_i & \text{if } l_i > x_i > u_i \\ u_i & \text{if } x_i > u_i \end{cases} \end{aligned} \quad (5.150)$$

where $-\vec{g}$ is the vector of steepest descent, $-\nabla J(\vec{x}_0)$, and t is the indexing variable. Since $J(x)$ is a quadratic function, it becomes a piecewise quadratic function between the breakpoints imposed by the constraints. Essentially along the solution path, there is a quadratic function between constraints. Because of this, we can quickly determine if there is a minimum value located between the constraints by calculating the location of the minimum value of the quadratic and

checking to see if it lies between the constraints. The first step is to locate the breakpoints. These values are given by

$$t_i^b = \begin{cases} \frac{(x_i(0) - u_i)}{g_i} & \text{if } g_i < 0 \text{ and } u_i < \infty \\ \frac{(x_i(0) - l_i)}{g_i} & \text{if } g_i > 0 \text{ and } l_i > -\infty \\ \infty & \text{if } g_i = 0 \text{ or } u_i = \pm\infty \end{cases} \quad (5.151)$$

Equations (5.150) and (5.151) can be combined so that the components of $\bar{x}(t)$ are given by

$$x_i(t) = \begin{cases} x_i(0) - tg_i & \text{if } t \leq t_i^b \\ x_i(0) - t_i^b g_i & \text{if } t > t_i^b \end{cases} \quad (5.152)$$

The next step is to re-order the breakpoints in ascending order and remove the duplicates. This allows us to look sequentially at each quadratic piecewise section to determine if a minimum value is found between those breakpoints.

$$[0, t_1^s], [t_1^s, t_2^s], [t_2^s, t_3^s], [t_3^s, t_4^s], \dots \quad (5.153)$$

where t^s are the breakpoint values in ascending order. If we assume that we are in between the two break points $[t_j, t_{j+1}]$, we can define a step direction p towards the next breakpoint as

$$\begin{aligned} \bar{x}(t) &= \bar{x}(t_j^s) + \Delta t \vec{p}_j \\ \vec{p}_{i,j} &= \begin{cases} -g_i & \text{if } t_j^s < t_i^b \\ 0 & \text{if } t_j^s \geq t_i^b \end{cases} \\ \Delta t &= t - t_j \quad \Delta t \in [0, t_{j+1} - t_j] \end{aligned} \quad (5.154)$$

where the j index represents the breakpoint and the i index represents the vector component. Essentially, a component of x will vary by g if the boundary has not yet been reached. If we substitute equation (5.154) into (5.149) we obtain

$$J(\bar{x}(t)) = (\vec{d}^T \bar{x}(t_j) + \frac{1}{2} \bar{x}(t_j)^T G \bar{x}(t_j)) + \Delta t (\vec{d}^T \vec{p}_j + \bar{x}(t_j)^T G \vec{p}_j) + \Delta t^2 (\vec{p}_j^T G \vec{p}_j) \quad (5.155)$$

From this equation we can quickly see that stationary point of the quadratic function is located at

$$\Delta t_{\min} = \frac{\vec{d}^T \vec{p}_j + \vec{x}(t_j)^T G \vec{p}_j}{\vec{p}_j^T G \vec{p}_j} \quad (5.156)$$

The point is a minimum point if

$$\vec{p}_j^T G \vec{p}_j > 0 \quad (5.157)$$

The minimum point must lie before the next break point for it to be valid.

$$\Delta t_{\min} \stackrel{?}{\in} [0, t_{j+1} - t_j) \quad (5.158)$$

If (5.158) is true, then the Cauchy point is given by

$$\vec{x}_c = \vec{x}(t_j + \Delta t_{\min}) \quad (5.159)$$

Also if

$$\vec{d}^T \vec{p}_j + \vec{x}(t_j)^T G \vec{p}_j > 0 \quad (5.160)$$

then the quadratic function is increasing at $\Delta t_{\min} = 0$. In either case, the Cauchy point is located at

$$\vec{x}_c = \vec{x}(t_j + \Delta t_{\min}) \quad (5.161)$$

If neither case happens then we move on to the next time interval and the process is repeated until a minimum value is found, or all the components of x are constrained. The above method leads to the following algorithm that was implemented in the MMA code **CauchyPoint[]**. (See below for syntax and usage.)

$$\vec{g} = G \bullet \vec{x}(0) + \vec{d}$$

Create $[t_1^b, t_2^b, \dots, t_n^b]$ from (5.147)

Sort into $[0, t_1^s, t_2^s, \dots, t_k^s]$

$$p_i = \begin{cases} -g_i & \text{if } t_i^b \neq 0 \\ 0 & \text{if } t_i^b = 0 \end{cases}$$

Create $\vec{m} = G \bullet \vec{p}$

Create $\vec{x} = \vec{x}(0)$

Begin Loop $j = 0, 1, 2, \dots, k$

$$f_1 = \vec{d}^T \vec{p} + \vec{x}^T \vec{m}$$

If $f_1 > 0$

$$\Delta t = 0$$

Break out of loop

$$f_2 = \vec{p} \bullet \vec{m}$$

$$\text{If } f_2 > 0 \text{ & } t_j^s \leq t_j^b - \frac{f_1}{f_2} < t_{j+1}^s$$

$$\Delta t = -\frac{f_1}{f_2}$$

Break out of loop

If $j = k$

$$\Delta t = t_k^s$$

Break out of loop

(5.162)

$$\text{Update } \vec{x} = (t_{j+1} - t_j) \vec{p}$$

$$\text{Update } \vec{m} = \vec{m} - G_i p_i$$

$$\text{Update } p_i = 0$$

where i is(are) the component(s) bounded at t_j^b

End Loop

$$\vec{x}_c = \vec{x}(t_j^b) + \Delta t$$

The update steps at the end of the for loop are designed to reduce the computational steps. Since G can be a large matrix, the right multiplication of \vec{p} can be very expensive. If the algorithm

was developed straight from the equations above, then the vector $G \cdot \vec{p}$ would have to be calculated twice per iterative loop. Instead, the vector is calculated only once at the beginning of the code. The vector multiplication is n times faster. Due to the simplicity of the constraints, we can easily update m by subtracting off the component of $G \cdot \vec{p}$ that hit the boundary at each iterative time step. This change is essential for the code to run efficiently.

The second step in the iterative process needs to know which variables are in the active set, along with the nullspace of the active constraint matrix. As stated earlier, typically the nullspace can be expensive to compute, however since we have simple bounded constraints, both the active constraint matrix and nullspace matrix are simply sparse matrices where each row is composed of zero's except for one index is a one. The column that the 1 is located in is associated with the index of a bounded constraint. The b vector lists the bounds for each constraint. For example, assume that there are five variables and that the Cauchy point lies on the lower bound of variable 2 & 3, and on the upper bound of variable 5. The resulting A, b, Z matrices are shown below.

$$\begin{aligned} A &= \begin{bmatrix} 0 & 1 & 0 & 0 & 0 \\ 0 & 0 & 1 & 0 & 0 \\ 0 & 0 & 0 & 0 & 1 \end{bmatrix} \\ \vec{b} &= [l_2 \ l_3 \ u_5] \\ Z^T &= \begin{bmatrix} 1 & 0 & 0 & 0 & 0 \\ 0 & 0 & 0 & 1 & 0 \end{bmatrix} \end{aligned} \tag{5.163}$$

The MMA code I wrote for finding the Cauchy point also outputs A, b, Z since the information is readily available and easily computed.

MATHEMATICA CODE: `CauchyPoint[G,d,l,u,x0]`

Description: *Find the Cauchy Point*

File: `Master EMFF Notebook.nb`

Section: `QPSolver`

Usage: *CauchyPoint*[*G,d,l,u,x₀*] = {*x_c,A,B,Z,s*}

x_c – The Cauchy Point

A – The Active Constraint Matrix

B – The Active Constraint Vector

Z – The Nullspace of *A*

s – List of Indices of Unbounded Variables

Example # 8 Cauchy Point

The following example uses the same *G* and *d* matrix and vectors from the previous example, but this time we are bounding the constraints from above and below using the following box constraints.

$$G = \begin{bmatrix} 10 & -2 & 0 & 0 & 0 \\ -2 & 2 & 1 & 0 & 0 \\ 0 & 1 & 1 & 0 & 0 \\ 0 & 0 & 0 & 4 & 0 \\ 0 & 0 & 0 & 0 & 1 \end{bmatrix} \quad \vec{d} = \begin{bmatrix} 2 \\ 4 \\ -6 \\ 3 \\ 5 \end{bmatrix} \quad \vec{l} = \begin{bmatrix} -5 \\ -2.25 \\ 0 \\ -\infty \\ -0.2 \end{bmatrix} \quad \vec{u} = \begin{bmatrix} 5 \\ 3 \\ 5 \\ 3 \\ 4 \end{bmatrix} \quad \vec{x}_0 = \begin{bmatrix} 1 \\ 1 \\ 1 \\ -2 \\ 1 \end{bmatrix} \quad (5.164)$$

The steepest descent direction is given by

$$-\vec{g} = \vec{p}_0 = [-10 \ -5 \ -5 \ 5 \ -6]^T \quad (5.165)$$

Because the search direction is in the $-g$ direction we know that the solutions will go towards the lower boundary for 1st, 2nd, 3rd and 5th components and on the upper boundary for the 4th component of *x*. The first step is to calculate the break points using (5.151)

$$\vec{t}^b = [0.15, 0.65, 0.2, 1.0, 0.2] \quad (5.166)$$

Next, we sort the break points, remove the duplicates and add a zero.

$$t^s = [0, 0.15, 0.2, 0.65, 1.0] \quad (5.167)$$

The first search range we look through is $t \in [0, 0.15]$. Calculating the characteristics of the quadratic we have

$$\begin{aligned} f_1 &= -211 \\ \Delta t_{\min} &= 0.164075 \end{aligned} \quad (5.168)$$

Since f_1 is negative, we know that the function is decreasing. The minimum value is located at 0.164075, but this value is outside the range, and the lower constraint on the first component of x will be reached (at 0.15) before we reach the minimum. Therefore we must move to the next range of $t \in [0.15, 0.2]$, but first we must update our new search direction to account for the new boundary. First we update our solution

$$\vec{x}(0.15) = \vec{x}(0) + 0.15 \vec{p}_0 = [-0.5 \ 0.25 \ 0.25 \ -1.25 \ 0.1]^T \quad (5.169)$$

To update \vec{p} all we do is simply set the component that reached the boundary to zero resulting in

$$\vec{p}_1 = [0 \ -5 \ -5 \ 5 \ -6]^T \quad (5.170)$$

The iteration is repeated resulting in

$$\begin{aligned} f_1 &= -53.1 \\ \Delta t_{\min} &= 0.109259 \end{aligned} \quad (5.171)$$

Once again, the quadratic function is continuing to decrease, and $\Delta t > (t_2^s - t_1^s)$. This time two variables reach their boundaries at the same time. The third and fifth variables reach their lower bound at $t=0.2$. Since we hit the boundary for two components, we must remove them both from \vec{p} .

$$\begin{aligned} \vec{x}(0.2) &= \vec{x}(0.15) + 0.05 \vec{p}_1 = [-0.5 \ 0 \ 0 \ -1 \ -0.2]^T \\ \vec{p}_2 &= [0 \ -5 \ 0 \ 5 \ 0] \end{aligned} \quad (5.172)$$

Solving for the next time interval $t \in [0.2, 0.65]$ we have

$$\begin{aligned}f_1 &= -30 \\ \Delta t_{\min} &= 0.2\end{aligned}\tag{5.173}$$

This time the minimum value is reached before the next boundary is reached. The resulting Cauchy point is thus

$$\vec{x}_c = \vec{x}(0.4) = \vec{x}(0.2) + 0.2 \vec{p}_2 = [-0.5 \ -1 \ 0 \ 0 \ -0.2]^T\tag{5.174}$$

The following figure is a plot of $J(x)$. The red points indicate the break points and the red lines are plots of $J(x)$ if the break point was not there. From the plot it is easy to see that the minimum is located at $x=0.4$.

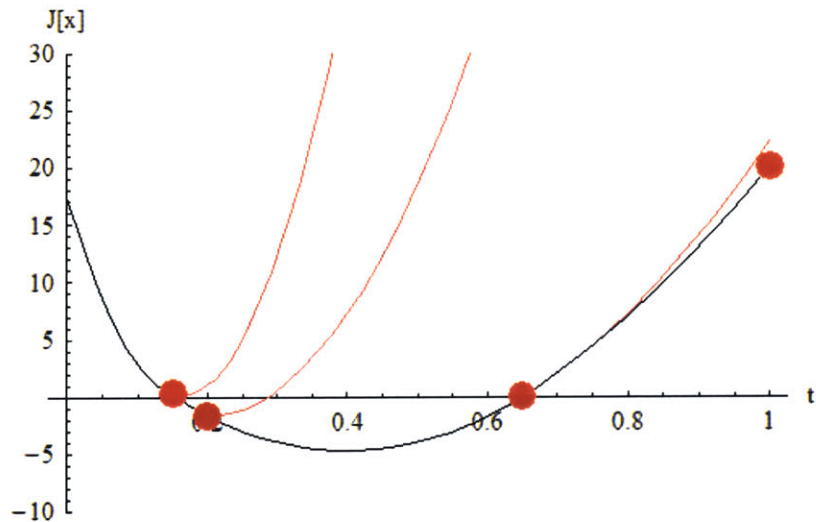


Figure 5-20: Plot of the Cost Function $J(x)$

Section 5.14.2 Part 2: Face Search

The second half of the iteration step, as described above, is to produce an improvement on the solution using the constraints created by finding the Cauchy point. If we use the box analogy for the constraints, this could be considered a search along one of the faces of the box.

$$\begin{aligned} \min_{\vec{x}} J(\vec{x}) &= \frac{1}{2} \vec{x}^T G \vec{x} + \vec{x}^T \vec{d} \\ \text{subject to } x_i &= x_i^c \quad i \in A \\ l_i &\leq x_i \leq u_i \quad i \notin A \end{aligned} \tag{5.175}$$

Once again, solving (5.175) can be very difficult. However, all that is needed is an improvement \vec{x}^+ on the Cauchy solution for convergence. This can be done using the nullspace method with the conjugate gradient method.

Our goal is now to find \vec{p} such that

$$\vec{x}^+ = \vec{x}_c + \vec{p} \text{ such that } J(\vec{x}^+) \leq J(\vec{x}_c) \tag{5.176}$$

Using the nullspace method, from equation (5.146), we are trying to find the minimization direction vector \vec{p} .

$$\vec{p} = Y\vec{p}_y + Z\vec{p}_z \tag{5.177}$$

\vec{p}_y is the component of the direction vector that brings the initial solution to a solution space that satisfies the constraints. Since our initial value already satisfies the constraints, \vec{p}_y is identically zero. Equation (5.147) simplifies to

$$\begin{aligned} \vec{0} &= \vec{0} \\ -GY\vec{p}_z + A^T \vec{\lambda} &= \vec{g} \end{aligned} \tag{5.178}$$

Multiplying through by Z , equation (5.148) can be simply written as

$$(Z^T G Z) \vec{p}_z = -Z^T \vec{g} \tag{5.179}$$

The matrix $Z^T G Z$ can easily be created by only keeping the rows and columns of G associated with the free variables (the variables that do not lie in the active set). Likewise the vector $Z^T \vec{g}$ can also simply be created in a similar manner. Equation (5.179) is now solved using a variation of the conjugate gradient method.

The conjugate gradient method assumes that no constraints are present. The equality constraints and active constraints are already incorporated into the solution by the nullspace method. Solving (5.179) will not violate those constraints. The other inequality constraints however are not represented by (5.179) and thus *could* be violated by the conjugate gradient method. Therefore to prevent the constraints from being violated, the method will be modified such that if a constraint boundary is reached, the iteration is stopped and the current solution is returned as the approximate minimum value. Since at each step in the conjugate gradient method, the solution is closer to the minimum than the previous step, we know that we will get a better solution than the Cauchy point every time.

Now since the Conjugate gradient algorithm also uses the variable \vec{p} , it can be confusing. Therefore, the algorithm described below is written to solve the following equation

$$\begin{aligned} \min_{\vec{x}} J(\vec{x}) &= \frac{1}{2} \vec{x}^T G \vec{x} + \vec{x}^T \vec{d} \\ \text{subject to } x_i &= x_i^c \quad i \in A \\ l_i &\leq x_i \leq u_i \quad i \notin A \end{aligned} \tag{5.180}$$

Remember, minimizing $\frac{1}{2} \vec{x}^T G \vec{x} + \vec{x}^T \vec{d}$ is equivalent to solving $G \vec{x} = -\vec{d}$. To change from equation (5.179) to (5.180) we must use the following conversions.

$$\begin{aligned} Z^T G Z &\rightarrow G \\ Z^T \vec{g} &\rightarrow \vec{d} \\ \vec{p}_z &\rightarrow \vec{x} \\ l_i - x_i^c | i \notin A &\rightarrow l_i \\ u_i - x_i^c | i \notin A &\rightarrow u_i \end{aligned} \tag{5.181}$$

The algorithm is given by

$$\vec{x}_0 = \vec{0}$$

$$\vec{r}_0 = G\vec{x}_0 + \vec{d}$$

$$\vec{p}_0 = -\vec{r}_0$$

Begin Loop k=1,2,...,n

$$\alpha_k = \frac{\vec{r}_k \vec{r}_k^T}{\vec{p}_k^T G \vec{p}_k}$$

$$\vec{x}_{k+1} = \vec{x}_k + \alpha_k \vec{p}_k$$

If $x_{k+1,i} > u_i$ OR $x_{k+1,i} < l_i$

$$\alpha_k = \min_{\substack{i \in [i|x_i > u_i] \\ j \in [j|x_j > u_j]}} \left(\frac{u_i - x_{k,i}}{p_{k,i}}, \frac{l_j - x_{k,j}}{p_{k,j}} \right)$$

$$\vec{x}_{k+1} = \vec{x}_k + \alpha_k \vec{p}_k$$

Break out of loop

$$\vec{r}_{k+1} = \vec{r}_k + \alpha_k G \vec{p}_k$$

$$\beta_{k+1} = \frac{\vec{r}_{k+1}^T \vec{r}_{k+1}}{\vec{r}_k^T \vec{r}_k}$$

$$\vec{p}_{k+1} = -\vec{r}_{k+1} + \beta_{k+1} \vec{p}_k$$

End of Loop

(5.182)

MATHEMATICA CODE: `QPConGradBC[G,d,l,u,x0]`

Description: Find the approximate minimum with bounding constraints.

File: Master EMFF Notebook.nb

Section: QPSolver

Usage: `QPConGradBC [G,d,l,u,x0]=x+`

x_o – Initial Solution

G – 2D Matrix

d – 1D Vector

l – Vector of lower constraints (-Infinity if variable is not constrained)

u – Vector of upper constraints -Infinity if variable is not constrained)

x^+ – Approximate minimum solution

**Example # 9 Application of the Nullspace Method and Gradient Projection Method
(Continuing Example # 8)**

Next, we continue the example from the Cauchy point section. The Cauchy point has been found and lies on the lower bound of the first, third, and fifth constraint. We are trying to minimize

$$\begin{aligned} \min_{\vec{x}} J(\vec{x}) &= \frac{1}{2} \vec{x}^T G \vec{x} + \vec{x}^T \vec{d} \\ \text{subject to} \\ x_1 &= -0.5 \\ x_3 &= 0 \\ x_5 &= -0.2 \\ -2 \leq x_2 &\leq 3 \\ -\infty \leq x_4 &\leq 3 \end{aligned} \tag{5.183}$$

At the Cauchy point, we have a cost value of

$$J(x_c) = -4.73 \tag{5.184}$$

The goal is to at least improve on this value, with the final goal of minimizing $J(x)$. Using the nullspace approach to solve (5.183), we must solve equation (5.179). Substituting, we are left with the following linear equation

$$\begin{bmatrix} 2 & 0 \\ 0 & 4 \end{bmatrix} \bar{p}_z = \begin{bmatrix} 3 \\ 3 \end{bmatrix} \tag{5.185}$$

We can't just solve (5.185) because $\vec{x}_c + \bar{p}_z$ may violate a constraint. Using the conjugate gradient method described above, we must solve (5.180) with the following change of variables

$$\begin{aligned}
 Z^T G Z &= \begin{bmatrix} 2 & 0 \\ 0 & 4 \end{bmatrix} \rightarrow G \\
 Z^T \vec{g} &= \begin{bmatrix} 3 \\ 3 \end{bmatrix} \rightarrow \vec{d} \\
 \vec{p}_z &\rightarrow \vec{x} \\
 l_i - x_c &= \begin{bmatrix} -1.25 \\ -\infty \end{bmatrix} \rightarrow l_i \\
 u_i - x_c &= \begin{bmatrix} 4 \\ 3 \end{bmatrix} \rightarrow u_i
 \end{aligned} \tag{5.186}$$

Using the algorithm of (5.182) we have

$$\begin{aligned}
 \vec{p}_0 &= [-3 \ -3]^T \\
 \alpha &= 0.3333 \\
 \vec{x}_1 &= [-1 \ -1]
 \end{aligned} \tag{5.187}$$

On the second iteration we have

$$\begin{aligned}
 \vec{p}_1 &= [-1.333 \ 0.6667]^T \\
 \alpha &= 0.375 \\
 \vec{x}_1 &= [-1.5 \ -0.75]
 \end{aligned} \tag{5.188}$$

This second solution violates the lower bound on the first component. We therefore must reduce alpha so that the solution is on the constraint.

$$\begin{aligned}
 \alpha &= 0.1875 \\
 \vec{x}_{\min} &= \vec{x}_1 = [-1.25 \ -0.875]
 \end{aligned} \tag{5.189}$$

This is the best we can do using the conjugate gradient method. The next step is to convert back to the original variables.

$$\vec{p} = Z \vec{p}_z = [0 \ -1.25 \ 0 \ -0.875 \ 0]^T \tag{5.190}$$

This gives a solution after one full iteration of

$$\vec{x}_1 = [-0.5 \ -2.25 \ 0 \ -0.875 \ -0.2]^T \quad (5.191)$$

The cost function is now

$$J(\vec{x}_1^+) = -8.011 \quad (5.192)$$

To find the minimum value for the original problem, we just re-iterate the process.

$$\begin{aligned} x_0 &= [1 \ 1 \ 1 \ -2 \ 1]^T & J(x_0) &= 17.5 \\ x_1^c &= [-0.5 \ -1 \ 0 \ 0 \ -0.2]^T & J(x_1^c) &= -4.73 \\ x_1^+ &= [-0.5 \ -2.25 \ 0 \ -0.875 \ -0.2]^T & J(x_1^+) &= -8.011 \\ x_2^c &= [-0.5 \ -2.25 \ 0.8268 \ -0.8249 \ -0.2]^T & J(x_2^c) &= -11.43 \\ x_2^+ &= [-0.5 \ -2.25 \ 0.825 \ -0.75 \ -0.2]^T & J(x_2^+) &= -11.45 \end{aligned} \quad (5.193)$$

The minimum value was found after just two iterations. The minimum value was verified by using the active set method along with using the built in minimization routine in MMA.

MATHEMATICA CODE: `QPGradProj[G,d,l,u,x0]`

Description: Find the solution to a boundary constrained QP.

File: Master EMFF Notebook.nb

Section: QPSolver

Usage: `QPGradProj[G,d,l,u,x0]=xmin`

x₀ – Initial Solution

G – 2D Matrix

d – 1D Vector

l – Vector of lower constraints (-Infinity if variable is not constrained)

u – Vector of upper constraints -Infinity if variable is not constrained)

x_{min} – Approximate minimum solution

Section 5.14.3 Synopsis

For solving quadratic programs, we have four routines in our arsenal.

- QPLinSolve
 - Solves unconstrained, and equality constrained QP.
 - Uses MMAs built in functions to solve the KKT matrix.
- QPConGrad
 - Solves unconstrained QP
 - Iterative method that uses conjugate vectors
- QPActiveSet
 - Solves inequality constrained QP
 - Uses QPLinSolve at each time step
- QPGradProj
 - Solves boxed constrained QP
 - Much faster than the active set method.

If we have a simple equality constrained QP, then either the QPLinSolve or the QPConGrad routine will work well. If there are inequality constraints then the active set method must be used. If we can reduce the problem to box constraints, then QPGradProj is the preferred routine to use.

Section 5.15 Application to EMFF

Example # 10 Minimizing the Angular Momentum Distribution for an EMFF System

The next section will apply the technique of minimizing the angular momentum at all points in time. The example will be similar to the previous example except the free dipole will have a magnitude of 60,000 Am². The initial dipole solution is

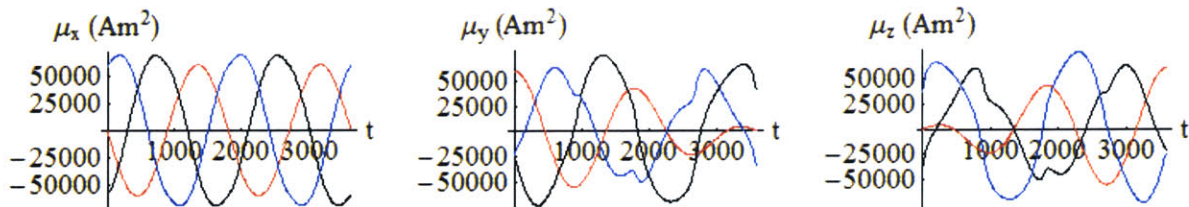


Figure 5-21: Initial Dipole Solution

This produces and angular momentum distribution of

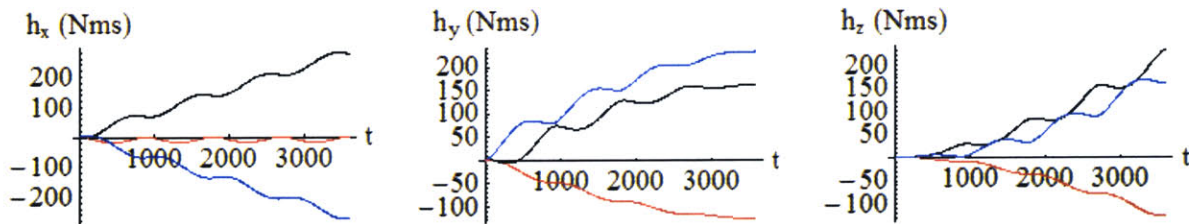


Figure 5-22: Initial Angular Momentum Distribution

From these plots it can be seen that the angular momentum distribution is not even among the satellites. Our goal is not to reduce the angular momentum to zero. Due to the conservation of angular momentum, the sum of angular momentum on each component cannot change. The goal is to have the angular momentum to be evenly distributed among the satellites. In the above figure this would be represented by having the lines in each plot coincide. Since we can't specifically control the torque distribution (from earlier section), the best we can do is have the solution oscillate about the average value.

The problem to solve is a quadratic program with bounded constraints as shown in equation (5.136). The matrix G and vector d are formed as described in equation (5.112). The following bounds were chosen

$$\begin{aligned}\vec{l} &= [-100000, -100000, -100000, \dots]^T \\ \vec{u} &= [100000, 100000, 100000, \dots]^T \\ \max \Delta\mu_i &= 10000 \text{Am}^2\end{aligned}\tag{5.194}$$

The l and u are bounds on the alphas while the max change in dipole strength is a bound on the change in dipole strengths between time steps. The bounds on the alphas (since the nullspace vectors have a length of one) can essentially be thought of bounds on the dipole solution. However, for this problem the bounds on the alphas are an order of magnitude larger than the bounds on the dipole solution. Therefore the bound on the change in dipole solution is really the limiting factor on the dipole solution.

The reason for this is two-fold. First, the bound on the change of the dipole solution isn't a ceiling constraint. Remember from equation (5.19)

$$\Delta\vec{\mu}_{\text{limited}} = \frac{\Delta\vec{\mu}}{\max(l, |\Delta\vec{\mu}_i|)} l\tag{5.195}$$

The largest component of the change in the dipole solution is found and the whole solution is scaled so that the largest component is not greater than the bound. Therefore if the change in the dipole solution is smooth, it will remain as such. This is different than just chopping dipole components off at a certain value. This would be given by the following formula

$$\Delta\vec{\mu}_{i,\text{limited}} = \min(u, \max(l, \Delta\vec{\mu}_i))\tag{5.196}$$

Equation (5.195) suffers from the problem that sometimes the dipole solution has large excursions away from the origin or singular type points. Because C is very large typically, one can assume that the space is spanned fairly well. However, if this is not the case, then the solution will typically have large excursions away from zero that dominate the solution. If the

solution is scaled by equation (5.195), then only the large excursion will remain in the solution and the rest of the information is lost. It is for this reason that the box constraints are implemented.

Continuing the example problem with the specified constraints, the conjugate gradient method is used to solve (5.136). The solution produces the following alpha values

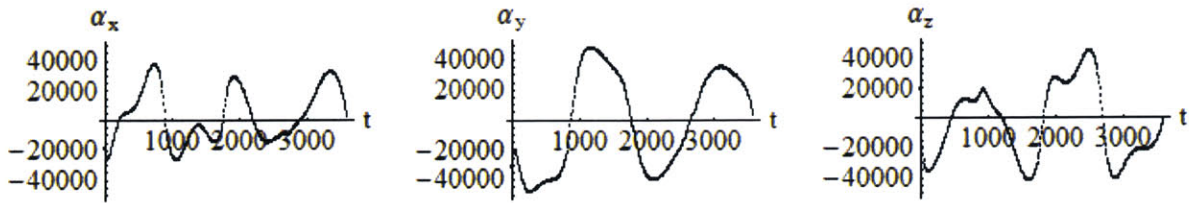


Figure 5-23: Alpha Values

In this example, the alpha values behaved well and remained below the bounds of 100,000. The change in dipole strength is calculated using equation (5.6). The linearization errors are removed from the dipole solution by re-solving the non-linear EOM with the new dipole solution as the initial value. This produced a change in dipole strength of

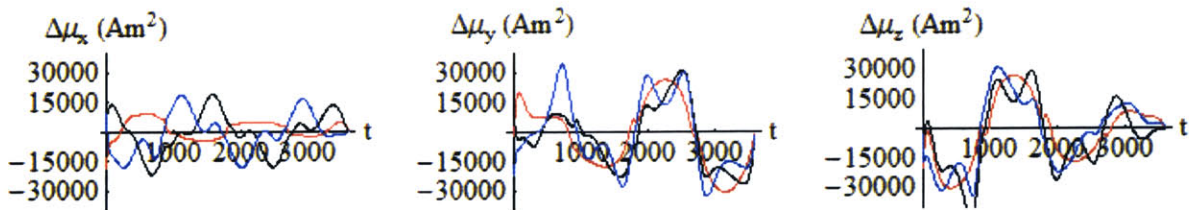
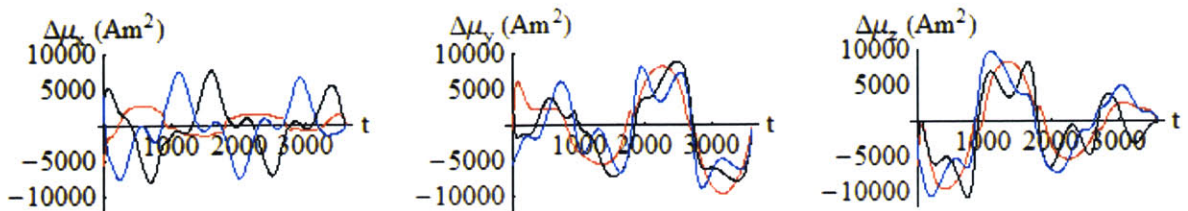


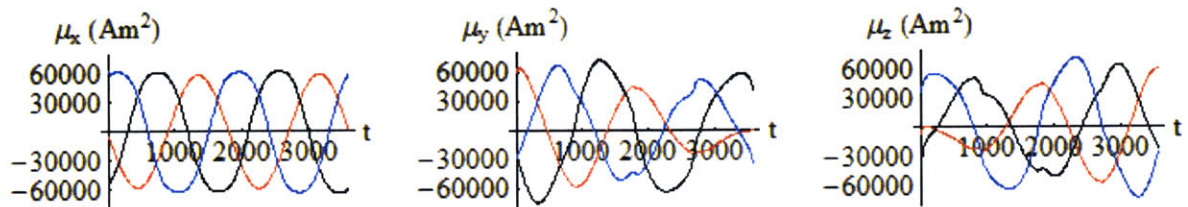
Figure 5-24: Un-scaled Change in Dipole Solution

Because the change in dipole strength is over the maximum allowable as specified in equation (5.195), the change in dipole strength is scaled using equation (5.195).

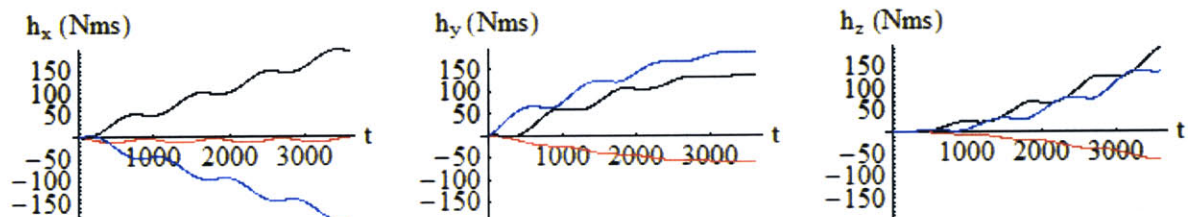
**Figure 5-25: Scaled Change in Dipole Solution**

The reason why the plots are not exact scales of each other is that the scaling operation is done before the resolving of the non-linear EOM step. Thus the solutions are slightly different.

Using the scaled change in the dipole solution produces the following dipole solution

**Figure 5-26: Resulting Dipole Solution After One Iteration**

And a resulting angular momentum distribution of

**Figure 5-27: Resulting Angular Momentum Distribution After One Iteration**

This is an improvement over the initial angular momentum distribution, but since we limited the change in the dipole solution, our goal was not met and the angular momentum was not driven all the way to equality. Therefore more iterations are performed.

After fifteen iterations, the angular momentum distribution has been driven to the desired goal.

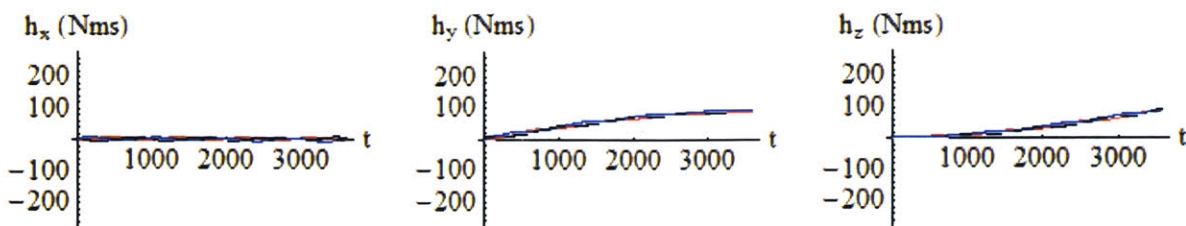


Figure 5-28: Final Angular Momentum Distribution

All three solutions have been aligned. Zooming-in on the plots, one can see that the solutions tend to oscillate around the mean angular momentum as expected.

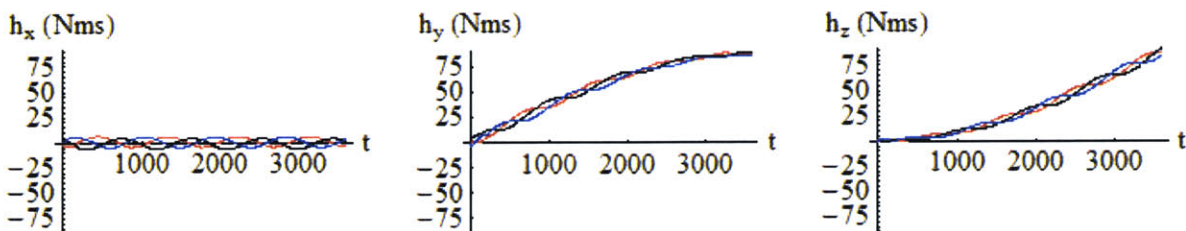


Figure 5-29: Final Angular Momentum Distribution (Zoomed In)

The overall change in the dipole solution is given by

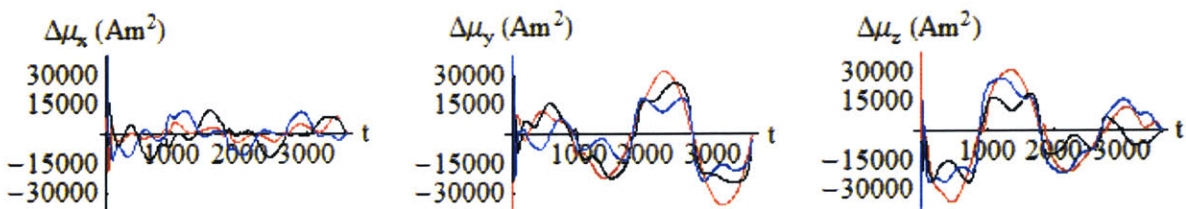
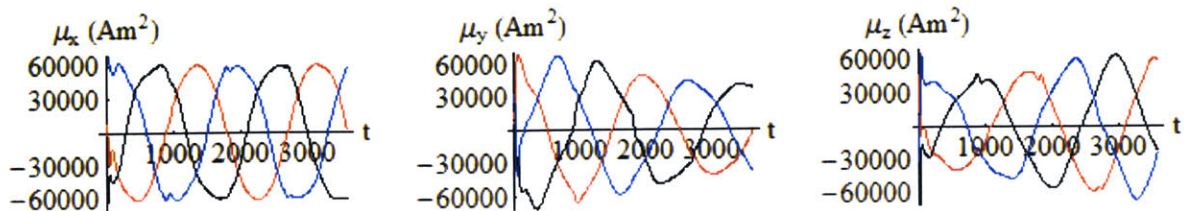


Figure 5-30: Overall Change in the Dipole Solution

The final dipole solution is given by

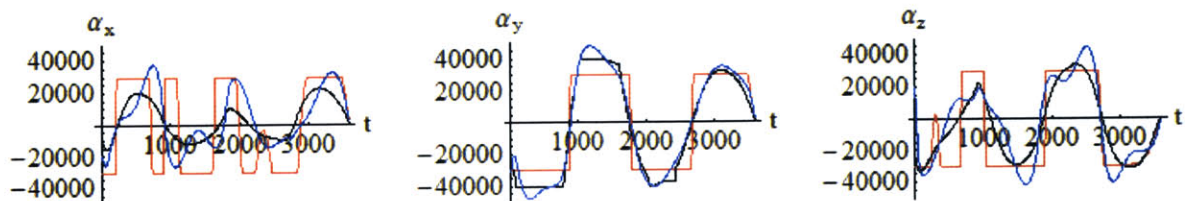
**Figure 5-31: Final Dipole Solution**

The final dipole solution, while different from the initial dipole solution isn't a drastic change from the initial dipole solution.

Section 5.15.2 Changing the Box Constraints

As an observation, when part of the solution lies on the boundary, it tends to drive every component of the solution to lie on the boundary. This makes intuitive sense. If a component of the solution is restricted by the boundary, other components will have to make up the slack so that the minimum is reached. Also, each alpha corresponds to a vector in the basis. Since the vectors don't point in the same direction, when a component of the solution is bounded, the other solutions will have to "work harder" to achieve the same goal. These phenomena have the combined effect that when a solution begins to encounter a boundary, it quickly lies completely on the boundary.

The following example looks at the effects of reducing the box constraints on the alphas from 100,000 (blue), to 40,000 (black), to 30,000 (red).

**Figure 5-32: Alpha Solutions with Varying Box Constraints**

The blue plot shows that the alphas are unrestricted since they are less than 100,000. The black plot shows that with a restriction of 40,000, only a small part of the solution is bounded. The rest remains fairly unchanged. However, when we solution is restricted to 30,000 (red), nearly the entire solution lies almost completely on the boundary. Even sections where the original alpha solution was less than 30,000 in the unbounded case move to the boundary when the solution is restricted to 30,000.

Example # 11 Box Constraints set to 10,000

The following example uses the box constraints set to 10,000. As expected, the alpha solutions lie exclusively on the boundary.

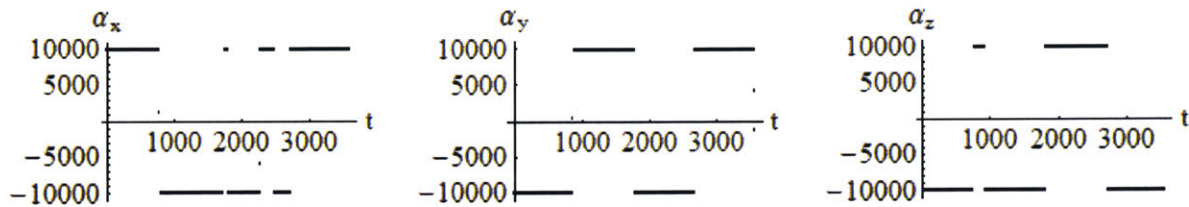


Figure 5-33: Alpha Solution with Box Constraints Limits at 10,000

This produces a change in the dipole solution of

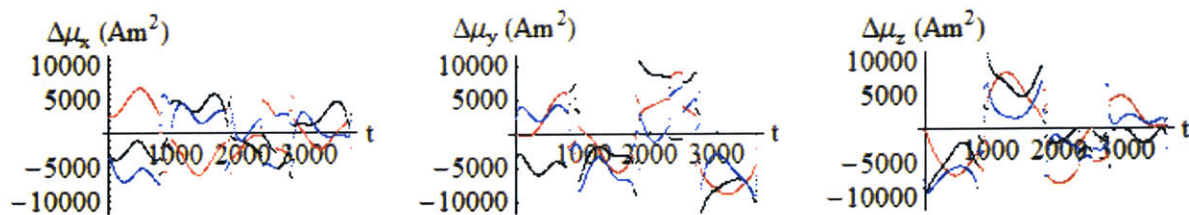
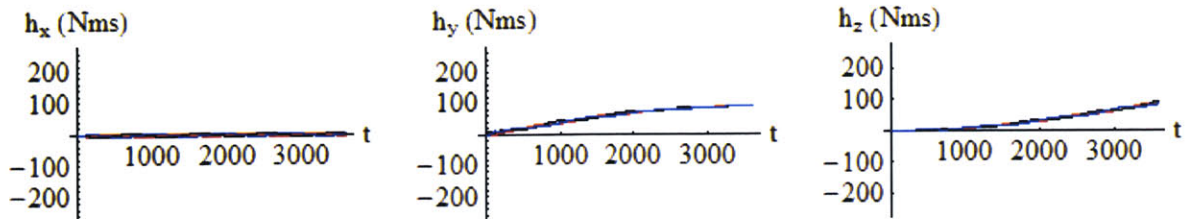
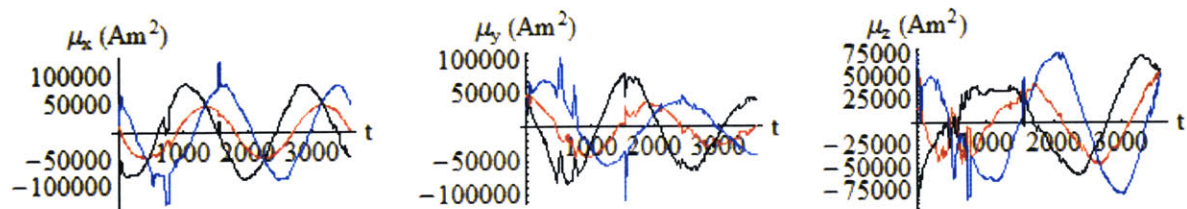


Figure 5-34: Resulting Change in Dipole Solution

Because the alphas did not vary smoothly, the change in dipole solution also does not vary smoothly. If we run through multiple iterations, we do achieve the desired torque solution

**Figure 5-35: Final Angular Momentum Distribution**

But the final dipole solution is not smooth

**Figure 5-36: Final Dipole Solution**

Therefore, when limiting the change in dipole solution it is better to use the limit given by equation (5.195) than to impose tight box constraints. However, the box constraints should be employed so that large singularities do not dominate the solution.

Section 5.15.3 Solutions that Move Into the Imaginary Plane

Above, we were able to move the initial solution to one that produced the desired angular momentum distribution. Sometimes when adjusting the solution, the solution begins to have imaginary components.

Example # 12 Different Initial Solution

In the above example there were two possible initial solutions. The second dipole solution is given by

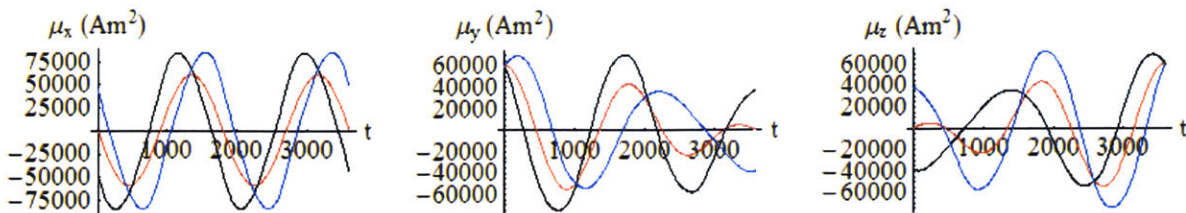


Figure 5-37: Initial Dipole Solution

This dipole solution produces an angular momentum distribution of

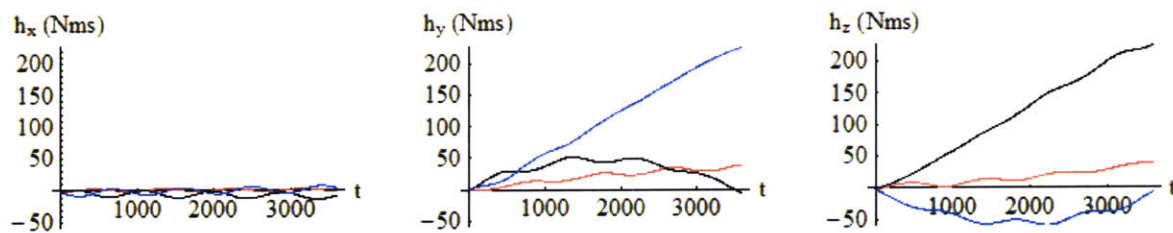


Figure 5-38: Initial Angular Momentum Distribution

The first iterative step goes without a problem producing an alpha solution of

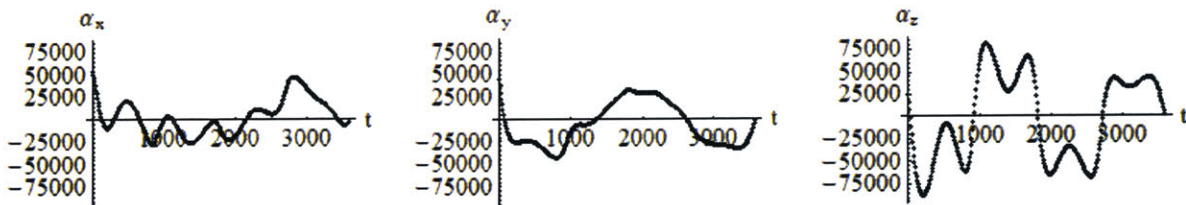


Figure 5-39: Alpha Solutions

and a change in dipole solution which has been limited to 10,000 of

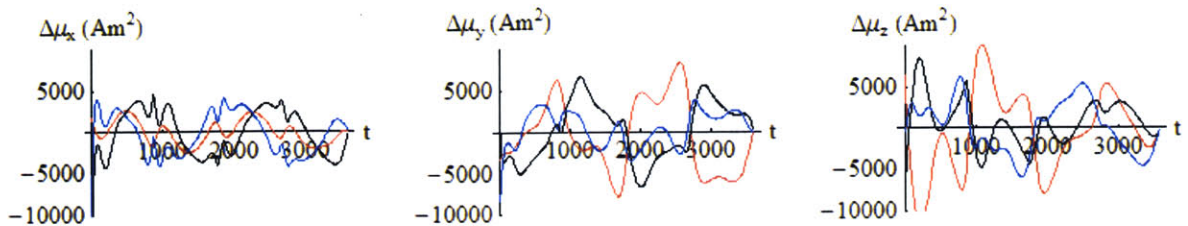


Figure 5-40: Initial Change in Dipole Solution

At the second iterative step, the desired change in dipole solution (before running it through the non-linear EOM) is

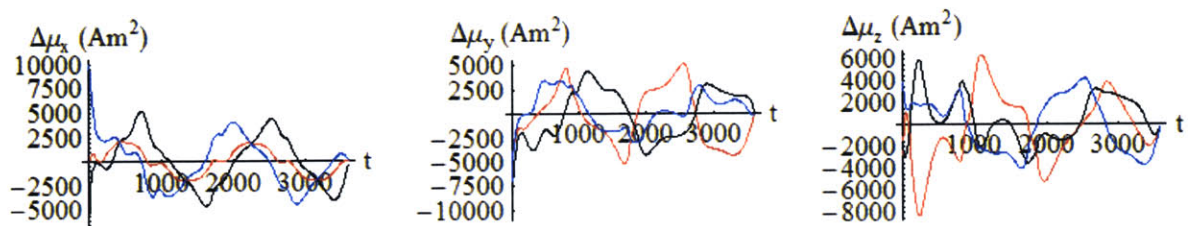


Figure 5-41: Change in Dipole Solution - Second Iteration

When we apply this change in dipole solution and then run the changed solution through the non-linear EOM (assuming that the first dipole is fixed), we find that the solution becomes imaginary from $t = 50, 740 \leq t \leq 790, 2630 \leq t \leq 2800$. Once the solution becomes imaginary, it becomes difficult to decide on a method to continue the minimization process. One solution is not to change the part of the solution that would become imaginary. This will lead to discretizations of the solution because some points will be changing while others don't. Using this method, the angular momentum can still be brought close to the desired distribution.

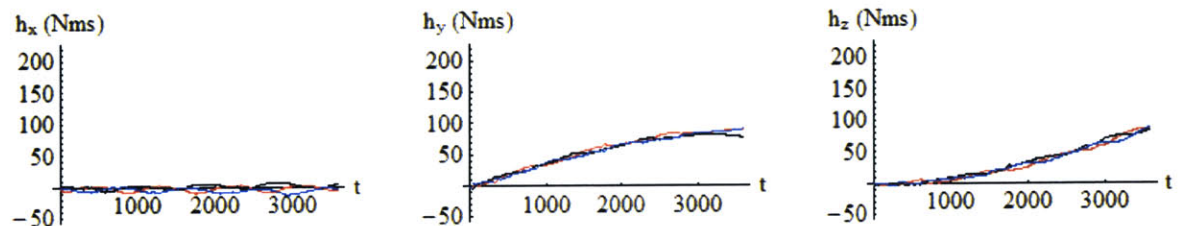


Figure 5-42: Final Angular Momentum Distribution

The resulting dipole solution is

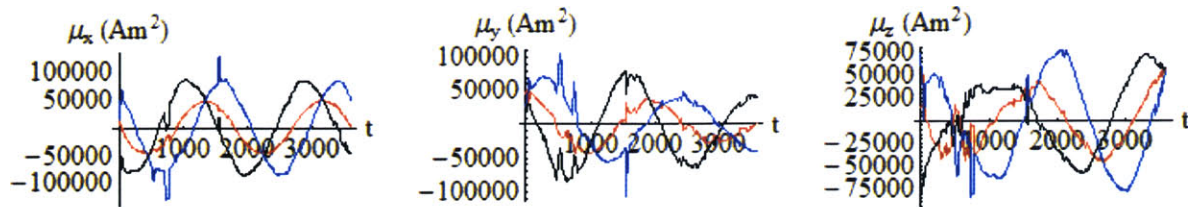


Figure 5-43: Final Dipole Solution

Because the sections that would have become imaginary didn't change, the dipole solution ends up discretized. Therefore when a solution begins to have imaginary sections it is typically best to attempt a different initial dipole solution.

Section 5.16 Conclusions

In this section, we started with a dipole solution that was created by using an arbitrarily chosen free dipole. This solution, while satisfying the force constraints, typically produces an undesirable torque and angular momentum distribution. Because of the existence of the free dipole, there is room to adjust the dipole solution and produce a better torque and angular momentum distribution. However, there is a limit to the degree of control that is available to change the torque distribution, and it is not possible to find a direct solution for satellite formations containing more than two satellites. A change in dipole solution was made under the constraint that the force distribution remained unchanged. To accomplish this, the EOM were linearized and the nullspace of the linearized EOM was found. The nullspace described the allowable changes in the dipole solution. Three different desired conditions or end goals were discussed: specifying the torque at one point in time, specifying the angular momentum at one point in time, and minimizing the angular momentum distribution over all time.

When attempting to minimize the torque at one point in time, difficulties arose due to the fact that the free dipole only allows for control of three dimensions of a 3N-3 dimensions space where N is the number of vehicles. This was also represented by the fact that the nullspace, in

which the solution could move, had a dimension of three. By not having the ability to completely move through the 3N-3 space, the desired torque distribution could not be achieved while maintaining the desired force distribution. Therefore, the ‘closest’ or minimum solution was obtained. Due to the non-linearity of the EOM, there were multiple minimum local solutions. The global solution was found by randomly searching the space.

When attempting to specify the angular momentum distribution at one point in time, there was a greater ability to change the desired angular momentum distribution. Since the angular momentum distribution at one point in time is based on the torque distribution at every point in time leading up to the specified time, the desired angular momentum distribution could be changed by not only the dipole solution at the specified time, but at all the previous time steps. Because at each time step the solution can move through a slightly different space, the overall space in which the final dipole solution could move was large and typically complete. The desired angular momentum could be achieved.

Finally, instead of specifying the angular momentum distribution at one point in time, the goal was to specify the angular momentum distribution at all points in time. Just like trying to specify the torque distribution, there aren’t enough degrees of control to completely specify the angular momentum distribution at every point in time. Therefore, the goal is to instead minimize the angular momentum distribution at every point in time. This formulation presents itself as a quadratic cost function with linear constraints. This problem is called a quadratic program. Much work has been done on quadratic programming, and two solution methods were explored and implemented: the active set method, and the gradient projection method. The latter was used for the EMFF example because of its speed in finding a solution.

The goal of this section was to present and implement different methods of adjusting the dipole solution to achieve a goal. This chapter has laid out a framework for doing just that. Besides discussing and implementing methods for the three cases above (which are believed to be necessary for every mission), the framework presented can easily be adjusted to accomplish other goals that the mission may place on the dipole solution. The following chapters will look at

specific mission constraints such as working in LEO and in the presence of Earth's magnetic field.

Chapter 6

THE EARTH'S GRAVITATIONAL FIELD

Using EMFF in low earth orbit (LEO) produces a new set of challenges. The two primary challenges that are addressed in this thesis are the effects of the Earth's magnetic field and the Earth's gravitational field including the J₂ geopotential. The gravitational field is addressed in this chapter, while the Earth's magnetic field will be addressed in Chapter 7.

Section 6.1 Operating within the Earth's Gravitational Field (Spherical Earth)

When operating in LEO, satellite formations are affected by the Earth's gravitational forces. In this section the Earth is modeled as a perfect sphere, and the formation is in a circular orbit. To calculate the relative forces on the satellites in the formation, the Clohessy-Wiltshire (CW) or Hill's equations are used. In the following section the equations developed by Schweighart and Sedwick^{14,37} are used to include the effects of the J₂ geopotential.

Section 6.1.1 The CW Equations

The CW equations are derived by linearizing the gravitational forces about a circular reference orbit. The result is a set of three differential equations of motion.¹

$$\begin{aligned}\frac{\vec{F}_{\hat{x}}^{CW}}{m} &= 3n^2 \hat{x} + 2n\hat{y}' \\ \frac{\vec{F}_{\hat{y}}^{CW}}{m} &= -2n\hat{x}' \\ \frac{\vec{F}_{\hat{z}}^{CW}}{m} &= -n^2 \hat{z}\end{aligned}\tag{6.1}$$

The coordinates $(\hat{x}, \hat{y}, \hat{z})$ are a local curvilinear coordinate system that rotates with the formation as it orbits the Earth. The \hat{x} direction points in the radial (zenith) direction. The \hat{z} direction is normal to the orbital plane, and the \hat{y} direction points in the plane and in the direction of motion.

In this chapter the origin will be located at the formation's center of mass so that the sum of the gravitational forces remains zero. n is the orbital frequency and is given by

$$n = \sqrt{\frac{\hat{\mu}}{r^3}} \quad (6.2)$$

$\hat{\mu}$ is the gravitational constant for the Earth and is given by the following equation. r is the orbital radius of the formation. The caret is included to avoid confusion with the magnetic dipoles.

$$\hat{\mu} = 3.986e5 \frac{\text{km}^3}{\text{s}^2} \quad (6.3)$$

Up to this point, an inertial coordinate system has been used. This is because the coordinate system had no need to rotate, but more importantly the angular momentum and torque calculations are all inertially based. Therefore the accelerations produced in equation (6.1) will be converted through a series of coordinate transformations to an inertial coordinate system with its origin at the center of mass of the formation.

Section 6.1.2 Free Orbit Ellipse

Solving the CW equations and setting the initial conditions so that the satellites remain in formation results in a set of equations that describe a zero-force formation. These formations are called “free orbit ellipses”. Essentially satellites in a free-orbit ellipse do not need to expend any propellant to stay in formation (according to the CW equations). These solutions are

$$\begin{aligned}\hat{x} &= \hat{x}_0 \cos nt + \hat{y}_0 \sin nt \\ \hat{y} &= \hat{y}_0 \cos nt - 2x_0 \sin nt \\ \hat{z} &= \hat{z}_0 \cos nt + \frac{\hat{z}'}{n} \sin nt\end{aligned} \quad (6.4)$$

From the equations, it can be seen that the \hat{x} and the \hat{y} motion are coupled. The satellites in the free orbit ellipse orbit around the origin once per orbit. The formation always projects a 1x2 ellipse onto the $\hat{x} - \hat{y}$ plane.

Unfortunately many missions require configurations that are not free-orbit ellipses. Because of this, they will have to expend propellant, or use EMFF to provide the necessary forces to remain in formation. Three such configurations are explored in the following section. The first configuration is a formation in which the satellites remain fixed with respect to the rotating coordinate system. Such a formation would be useful for Earth-looking telescopes. The second formation type is a fixed formation with respect to the inertial coordinate system. Such a formation would be useful for space-looking telescopes. Finally, interferometer missions require the satellites to remain in a specified formation and rotate in a plane perpendicular to the object they are imaging. This is the third configuration evaluated.

Section 6.1.3 Incorporating the Gravitational Forces into the EOM

The gravitational forces, \vec{F}_j^G are incorporated into the EOM.

$$\begin{aligned}\vec{F}_1(\vec{r}_1, \dots, \vec{r}_N, \vec{\mu}_1, \dots, \vec{\mu}_N) - \vec{f}_1 + \vec{F}_1^G &= 0 \\ \vec{F}_2(\vec{r}_1, \dots, \vec{r}_N, \vec{\mu}_1, \dots, \vec{\mu}_N) - \vec{f}_2 + \vec{F}_2^G &= 0 \\ &\vdots \\ \vec{F}_{N-1}(\vec{r}_1, \dots, \vec{r}_N, \vec{\mu}_1, \dots, \vec{\mu}_N) - \vec{f}_{N-1} + \vec{F}_{N-1}^G &= 0 \\ \vec{F}_N(\vec{r}_1, \dots, \vec{r}_N, \vec{\mu}_1, \dots, \vec{\mu}_N) - \vec{f}_N + \vec{F}_N^G &= 0\end{aligned}\tag{6.5}$$

Recall that \vec{F}_j is the magnetic force produced on satellite j , and \vec{f}_j is the desired force acting on satellite j . The next sections will determine the magnetic forces necessary to hold a satellite formation in a given configuration. They also will examine the torques and average angular momentum change placed on the formation by the Earth's gravitational potential.

Section 6.1.4 Stationary Formations Relative to the Rotating Coordinate Frame

One possible mission application would be an Earth observing telescope where one satellite is the primary mirror, and the second satellite is the secondary mirror. These satellites are held in a stationary position relative to the local rotating coordinate system.

These formations are typically not standard Hill's formations and require applied forces to maintain their configuration. For these derivations, the satellites have the same mass, and the center of the coordinate system coincides with the center of mass. The satellites' fixed position relative to the rotating coordinate system is

$$\vec{r}^{(R)} = \begin{pmatrix} \hat{x} \\ \hat{y} \\ \hat{z} \end{pmatrix} \quad (6.6)$$

The gravitational forces given by the CW equations are

$$\vec{F}^{CW(R)} = m \begin{pmatrix} 3\hat{x}n^2 \\ 0 \\ -\hat{z}n^2 \end{pmatrix} \quad (6.7)$$

The forces are now converted to an inertial coordinate system. The inertial coordinate system (*X-Y-Z*) is initially aligned with the rotating coordinate system. θ is the true anomaly of the formation which can be visualized as the angle by which the rotational coordinate system is rotated along its \hat{z} axis to align with the inertial coordinate system.

When converting over, it is important to remember the centrifugal and Coriolis accelerations introduced by the rotating coordinate system in addition to the gravitational forces from the CW equations.

$$\vec{F}^G = m \begin{pmatrix} n^2(2x \cos \theta + y \sin \theta) \\ n^2(2x \sin \theta - y \cos \theta) \\ -z n^2 \end{pmatrix} \quad (6.8)$$

The desired force profile is given by,

$$\vec{f} = m \begin{pmatrix} -n^2(x \cos \theta - y \sin \theta) \\ -n^2(x \sin \theta + y \cos \theta) \\ 0 \end{pmatrix} \quad (6.9)$$

From equation (6.5), the forces that the EMFF system will have to produce are

$$\vec{F}_1 = m \begin{pmatrix} 3n^2x \cos \theta \\ 3n^2x \sin \theta \\ -z n^2 \end{pmatrix} \quad \vec{F}_2 = m \begin{pmatrix} -3n^2x \cos \theta \\ -3n^2x \sin \theta \\ z n^2 \end{pmatrix} \quad (6.10)$$

When these forces are produced, the following torques are placed onto the satellite formation.

$$\vec{\tau}_j = \vec{F}_j \times \vec{r}_j$$

$$\vec{\tau} = m \begin{pmatrix} (y \cos \theta + 4x \sin \theta) z n^2 \\ (4x \cos \theta - y \sin \theta) z n^2 \\ -3xy n^2 \end{pmatrix} \quad (6.11)$$

Averaging the torques over the course of one orbital period results in the following time averaged torque.

$$\vec{\tau}_{avg} = m \begin{pmatrix} 0 \\ 0 \\ -3xy n^2 \end{pmatrix} \quad (6.12)$$

From equation (6.12), it can be seen that any in-plane offset (except when $x = 0$ or $y = 0$) will produce an average torque in the z direction that will cause a buildup in the angular momentum stored on the reaction wheels.

The next section provides a series of examples that show the forces and torques for a two satellite formation oriented in different directions. In these examples, each satellite has a mass of 400 kg. The formation is at an altitude of 500km and an inclination of 0^0 . The satellites are separated by a distance of 10m.

Example # 1 In-Plane Offset

In this formation, two vehicles are in the same orbit but have different true anomalies.

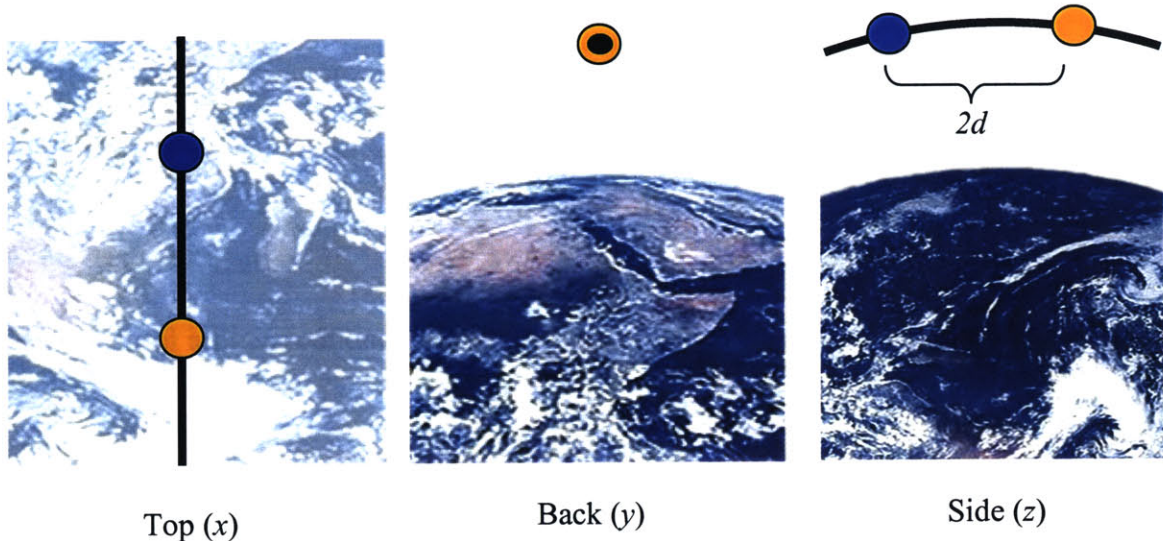


Figure 6-1: In-Plane Offset

This formation is relatively trivial to analyze. Assuming the satellites have equal mass, their relative position is given by

$$\vec{r}_1^{(R)} = \begin{pmatrix} 0 \\ 5 \\ 0 \end{pmatrix} \text{m} \quad \vec{r}_2^{(R)} = \begin{pmatrix} 0 \\ -5 \\ 0 \end{pmatrix} \text{m} \quad (6.13)$$

Substituting equation (6.13) into (6.1) and incorporating in the accelerations due to the rotating coordinate system shows that no forces are needed.

$$\vec{F}_1^{G(R)} = \vec{F}_1^G = \begin{pmatrix} 0 \\ 0 \\ 0 \end{pmatrix} \quad \vec{F}_2^{G(R)} = \vec{F}_2^G = \begin{pmatrix} 0 \\ 0 \\ 0 \end{pmatrix} \quad (6.14)$$

Satellites in this formation do not require the EMFF vehicle to provide any forces or absorb any angular momentum.

Example # 2 Cross-Track Offset

In the second formation, two satellites only vary in their cross-track position. In this configuration, if uncontrolled, the satellites will oscillate along the z axis.

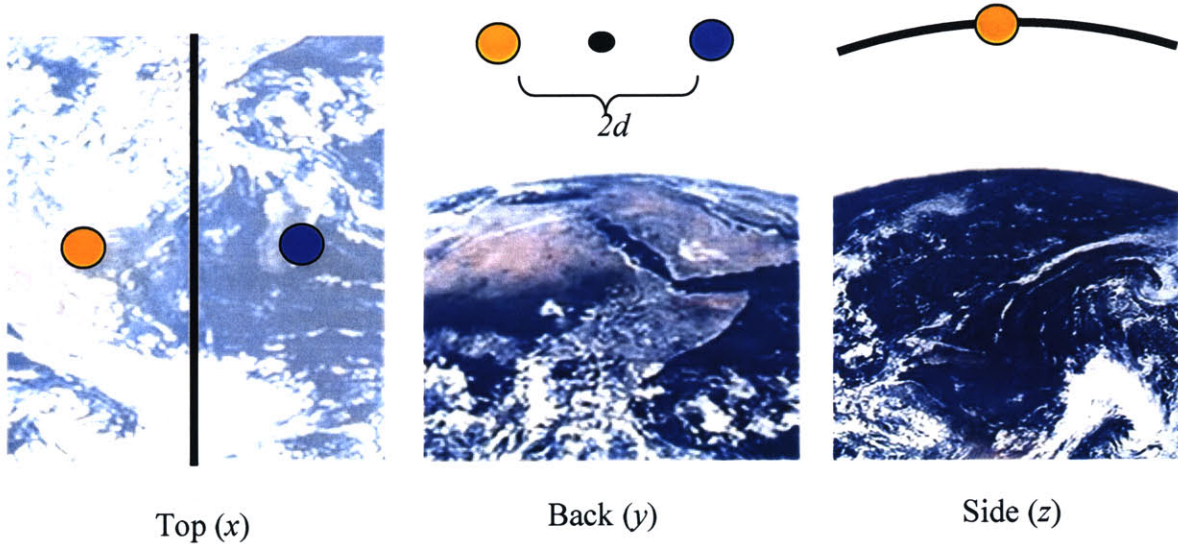


Figure 6-2: Cross-Track Offset

Their positions are given by

$$\vec{r}_1^{(R)} = \begin{pmatrix} 0 \\ 0 \\ 5 \end{pmatrix} \text{m} \quad \vec{r}_2^{(R)} = \begin{pmatrix} 0 \\ 0 \\ -5 \end{pmatrix} \text{m} \quad (6.15)$$

Substituting into equation (6.1) produces the following forces.

$$\vec{F}_1^{CW(R)} = \begin{pmatrix} 0 \\ 0 \\ -2.5 \end{pmatrix} \text{mN} \quad \vec{F}_2^{CW(R)} = \begin{pmatrix} 0 \\ 0 \\ 2.5 \end{pmatrix} \text{mN} \quad (6.16)$$

The resulting required EMFF forces (in the inertial coordinate system are)

$$\vec{F}_1 = \begin{pmatrix} 0 \\ 0 \\ 2.5 \end{pmatrix} \text{mN} \quad \vec{F}_2 = \begin{pmatrix} 0 \\ 0 \\ -2.5 \end{pmatrix} \text{mN} \quad (6.17)$$

These forces can be created with a dipole solution of

$$\vec{\mu}_1^{(R)} = \begin{pmatrix} 0 \\ 0 \\ 6390.04 \end{pmatrix} \text{Am}^2 \quad \vec{\mu}_2^{(R)} = \begin{pmatrix} 0 \\ 0 \\ -6390.4 \end{pmatrix} \text{Am}^2 \quad (6.18)$$

Note that this is only one of many possible dipole solutions that could create this force. The torque on the formation is given by

$$\bar{\tau}^{CW} = 0 \quad (6.19)$$

In this configuration no torques are produced, and thus no angular momentum needs to be stored.

Example # 3 Radial Offset

In this configuration, both satellites orbit with the same orbital period, but one satellite has a higher altitude than the other satellite. Normally, given the difference in altitude, the periods of the satellites would be different, so active control is required.

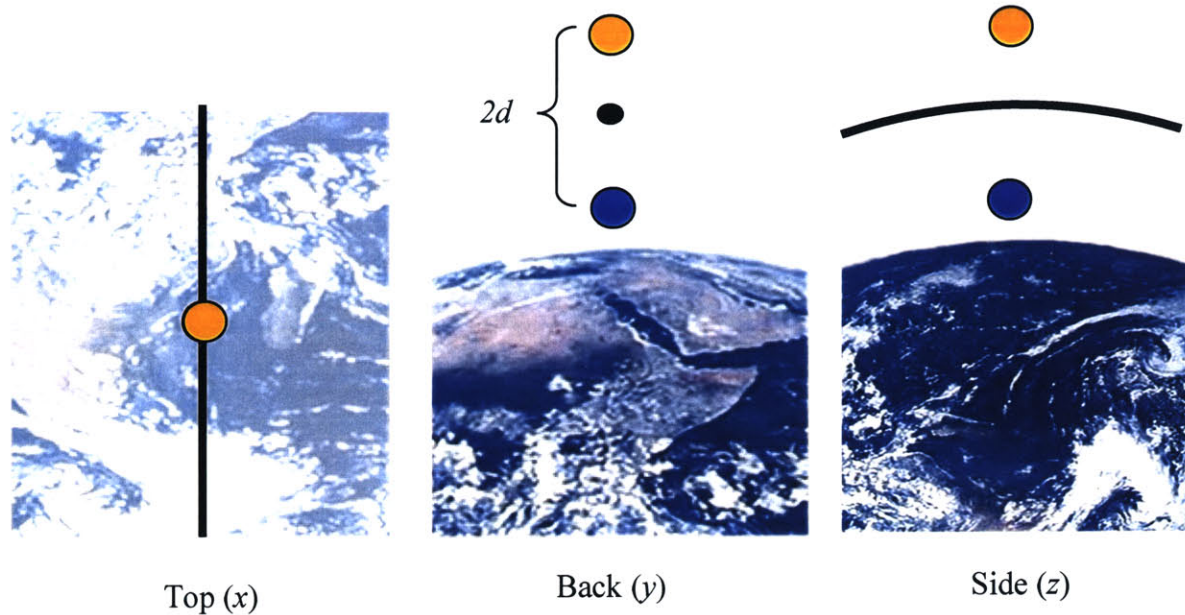


Figure 6-3: Radial Offset

The satellite positions are given by

$$\vec{r}_1^{(R)} = \begin{pmatrix} 5 \\ 0 \\ 0 \end{pmatrix} \quad \vec{r}_2^{(R)} = \begin{pmatrix} -5 \\ 0 \\ 0 \end{pmatrix} \quad (6.20)$$

Substituting into equation (6.1) produces the following forces.

$$\vec{F}_1^{CW(R)} = \begin{pmatrix} 7.35 \\ 0 \\ 0 \end{pmatrix} \text{mN} \quad \vec{F}_2^{CW(R)} = \begin{pmatrix} -7.35 \\ 0 \\ 0 \end{pmatrix} \text{mN} \quad (6.21)$$

The resulting required EMFF forces in the inertial frame are

$$\vec{F}_1 = \begin{pmatrix} -7.35 \cos \theta \\ -7.35 \sin \theta \\ 0 \end{pmatrix} \text{mN} \quad \vec{F}_2 = \begin{pmatrix} 7.35 \cos \theta \\ 7.35 \sin \theta \\ 0 \end{pmatrix} \text{mN} \quad (6.22)$$

These forces can be produced with the following dipole strengths.

$$\vec{\mu}_1^{(R)} = \begin{pmatrix} 9306.93 \\ 0 \\ 0 \end{pmatrix} \text{Am}^2 \quad \vec{\mu}_2^{(R)} = \begin{pmatrix} 9306.93 \\ 0 \\ 0 \end{pmatrix} \text{Am}^2 \quad (6.23)$$

The torque produced on the satellite formation is

$$\vec{\tau} = \begin{pmatrix} 0 \\ 0 \\ 0 \end{pmatrix} \text{Nm} \quad (6.24)$$

Example # 4 Side-Looking

The next example is a side looking formation.

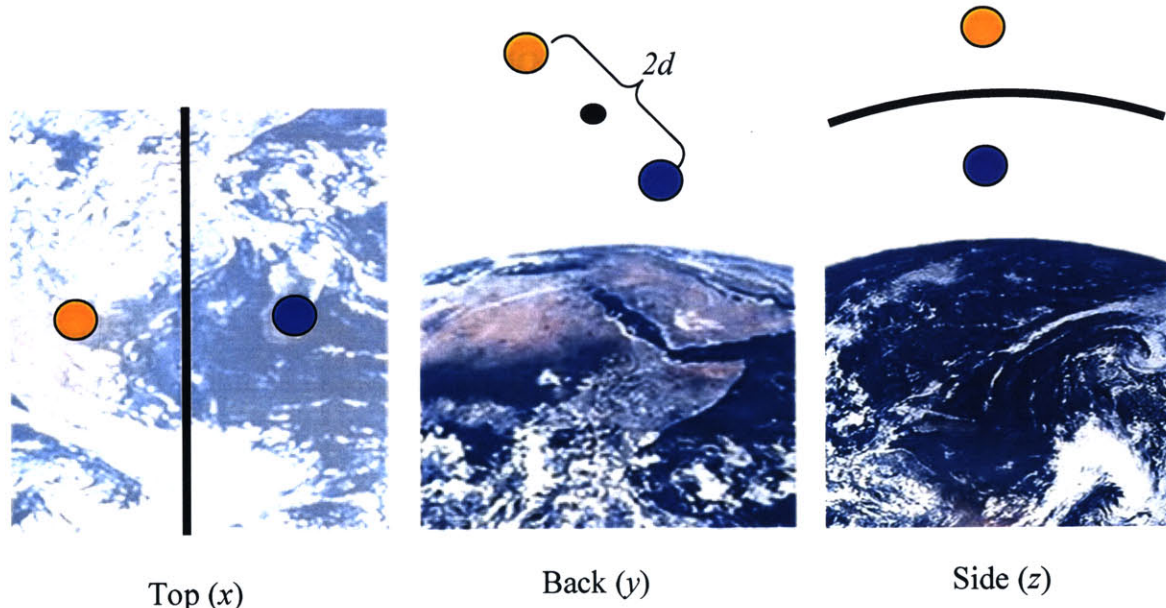


Figure 6-4 Side-Looking Offset

Their positions are given in the rotating coordinate system by

$$\vec{r}_1^{(R)} = \begin{pmatrix} \frac{5}{\sqrt{2}} \\ 0 \\ \frac{5}{\sqrt{2}} \end{pmatrix} \text{m} \quad \vec{r}_2^{(R)} = \begin{pmatrix} -\frac{5}{\sqrt{2}} \\ 0 \\ -\frac{5}{\sqrt{2}} \end{pmatrix} \text{m} \quad (6.25)$$

Substituting into equation (6.1) produces the following forces.

$$\vec{F}_1^{CW(R)} = \begin{pmatrix} 5.20 \\ 0 \\ -1.73 \end{pmatrix} \text{mN} \quad \vec{F}_2^{CW(R)} = \begin{pmatrix} -5.20 \\ 0 \\ 1.73 \end{pmatrix} \text{mN} \quad (6.26)$$

The required EMFF forces are

$$\vec{F}_1 = \begin{pmatrix} -5.20 \cos \theta \\ -5.20 \sin \theta \\ 1.73 \end{pmatrix} \text{mN} \quad \vec{F}_2 = \begin{pmatrix} 5.20 \cos \theta \\ 5.20 \sin \theta \\ -1.73 \end{pmatrix} \text{mN} \quad (6.27)$$

The torques are given by

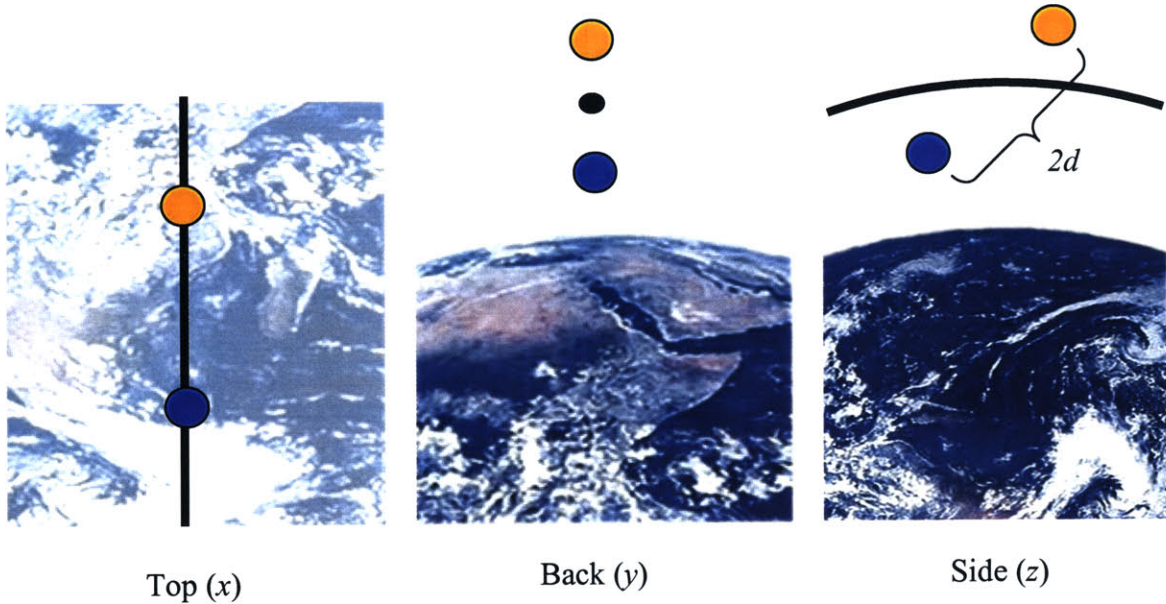
$$\vec{\tau} = m \begin{pmatrix} -51.9 \sin \theta \\ 51.9 \cos \theta \\ 0 \end{pmatrix} \text{mNm} \quad (6.28)$$

Integrating over one orbital period, the angular momentum accumulated by the formation is zero. However, during the orbit, the formation must store up to

$$H_{\max} = 44.27 \text{ Nms} \quad (6.29)$$

Example # 5 Forward-Looking

The final example is a forward-looking formation.

**Figure 6-5 Forward Looking Offset**

Their positions are given in the rotating coordinate system by

$$\vec{r}_1^{(R)} = \begin{pmatrix} \frac{5}{\sqrt{2}} \\ -\frac{5}{\sqrt{2}} \\ 0 \end{pmatrix} \text{m} \quad \vec{r}_2^{(R)} = \begin{pmatrix} -\frac{5}{\sqrt{2}} \\ \frac{5}{\sqrt{2}} \\ 0 \end{pmatrix} \text{m} \quad (6.30)$$

Substituting into equation (6.1) produces the following forces.

$$\vec{F}_1^{CW(R)} = \begin{pmatrix} 5.20 \\ 0 \\ 0 \end{pmatrix} \text{mN} \quad \vec{F}_2^{CW(R)} = \begin{pmatrix} -5.20 \\ 0 \\ 0 \end{pmatrix} \text{mN} \quad (6.31)$$

The required EMFF forces are

$$\vec{F}_1 = \begin{pmatrix} -5.20 \cos \theta \\ -5.20 \sin \theta \\ 0 \end{pmatrix} \text{mN} \quad \vec{F}_2 = \begin{pmatrix} 5.20 \cos \theta \\ 5.20 \sin \theta \\ 0 \end{pmatrix} \text{mN} \quad (6.32)$$

This produces a constant torque on the formation of

$$\vec{\tau} = \begin{pmatrix} 0 \\ 0 \\ 18.37 \end{pmatrix} \text{mN m} \quad (6.33)$$

Left unchecked, the formation will build up angular momentum at a rate of

$$\Delta H = 37.2 \frac{\text{Nm s}}{\text{orbit}} \quad (6.34)$$

Section 6.1.5 Stationary Orbits with Respect to an Inertial Frame

Instead of holding a formation fixed with respect to the relative coordinate system, the formation could be held fixed in inertial space. This formation could be used for a space-looking telescope imaging a fixed star or planet.

The position of the satellites are given (in the inertial coordinate system) as

$$\vec{r} = \begin{pmatrix} X \\ Y \\ Z \end{pmatrix} \quad (6.35)$$

The forces due to the Earth's gravitational potential are given by

$$\vec{F}^G = m \begin{pmatrix} \frac{1}{2} n^2 (X + 3X \cos 2\theta + 3Y \sin 2\theta) \\ -\frac{1}{2} n^2 (-Y - 3X \sin 2\theta + 3Y \cos 2\theta) \\ -Z n^2 \end{pmatrix} \quad (6.36)$$

Since the satellite formation is kept inertially fixed, the total desired forces are zero and the required EMFF forces are simply the opposite of the gravitational forces.

$$\vec{F}_1 = m \begin{pmatrix} -\frac{1}{2}n^2(X + 3X\cos 2\theta + 3Y\sin 2\theta) \\ \frac{1}{2}n^2(-Y - 3X\sin 2\theta + 3Y\cos 2\theta) \\ Zn^2 \end{pmatrix} \quad (6.37)$$

The torque applied to the satellite is given by

$$\vec{\tau} = m \begin{pmatrix} -3Zn^2\sin\theta(X\cos\theta + Y\sin\theta) \\ 3Zn^2\cos\theta(X\cos\theta + Y\sin\theta) \\ \frac{3}{2}n^2(-2XY\cos 2\theta + (X^2 - Y^2)\sin 2\theta) \end{pmatrix} \quad (6.38)$$

The average torque over one orbital period is given by

$$\vec{\tau} = m \begin{pmatrix} -\frac{3}{2}nYZ \\ \frac{3}{2}nXZ \\ 0 \end{pmatrix} \quad (6.39)$$

Example # 6 Inertially Pointing Formation

The parameters from the previous examples are used. The satellites have the following positions in the inertial coordinate frame.

$$\vec{r}_1 = \begin{pmatrix} \frac{5}{\sqrt{6}} \\ \frac{5}{\sqrt{3}} \\ \frac{5}{\sqrt{2}} \end{pmatrix} \quad \vec{r}_2 = \begin{pmatrix} -\frac{5}{\sqrt{6}} \\ -\frac{5}{\sqrt{3}} \\ -\frac{5}{\sqrt{2}} \end{pmatrix} \quad (6.40)$$

The forces needed to counteract the gravitational forces are

$$\vec{F}_1 = \begin{pmatrix} -0.500 - 1.50\cos 2\theta - 2.12\sin 2\theta \\ -0.707 + 2.12\cos 2\theta - 1.5\sin 2\theta \\ 1.732 \end{pmatrix} \text{mN} \quad \vec{F}_2 = \begin{pmatrix} 0.500 + 1.50\cos 2\theta + 2.12\sin 2\theta \\ 0.707 - 2.12\cos 2\theta + 1.5\sin 2\theta \\ -1.732 \end{pmatrix} \text{mN} \quad (6.41)$$

The resulting torques on each satellite are given by

$$\vec{\tau}_1 = \begin{pmatrix} -7.50 + 7.50\cos 2\theta - 5.30\sin 2\theta \\ -5.30 + 5.30\cos 2\theta + 7.5\sin 2\theta \\ -8.66\cos 2\theta - 3.06\sin 2\theta \end{pmatrix} \text{mN-m} \quad \vec{\tau}_2 = \begin{pmatrix} -7.50 + 7.50\cos 2\theta - 5.30\sin 2\theta \\ -5.30 + 5.30\cos 2\theta + 7.5\sin 2\theta \\ -8.66\cos 2\theta - 3.06\sin 2\theta \end{pmatrix} \text{mN-m} \quad (6.42)$$

The average torque is

$$\vec{\tau}_1^{\text{avg}} = \begin{pmatrix} -7.50 \\ -5.30 \\ 0 \end{pmatrix} \text{mN-m} \quad \vec{\tau}_2^{\text{avg}} = \begin{pmatrix} -7.50 \\ -5.30 \\ 0 \end{pmatrix} \text{mN-m} \quad (6.43)$$

The angular momentum gain on the formation as a whole over one orbital period is

$$\Delta H = \begin{pmatrix} -85.1 \\ 60.2 \\ 0 \end{pmatrix} \frac{\text{Nms}}{\text{Orbit}} \quad (6.44)$$

Section 6.1.6 Rotating Formations

Some satellite formations must rotate to accomplish their missions. One such example is an interferometer. The satellites typically lie in a plane, and the object that the satellites are imaging lies normal to this plane. It can be desirable to have the formation spin at a rate faster than the orbital period. This section looks at the average momentum gain of satellite formations in this configuration in LEO. The forces and instantaneous torques are not shown herein due to their complicated form. However, the time-averaged torque can be shown and is important since it is the secular component of the change in angular momentum imparted onto the formation.

The normal to the plane of the satellite formation is defined by

$$\vec{r} = \begin{pmatrix} X \\ Y \\ Z \end{pmatrix} \text{ where } \sqrt{X^2 + Y^2 + Z^2} = 1 \quad (6.45)$$

The satellites in the formation are separated from the center of mass by a distance d . The satellite formation will rotate at a rate of kn where n is the orbital frequency.

Example # 7 Normal is Fixed Relative to the Rotating Coordinate System

For satellites that have a fixed normal relative to the rotating coordinate system, the torque is given by

$$\vec{\tau} = d^2 mn^2 \begin{pmatrix} \frac{1}{4k^2 - 1} \sin(2\pi k) (C_1 \cos(2\pi k) + C_2 \sin(2\pi k)) \\ \frac{1}{4k^2 - 1} \sin(2\pi k) (C_3 \cos(2\pi k) + C_4 \sin(2\pi k)) \\ \frac{1}{k} (C_5 \cos(2\pi k) + C_6 \sin(2\pi k)) \end{pmatrix} \quad (6.46)$$

where each C_i is a constant based on the normal vector. From equation (6.46) it can be seen that in the x and y direction, the secular component can be removed when k is a multiple of $\frac{1}{2}$, greater than or equal to one.

$$\tau^{AVG} = \begin{pmatrix} 0 \\ 0 \\ 3md^2 n^2 XY \end{pmatrix} \quad \text{for } k = [1, \frac{3}{2}, 2, \frac{4}{2}, 3, \dots] \quad (6.47)$$

Example # 8 Normal is Fixed Relative to the Inertial Coordinate System

For satellites that have a fixed normal relative to the inertial coordinate system, the torque is given by

$$\vec{\tau} = d^2 mn^2 \begin{pmatrix} \frac{1}{k(k^2 - 1)} (C_1 + C_2 \sin(4\pi k) + C_3 \cos(4\pi k)) \\ \frac{1}{k(k^2 - 1)} (C_4 + C_5 \sin(4\pi k) + C_6 \cos(4\pi k)) \\ \frac{1}{(k^2 - 1)} \sin(2\pi k) (C_7 \cos(2\pi k) + C_8 \sin(2\pi k)) \end{pmatrix} \quad (6.48)$$

where each C_i is a constant based on the normal vector. From equation (6.48) it can be seen that in the z direction, the secular component can be removed when k is a multiple of $\frac{1}{2}$.

$$\vec{\tau}^{AVG} = md^2 n \begin{pmatrix} \frac{3}{2}YZ \\ -\frac{3}{2}YZ \\ 0 \end{pmatrix} \quad \text{for } k = [\frac{1}{2}, \frac{3}{2}, 2, \frac{5}{2}, 3, \dots] \quad (6.49)$$

Section 6.1.7 Conclusions

Operating in the Earth's gravitational field poses a challenge for any satellite formation. Attempting to maintain a formation that is not a free-orbit ellipse requires the application of forces onto the satellites. For traditional thrusters this would require a large amount of propellant. For EMFF systems, the difficulty lies in the angular momentum management. It has been shown that except for certain specific formations, there is a secular component to the change in angular momentum. This will cause reaction wheels to saturate if left unchecked.

However, it is possible to dump the angular momentum gained, by rotating the formation in such a way that the change in angular momentum is now in the opposite direction. This is typically done by 'pointing the other way'. In fact, the Earth's gravitational field can be useful to manage angular momentum. If the formation has a large amount of angular momentum stored, then it only needs to move into a configuration with a favorable change in angular momentum and dump its momentum into the Earth's gravitational field.

Finally, another means of combating the unwanted torques and angular momentum from the Earth's gravitational potential is to use the Earth's magnetic field. The following chapter discuss the effects of the Earth's magnetic field and how it can be exploited for angular momentum management, but first a look at the non-spherical gravitational geopotential.

Section 6.2 The J_2 Geopotential

In the previous section, the Earth is modeled as a perfect sphere. However, the Earth is more accurately modeled as an oblate spheroid. This can be visualized by squishing the Earth at the

poles and letting it bulge at the equator. In order to account for this and other asymmetries, the Earth's gravitational potential can be modeled by a series of orthogonal Legendre functions. The first term in this series is the J_2 term that captures the equatorial bulge described earlier.

In a local relative coordinate system, the specific force on a satellite due to J_2 is given by¹

$$\vec{J}_2(\vec{r}) = -\frac{3}{2} \frac{J_2 n^2 R_E^2}{r} \begin{pmatrix} 1 - 3 \sin^2 i \sin^2 \theta \\ 2 \sin^2 i \sin \theta \cos \theta \\ 2 \sin i \cos i \sin \theta \end{pmatrix} \quad (6.50)$$

However for satellites flying in formation, what is important are the relative forces applied to the satellites. Much research has been done on modeling the relative forces on satellites flying in formation in the presence of the J_2 geopotential. One such method is a set of linearized differential equations by Schweighart and Sedwick.^{14,37} The equations are similar to the CW equations but incorporate the effects of the J_2 geopotential. The equations are reproduced below.

$$\begin{aligned} \ddot{x} - 2nc\dot{y} - (5c^2 - 2)n^2x &= 0 \\ \ddot{y} + 2nc\dot{x} &= 0 \\ \dot{y} - nb \cos \gamma &= 0 \\ \dot{\Phi} - nb \Phi \cos \gamma \sin \gamma &= 0 \\ \text{where } z &= \Phi \sin(knt - \gamma) \end{aligned} \quad (6.51)$$

Just as in the CW equations, x is the radial motion, y is the in-track motion, and z is the cross-track motion. However, the cross-track motion is modeled by two new variables. Φ is amplitude of the cross-track motion and γ is the phase angle. The two references by Schweighart and Sedwick offer a more in-depth explanation of the equations and associated variables and parameters.^{14,37}

The J_2 geopotential affects the satellite formation in several ways. The most prevalent and important is that the J_2 geopotential will cause the formation to drift apart in the cross-track direction. This is due to the fact that satellites in different orbital planes with different inclinations have different variations in the longitude of the ascending node. Because the orbital

planes precess at different rates, the formation eventually starts to separate. The other effects of the J_2 geopotential can be found in the prior publications by the author of this thesis.^{7,14,37}

Section 6.2.1 Combating Formation Separation

Formation separation is governed by Φ , the amplitude of the cross-track motion. From equation (6.51), the rate of change of the amplitude of the cross-track motion is³⁷

$$\begin{aligned}\dot{\Phi} &= nb \cos \gamma \sin \gamma \Phi \\ b &= \frac{3J_2 R_E^2}{2r_{ref}^2} \sin^2 i\end{aligned}\quad (6.52)$$

When a specific force is applied to the satellite in the z direction, the amplitude is changed by³⁷

$$\dot{\Phi} = \frac{a_z \cos(\gamma - \theta)}{n k r_{ref}} \quad (6.53)$$

Solving for the required force

$$F_z^{\Phi(R)} = m a_z = m \frac{r_{ref} n^2 k b \cos \gamma \sin \gamma \Phi}{\cos(\gamma - \theta)} \quad (6.54)$$

From equation (6.54) it can be seen that when $\cos(\gamma - \theta) = 0$, the required force is infinite. This is due to the fact that when the satellite is at its farthest reach, the amplitude cannot be changed. Therefore a force is applied so that the average change in amplitude is the desired change. The required force to counteract the mean change in cross-track amplitude is given by

$$\vec{F}^{\Phi(R)} = m \begin{pmatrix} 0 \\ 0 \\ 2 \cos(\gamma - \theta) r_{ref} n^2 k b \cos \gamma \sin \gamma \Phi \end{pmatrix} \quad (6.55)$$

Section 6.2.2 Angular Momentum Buildup

It is assumed that the satellites are in the free-orbit ellipse that is defined by the new equations. This is so that the effects of the cross-track separation can be identified. Formations other than

free-orbit ellipses can be created using the same technique as in the previous section. The position of the satellites is ³⁷

$$\vec{r}^{(R)} = \begin{pmatrix} x_0 \cos(gnt) + \frac{g}{2c} y_0 \sin(gnt) \\ -2 \frac{c}{g} x_0 \sin(gnt) + y_0 \cos(gnt) \\ r_{ref} \Phi \sin(knt - \gamma) \end{pmatrix} \quad (6.56)$$

For now, it is assumed that $g \approx k$, since they are both approximately equal to one. Therefore $gnt \approx knt = \theta(t)$. g and k will be set to their exact value, and the resulting angular momentum buildup will be examined at the end of this section. The torque vector (in the rotating coordinate system) is given by

$$\vec{\tau}^{(R)} = \begin{pmatrix} 2 \cos(\gamma - knt) r_{ref} n^2 kb \cos \gamma \sin \gamma \Phi (x_0 \cos knt + \frac{k}{2c} y_0 \sin knt) \\ 2 \cos(\gamma - knt) r_{ref} n^2 kb \cos \gamma \sin \gamma \Phi (x_0 \cos knt + \frac{k}{2c} y_0 \sin knt) \\ 0 \end{pmatrix} \quad (6.57)$$

Since the equation in (6.57) is starting to become messy, it is important to note that the torques are simply functions of

$$\vec{\tau}^{(R)} = \begin{pmatrix} \cos(\gamma - \theta) (C_1 \cos \theta + C_2 \sin \theta) \\ \cos(\gamma - \theta) (C_3 \cos \theta + C_4 \sin \theta) \\ 0 \end{pmatrix} \quad (6.58)$$

where the C_i are (not necessarily equal) constants. From equation (6.58) it can be seen that the torque is simply a linear combination of products of two trigonometric functions. The next step is to change the torque vector into the inertial coordinate system. This process will multiply the x and y components by another sine/cosine function.

$$\vec{\tau} = \begin{pmatrix} \cos\theta \cos(\gamma - \theta) (C_1 \cos\theta + C_2 \sin\theta) \\ \sin\theta \cos(\gamma - \theta) (C_3 \cos\theta + C_4 \sin\theta) \\ 0 \end{pmatrix} \quad (6.59)$$

By inspection it can be seen that equation (6.59) will integrate to zero. Therefore combating the change in amplitude of the cross-track motion will result in a zero-net gain in the angular momentum.

It should be noted that the zero-net gain result is only a first order approximation. In order for equation (6.59) to integrate to zero over one orbital period, the period of all the cosine and sine functions must be the same. In this example we assumed that $g \approx k$. However, there is a slight difference in the two constants. Also, it was assumed that the rotating coordinate system and the inertial coordinate system share the same z direction. However, due to J_2 , the orbital planes precess about the Earth's axis. Therefore, over the course of one orbital period the torques do not integrate to zero since torques on one side of the orbit that originally canceled with torques on the other side of the orbit, now no longer point in the opposite direction

However, these extra torques are very small and can be neglected when compared to the torques from the Earth's magnetic field. Chapter 7 discusses operating within the Earth's magnetic field and the methods used to manage the torques from the Earth's magnetic field will be able to handle the small torques produced by the J_2 geopotential.

Example # 9 Counteracting the Cross-Track Separation

Continuing with the parameters from the previous examples, consider a formation with the following initial conditions.

$$\begin{pmatrix} x_0 \\ y_0 \\ \gamma_0 \\ r_{ref}\Phi_0 \\ z_0 \end{pmatrix} = \begin{pmatrix} 5\text{m} \\ 0\text{m} \\ 45^\circ \\ 5\text{m} \\ \frac{s}{\sqrt{2}}\text{m} \end{pmatrix} \quad (6.60)$$

This produces the following constants. (Refer to references 14 and 37 for explanations).

$$\begin{pmatrix} g \\ c \\ k \\ n \\ b \end{pmatrix} = \begin{pmatrix} 1.00016 \\ 0.999838 \\ 1.00076 \\ 0.00110679 \\ 0.00114701 \end{pmatrix} \quad (6.61)$$

From equation (6.55), the maximum force needed to counteract the formation expansion is

$$\vec{F}_{\max}^{J_2(R)} = \begin{pmatrix} 0 \\ 0 \\ 2.8122 \end{pmatrix} \mu\text{N} \quad (6.62)$$

The maximum torque (per (x,y,z) component) is given by

$$\begin{pmatrix} \vec{\tau}_x^{J_2(R)\max} \\ \vec{\tau}_y^{J_2(R)\max} \\ \vec{\tau}_z^{J_2(R)\max} \end{pmatrix} = \begin{pmatrix} 4.1504 \\ 2.0435 \\ 0 \end{pmatrix} \mu\text{N m} \quad (6.63)$$

Converting to the inertial coordinate system, the torques applied to the satellite are shown in the following plot.

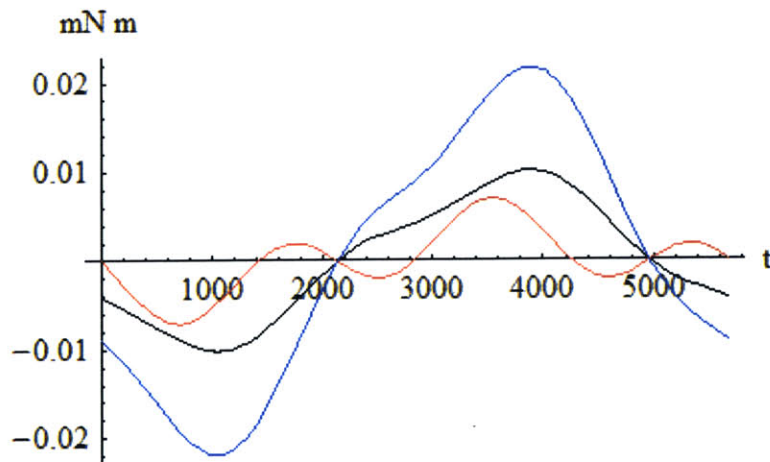


Figure 6-6 Torques Applied to the Satellite

The maximum angular momentum ever accumulated in each direction is

$$\vec{H}_{\max}^{J_2} = \begin{pmatrix} -5.98149 \\ -14.3678 \\ -30.8119 \end{pmatrix} \text{mN-m-s} \quad (6.64)$$

and the total gain over one orbital period is

$$\vec{H}^{J_2} = \begin{pmatrix} 0 \\ 0 \\ 0 \end{pmatrix} \text{N-m-s} \quad (6.65)$$

If the simplifying assumptions are removed and the rotation of the coordinate system due to the precession of the orbital planes is incorporated, it results in the following change of angular momentum over one orbital period. Notice the units are picoN-m-s.

$$\vec{H}_{\text{orbit}}^{J_2} = \begin{pmatrix} -0.0300 \\ 0.0142 \\ 0 \end{pmatrix} \text{pN-m-s} \quad (6.66)$$

If $g \neq k$, but are instead defined by equation (6.61), then

$$\vec{H}_{\text{orbit}}^{J_2} = \begin{pmatrix} 5.615 \\ 0.5948 \\ 1.271 \end{pmatrix} \mu\text{N-m-s} \quad (6.67)$$

Section 6.2.3 Conclusions

From equation (6.62), it can be seen that the amount of force needed to counteract the J_2 disturbance is quite small. However, integrated over one orbit, or one day, or the mission lifetime, the small force can contribute to a large ΔV which may prevent some propulsion methods from being feasible. EMFF does not suffer the ΔV limitation, and the force needed is well within its capabilities. From equation (6.63) and (6.67), the torques and resulting angular momentum buildup is very small, much smaller than the torques produced by operating in the

Earth's magnetic field or when in one of the formations listed in Section 1. Therefore the methods used to handle the angular momentum buildup due to the Earth's magnetic field or gravitational forces will be able to accommodate the angular momentum buildup from the J_2 disturbance.

Chapter 7

THE EARTH'S MAGNETIC FIELD

Section 7.1 Operating in the Earth's Magnetic Field – Overview

The Earth's magnetic field has been exploited by satellites for years. Many satellites in LEO use magnetic torque rods to dump their angular momentum or de-saturate their reaction wheels. The magnetic torque rods are simple electromagnets. When energized in the Earth's magnetic field, the magnets produce a torque on the spacecraft. The torque produced is specified in the opposite direction of the angular momentum stored in the reaction wheels, thus they are able to dump their angular momentum into the Earth.

EMFF satellites operating in the Earth's magnetic field will be similarly affected. In fact, typical EMFF vehicles will have significantly larger magnetic dipoles making the effects of the Earth's magnetic field that much more influential. This influence is a mixed blessing. When the magnets are energized, considerable torques can be placed on the vehicles. However, these torques can be used to dump angular momentum and to counteract the torques produced by operating in the Earth's gravitational potential.

Section 7.2 Modeling the Earth's Magnetic Field

The Earth's magnetic field is not simple. The field is dynamic and changes from year to year, with the location of North and South Poles wandering around. History has shown that the Earth's magnetic field has completely flipped polarity several times. At the same time, the overall magnetic field can be approximated fairly well by assuming the magnetic field is created by one large dipole. It is for this reason, that the Earth's field is pictured as one large bar magnet with the S of the magnet at the North Pole and the N at the South Pole.

Just like the Earth's gravitational field, the Earth's magnetic field can be represented by a series of orthogonal functions. When this series is truncated to the first term, the model predicts that the Earth's magnetic field is created by a large magnetic dipole. In this thesis the Earth's magnetic

field will be modeled as a dipole. The dipole is pointed towards the South geomagnetic pole which is tilted approximately 11° from the Earth's rotational axis.

Section 7.3 Magnitude of the Forces and Torques

The magnitude of the disturbance force and torque produced by the Earth's magnetic field is a function of the satellite's dipole strength, its distance from the Earth, and the relative angles between the Earth's dipole and the satellite's dipole.

Section 7.3.1 The Disturbance Force

From Chapter 3, the magnetic force is a function of the gradient of the local magnetic field.

$$\vec{F}_s = \nabla B_E \cdot \vec{\mu}_s \quad (7.1)$$

As would be expected, the gradient of the Earth's magnetic field is very small. It is a function of the distance between the satellite and the Earth, and the strength of magnetic dipole.

$$\nabla \vec{B}_E \propto \frac{\mu_E}{d^4} \quad (7.2)$$

The distance between the satellite and the Earth is very large (~7,000,000 m) compared to the meters between satellites. However, the Earth's magnetic field has a large strength (8×10^{22} Am). In the end though, the very large distance raised to the 4th power dominates over the large dipole strength when the Earth-generated force is compared to the force generated by the presence of another EMFF vehicle.

The force between any two magnetic dipoles is a function of

$$\vec{F}_{ES} \propto \frac{\mu_E \mu_S}{d_{ES}^4} \quad (7.3)$$

For comparison, two EMFF satellites are separated by a distance d_{SS} and produce a force of F_{SS} . Let the force between two satellites with their dipoles aligned be

$$F_{SS} = 1\text{mN} \quad (7.4)$$

Assuming that each satellite has the same dipole strength, are separated by a distance of 10m, the required dipole strength is

$$\mu_s = 4082 \text{ Am} \quad (7.5)$$

Assuming that the satellite formation is orbiting at an altitude of 500km and that the dipoles are aligned with the Earth's magnetic field (producing the worst-case disturbance force), the resulting disturbance force is

$$F_{ES} = 0.087 \mu\text{N} \quad (7.6)$$

The disturbance force is over 3 orders of magnitude less than the inter-satellite forces.

It is interesting to plot the disturbance force on a satellite if parameters are varied. For example, how does the disturbance force vary if the desired force is kept constant, but the separation distance between the vehicle changes. (Since the separation distance changes, the magnetic dipole strength must also change.)

Solving equation (7.4) for the magnetic dipole strength, and assuming that both satellites have the same dipole strength μ_s , results in

$$\mu_s = 1000 \sqrt{\frac{5}{3}} d_s^2 \sqrt{F_s} \quad (7.7)$$

The magnetic dipole strength varies as the distance squared and the square root of the desired force. Incorporating equation (7.7) results in

$$F_{ES} = \frac{\sqrt{3}}{1000\sqrt{5}} \frac{\mu_E}{d_{ES}^4} d_{ss}^2 \sqrt{F_{ss}} \quad (7.8)$$

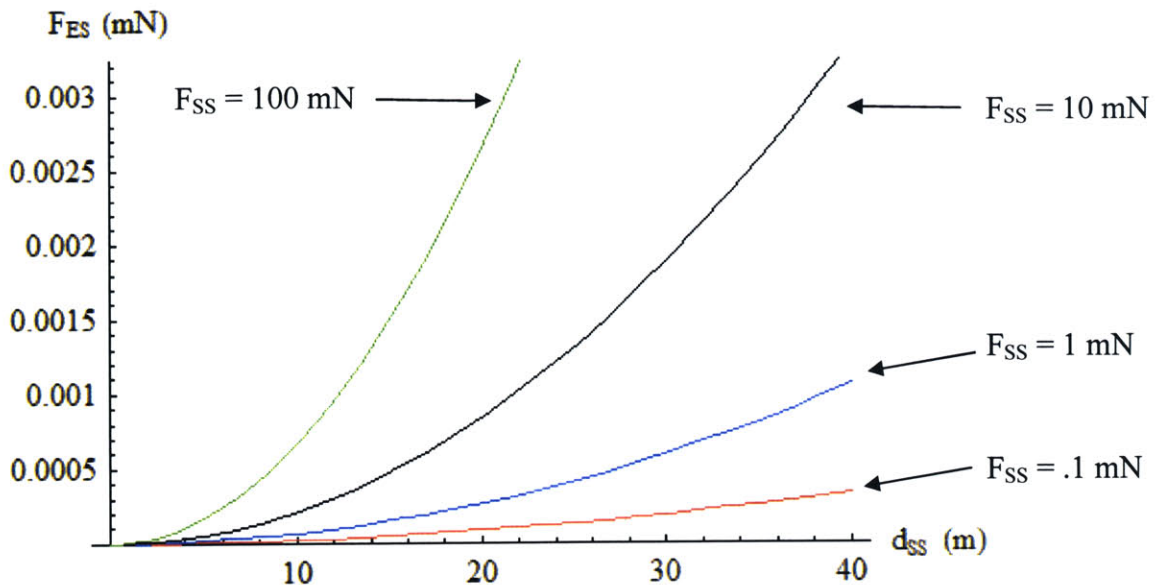


Figure 7-1: Comparing the Disturbance Force to the Inter-satellite Forces

The ratio of the disturbance force compared to the inter-satellite forces is given by

$$\frac{F_{ES}}{F_{SS}} = \frac{\sqrt{3}}{1000\sqrt{5}} \frac{\mu_E}{d_{ES}^4} \frac{d_{SS}^2}{\sqrt{F_{SS}}} \quad (7.9)$$

The ratio increases for larger distances (because the magnets must be stronger), and decreases for larger forces (since each satellite contributes to F_{SS} but only one satellite contributes to F_{ES}).

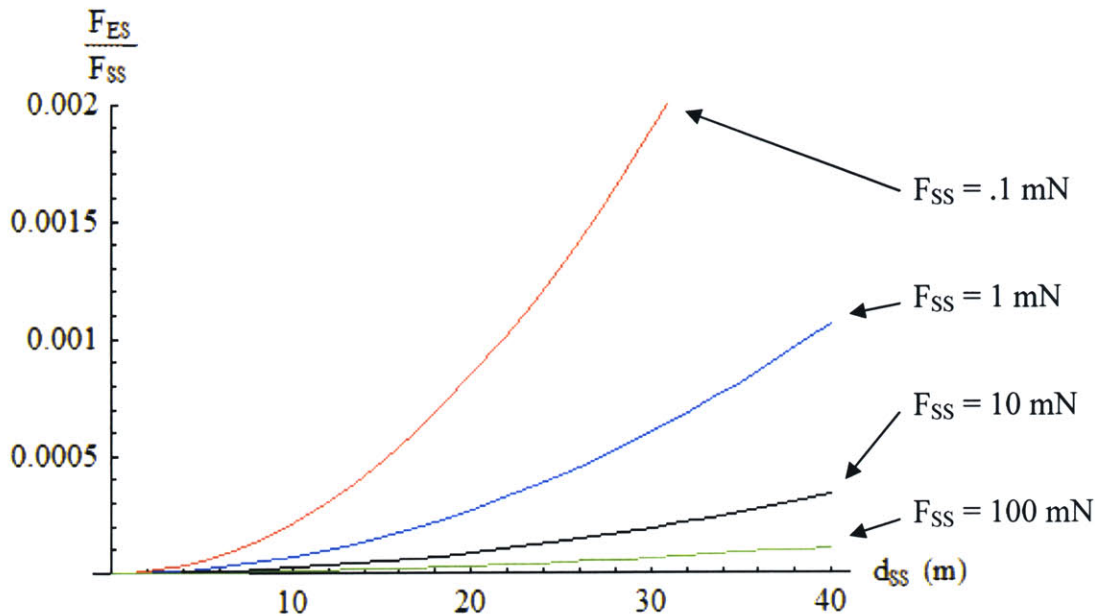


Figure 7-2: Ratio Between the Disturbance and the Inter-Satellite Forces

From this plot it can be seen that the ratio is less than a few tenths of a percent. Because the ratio is so small the magnetic disturbance force is typically neglected, however, in a later section methods for incorporating the relative effects of the Earth's magnetic field are discussed.

Section 7.3.2 The Disturbance Torque

From Chapter 3, the magnetic torque is not a function of the gradient of the magnetic field but instead is a function of the field strength.

$$\vec{\tau}_S = \vec{\mu}_S \times \vec{B}_E \quad (7.10)$$

Whereas the gradient of the magnetic field was a function of the distance to the 4th power, the magnetic field itself is a function of the distance to the 3rd power.

$$\vec{B}_E \propto \frac{\mu_E}{d_E^3} \quad (7.11)$$

The disturbance force was small due to the 4th power in the denominator. Now that the denominator is only to the 3rd power, the torque can have a much larger value. Assuming the

dipoles are aligned perpendicularly, the magnitude of the magnetic torque produced between two dipoles is

$$\tau_{12} = 10^{-7} \frac{\mu_1 \mu_2}{d_{12}^3} \quad (7.12)$$

Using the satellites' magnetic dipole strength given above of $\mu_s = 4087 \text{ Am}$, the maximum possible disturbance torque

$$\tau_{SE} = 0.100 \text{ Nm} \quad (7.13)$$

The maximum torque between the two satellites is

$$\tau_{SS} = 0.00167 \text{ Nm} \quad (7.14)$$

In this configuration, the disturbance torque is sixty times larger than the inter-satellite torques. The following plot looks at the maximum inter-satellite torque and the maximum disturbance torques for different dipole strength and separation distances. The thick orange line is the plot of the disturbance torque, τ_{ES} , and the other lines are the inter-satellite torques with the inter-satellite separation labeled for each curve.

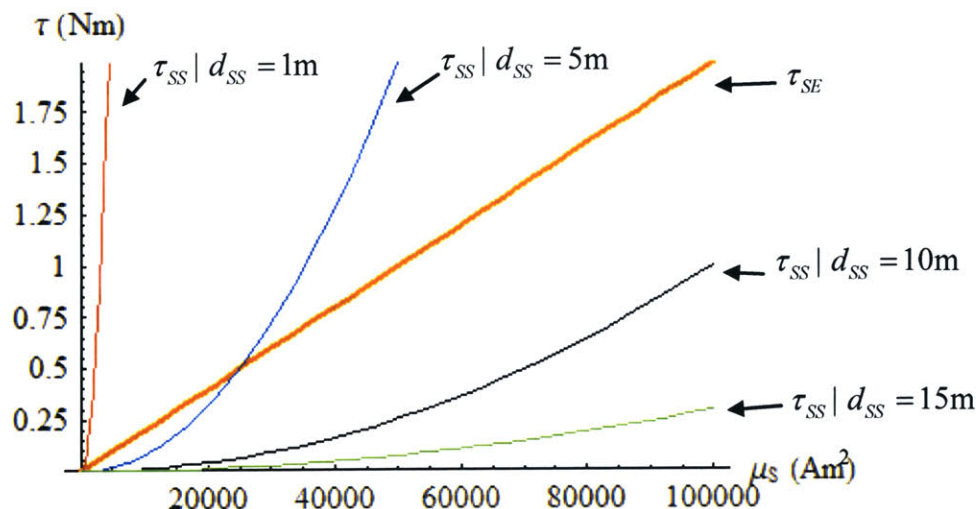


Figure 7-3: Comparing the Disturbance Torques to the Inter-Satellite Torques

The plot shows that small formations, due to their small separation distances, have larger inter-satellite torques than disturbance torques. The size of the formation has no impact on the size of the disturbance torques. However, if it can be assumed that an EMFF vehicle is designed to handle the inter-satellite torques, then the relative size of the Earth's disturbance torques is important.

Plotting the cut-off point where the inter-satellite torques and the disturbance torques are equated, it can be seen that the separation distance varies as the dipole strength to the one-third power. Points above the line have larger disturbance torques while points below the line have larger inter-satellite torques.

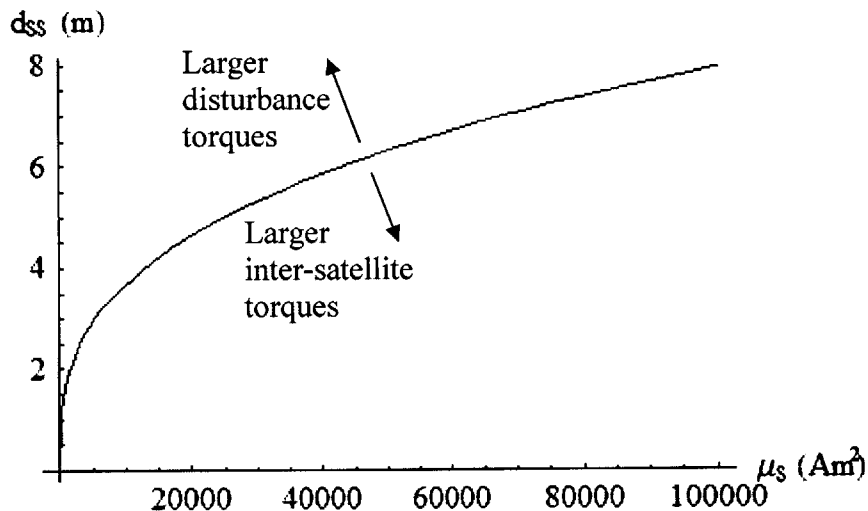


Figure 7-4: Configurations where the Disturbance and Inter-Satellite Torques are Equal

Section 7.3.3 Conclusions

The amount of disturbance force produced on a satellite due to the Earth's magnetic field is negligible. Depending on the fidelity of the hardware and control system, these forces may be in the noise. However, it is acknowledged that some systems may require extremely precise positioning from the EMFF system. In those cases the relative disturbance forces must be incorporated. (See the following section.)

The disturbance torque however cannot be neglected. In fact for many mission architectures the disturbance torque is on the same order or larger than the inter-satellite torques. As will be seen, this is a mixed blessing. The disturbance torques can be large and require constant adjustments, but at the same time they allow for a mechanism of off-loading angular momentum from the formation into the Earth.

Section 7.4 Incorporating the Earth's Magnetic Field into the Force Equations of Motion

Section 7.4.1 The Earth as Another Dipole

From Chapter 4, in the absence of the Earth's magnetic field, there are $3N$ force equations of motion and $3N$ variables. (N vector equations with 3 components each. N is the number satellites and the variables are the magnetic dipole components, $\vec{\mu}$.)

$$\begin{aligned}\vec{F}_1(\vec{r}_1, \dots, \vec{r}_N, \vec{\mu}_1, \dots, \vec{\mu}_N) - \vec{f}_1 &= 0 \\ \vec{F}_2(\vec{r}_1, \dots, \vec{r}_N, \vec{\mu}_1, \dots, \vec{\mu}_N) - \vec{f}_2 &= 0 \\ &\vdots \\ \vec{F}_{N-1}(\vec{r}_1, \dots, \vec{r}_N, \vec{\mu}_1, \dots, \vec{\mu}_N) - \vec{f}_{N-1} &= 0 \\ \vec{F}_N(\vec{r}_1, \dots, \vec{r}_N, \vec{\mu}_1, \dots, \vec{\mu}_N) - \vec{f}_N &= 0\end{aligned}\tag{7.15}$$

However, due to Newton's 3rd law,

$$\sum_{j=1}^N \vec{f}_j = 0\tag{7.16}$$

the sum of the forces must equal zero, and three of the equations are dependent on the other equations. Thus, there are $3N-3$ independent equations of motion and $3N$ variables.

$$\begin{aligned}
 \vec{F}_1(\vec{r}_1, \dots, \vec{r}_N, \vec{\mu}_1, \dots, \vec{\mu}_N) - \vec{f}_1 &= 0 \\
 \vec{F}_2(\vec{r}_1, \dots, \vec{r}_N, \vec{\mu}_1, \dots, \vec{\mu}_N) - \vec{f}_2 &= 0 \\
 &\vdots \\
 \vec{F}_{N-1}(\vec{r}_1, \dots, \vec{r}_N, \vec{\mu}_1, \dots, \vec{\mu}_N) - \vec{f}_{N-1} &= 0
 \end{aligned} \tag{7.17}$$

Because there are more variables than equations of motion, three of the variables can be set arbitrarily (the free dipole), and the force equations of motion can be solved. From Bezout's theorem³, there are 2^{3N-6} solutions. Chapter 5 exploited the free dipole in order to manage torque and angular momentum distribution.

As stated earlier, the Earth's magnetic field can be approximated as a magnetic dipole. Because of this, the Earth can be treated just like another EMFF vehicle for the purposes of solving the equations of motion. However, unlike the EMFF vehicles, the Earth's EM field is fixed for our purposes.

If the Earth is treated like an EMFF vehicle, then there are now $3N$ independent equations of motion and $3N+3$ variables. The reference frame for the desired forces up to this point has been centered around the formation's center of mass. With the addition of the Earth into the EOM, the center of mass now moves almost entirely to the center of the Earth. This will be examined further in the next section.

$$\begin{aligned}
 \vec{F}_1(\vec{r}_1, \dots, \vec{r}_N, \vec{r}_E, \vec{\mu}_1, \dots, \vec{\mu}_N, \vec{\mu}_E) - \vec{f}_1 &= 0 \\
 \vec{F}_2(\vec{r}_1, \dots, \vec{r}_N, \vec{r}_E, \vec{\mu}_1, \dots, \vec{\mu}_N, \vec{\mu}_E) - \vec{f}_2 &= 0 \\
 &\vdots \\
 \vec{F}_{N-1}(\vec{r}_1, \dots, \vec{r}_N, \vec{r}_E, \vec{\mu}_1, \dots, \vec{\mu}_N, \vec{\mu}_E) - \vec{f}_{N-1} &= 0 \\
 \vec{F}_E(\vec{r}_1, \dots, \vec{r}_N, \vec{r}_E, \vec{\mu}_1, \dots, \vec{\mu}_N, \vec{\mu}_E) - \vec{f}_E &= 0
 \end{aligned} \tag{7.18}$$

The Earth's magnetic field is fixed and thus its dipole cannot be treated as a variable. Therefore there are still only $3N$ degrees of freedom. Because there are an equal number of variables and equations, the free dipole no longer exists. The force EOM can still be solved with 2^{3N-3} possible solutions.

Section 7.4.2 The Force on the Formation's Center of Mass

Looking at equation (7.18), we see that \vec{f}_E has yet to be defined. (\vec{f}_E is the desired force applied to the Earth.) Because of Newton's third law, $-\vec{f}_E$ can also be thought of as the force applied to the formation's center of mass. Up to this point, there have been no outside forces and thus no force could be applied to the formation as a whole. With the introduction of the Earth's magnetic field, there is now the ability to change the satellite formation's center of mass.

By having the ability to apply a force to the satellite formation's center of mass, the formation's orbital parameters can now be changed. However, as seen from the previous section, the force produced by the Earth's magnetic field is very small. If the EOM are forced to produce a significant force on the satellite formation's center of mass (by setting \vec{f}_E to a substantial value), then the resulting dipole solution will be inordinately large.

It is safe to assume that Earth will not provide a sizeable force on the satellite formation. That said, there is still the question of what value \vec{f}_E should be set to. The obvious choice is to set \vec{f}_E to be zero.

The last equation in (7.18) will force \vec{f}_E to be the desired value (typically zero). However, we have stated that the Earth's magnetic field produces no appreciable forces on the satellites, or the satellite formation's center of mass. This constraint equation has no real benefit, and it prevents the existence of the free dipole. Can it just be ignored? Unfortunately, No.

The EOM in (7.18) already have one vector equation removed ($\vec{F}_N - \vec{f}_N = 0$) because it is linearly dependent on the other equations. If the last equation ($\vec{F}_E - \vec{f}_E = 0$) in (7.18) is removed, then $\vec{F}_N - \vec{f}_N = 0$ is no longer dependent and must be added to the EOM. Therefore just removing $\vec{F}_E - \vec{f}_E = 0$ has no real benefit. The number of equations will remain the same and thus there is still no free dipole.

Stepping back for a moment, it helps to revisit our goal. The disturbance force produced by the Earth's magnetic field on each satellite is very small and could be neglected. However before throwing in the towel and just completely neglecting the forces, it is worth an attempt to incorporate them. By treating the Earth as another dipole, we have essentially traded the free dipole for the Earth's dipole. This allows for the exact calculation of the disturbance force, but at a cost of losing the free dipole. Since this force is essentially insignificant, removing three degrees of freedom (the free dipole) to include the Earth's disturbance force is simply pointless.

However, it was recognized that by adding in the Earth into the EOM as another dipole, the force applied to the Earth must be chosen. This is equivalent to choosing the force on the formation's center of mass. Since no appreciable force can be generated on the formation's center of mass that would be of use, this force is typically set to zero.

But this force can be set arbitrarily. The three extra degrees of freedom are now the force on the formation center of mass. The “free dipole” is now the “free force”. But having the free degrees of freedom reserved as the force on the center of mass does not do us any good. However, the fact that there are still three extra degrees of freedom gives hope that the free dipole can be still be realized.

For the moment, \vec{f}_E is kept as a variable. By Newton's third law

$$\vec{f}_E + \sum_{j=1}^N \vec{f}_j = 0 \quad (7.19)$$

Since \vec{f}_j is already defined by the user, \vec{f}_E would be completely defined by (7.19). It would initially appear that that this “free force” is not really free at all. However, remember from earlier that because the Earth is being treated as another dipole, the reference frame for (7.19) includes the Earth. Therefore \vec{f}_i must be defined with respect to this new center of mass.

EMFF is designed to provide *relative* position control, and the force relative to the Earth/formation center of mass is not important to EMFF. Therefore, the relative motion of the

Earth/formation center of mass is removed, and we now define \vec{f}'_j to be the desired force relative to just the formation's center of mass.

$$\vec{f}_j = \vec{f}'_j - \frac{\vec{f}_E}{N} \quad (7.20)$$

If the relative forces are restricted to sum to zero

$$\sum_j^N \vec{f}'_j = 0 \quad (7.21)$$

Then equation (7.19) is identically satisfied.

$$\begin{aligned} \vec{f}_E + \sum_{j=1}^N (\vec{f}'_j - \frac{\vec{f}_E}{N}) &= \\ \sum_{j=1}^N \vec{f}'_j + \vec{f}_E - \vec{f}_E \sum_{j=1}^N (\frac{1}{N}) &= \\ 0 + \vec{f}_E - \vec{f}_E &= 0 \end{aligned} \quad (7.22)$$

It is important to note that \vec{f}_E is independent of f'_j . No matter what the choice of f'_j (as long as it satisfies (7.21)), Newton's 3rd law will always be satisfied. Substituting equation (7.20) into (7.18) results in

$$\begin{aligned} \vec{F}_1(\vec{r}_1, \dots, \vec{r}_N, \vec{r}_E, \vec{\mu}_1, \dots, \vec{\mu}_N, \vec{\mu}_E) - \vec{f}'_1 + \frac{\vec{f}_E}{N} &= 0 \\ \vec{F}_2(\vec{r}_1, \dots, \vec{r}_N, \vec{r}_E, \vec{\mu}_1, \dots, \vec{\mu}_N, \vec{\mu}_E) - \vec{f}'_2 + \frac{\vec{f}_E}{N} &= 0 \\ &\vdots \\ \vec{F}_{N-1}(\vec{r}_1, \dots, \vec{r}_N, \vec{r}_E, \vec{\mu}_1, \dots, \vec{\mu}_N, \vec{\mu}_E) - \vec{f}'_{N-1} + \frac{\vec{f}_E}{N} &= 0 \\ \vec{F}_E(\vec{r}_1, \dots, \vec{r}_N, \vec{r}_E, \vec{\mu}_1, \dots, \vec{\mu}_N, \vec{\mu}_E) - \vec{f}_E &= 0 \end{aligned} \quad (7.23)$$

So there are $3N$ equations and $3N+3$ variables ($3N$ dipole variables, $\vec{\mu}_i$, and 3 force variables, \vec{f}_E). Substituting \vec{F}_E in for \vec{f}_E , (using the last equation in (7.23)) results in

$$\begin{aligned}\vec{F}_1(\vec{r}_1, \dots, \vec{r}_N, \vec{r}_E, \vec{\mu}_1, \dots, \vec{\mu}_N, \vec{\mu}_E) - \vec{f}'_1 + \frac{1}{N} \vec{F}_E(\vec{r}_1, \dots, \vec{r}_N, \vec{r}_E, \vec{\mu}_1, \dots, \vec{\mu}_N, \vec{\mu}_E) &= 0 \\ \vec{F}_2(\vec{r}_1, \dots, \vec{r}_N, \vec{r}_E, \vec{\mu}_1, \dots, \vec{\mu}_N, \vec{\mu}_E) - \vec{f}'_2 + \frac{1}{N} \vec{F}_E(\vec{r}_1, \dots, \vec{r}_N, \vec{r}_E, \vec{\mu}_1, \dots, \vec{\mu}_N, \vec{\mu}_E) &= 0 \\ &\vdots \quad (7.24) \\ \vec{F}_{N-1}(\vec{r}_1, \dots, \vec{r}_N, \vec{r}_E, \vec{\mu}_1, \dots, \vec{\mu}_N, \vec{\mu}_E) - \vec{f}'_{N-1} + \frac{1}{N} \vec{F}_E(\vec{r}_1, \dots, \vec{r}_N, \vec{r}_E, \vec{\mu}_1, \dots, \vec{\mu}_N, \vec{\mu}_E) &= 0 \\ \vec{F}_E(\vec{r}_1, \dots, \vec{r}_N, \vec{r}_E, \vec{\mu}_1, \dots, \vec{\mu}_N, \vec{\mu}_E) - \vec{f}_E &= 0\end{aligned}$$

The last equation of (7.24) can always be satisfied since \vec{f}_E is a variable and can be set at will. Therefore we can remove the last equation of (7.24). When we tried to remove the last equation in (7.18), we were unable due to the fact that the removed equation $F_N - f_N = 0$ was dependent on it. But since \vec{f}'_j is *independent* of \vec{f}_E , it can be removed.

This results in

$$\begin{aligned}\vec{F}_1(\vec{r}_1, \dots, \vec{r}_N, \vec{r}_E, \vec{\mu}_1, \dots, \vec{\mu}_N, \vec{\mu}_E) - \vec{f}'_1 + \frac{1}{N} \vec{F}_E(\vec{r}_1, \dots, \vec{r}_N, \vec{r}_E, \vec{\mu}_1, \dots, \vec{\mu}_N, \vec{\mu}_E) &= 0 \\ \vec{F}_2(\vec{r}_1, \dots, \vec{r}_N, \vec{r}_E, \vec{\mu}_1, \dots, \vec{\mu}_N, \vec{\mu}_E) - \vec{f}'_2 + \frac{1}{N} \vec{F}_E(\vec{r}_1, \dots, \vec{r}_N, \vec{r}_E, \vec{\mu}_1, \dots, \vec{\mu}_N, \vec{\mu}_E) &= 0 \\ &\vdots \\ \vec{F}_{N-1}(\vec{r}_1, \dots, \vec{r}_N, \vec{r}_E, \vec{\mu}_1, \dots, \vec{\mu}_N, \vec{\mu}_E) - \vec{f}'_{N-1} + \frac{1}{N} \vec{F}_E(\vec{r}_1, \dots, \vec{r}_N, \vec{r}_E, \vec{\mu}_1, \dots, \vec{\mu}_N, \vec{\mu}_E) &= 0\end{aligned} \quad (7.25)$$

\vec{f}_E does not appear in (7.25), therefore we have $3N-3$ equations and $3N$ variables. The free dipole is back!

Section 7.4.3 The Force on the Formation's Center of Mass (Another Derivation)

Using the technique of Section 4.5.5 and Section 4.5.6, we can systematically reduce the EMFF EOM represented below.

$$\begin{aligned}\vec{F}_1(\vec{r}_1, \dots, \vec{r}_N, \vec{r}_E, \vec{\mu}_1, \dots, \vec{\mu}_N, \vec{\mu}_E) - \vec{f}_1 &= 0 \\ \vec{F}_2(\vec{r}_1, \dots, \vec{r}_N, \vec{r}_E, \vec{\mu}_1, \dots, \vec{\mu}_N, \vec{\mu}_E) - \vec{f}_2 &= 0 \\ &\vdots \\ \vec{F}_{N-1}(\vec{r}_1, \dots, \vec{r}_N, \vec{r}_E, \vec{\mu}_1, \dots, \vec{\mu}_N, \vec{\mu}_E) - \vec{f}_{N-1} &= 0 \\ \vec{F}_N(\vec{r}_1, \dots, \vec{r}_N, \vec{r}_E, \vec{\mu}_1, \dots, \vec{\mu}_N, \vec{\mu}_E) - \vec{f}_N &= 0 \\ \vec{F}_E(\vec{r}_1, \dots, \vec{r}_N, \vec{r}_E, \vec{\mu}_1, \dots, \vec{\mu}_N, \vec{\mu}_E) - \vec{f}_E &= 0\end{aligned}\tag{7.26}$$

For this example, 3 satellites and the Earth are used.

$$\begin{aligned}\vec{F}_1(\vec{r}_1, \vec{r}_2, \vec{r}_3, \vec{r}_E, \vec{\mu}_1, \vec{\mu}_2, \vec{\mu}_3, \vec{\mu}_E) - \vec{f}_1 &= 0 \\ \vec{F}_2(\vec{r}_1, \vec{r}_2, \vec{r}_3, \vec{r}_E, \vec{\mu}_1, \vec{\mu}_2, \vec{\mu}_3, \vec{\mu}_E) - \vec{f}_2 &= 0 \\ \vec{F}_3(\vec{r}_1, \vec{r}_2, \vec{r}_3, \vec{r}_E, \vec{\mu}_1, \vec{\mu}_2, \vec{\mu}_3, \vec{\mu}_E) - \vec{f}_3 &= 0 \\ \vec{F}_E(\vec{r}_1, \vec{r}_2, \vec{r}_3, \vec{r}_E, \vec{\mu}_1, \vec{\mu}_2, \vec{\mu}_3, \vec{\mu}_E) - \vec{f}_E &= 0\end{aligned}\tag{7.27}$$

If we expand equation (7.27) into the form used in equation (4.63) we have

$$\begin{array}{ccccccccc}\vec{\mu}_3\vec{\mu}_2 & \vec{\mu}_3\vec{\mu}_1 & \vec{\mu}_2\vec{\mu}_1 & \vec{f}_E & \vec{\mu}_E\vec{\mu}_1 & \vec{\mu}_E\vec{\mu}_2 & \vec{\mu}_E\vec{\mu}_3 & \vec{f}'_j \\ \vec{F}_1 \rightarrow & \left(\begin{array}{ccccccc} 0 & C_2 & C_3 & -\frac{\vec{f}_E}{3} & C_4 & 0 & 0 & -\vec{f}'_1 \end{array} \right) \\ \vec{F}_2 \rightarrow & \left(\begin{array}{ccccccc} C_1 & 0 & -C_3 & -\frac{\vec{f}_E}{3} & 0 & C_5 & 0 & -\vec{f}'_2 \end{array} \right) \\ \vec{F}_3 \rightarrow & \left(\begin{array}{ccccccc} -C_1 & C_2 & 0 & -\frac{\vec{f}_E}{3} & 0 & 0 & C_6 & \vec{f}'_1 + \vec{f}'_2 \end{array} \right) \\ \vec{F}_E \rightarrow & \left(\begin{array}{ccccccc} 0 & 0 & 0 & \vec{f}_E & -C_4 & -C_5 & -C_6 & 0 \end{array} \right)\end{array}\tag{7.28}$$

Applying row reduction

$$\begin{array}{cccccccc}
 \vec{\mu}_3\vec{\mu}_2 & \vec{\mu}_3\vec{\mu}_1 & \vec{\mu}_2\vec{\mu}_1 & \vec{f}_E & \vec{\mu}_E\vec{\mu}_1 & \vec{\mu}_E\vec{\mu}_2 & \vec{\mu}_E\vec{\mu}_3 & \vec{f}'_j \\
 eqn_1 \rightarrow & \left(\begin{array}{ccccccc} 3C_1 & 0 & -3C_3 & 0 & -C_4 & 2C_5 & -C_6 & -3\vec{f}'_2 \end{array} \right) & & & & & & \\
 eqn_2 \rightarrow & \left(\begin{array}{ccccccc} 0 & 3C_2 & 3C_3 & 0 & 2C_4 & -C_5 & -C_6 & -3\vec{f}'_1 \end{array} \right) & & & & & & (7.29) \\
 eqn_3 \rightarrow & \left(\begin{array}{ccccccc} 0 & 0 & 0 & \vec{f}_E & -C_4 & -C_5 & -C_6 & 0 \end{array} \right) & & & & & & \\
 eqn_4 \rightarrow & \left(\begin{array}{ccccccc} 0 & 0 & 0 & 0 & 0 & 0 & 0 & 0 \end{array} \right) & & & & & &
 \end{array}$$

From (7.29), it can be seen that one row is all zeros indicating that one of the vector equations was dependent and can be removed. The 3rd row is the only row that contains \vec{f}_E . Since this 3rd row can always be satisfied by choosing \vec{f}_E appropriately, it can be ignored. What are left are the top two equations. There are two equations and three variables $(\vec{\mu}_1, \vec{\mu}_2, \vec{\mu}_3)$. Thus the free dipole is available. It should be noted that if $\vec{\mu}_i$ is chosen to be the free dipole, then it can be seen from (7.29) that the second equation will only be first order (since the only second order terms will be $\vec{\mu}_2\vec{\mu}_3$ and row #2 has a zero in that column). Therefore the number of solutions to (7.29) will be 2^3 or in general terms 2^{3N-6} which is the same number of solutions as when Earth's field was neglected.

From equation (7.29) we can back out (7.25). The first equation is

$$3\vec{F}_{32} - 3\vec{F}_{21} - \vec{F}_{E1} + 2\vec{F}_{E2} - \vec{F}_{E3} - 3\vec{f}'_2 = 0 \quad (7.30)$$

where F_{ij} is the force on j from satellite i . Rearranging,

$$\begin{aligned}
 3\vec{F}_{32} + 3\vec{F}_{12} + 3\vec{F}_{E2} - \vec{F}_{E1} - \vec{F}_{E2} - \vec{F}_{E3} - 3\vec{f}'_2 &= 0 \\
 \vec{F}_{32} + \vec{F}_{12} + \vec{F}_{E2} + \frac{\vec{F}_{1E} + \vec{F}_{2E} + \vec{F}_{3E}}{3} - \vec{f}'_2 &= 0 \\
 \vec{F}_{(3,1,E)2} + \frac{\vec{F}_{(1,2,3)E}}{3} - \vec{f}'_2 &= 0
 \end{aligned} \tag{7.31}$$

The other two equations can be reduced in the same way resulting in the final 3 equations

$$\begin{aligned}
 \vec{F}_{(3,2,E)1} + \frac{\vec{F}_{(1,2,3)E}}{3} - \vec{f}'_1 &= 0 \\
 \vec{F}_{(3,1,E)2} + \frac{\vec{F}_{(1,2,3)E}}{3} - \vec{f}'_2 &= 0 \\
 \vec{F}_{(1,2,3)E} - \vec{f}_E &= 0
 \end{aligned} \tag{7.32}$$

which are the exact same equations as equation (7.25).

Example # 1

In this example, the set-up used in the examples of Chapter 4 is used. There are 3 satellites in an equilateral triangle configuration. The free dipole has a magnitude of $40,000 \text{ Am}^2$. One of the dipole solutions is

$$\vec{\mu} = \begin{pmatrix} 0 \\ 40000 \\ 0 \\ -84652.1 \\ -10000. \\ 117725 \\ 84652.1 \\ -10000. \\ -3493.14 \end{pmatrix} \tag{7.33}$$

The Earth's magnetic field is now incorporated and the new EOM are used. The formation's center of mass is located at an arbitrary point in LEO, and the Earth's magnetic dipole is given as

$$\vec{r}_f = - \begin{pmatrix} 6878.12 \cos 15^\circ \\ 0 \\ 6878.12 \sin 15^\circ \end{pmatrix} \text{km} \quad \vec{\mu}_E = \begin{pmatrix} 0 \\ 8e22 \sin 11^\circ \\ 8e22 \cos 11^\circ \end{pmatrix} \text{Am}^2 \quad (7.34)$$

There are a total of 8 solutions that vary slightly from the solutions that were produced when the Earth's magnetic field was not incorporated. The matching dipole solution to equation (7.33) when the Earth's magnetic field is incorporated is

$$\vec{\mu} = \begin{pmatrix} 0 \\ 40000 \\ 0 \\ -84651.5 \\ -9996.39 \\ -117717. \\ 84651.9 \\ -9995.60 \\ -3489.20 \end{pmatrix} \quad (7.35)$$

The force on the formation's center of mass is

$$-\vec{F}_E = \begin{pmatrix} 0.496197 \\ -0.812529 \\ -1.12836 \end{pmatrix} \mu\text{N} \quad (7.36)$$

The overall force on vehicle #1 is (the forces on the other vehicles are omitted for brevity)

$$\vec{F}_1 = \begin{pmatrix} -30.4620 \\ 2.09590e-5 \\ 7.61516 \end{pmatrix} \text{mN} \quad (7.37)$$

The force relative to the formation's center of mass is

$$\vec{F}_1 - \left(-\frac{\vec{F}_E}{3}\right) = \begin{pmatrix} -30.4617 \\ 0 \\ 7.61544 \end{pmatrix} \text{mN} = f'_1 \quad (7.38)$$

which is equal to our desired force relative to the formation's center of mass.

Incorporating the Earth's magnetic field required a change in the satellites' magnetic dipole strength of

$$\Delta\mu = \begin{pmatrix} 0 \\ 0 \\ 0 \\ -0.525229 \\ -3.60775 \\ -7.49547 \\ 0.210909 \\ -4.40013 \\ -3.9478 \end{pmatrix} \text{Am}^2 \quad (7.39)$$

or a variation of less than 0.007% in the magnitude of any dipole.

If the Earth's magnetic field is not incorporated by the equations of motion, the error in the force calculated on satellite #1 is

$$\vec{F}_{1,error} = \begin{pmatrix} -0.171716 \\ -0.104330 \\ -0.0379729 \end{pmatrix} \mu\text{N} \quad (7.40)$$

or an error of less than 0.005% in the magnitude of the force applied to any of the satellites.

Section 7.4.4 Conclusions

The disturbance force applied to the satellites in the Earth's magnetic field is very small. In the example problem, the magnitude of the forces was over 5 orders of magnitude smaller. However, some mission designers may still wish to incorporate these disturbance forces.

Fortunately, the *relative* disturbance forces may be incorporated into the force EOM model (equation (7.25)). This allows for the mission designer to specify the desired relative forces and calculate the correct magnetic dipole moment on each satellite that will produce the desired force even in the presence of an external field such as the Earth's magnetic field.

In order to allow for the existence of the free-dipole, the force on the formation's center of mass cannot be controlled. This force is also very small and can be neglected. However if desired, it can be easily calculated.

Section 7.5 Setting the Torque on One Satellite

This section will attempt to create a specified torque distribution on the formation at one point in time. Typically, the goal will be to reduce the torques applied to the formation, but the torques could be chosen in such a way as to remove angular momentum from the formation.

Even with formations of just two satellites, it is not possible to directly specify the torque on each satellite in the presence of the Earth's magnetic field.

From (7.17), the force equations of motion are given as

$$\begin{aligned}\vec{F}_1(\vec{r}_1, \dots, \vec{r}_N, \vec{\mu}_1, \dots, \vec{\mu}_N) - \vec{f}_1 + \vec{f}_1^G &= 0 \\ \vec{F}_2(\vec{r}_1, \dots, \vec{r}_N, \vec{\mu}_1, \dots, \vec{\mu}_N) - \vec{f}_2 + \vec{f}_2^G &= 0 \\ \vdots \\ \vec{F}_{N-1}(\vec{r}_1, \dots, \vec{r}_N, \vec{\mu}_1, \dots, \vec{\mu}_N) - \vec{f}_{N-1} + \vec{f}_{N-1}^G &= 0\end{aligned}\tag{7.41}$$

For the time being, satellite formations with two satellites will be considered. The torque equations are given as

$$\begin{aligned}\vec{T}_1(\vec{r}_1, \vec{r}_2, \vec{r}_E, \vec{\mu}_1, \vec{\mu}_2, \vec{\mu}_E) - \vec{\tau}_1 &= 0 \\ \vec{T}_2(\vec{r}_1, \vec{r}_2, \vec{r}_E, \vec{\mu}_1, \vec{\mu}_2, \vec{\mu}_E) - \vec{\tau}_2 &= 0 \\ \vec{T}_E(\vec{r}_1, \vec{r}_2, \vec{r}_E, \vec{\mu}_1, \vec{\mu}_2, \vec{\mu}_E) - \vec{\tau}_E &= 0\end{aligned}\tag{7.42}$$

Due to the conservation of angular momentum, one of the torque vector equations is dependent on the other two and can be removed. Combining the force and torque equations,

$$\begin{aligned}\vec{F}_1(\vec{r}_1, \vec{r}_2, \vec{r}_E, \vec{\mu}_1, \vec{\mu}_2, \vec{\mu}_E) - \vec{f}_1 &= 0 \\ \vec{T}_1(\vec{r}_1, \vec{r}_2, \vec{r}_E, \vec{\mu}_1, \vec{\mu}_2, \vec{\mu}_E) - \vec{\tau}_1 &= 0 \\ \vec{T}_E(\vec{r}_1, \vec{r}_2, \vec{r}_E, \vec{\mu}_1, \vec{\mu}_2, \vec{\mu}_E) - \vec{\tau}_E &= 0\end{aligned}\tag{7.43}$$

there are $3N+3$ equations and only $3N$ variables.

When dealing with the forces produced by the Earth's magnetic field, it was possible to separate the force acting on the formation's center of mass. Unfortunately, this is not possible with the torques.

From equation (7.43), it appears that the torque on one satellite can be set at will. (Make $\vec{\mu}_1, \vec{\mu}_2, \vec{\tau}_E$ the dependent variables.) However, when the Earth's magnetic field is not present it is not possible to arbitrarily set the torque on one satellite even though there are just two equations and two variables. Refer to Chapter 3. From (7.61) and (7.1), it can be seen that the force and torque equations are not completely independent as they are both functions of the angle of the magnetic field.

With the addition of another magnetic field (such as the Earth's magnetic field), it appears that it may be possible to choose any torque on the satellite since the local magnetic field is not exclusively dependent on the other satellite. Especially since the gradient of the Earth's magnetic field is negligible, the force and torque equations are de-coupled. Unfortunately, the equations can become too complex to solve analytically and examples must then be used to evaluate them.

Section 7.5.1 Zero-Torque Solutions

Setting the torque on a satellite to zero can (almost) always be achieved when working in the Earth's magnetic field. The torque on the satellite B is given by

$$\vec{\tau}_B = \vec{\mu}_B \times \vec{B}_A + \vec{\mu}_B \times \vec{B}_E = \vec{\mu}_B \times (\vec{B}_A + \vec{B}_E)\tag{7.44}$$

As long as the sum of the magnetic fields is zero, then the torque on satellite B is zero.

$$\vec{B}_A + \vec{B}_E = 0\tag{7.45}$$

where

$$\vec{B}(\vec{d}) = \frac{\mu_0}{4\pi} \left(\frac{3\vec{d}(\vec{\mu} \bullet \vec{d})}{d^5} - \frac{\vec{\mu}}{d^3} \right) \quad (7.46)$$

(Section 7.5.2 looks at zero-torque solutions where satellite B's magnetic dipole is aligned with the local magnetic field.)

If the position of satellite A and the location of the Earth are defined in general terms, the solution is very messy and too complicated to print here. However if the coordinate system is aligned with the dipoles, the solution becomes much simpler.

$$\vec{d}^A = \begin{pmatrix} d_x^A \\ 0 \\ 0 \end{pmatrix} \quad (7.47)$$

Also, if the disturbance forces from the Earth are neglected, the gradient of the Earth's magnetic field can be neglected. Since the direction of the magnetic field is simply a combination of the location of the Earth and the direction of the Earth's dipole, either one can be set arbitrarily. Therefore the location of the Earth is set to

$$\vec{d}^E = \begin{pmatrix} d_x^E \\ 0 \\ 0 \end{pmatrix} \quad (7.48)$$

Solving for the required magnetic dipole strengths on satellite A results in

$$\vec{\mu}^A = \begin{pmatrix} -\frac{d_x^A}{d_x^E} \mu_x^E \\ -\frac{d_y^A}{d_y^E} \mu_z^E \\ -\frac{d_z^A}{d_z^E} \mu_z^E \end{pmatrix} \quad (7.49)$$

Solving the force EOM for the dipole on satellite B results in

$$\vec{\mu}^B = \frac{4\pi d_x^A d_x^{E^3}}{3\mu_0 \mu_x^E (\mu_x^{E^2} + |\mu^E|^2)} \begin{pmatrix} \mu_x^E (-f_x^B \mu_x^E + f_y^B \mu_y^E + f_z^B \mu_z^E) \\ (f_y^B (2\mu_x^{E^2} + \mu_z^{E^2})^2 + 2f_x^B \mu_x^E \mu_y^E - f_z^B \mu_z^E \mu_y^E) \\ (f_z^B (2\mu_x^{E^2} + \mu_y^{E^2})^2 + f_x^B \mu_x^E \mu_z^E - f_y^B \mu_z^E \mu_y^E) \end{pmatrix} \quad (7.50)$$

From equation (7.49) and (7.50), it can be seen that given any desired force profile, it is possible to set the torque on one satellite to zero. The exception is when $\mu_x^E = 0$. When $\mu_x^E = 0$, from equation (7.49), then $\mu_x^A = 0$. In Section 4.2, it was shown that when the magnetic dipole is perpendicular to the axis connecting the two satellites then no force can be created in a direction that is perpendicular to both the dipole and the axis connecting the vectors. The same phenomenon is present here. From equation (7.50), when $\mu_x^E = 0$ then $\vec{\mu}^B$ has the possibility of approaching infinity depending on the desired forces on satellite B.

Having the ability to arbitrarily set the torque to zero for a specific satellite raises the possibility of having a satellite that does not need reaction wheels for angular momentum control. However, always setting the torque on one satellite to zero prevents the ability to control the angular momentum build-up on the other satellites. Essentially all the free degrees of control have been used to prevent torques from being applied to one satellite.

One such mission application would be the space-based telescope. The primary mirror could have the EMFF coils and the reaction wheels while the smaller secondary could have only EMFF coils. One simple way of managing angular momentum would be for the primary mirror to store the angular momentum build-up. Once the angular momentum stored on the satellite became too large, then the formation could enter into a free-orbit ellipse and the primary satellite could dump its angular momentum. While not elegant, it is a viable solution. As stated in the next section, other zero-torque configurations exist, and these may release enough control to manage the torque (at least partially) on the primary mirror also.

It should also be noted that the sizing of the dipole on satellite A is based solely on counteracting the Earth's magnetic field, which is a function of the distance to the third power. The sizing of the dipole on satellite B is based on both the size of the dipole on satellite A and on the desired forces and the separation distance to the 4th power. These characteristics will have to be taken into account when designing such a mission in order to balance the dipole requirements for each vehicle.

Example # 2 Zero-Torque Solution (Canceling the B-Field)

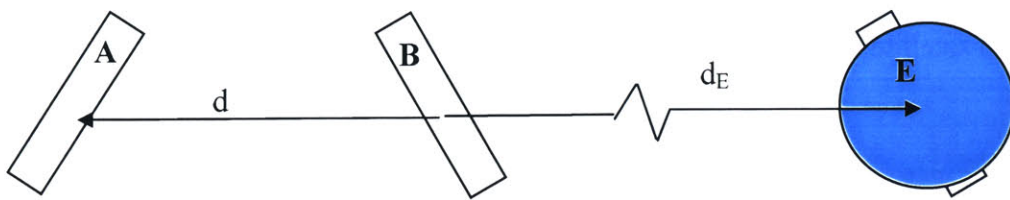


Figure 7-5: Dipole Configuration for Example #2

The formation has the following parameters.

$$\vec{d} = \begin{pmatrix} -5\text{m} \\ 0 \\ 0 \end{pmatrix} \quad \vec{d}^E = \begin{pmatrix} 6878\text{km} \\ 0 \\ 0 \end{pmatrix} \quad \vec{\mu}^E = 8e22 \begin{pmatrix} \frac{1}{\sqrt{2}} \\ \frac{1}{\sqrt{3}} \\ \frac{1}{\sqrt{6}} \end{pmatrix} \text{Am}^2 \quad \vec{f}^B = \begin{pmatrix} 10\text{mN} \\ 20\text{mN} \\ -20\text{mN} \end{pmatrix} \quad (7.51)$$

The magnetic field from the Earth at point B is given by

$$\vec{B}^E = \begin{pmatrix} 19.2391 \\ -7.85431 \\ -5.55384 \end{pmatrix} \mu\text{T} \quad (7.52)$$

The dipole solution for satellite A to counteract the B-field is given by

$$\vec{\mu}^A = \begin{pmatrix} -12024.4 \\ -9817.89 \\ -6942.30 \end{pmatrix} \text{Am}^2 \quad (7.53)$$

Solving for satellite B's dipole solution to satisfy the desired force distribution produces

$$\vec{\mu}^B = \begin{pmatrix} 301.301 \\ -3711.18 \\ 3291.22 \end{pmatrix} \text{Am}^2 \quad (7.54)$$

Section 7.5.2 Zero-Torque Solutions (Non-Zero Magnetic Fields)

The torque on satellite B can also be zero when its dipole is aligned with the local magnetic field.

$$\vec{\tau}^B = \vec{\mu}^B \times (\vec{B}^E + \vec{B}^A) \quad (7.55)$$

Aligning the dipole only takes two degrees of freedom since the magnitude of the dipole does not matter. Therefore there is still one degree of freedom available. In the following example the x component on satellite B is arbitrarily chosen as the free component. The equations of motion are

$$\begin{aligned} \vec{F}_1(\vec{r}_1, \vec{r}_2, \vec{r}_E, \vec{\mu}_1, \vec{\mu}_2, \vec{\mu}_E) - \vec{f} + \vec{f}_1^G &= 0 \\ \vec{T}_1(\vec{r}_1, \vec{r}_2, \vec{r}_E, \vec{\mu}_1, \vec{\mu}_2, \vec{\mu}_E) - \vec{\tau}_1 &= 0 \end{aligned} \quad (7.56)$$

The equations of motion can be solved for the dipole solutions. They will be a function of this remaining free component. Unfortunately the solution to these equations (from Mathematica) is very messy and pages long. Therefore an example will be used to demonstrate the concept.

Example # 3 Zero-Torque Solutions (Aligning the Dipole with the B-Field)

Using the parameters from Example # 2, equation (7.56) is now solved. The dipole solutions as a function of the x -component of satellite B's dipole are plotted below.

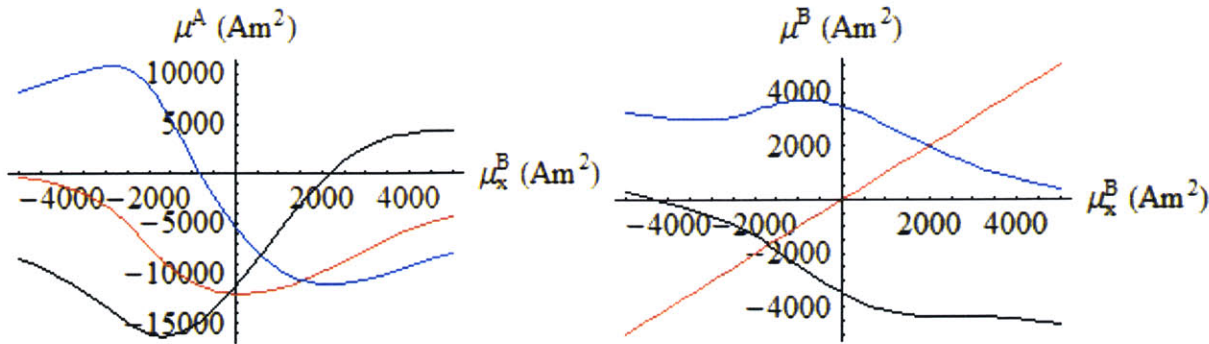


Figure 7-6: Zero-Torque Dipole Solutions

x-red y-Black z-Blue

The torque on satellite B has been set to zero, and the desired force profile has been achieved for any choice of μ_x^B . All that is remaining is to set the value of μ_x^B based on the torque distribution on satellite A. The following plot shows the possible torque distribution on satellite A.

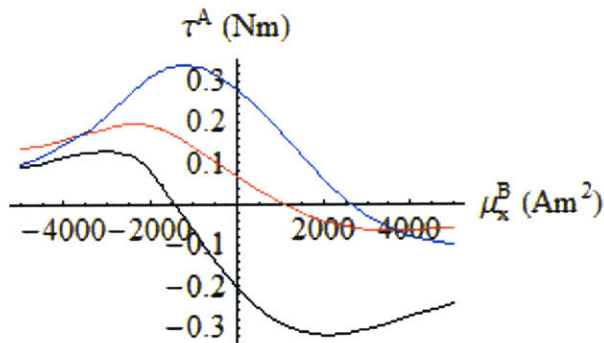


Figure 7-7: Torques on Satellite A

x-red y-Black z-Blue

Section 7.5.3 Specifying a Non-Zero Torque

Instead of looking at the zero-torque solution, it may be desirable to set the torque on one satellite to a specific direction and magnitude. Or it may be enough to specify the direction of the torque. If a satellite has a large amount of angular momentum stored, then it would be desirable to set the torque vector to be opposite of the stored angular momentum.

From equation (7.61), in order for the desired torque on satellite B to be set to a specified value, both the magnetic field at point B and satellite B's dipole must be perpendicular to the desired torque (this requires 2 degrees of control), and there is a relation between their magnitudes and angles (another degree of control). Therefore to specify a non-zero torque on a satellite requires 3 degrees of control. Solving the force equation requires another 3 degrees of control. Therefore there are 6 equations and 6 variables. Therefore, there will not be a free parameter (as was the case with the zero-torque solution).

There will be a finite number of solutions due to the fact that the equations are polynomials. Since there are 6 equations and each equation is degree 2, then from Bezout's theorem there will be no more than 2^6 solutions. However, from running multiple examples, only 3 finite solutions have been found. Therefore, the equations must be reducible. Unfortunately, applying the reduction method in Chapter 4 does not reduce the equations any more due to the limitations of the reduction method. The benefit of having three solutions is that there will always be one real solution to the equations. (Complex solutions must always appear in pairs since the equations have real coefficients).

Example # 4 Specifying a non-zero torque

Using the parameters from the previous example,

$$\vec{d} = \begin{pmatrix} -5\text{m} \\ 0 \\ 0 \end{pmatrix} \quad \vec{d}^E = \begin{pmatrix} 6878\text{km} \\ 0 \\ 0 \end{pmatrix} \quad \vec{\mu}^E = 8e22 \begin{pmatrix} \frac{1}{\sqrt{2}} \\ \frac{1}{\sqrt{3}} \\ \frac{1}{\sqrt{6}} \end{pmatrix} \text{ Am}^2 \quad \vec{f}^B = \begin{pmatrix} 10\text{ mN} \\ 20\text{ mN} \\ -20\text{ mN} \end{pmatrix} \quad (7.57)$$

we now include the desired non-zero torque on satellite B.

$$\vec{\tau}_B = \begin{pmatrix} 10 \\ 12 \\ 40 \end{pmatrix} \text{ mN-m} \quad (7.58)$$

Solving the equations of motion (equation (7.56)) produces the following three finite dipole solutions.

$$\begin{aligned}\vec{\mu}^A &= \begin{pmatrix} -3571.65 \\ 2485.59 \\ -6406.96 \end{pmatrix} \text{Am}^2 \quad \vec{\mu}^B = \begin{pmatrix} 6116.69 \\ -7409.21 \\ 693.59 \end{pmatrix} \text{Am}^2 \\ \vec{\mu}^A &= \begin{pmatrix} -6372.48 \pm 19280.7i \\ 28305.4 \pm 5678.17i \\ -15553.3 \pm 7936.91i \end{pmatrix} \text{Am}^2 \quad \vec{\mu}^B = \begin{pmatrix} 3001.54 \pm 2645.65i \\ -3861.51 \pm 2742.53i \\ 408.069 \mp 1484.17i \end{pmatrix} \text{Am}^2\end{aligned}\tag{7.59}$$

The torque on satellite A using the real solution is given by

$$\vec{\tau}_A = \begin{pmatrix} -27.53 \\ -207.8 \\ -65.26 \end{pmatrix} \text{mN-m}\tag{7.60}$$

Section 7.6 Angular Momentum Management Overview

Section 7.6.1 The Obtainable Torques

$$\vec{\tau} = \vec{\mu} \times \vec{B}^E\tag{7.61}$$

From equation (7.61), it can be seen that the disturbance torque applied to the satellites is perpendicular to the Earth's magnetic field. This means that no component of the disturbance torque can lie in the same direction as the Earth's magnetic field. Torques can only be produced in the plane perpendicular to the Earth's magnetic field. This also prevents a satellite from being able to dump angular momentum into the Earth in an arbitrary direction. Luckily, as the satellite orbits the Earth, the direction of the Earth's magnetic field will point in a different direction. (The exception is the orbit with its normal aligned with the Earth's magnetic dipole. However, over the course of a day, the Earth, and thus its magnetic field will rotate and will no longer be aligned with the orbit.) Therefore any torque direction is achievable by summing torques from

different points in orbit. For satellites with higher inclination orbits, any torque direction can be achieved at some point in the orbit.

Equation (7.61) also means that no disturbance torques are produced when the magnetic dipoles are aligned with the Earth's magnetic field. This allows for the possibility of having large dipoles that produce no torques because they are aligned with the Earth's magnetic field.

The following sections discuss methods for exploiting equation (7.61) to manage the satellites' angular momentum.

Section 7.7 Angular Momentum Management Algorithm

This section discusses an algorithm for managing the angular momentum of satellites flying in formation in LEO. The algorithm consists of two parts: the Normal mode and the Angular Momentum Reduction mode. (For consistency with the above examples, satellite B will be considered the satellite that requires its angular momentum to be managed.)

Section 7.7.1 Overview

The algorithm begins in the Normal mode. In this mode, angular momentum is not being actively managed. The free dipole is chosen at will, either arbitrarily or to achieve some goal such as minimizing the disturbance torques from the Earth's magnetic field. Regardless, as time goes by, the satellites in the formation will pick up angular momentum from the Earth's magnetic field along with other possible sources including the Earth's gravitational potential. Eventually the angular momentum stored on a satellite will surpass a threshold indicating that the angular momentum on that satellite should be reduced.

The algorithm then switches to the Angular Momentum Reduction mode. At this point in time, the satellite with the angular momentum build-up is chosen to have its angular momentum transferred to the Earth. The free dipole is used to align this satellite with the Earth's magnetic field in such a way that the torque from the Earth is applied in the direction opposite to the

angular momentum stored on the satellite. Once the angular momentum has been removed, the algorithm returns to the Normal mode.

Two concerns are immediately apparent from this method. First, if the satellites in the formation gain angular momentum faster than can be removed, this method cannot work. A quick test is while a satellite is dumping angular momentum, the sum of the angular momenta on the other satellites must be less than the angular momentum being removed from the first satellite. Therefore there is a net flow of angular momentum out of the formation. The net flow is a function of the maximum size a dipole can achieve since the larger the dipole can be set while dumping, the faster it can dump momentum. Also, the larger the dipole can be set, the smaller the dipoles on the other satellites; thus, they gain momentum more slowly. Therefore a minimum dipole size is set by the algorithm.

Second, angular momentum can only be removed in a direction that is perpendicular to the local magnetic field. The angular momentum gained from the Earth's magnetic field can typically be returned to the Earth since the disturbance torques are in the same direction as the torques needed to remove the angular momentum. However if angular momentum from other sources needs to be removed, or if the angular momentum from the Earth's field is not removed right away, then the desired torque vector may not lie perpendicular to the Earth's magnetic field. The inclination of the orbit determines the direction of the local magnetic field over the course of an orbit and thus it determines what directions the torque vector can be pointed. Over the course of one orbit, it is possible to use a combination of torques to produce the desired change in angular momentum.

The next sections discuss different methods of accomplishing the different modes and provide a working algorithm for operating in the Earth's magnetic field.

Section 7.7.2 Normal Mode Overview

In this mode, the satellites are flying in formation, but none of the satellites have an excess of angular momentum. Angular momentum is not being actively managed or removed from any of the satellites. The free dipole can be used in many ways to accomplish other goals including

- Minimize the overall magnetic dipole strength
- Minimize the torque distribution on the formation (Section 7.8.1)
- One satellite has zero-torque

Regardless of the use of the free dipole, this algorithm assumes that eventually one of the satellites will gain an excess of angular momentum that must be removed. When this happens, the second mode of the algorithm is used.

Section 7.7.3 Angular Momentum Reduction Mode Overview

Over the course of a mission, it stands to reason that at some point in time, a satellite may gain a large amount of angular momentum on its reaction wheels. Ideally the torque on that satellite would be in the opposite direction of the satellite's angular momentum vector. (It is assumed that the satellite needed angular momentum removal is satellite B.)

$$\frac{\vec{\tau}^B \cdot \vec{H}^B}{|\vec{\tau}^B| |\vec{H}^B|} = -1 \quad (7.62)$$

However, from equation (7.61), angular momentum cannot be dumped into the Earth except in a direction that is perpendicular to the Earth's dipole. Therefore only the component of the angular momentum that is perpendicular to the Earth's magnetic field can be dumped into the Earth at one point in time. The desired torque vector is restricted by

$$\vec{\tau}_{dump}^B \perp \vec{B}^E \quad (7.63)$$

The desired torque direction can be found by using

$$\frac{\vec{\tau}_{des}^B}{|\vec{\tau}_{des}^B|} = \frac{(\vec{H}^B \times \vec{B}^E) \times \vec{B}^E}{|(\vec{H}^B \times \vec{B}^E) \times \vec{B}^E|} \quad (7.64)$$

Equation (7.64) only sets the direction of the torque on satellite B. The magnitude of the torque must also be set. One good idea is to set the torque to a high value so that the angular momentum is removed quickly from the satellite. However, a better reason for setting the torque to a high value stems from the fact that the inter-satellite forces are a function of the product of dipoles.

$$\vec{F}_{BA} \propto \vec{\mu}^A \vec{\mu}^B \quad (7.65)$$

In order to increase the torque on satellite B, its dipole strength must be increased. Since the inter-satellite forces must remain unchanged, when the magnitude of satellite B's dipole increases, the magnitude of the dipole on satellite A decreases inversely proportionally. The benefit of having satellite A's dipole decrease is that the disturbance torque from the Earth on satellite A will also decrease proportionally. Since the torque on B is high and in a direction that removes angular momentum, and the torque on satellite A is low, the net flow of angular momentum will still be out of the formation as long as the torque on B is high enough.

The following sections discuss different methods of creating this desired torque vector and removing the angular momentum from the satellite formations. Each method (except for method #1) allows for the desired inter-satellite forces to be provided at all times. Thus the angular momentum management is invisible to the inter-satellite forces of the formation.

Section 7.7.3.1 Angular Momentum Reduction Method #1 – Free-Orbit Ellipse

This method of angular momentum reduction is the most simple, yet does not allow for inter-satellite forces to be applied to the satellites. It is included herein for completeness and because satellite formations that utilize a satellite without reaction wheels may need to use this method.

When a satellite has too much angular momentum, all the satellites are moved into a free-orbit ellipse. (Moving to a free-orbit ellipse can be as simple as turning off the EMFF coils. However, it may be necessary to place the formation into a different free-orbit ellipse.) Once in the ellipse,

all the satellites turn off their EMFF coils except for the satellite selected to dump angular momentum into the Earth. This allows for one satellite to remove its angular momentum without any of the other satellites in the formation experiencing an undesirable force, or torque.

The selected satellite's dipole is aligned in such a way that the torques produced from the Earth's magnetic field are in the opposite direction of the angular momentum stored on the satellite. As stated in Section 7.6, the torque due to the Earth's magnetic field can only be perpendicular to the local magnetic field. This prevents the direct removal of angular momentum unless the angular momentum happens to lie perpendicular to the local magnetic field. Therefore, to remove angular momentum from the satellite in any direction, a series of torques applied at different points in the orbit, and thus at different local magnetic fields, must be used to completely remove the angular momentum from the satellite.

Once the excess angular momentum has been removed, the formation returns to its operating position and continues in the Normal mode.

This method has the obvious issues of needing to move into a free orbit ellipse, and then losing the ability to provide magnetic forces between the satellites during the angular momentum management process. The algorithms in the next section have no such restrictions but do require that all the satellites have reaction wheels.

Section 7.7.4 Angular Momentum Reduction Method #2 – Specifying the Torque on a Satellite

This method attempts to remove angular momentum from the satellite by directly specifying the torque on the satellite just as in Section 7.5.3.

Section 7.7.4.1 Specified Torque is Perpendicular to the Earth's Magnetic Field

This method attempts to set the torque direction on Satellite B to be exactly that given in equation (7.64). From (7.61), the torque on satellite B due to the Earth and satellite A is given by

$$\bar{\tau}^B = \bar{\mu}^B \times \vec{B}^E + \bar{\mu}^B \times \vec{B}^A \quad (7.66)$$

Since torque can only be applied from Earth in a direction that is perpendicular to the local magnetic field from the Earth, one option is to specify the total torque on the satellite to also be perpendicular to the local magnetic field due to the Earth.

If the torque on satellite B is defined to be perpendicular to the Earth's magnetic field, then from equation (7.66), the magnetic field from satellite A is also restricted.

$$\vec{B}^A \perp \vec{\tau}_{des}^B \quad \text{or} \quad \vec{B}^A = 0 \quad \text{or} \quad \vec{\mu}^B = 0 \quad (7.67)$$

Either the local magnetic field from satellite A must be perpendicular to the desired torque, the field itself must be zero, or the dipole on satellite B must be zero. The last two cannot happen since for the force EOM to be satisfied, the dipole on neither satellite can be zero. Therefore, the magnetic field from satellite A is perpendicular to the desired torque vector.

Because the magnetic field on satellite A is restricted to be in a plane, it forces the dipole on satellite A to also reside on a surface of possible solutions. Also from equation (7.66)

$$\vec{\mu}_B \perp \vec{\tau}_B \quad (7.68)$$

This forces the dipole on satellite B to reside in a plane. (Not necessarily the same surface as the dipole for satellite A.) Unfortunately, the force equation cannot find a real solution when the dipole vectors are restricted in such a way.

The problem lies in the fact that the desired torque is perpendicular to the Earth's magnetic field. When the desired torque lies in a direction that is not perpendicular to the Earth's magnetic field, the magnetic field from satellite A must move the local magnetic field perpendicular to the desired torque, and there are different ways or degrees of freedom in which it can do that. However, when the Earth's magnetic field is already perpendicular to the desired torque, then the magnetic field from satellite A is zero, or it must also lie perpendicular to the desired torque. This reduction of freedom for satellite A's magnetic field prevents a real solution from being found.

Example # 5 Approaching Perpendicularity

This example will look at what happens when the desired torque approaches perpendicularity to the Earth's magnetic field. The same parameters are being used as the previous example except that the desired torque will approach being perpendicular to the local magnetic field.

$$\vec{\tau}_{des}^B = \vec{\tau}^\perp + (1-\alpha) \begin{pmatrix} 10 \\ 10 \\ 10 \end{pmatrix} \text{mN-m} \quad (7.69)$$

where

$$\vec{\tau}^\perp \perp \vec{B}^E \quad (7.70)$$

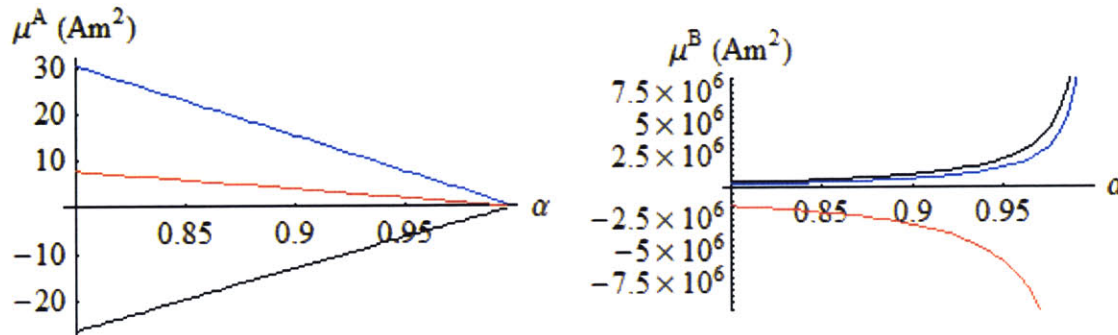


Figure 7-8: Dipole strength on satellite A and B

x-red y-Black z-Blue

From the plots we can see why no solution could be found under the restrictions of (7.67). As the desired torque approached perpendicularity to the Earth's magnetic field, the magnetic field from satellite A does not need to create as much of a change the local magnetic field so that it is perpendicular to the desired torque. When the desired torque became perpendicular to the Earth's magnetic field, the component of magnetic field from satellite A that used to move the local magnetic field goes to zero. Because satellite A's dipole is already constrained by the force equations, when one component goes to zero, the whole dipole must go to zero. To satisfy the force equations, since dipole A went to zero, satellite B's dipole must go to infinity. Therefore

when the desired torque is exactly perpendicular to the Earth's magnetic field, there is no solution.

Section 7.7.4.2 Desired Torque is NOT perpendicular to the Earth's magnetic field.

If the restriction from equation (7.63) is lifted, and the desired torque is not perpendicular to the Earth's magnetic field, then a solution can be found as expected from Section 7.5.3. In this case the desired torque is once again chosen, but since the dipole is not perpendicular to the Earth's magnetic field, all of the angular momentum removed does not go into the Earth. The remaining angular momentum is transferred into the other satellite. This is best illustrated by an example.

Example # 6 Desired Torque not Perpendicular to the Earth's Magnetic Field

This example will use the same parameters as Example # 4 except that the size of the torque desired will be varied by a parameter α .

$$\vec{\tau}_{des}^B = \alpha \begin{pmatrix} 10 \\ 12 \\ 40 \end{pmatrix} \text{mN-m} \quad (7.71)$$

As the parameter α is varied, the torque on satellite B is exactly what was specified in equation (7.71).

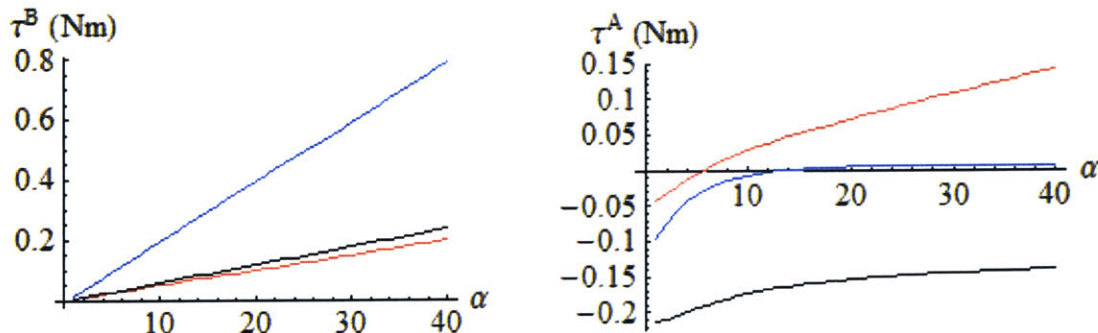


Figure 7-9: Torque on Satellite B and on the Earth

x-red y-Black z- Blue

Therefore the remaining angular momentum gain from satellite B must be coming from satellite A, and from the figure we see that it is true. Essentially satellite B dumps all the angular momentum it can (the component that is perpendicular to the Earth's B field) into the Earth, but the remaining torque must be dumped into the other satellite.

The dipole strengths on both satellites are given in the following plots.

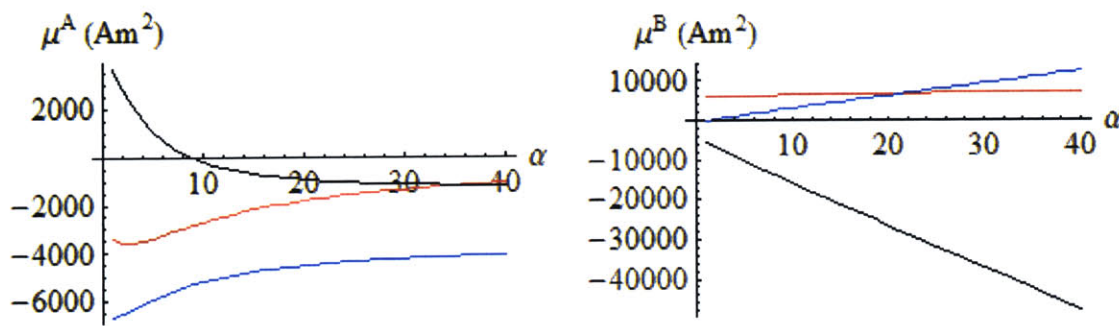


Figure 7-10:Dipole Strength on Satellite A and B

x-red y-Black z-Blue

The plot on the right shows that the strength of satellite B's dipole is steadily increasing as the desired torque on that satellite is increasing. This makes sense as the torque on satellite B is a direct function of its dipole strength. The dipole strength on satellite A also starts to decrease as the torque on satellite B increases, but then levels off. This is because satellite A must make the magnetic field at point B point in the right direction. The solution that satellite A's dipole is approaching is the **minimum** dipole solution that forces the magnetic field at point B to be perpendicular to the desired torque.

$$\vec{\tau}_{des}^B \perp (\vec{B}^E + \vec{B}^A) \quad (7.72)$$

Since satellite A's dipole no longer decreases, the torque from the Earth's magnetic field on satellite A remains constant. However, the torque from satellite B continues to increase since its dipole strength also increases.

It would appear that the force EOM must be violated as satellite A's dipole remains fairly constant, and satellite B's dipole is increasing. How does the inter-satellite force remain constant? The answer is that the component of satellite B's dipole that is increasing is perpendicular to the gradient of satellite A's magnetic field. Therefore it doesn't affect the inter-satellite forces.

This raises the possibility of being able to directly transfer angular momentum from one satellite to another in the presence of the Earth's field, but that topic is not addressed herein.

From this example it appears that having the desired torque lie perpendicular to the Earth's magnetic field would be best since the B field necessary from satellite A would be zero, and its momentum change would be zero. However, as was seen in Section 7.7.4 no solution can be found when the dipole is directly perpendicular to the Earth's magnetic field.

Section 7.7.4.3 Method #2 Conclusions

Using the ability to directly specify the torque on a satellite seems like a good option. Ideally one would specify the torque on the satellite to be perpendicular to the Earth's magnetic field. However, no solution can be found in this case. The desired torque can be chosen so that it is not perpendicular to the local magnetic field, but the open-ended question is how far away from the magnetic field should the desired torque vector point.

The problem is that due to the inter-satellite forces, torques will be applied to each satellite that are in the opposite direction of the angular momentum gained by the movement of the satellites. The component of this torque that is not perpendicular to the Earth's magnetic field should not be restricted to zero, however, the above method is doing just that by specifying the torque on the satellite to only be perpendicular to the Earth's magnetic field. When the torque is restricted in this way, the torque from the inter-satellite forces is being completely placed on satellite A.

The solution is to separate the two torques. Specify the dipole in such a way that the torque from the Earth's magnetic field on satellite B is in the direction opposite of the angular momentum

vector, but ignore the torques applied from satellite A. The next section discusses this method in detail.

Section 7.7.5 Method #3 - Setting the Dipole to be Perpendicular to the Earth's B Field

In this section, the overall torque on satellite B is not directly specified. Instead, the focus is on the torque on satellite B from the Earth's magnetic field. Essentially, the torque from satellite A is not considered. Once the torque from satellite A is not considered, then the constraint on the magnetic field of satellite A no longer holds and a dipole solution can be found.

Section 7.7.5.1 Overview

Once again, the component of angular momentum that can be transferred to the Earth is perpendicular to the local Earth's magnetic field. Therefore, the desired torque on the satellite B *from the Earth's magnetic field* is perpendicular to the Earth's magnetic field. The requirement forces satellite B's dipole to be perpendicular to the Earth's magnetic field.

$$\vec{\mu}^B \perp \vec{B}^E \quad (7.73)$$

Since the magnetic field from satellite A is neglected, satellite B's dipole can be found from

$$\vec{\tau}_{des}^{BE} = \vec{\mu}^B \times \vec{B}^E \quad (7.74)$$

where

$$\frac{\vec{\tau}_{des}^{BE}}{|\vec{\tau}_{des}^{BE}|} = \frac{(\vec{H}^B \times \vec{B}^E) \times \vec{B}^E}{|(\vec{H}^B \times \vec{B}^E) \times \vec{B}^E|} \quad (7.75)$$

Even though the inter-satellite torques are not considered when determining satellite B's dipole, the overall torque on satellite B is still given by

$$\vec{\tau}^B = \vec{\tau}^{BA} + \vec{\tau}_{des}^{BE} \quad (7.76)$$

This method also takes advantage of the fact that when satellite B increases its dipole strength, satellite A's dipole strength will decrease (as long as satellite B's dipole does not increase along

a direction that is perpendicular to the gradient of satellite A's magnetic field). This allows the torque on satellite B from the Earth to increase while at the same time decreasing the torque on satellite A from the Earth.

The torque on satellite B from satellite A remains constant no matter what the strength of satellite B's dipole is since the product of the magnitudes must remain fixed to maintain a constant force. The sum of the torque on satellite A from satellite B and on satellite B from satellite A is constant. This sum is equal and opposite of the angular momentum gained from the forces applied to the formation. Typically, depending on the orientation of the dipoles, the distribution of this torque can vary on the satellites. However, the dipole on satellite B (and thus satellite A) is fixed from equation (7.74). Therefore the torque is only a function of the product of the dipoles. However from the force equation of motion, the product of the dipole strength is fixed. Therefore the inter-satellite torques remain constant.

Example # 7 Dipole is Perpendicular to the Earth's Magnetic Field

Once again using the same parameters as the previous example, the desired torque direction is

$$\frac{\vec{\tau}_{des}}{|\vec{\tau}_{des}|} = \begin{pmatrix} 0.419324 \\ 0.484058 \\ 0.768020 \end{pmatrix} \quad (7.77)$$

The Earth's magnetic field at the formation's location is

$$\vec{B}^E = \begin{pmatrix} 19.2391 \\ -7.85431 \\ -5.55384 \end{pmatrix} \mu\text{T} \quad (7.78)$$

Solving for satellite B's dipole produces a dipole direction of

$$\frac{\vec{\mu}_B}{|\vec{\mu}_B|} = \begin{pmatrix} -0.155458 \\ -0.795207 \\ 0.586071 \end{pmatrix} \quad (7.79)$$

The magnitude is left as a variable. Solving the force EOM for dipole A produces

$$\vec{\mu}_A = \frac{1}{|\vec{\mu}_B|} \begin{pmatrix} 3.25132e6 \\ 3.80934e7 \\ 5.3029e7 \end{pmatrix} A^2 m^4 \quad (7.80)$$

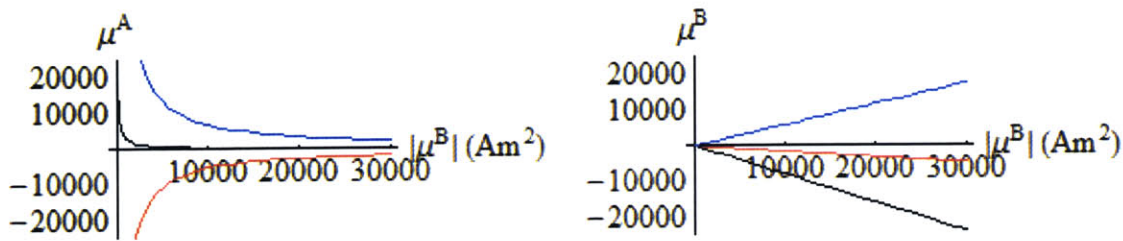


Figure 7-11: Dipole Strength on Satellite A and B

As expected, as the dipole strength of satellite B is increased, the dipole strength of satellite A comes down rapidly.

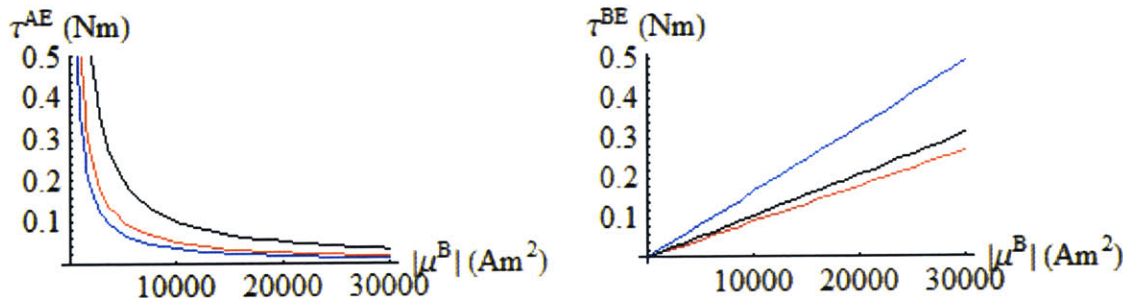


Figure 7-12: Torque from the Earth on Satellite A and B

From the above plots, it can be seen that as satellite B increases its dipole strength, it is able to dump more angular momentum. Also, as satellite B's dipole increases in strength, the torque from the Earth on satellite A decreases rapidly. The inter-satellite torques remain constant, and

as satellite B's dipole strength increases, they are much smaller than the torque applied by the Earth.

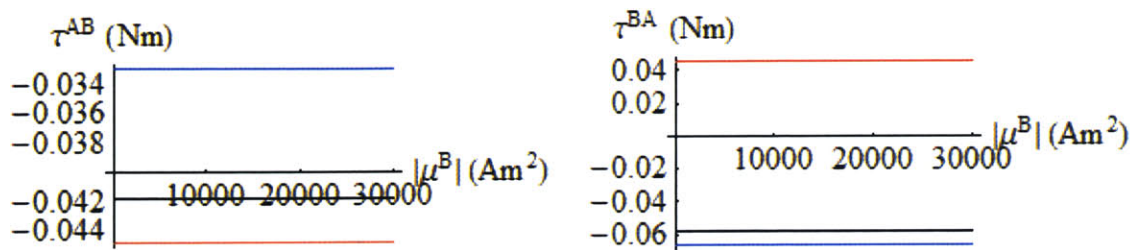


Figure 7-13: Inter-Satellite Torques

Section 7.7.5.2 Difficulty #1: Direction of Satellite B's Dipole

One problem with this method is that the direction of satellite B's dipole is defined from the beginning. If satellite B's dipole lies in the plane that is perpendicular to the vector between the two satellites, then there is no dipole configuration for satellite A to produce a force that is not in the same plane spanned by satellite B's dipole, and the vector connecting the satellites.

In other words, as the angle between satellite B's dipole and the vector connecting the two satellites approaches 90°, then the product of the magnitude of the dipoles of the two satellites approaches infinity. Since satellite B's dipole is limited by a maximum value set by the hardware, satellite A's dipole will have to take the increase.

This is best visualized with an example.

Example # 8 : Difficulty #1

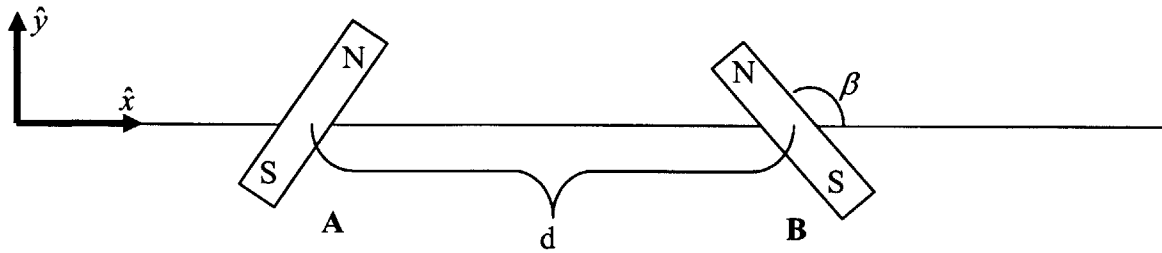


Figure 7-14: Schematic of Two Dipoles

Imagine two dipoles in the configuration above. Using the same parameters as the previous examples, we have

$$\vec{d}^A = \begin{pmatrix} -5\text{m} \\ 0 \\ 0 \end{pmatrix} \quad \vec{f}^A = \begin{pmatrix} -10\text{mN} \\ -20\text{mN} \\ 20\text{mN} \end{pmatrix} \quad (7.81)$$

Dipole B is set by equation (7.74) to be perpendicular to the Earth's magnetic field, and the desired torque vector. For this example, it is assumed that these equations constrain satellite B in such a way that it resides in the x - y plane and has an angle β from the x axis as shown in Figure 7-14. As β is varied and approaches 90° , the force equations of motion solve for a larger and larger product for the dipole strengths. When β equals 90 degrees, the product is infinite. Please refer to Section 4.2 for more explanation.

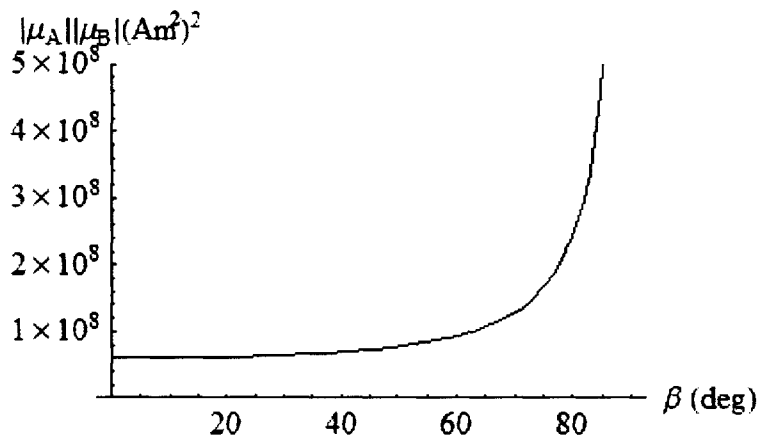


Figure 7-15: Resulting Product of Dipole Strengths to Satisfy Force EOM

If the maximum value for the Dipole on satellite B is $30,000 \text{ Am}^2$, then the magnitude of the dipole on satellite A is given by Figure 7-16.

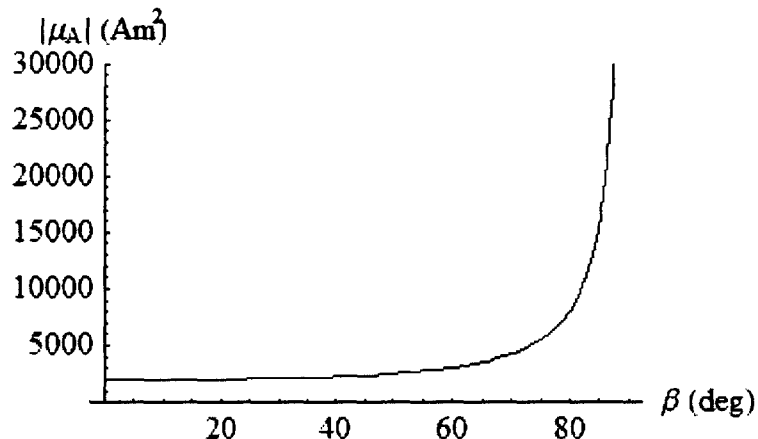


Figure 7-16: Required Strength on Satellite A's Dipole to Satisfy Force EOM

Section 7.7.5.3 Difficulty #1 Continued

Remember, our goal of increasing satellite B to its hardware maximum level is so that the magnitude on satellite A is small, and thus the disturbance torques are small. From Figure 7-16, as long as β is less than approximately 82 degrees, then the goal is accomplished. However, if

β is close to 90 degrees, then the dipole on satellite A is large, possibly even larger than the hardware maximum for that coil. In this example, satellite A's dipole reaches $30,000\text{Am}^2$ at 87.3 degrees.

This phenomenon does not prevent the idea in this section from working. Most of the time β is not near 90 degrees. For the times that it is near 90 degrees, it can be artificially restricted.

$$\left(\beta \equiv \cos^{-1}\left(\frac{\vec{r}_{BA} \cdot \vec{\mu}_B}{|\vec{r}_{BA}| |\vec{\mu}_B|}\right) \right) < \beta_{\text{restrict}} \quad (7.82)$$

β_{restrict} could be set at a value of 80~85 degrees. Since equation (7.82) places a restriction on satellite B's dipole, equation (7.73) is no longer satisfied and the satellite's dipole is no longer perpendicular to the Earth's magnetic field. However the dipole on satellite B will only be restricted by a few degrees, therefore the actual torque achieved will be very close to the desired torque. Furthermore, the Earth's magnetic field will vary over the course of the orbit, and thus if satellite B's dipole is restricted at one point in time, chances are it won't be restricted long, and then the desired torque can again be achieved.

Section 7.7.5.4 Difficulty #2 –Torque Vector Aligned with the Earth's Magnetic Field

From equation (7.75), and reproduced here, the desired torque vector is by definition perpendicular to the Earth's magnetic field.

$$\frac{\vec{\tau}_{\text{des}}^{BE}}{|\vec{\tau}_{\text{des}}^{BE}|} = \frac{(\vec{H}^B \times \vec{B}^E) \times \vec{B}^E}{|(\vec{H}^B \times \vec{B}^E) \times \vec{B}^E|} \quad (7.83)$$

However, as the torque vector is applied, and the angular momentum vector is reduced, eventually there will be a component of the angular momentum vector that is aligned with the Earth's magnetic field. When the angular momentum vector is aligned with the Earth's magnetic field, the desired torque is zero even though the angular momentum vector is not. Also, as the Earth's vector moves, by constantly removing the component that is perpendicular to the Earth's magnetic field, the angular momentum vector has a tendency to rotate instead of being reduced.

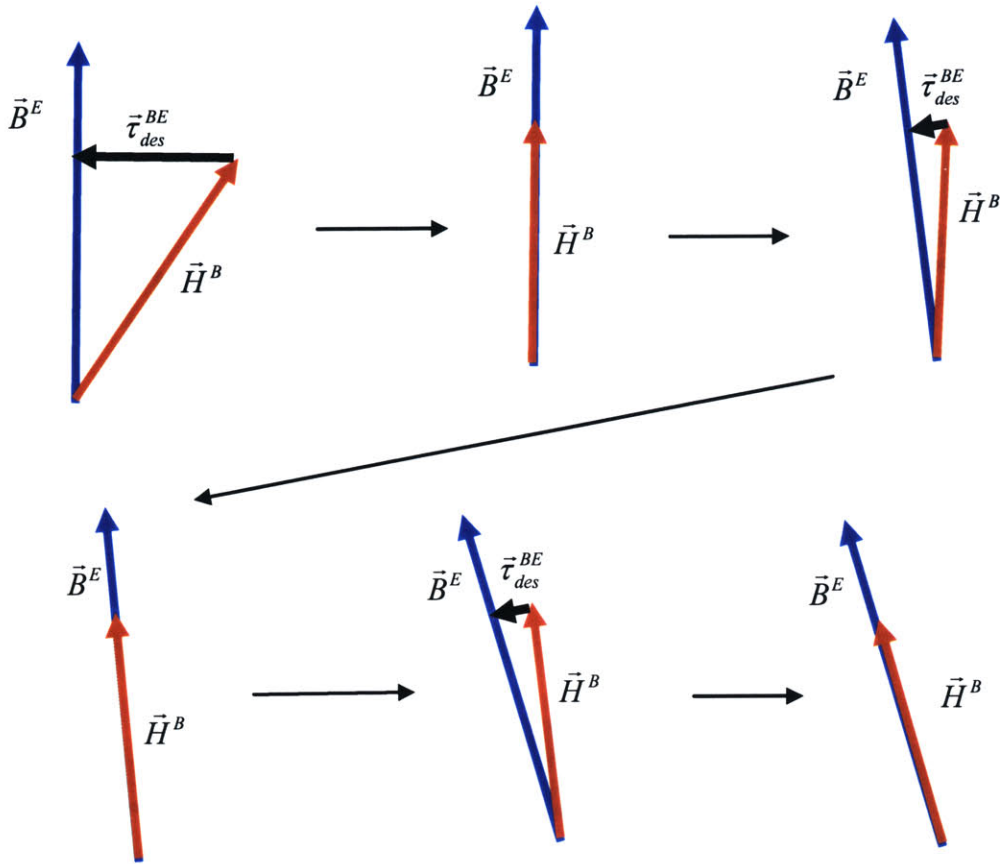


Figure 7-17: Pictorial representation of the Angular Momentum Vector Following the Magnetic Field Vector

In Figure 7-17 the angular momentum vector is being reduced. In the first step, the magnitude of the angular momentum vector is reduced, but only to the point where the angular momentum vector is aligned with the Earth's magnetic field. As the Earth's magnetic field moves, a new component of the angular momentum vector can be reduced. However, this vector (while perpendicular to the Earth's magnetic field) is essentially perpendicular to the angular momentum vector and thus the vector rotates instead of reduces.

One solution to this problem is to wait for the Earth's magnetic field to rotate more significantly before applying the torque.

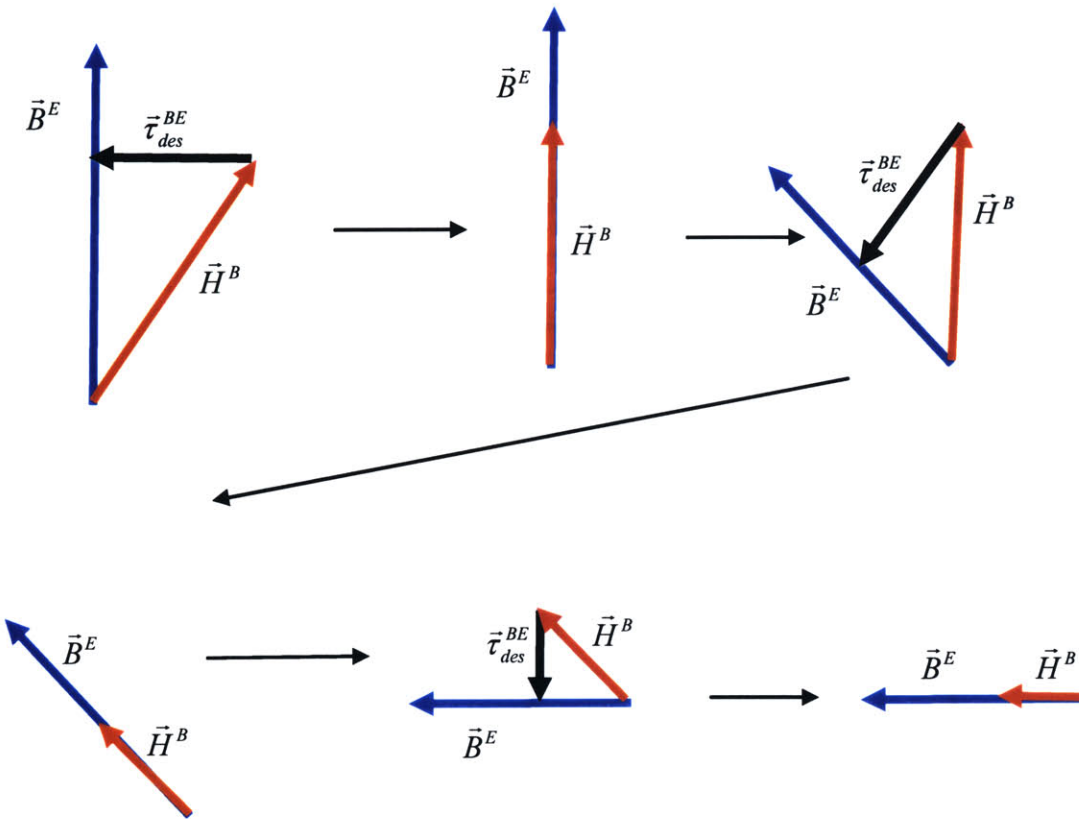


Figure 7-18: Minimizing the Angular Momentum Vector by Waiting for the Magnetic Field to Move

While waiting for the Earth's magnetic field to rotate, the free dipoles still need to be set. During this period the formation can either switch to the normal mode, or the angular momentum from satellite A can be reduced. The latter is a good option since when satellite A's angular momentum is being reduced, satellite B's dipole is small, and thus the angular momentum on Satellite B does not change significantly.

Section 7.7.5.5 Difficulty #3 – Overshooting the Angular Momentum Vector

In this algorithm, the desired torque vector is always increased to a maximum value. However, if the angular momentum vector is close to the magnetic field vector, then the angular momentum vector can overshoot the magnetic field vector.

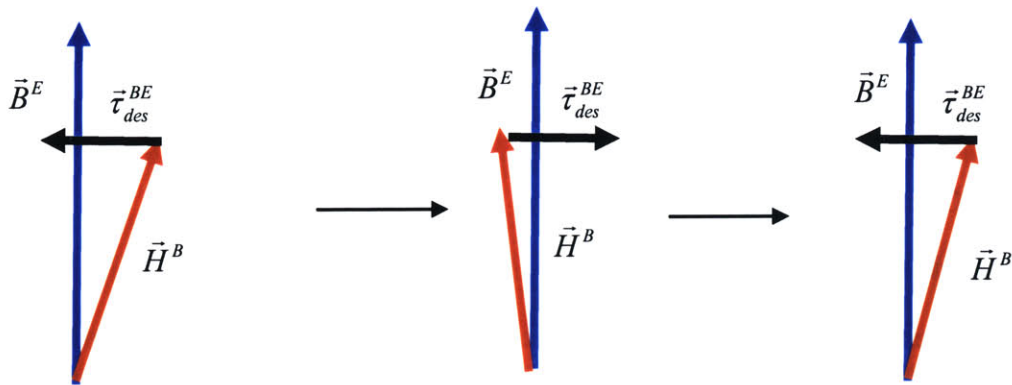


Figure 7-19: Overshooting the Magnetic Field

Once the angular momentum vector overshoots, on the next iteration step, it will overshoot the other direction, and the solution tends to oscillate about the angular momentum vector. One idea is to reduce the size of the desired torque vector so that the angular momentum vector will align with the Earth's magnetic field after an iteration step.

However, this does not work because if the angular momentum vector is closely aligned to the Earth's magnetic field, then the magnitude of the desired torque vector is small. Since the direction of satellite B's vector is fixed, the only way to reduce the size of the torque is to reduce the magnitude of satellite B's dipole strength. By reducing satellite B's dipole strength satellite A's dipole strength increases, and thus the torque from the Earth's magnetic field onto satellite A must increase, sometimes significantly.

The solution to this problem is to determine satellite B's dipole so that the desired torque aligns the angular momentum vector with the magnetic field. Relax the constraint that satellite B's dipole must be perpendicular to the Earth's magnetic field. Then add to satellite B's dipole a component that is parallel to the Earth's magnetic field, and increases the magnitude of satellite B's dipole strength to maximum. This added dipole component will not affect the desired torque on satellite B from the Earth's magnetic field, and will keep satellite A's dipole small.

It should be noted however, that the solution to difficulty #2 will typically prevent the situation in difficulty #3 since it keeps the angular momentum vector from aligning with the Earth's magnetic field.

Section 7.7.5.6 Overview of the Final Algorithm

- **Normal Mode**
 - When in this mode, arbitrarily pick the free dipole. To prevent the gradient of the magnetic field from being zero, align the free dipole with the vector connecting the two satellites. If there are more than two satellites, align it with the formation's center of mass. Set the magnitude of the dipole so that the magnitude of the other satellites' dipoles are comparable.
- OR
- Choose the free dipole so that the disturbance torques on each satellite is minimized. (See Section 7.8)
- Once a satellite's angular momentum crosses an upper threshold, select that satellite for angular momentum reduction. (For clarity, let's assume that satellite is satellite B.)
- **Angular Momentum Reduction Mode**
 - The angular momentum and local magnetic field due to the Earth are calculated for satellite B. \vec{B}^E, \vec{H}^B

- To prevent difficulty #2, the angle between \vec{B}^E and \vec{H}^B is calculated.

$$\angle^{BH} = \cos^{-1} \frac{\vec{B}^E \cdot \vec{H}^B}{|\vec{B}^E| |\vec{H}^B|} \quad (7.84)$$

- If \angle^{BH} is near zero, (typically within 10 degrees), then select another satellite in the formation for angular momentum reduction, or switch to the normal mode until \angle^{BH} is no longer too close to the Earth's magnetic field.
- Create the desired torque vector direction.

$$\frac{\vec{\tau}_{des}^{BE}}{|\vec{\tau}_{des}^{BE}|} = \frac{(\vec{H}^B \times \vec{B}^E) \times \vec{B}^E}{|(\vec{H}^B \times \vec{B}^E) \times \vec{B}^E|} \quad (7.85)$$

- Define the direction and magnitude of satellite B's dipole.

$$\vec{\mu}^B = -|\vec{\mu}_{max}| \frac{\vec{\tau}_{des}^{BE} \times \vec{B}^E}{|\vec{\tau}_{des}^{BE} \times \vec{B}^E|} \quad (7.86)$$

- If the desired torque will cause the angular momentum vector to oscillate about the magnetic field vector (difficulty #3), then adjust satellite B's dipole as appropriate.
- Check to see if satellite B's dipole is perpendicular to the vector connecting satellite B to satellite A (difficulty #1). (A variation is used for multiple spacecraft.) If so, adjust the dipole.

$$\alpha^{\mu r} = \cos^{-1} \frac{\vec{\mu}^B \cdot \vec{r}^{BA}}{|\vec{\mu}^B| |\vec{r}^{BA}|}$$

If $80^\circ < \alpha^{\mu r} < 100^\circ$

Then

(7.87)

$$\vec{n} \equiv \frac{\vec{r}^{BA} \times (\vec{\mu}^B \times \vec{r}^{BA})}{|\vec{r}^{BA} \times (\vec{\mu}^B \times \vec{r}^{BA})|}$$

$$\vec{\mu}_{adj}^B = \left| -\mu_{\max} \right| \left(\frac{\vec{n} + \text{sign}(90^\circ - \alpha^{\mu r}) \tan 10^\circ \frac{\vec{r}^{BA}}{|\vec{r}^{BA}|}}{\left| \vec{n} + \text{sign}(90^\circ - \alpha^{\mu r}) \tan 10^\circ \frac{\vec{r}^{BA}}{|\vec{r}^{BA}|} \right|} \right)$$

- Solve the force equation of motion for the remaining satellite dipoles
- Once satellite B's angular momentum is below a lower bound, return to the normal mode.

Example # 9 Two Satellite Angular Momentum Management Algorithm

This example will use the above algorithm to manage the angular momentum for a satellite formation in LEO. (The free dipole is chosen arbitrarily in the normal mode.) The satellite formation has the following orbital parameters.

$$\begin{aligned} a &= 6878 \text{ km} \\ e &= 0 \\ i &= 65^\circ \\ \theta_0 &= 0^\circ \end{aligned} \tag{7.88}$$

The satellites have the following mass parameters.

$$\begin{aligned} m_A &= 300 \text{ kg} \\ m_B &= 100 \text{ kg} \end{aligned} \tag{7.89}$$

The satellites are held in a fixed position relative to the rotating coordinate frame (Earth pointing, side/forward looking).

$$\vec{r}^A = \begin{pmatrix} 2 \\ .2 \\ .2 \end{pmatrix} \text{m} \quad \vec{r}^B = \begin{pmatrix} -6 \\ -.6 \\ -.6 \end{pmatrix} \text{m} \quad (7.90)$$

The gravitational forces produced on the satellites over an orbital period are

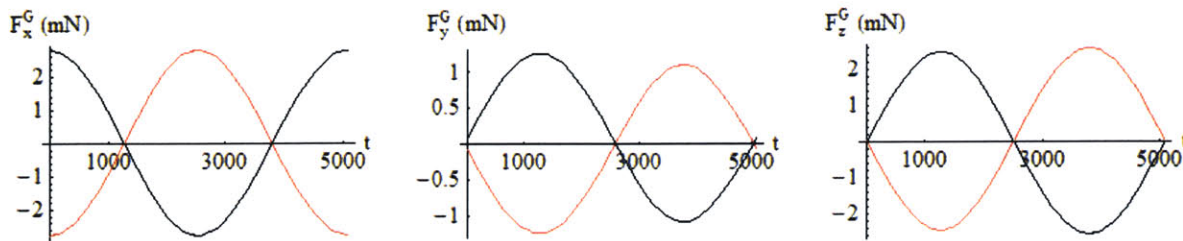


Figure 7-20: Gravitational Forces on Each Satellite
Satellite A – Red Satellite B -- Black

In the rotating coordinate frame the gravitational forces are

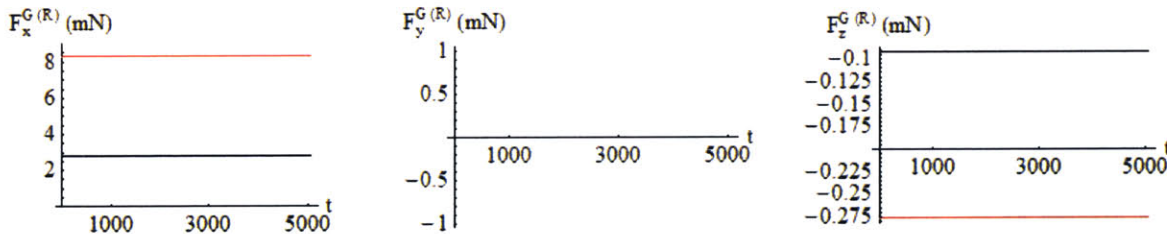
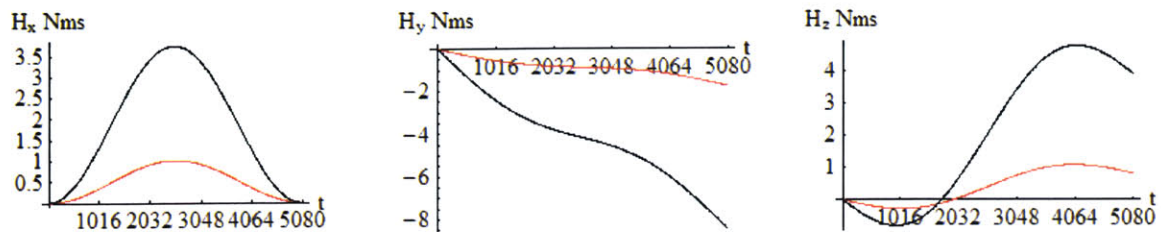


Figure 7-21 Gravitational Forces on Each Satellite in the Rotating Coordinate Frame
Satellite A – Red Satellite B – Black

Ignoring the affects of the Earth's magnetic field and choosing a free dipole of

$$\vec{\mu}_A = \begin{pmatrix} 4587.8 \\ 0 \\ 0 \end{pmatrix} \text{Am}^2 \quad (7.91)$$

The satellites have the following angular momentum after one orbital period.



**Figure 7-22: Satellite Angular Momentum over One Orbit
Excluding the Earth's Magnetic Field**

Over twenty orbital periods the angular momentum is

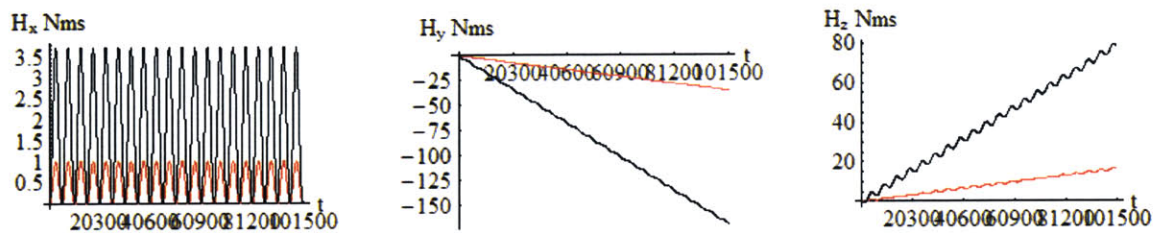


**Figure 7-23: Satellite Angular Momentum over 20 Orbital Periods
Excluding the Earth's Magnetic Field**

The angular momentum on the two satellites is not evenly distributed, and is secular in nature.

If the effects of the Earth's magnetic field are included, then the angular momentum over one orbital period is

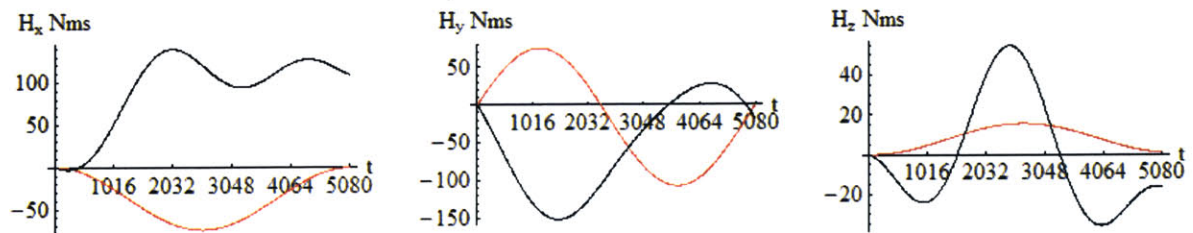


**Figure 7-24: Satellite Angular Momentum over 20 Orbital Periods
Including the Earth's Magnetic Field**

Over twenty orbital periods the angular momentum is

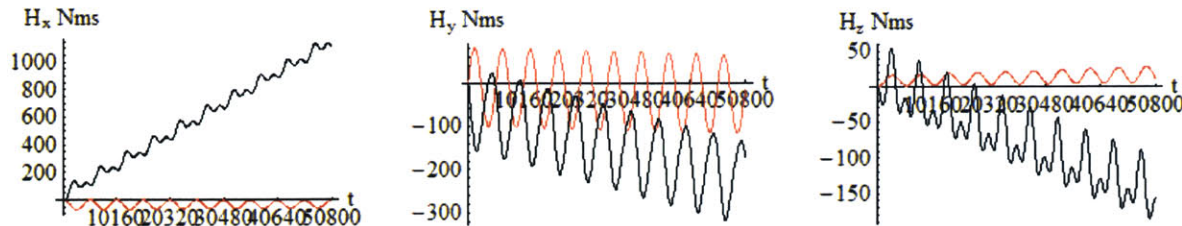


Figure 7-25: Satellite Angular Momentum over 20 Orbits

Including the Earth's Magnetic Field

As can be seen from the plots, the torque from the Earth's magnetic field can cause a significant increase in the angular momentum applied to the satellite formation. The next step is to implement the algorithm of Section 7.7.5.6.

The parameters of the algorithm are as follows

$$\begin{aligned} |\vec{H}|^{\text{Upper Bound}} &= 40 \text{ Nms} \\ |\vec{H}|^{\text{Lower Bound}} &= 20 \text{ Nms} \\ |\vec{\mu}_{\max}| &= 10,000 \text{ Am}^2 \end{aligned} \quad (7.92)$$

Over one orbital period, the angular momentum build-up is

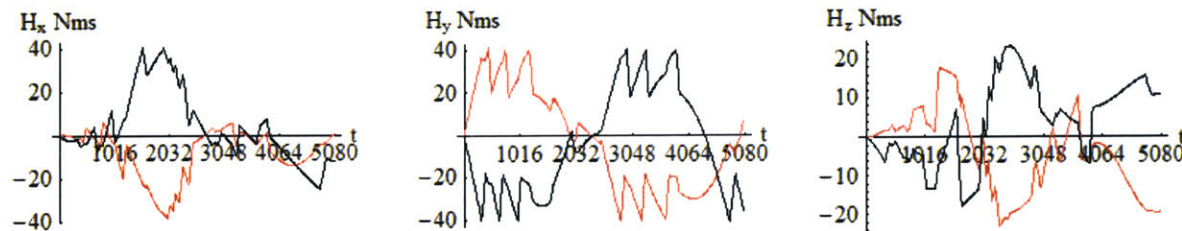


Figure 7-26: Satellite Angular Momentum Management Using the Algorithm

Figure 7-27 zooms in on the first 1500 seconds of the orbit. As the angular momentum builds up, it builds up the fastest on satellite B's y component. When it reaches -40 Nms , the algorithm switches to the next mode at which point the angular momentum is driven down until it reaches

the lower bound of -20Nms. Once the lower bound is reached, it switches back into the normal mode until satellite A's y component of angular momentum reaches 40Nms. The algorithm switches modes and reduces satellite A's angular momentum to 20Nms. The algorithm moves back into the normal mode for a while until the next satellite's component of angular momentum reach 40Nms and the process is repeated.

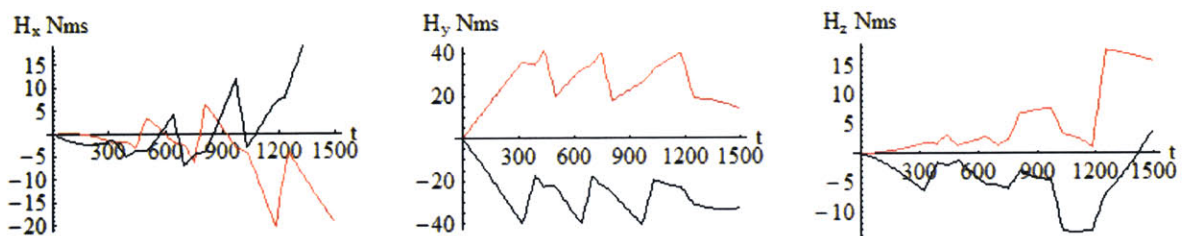


Figure 7-27: Zoomed in Plot of Angular Momentum Management

It should be noted that when one satellite's angular momentum is being reduced, the other satellite's angular momentum does not change very much. This is due to the fact that its dipole is very small, and thus there is only a small disturbance torque on the satellite.

The satellite dipole strength is given as

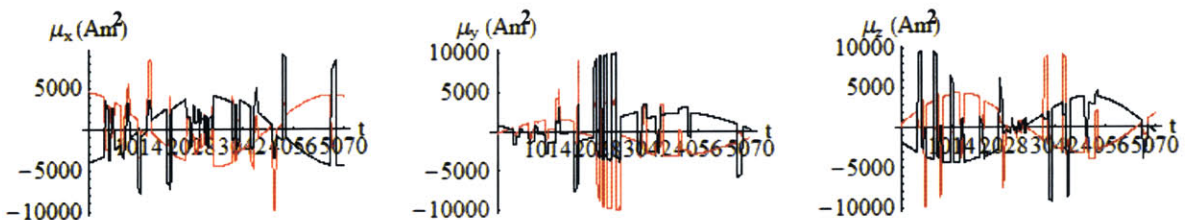


Figure 7-28: Satellite Dipole Strength

From the plot, the Normal mode dipole strength can be seen as a sinusoidal solution. (Recall, this solution was chosen arbitrarily.) When the algorithm is in the Angular Momentum Reduction node, the dipole strength on one satellite increases while the dipole strength on the other satellite decreases.

Looking at the modes that the algorithm is in, the following plot shows when the algorithm is reducing satellite A, satellite B or in the Normal mode.

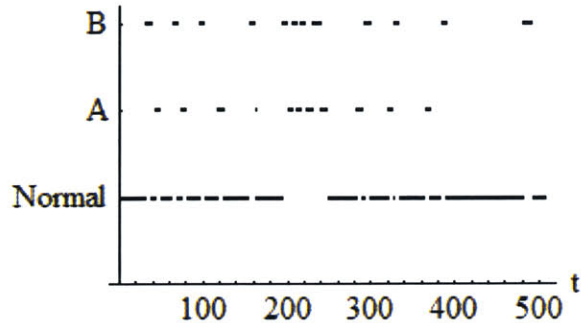


Figure 7-29: Algorithm Mode

The formation is in the normal mode 70% of the time and reducing the angular momentum the remaining 30% of the time.

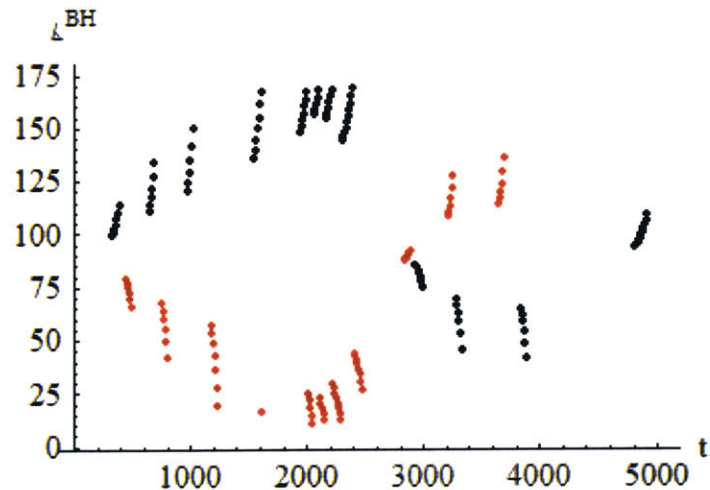


Figure 7-30 Angle Between the Satellite Angular Momentum Vector and the Earth's Magnetic Field (Angle is Only Shown when the Satellite is Reducing Angular Momentum)

Difficulty number two was encountered at approximately 1800 seconds. From Figure 7-30, the angle between angular momentum vector of the satellite being actively dumped and the Earth's magnetic field is shown. As expected, the angle between the angular momentum and the Earth's

magnetic field approaches 0 degrees (or 180 degrees) as the angular momentum is being removed. At approximately 1800 seconds, Satellite B is removing its angular momentum. The angle between Satellite B's angular momentum and the magnetic field approaches 10 degrees. At which time, the algorithm attempts to reduce satellite A's angular momentum. Quickly satellite A's angular momentum and the Earth's magnetic field also approach 10 degrees. The algorithm then goes into the Normal mode until one of the satellites angular momentum reaches the upper bound of 40 Nms and the algorithm switches modes again.

As can be seen, the difficulty was overcome by the algorithm. Because the angle between the angular momentum vector and the Earth's magnetic field was forced to be at least 10 degrees, the angular momentum vector was reduced and not rotated significantly.

Difficulty number one was also encountered.

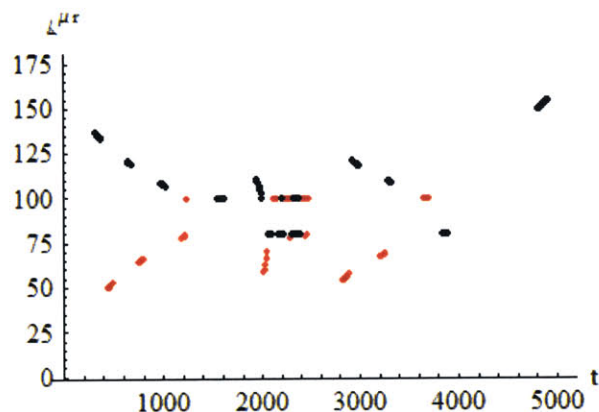


**Figure 7-31: Angle Between the Satellite Dipole and the Vector Connecting the Satellites
(Angle is Only Shown when the Satellite is Reducing Angular Momentum)**

From Figure 7-32, it can be seen that between approximately 1200 seconds and 2200 seconds, the satellites dipole is not allowed to be within 10 degrees of being perpendicular to the position vector connecting the two satellites. This kept the dipole strength on the satellite not being actively reduced to a small value.

If we now let the simulation run for twenty orbits, we have the following angular momentum plots.

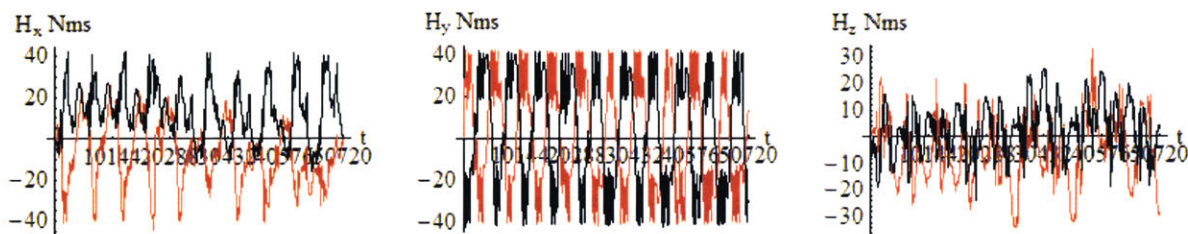


Figure 7-32: Satellite Angular Momentum over 20 Orbits using the Algorithm

From the plots, it can be seen that the algorithm successfully keeps the angular momentum within the bounds specified. The angular momentum gain from the Earth is managed and also the angular momentum gain from the gravitational forces is also successfully transferred to the Earth.

Example # 10 Insufficient Maximum Dipole Strength

If the maximum dipole component strength is reduced from 10,000Am to 5,500Am, then satellite's dipole strength will be more evenly matched during the angular momentum management mode. This increases the time it takes for a satellite to remove angular momentum. It also increases the disturbance torque on the other satellites in the formation. Typically, both satellites need approx 4,600 Am each to produce the desired force, by setting the maximum to 5,500Am, the other satellite's dipole will be approximately 3,600 Am. This is not a very good ratio, but it will allow for a demonstration to see what happens if the maximum dipole strength is not large enough. Over one orbital period, the satellites have the following angular momentum.

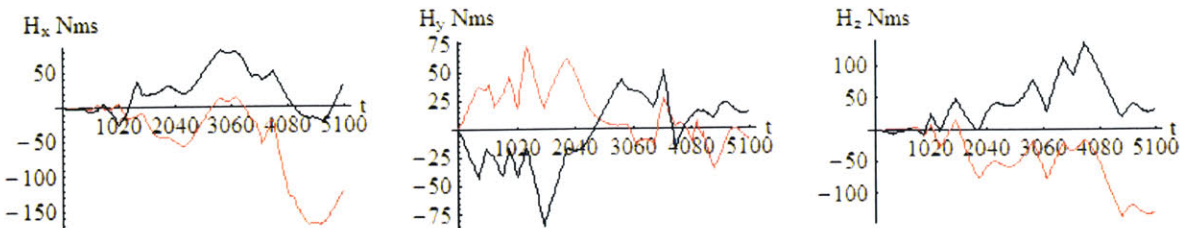


Figure 7-33: Satellite Angular Momentum – Insufficient Maximum Dipole Component Strength of 5,500Am

At first the algorithm keeps up with the angular momentum gain, however, it quickly gets behind. As one satellite is dumping its angular momentum, the other satellite is gaining it just as fast. Once the algorithm gets behind, it ends up spending all of its time attempting to reduce the angular momentum of the formation. This can be seen in Figure 7-34.

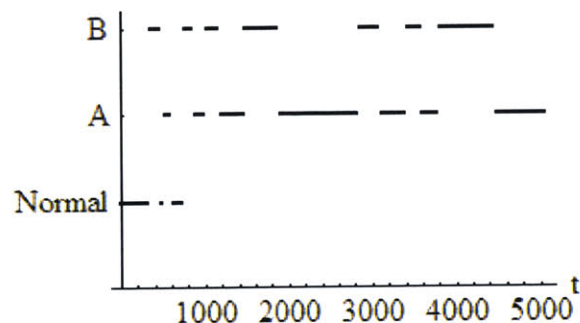


Figure 7-34: Algorithm Mode Usage – Insufficient Dipole Component Strength

Section 7.7.6 Conclusions

The algorithm presented in this section effectively manages angular momentum in the presence of the Earth's magnetic field. It also shows that angular momentum gained from other sources can also be dumped into the Earth's magnetic field. The difficulties encountered in the algorithm can be overcome as was shown in the example. The only requirement is that each satellite has reaction wheels and the ability to increase its dipole strength past the nominal strength required for the forces.

This algorithm can be improved on and the next section presents different methods and examples of the improvements.

Section 7.8 Minimizing/Specifying the Torque on Every Satellite

In the previous section a method for managing angular momentum was presented. This algorithm was a somewhat “brute force” method of angular momentum. During the normal mode, angular momentum management was neglected until a satellite gained too much angular momentum and then its dipole strength was increased to maximum causing the momentum to be removed from that satellite as quickly as possible.

Section 7.8.1 Minimizing the Torque during the Normal Mode

A more elegant solution would be, during the normal mode, attempt to minimize the torques applied by the Earth’s magnetic field onto the satellite formation. This minimization process is done using the same methods of Chapter 5.

Section 7.8.1.1 Minimizing the Torque in the Earth’s Magnetic Field

In Section 5.4, a method was presented to specify the torque distribution at one point in time. The same method is used here with the Earth’s magnetic field incorporated into the torque equations of motion. A brief review of the method is presented here.

The A and B matrices are created.

$$A(t) \equiv \frac{\partial \vec{F}(\vec{\mu}_1, \dots, \vec{\mu}_N, \vec{r}_1, \dots, \vec{r}_N, t)}{\partial \vec{\mu}} \quad B(t) \equiv \frac{\partial \vec{T}(\vec{\mu}_1, \dots, \vec{\mu}_N, \vec{\mu}_E, \vec{r}_1, \dots, \vec{r}_N, \vec{r}_E, t)}{\partial \vec{\mu}} \quad (7.93)$$

The nullspace of A is created.

$$\text{NullSpace}(A(t)) = N(A) = [\vec{n}_A(t) \quad \vec{n}_B(t) \quad \vec{n}_C(t)] \quad (7.94)$$

The desired change in the dipole solution is given by

$$\Delta \vec{\mu}(t) = N(A(t)) \bullet \begin{bmatrix} \alpha_A(t) \\ \alpha_B(t) \\ \alpha_C(t) \end{bmatrix} = \alpha_A(t) \vec{n}_A(t) + \alpha_B(t) \vec{n}_B(t) + \alpha_C(t) \vec{n}_C(t) \quad (7.95)$$

The C matrix, and the change in torque is created by

$$\begin{aligned} \Delta \vec{\tau}(t_i) &= C(t_i) \bullet \vec{\alpha}(t_i) \\ C(t_i) &\equiv \begin{bmatrix} B(t_i) \bullet \vec{n}_1(t_i) \\ B(t_i) \bullet \vec{n}_2(t_i) \\ B(t_i) \bullet \vec{n}_3(t_i) \end{bmatrix}_{3N \times 3}^T & \vec{\alpha}(t_i) &\equiv \begin{bmatrix} \alpha_A(t_i) \\ \alpha_B(t_i) \\ \alpha_C(t_i) \end{bmatrix}_{3 \times 1}^T \end{aligned} \quad (7.96)$$

Given an initial dipole solution, $\vec{\mu}_0$, an initial torque distribution is found, $\vec{\tau}_0$. By minimizing the following function, the torque distribution is minimized.

$$\min_{\vec{\alpha}} |(C \bullet \vec{\alpha} + \vec{\tau}_0)| \quad (7.97)$$

In chapter 5, equation (7.97) was solved using MMA's internal minimization routine. Using the active set method presented in the second half of Chapter 5, bounds on the dipole strength can be implemented. The matrices and vectors G, d can be calculated as follows. See equation 5.109.

$$\begin{aligned} G &= C^T C \\ \vec{d} &= (\vec{\tau}_0 - \vec{\tau}_{des})^T C \end{aligned} \quad (7.98)$$

The variables to be minimized are the three alpha values, but the constraints are on the dipole strengths. These constraints are defined as

$$\begin{aligned} |\mu_i^{\max}| &\equiv \text{Maximum Dipole Component} \\ |\Delta \mu_i^{\max}| &\equiv \text{Maximum Change in Dipole Component} \end{aligned} \quad (7.99)$$

$|\mu_i^{\max}|$ is the maximum value a dipole component can be set to. This could be the maximum value that the actual hardware can achieve, or a theoretical maximum value.

Because linearized equations are being used, small changes in the dipole strength must be used. After each iterative step the non-linear EOM are used to correct for the linearization errors.

Originally, the change in dipole strength was limited by using equation (5.191). These equations just reduced the magnitude of the change in the overall dipole strength. If the change in the magnitude of the whole dipole is quite large, rescaling the whole dipole will make the dipole components that are already limited that much smaller. For example, if the maximum dipole component is 10,000, and the current dipole strength and desired change is

$$\bar{\mu} = \begin{pmatrix} 9950 \\ 4000 \\ -3000 \end{pmatrix} \text{Am}^2 \quad \Delta\bar{\mu} = \begin{pmatrix} 50 \\ 2240 \\ -4324 \end{pmatrix} \text{Am}^2 \quad (7.100)$$

then since the limit on the dipole is 10,000 the change in the x direction will no be greater than 50. However, if the change in dipole strength is limited by

$$|\Delta\bar{\mu}|_{\max} = 1000 \text{Am}^2 \quad (7.101)$$

then the whole change in dipole is rescaled to

$$\Delta\mu_{\max} = \begin{pmatrix} 10.2 \\ 459.9 \\ -887.8 \end{pmatrix} \text{Am}^2 \quad (7.102)$$

The limit on the x component which should be 10,000 is not reached.

The solution is to incorporate the max change into the limits using the active set method.

Lower Limits:

$$-\min(|\Delta\mu_i^{\max}|, |\mu_i^{\max}| - \mu_{0,i}) \quad (7.103)$$

Upper Limits:

$$\min(|\Delta\mu_i^{\max}|, |\mu_i^{\max}| + \mu_{0,i})$$

Since the constraints are defined as

$$A\vec{x} \geq \vec{b} \quad (7.104)$$

the A_2 and b_2 matrix and vector can be defined as

$$A_2 = \begin{pmatrix} N(A) \\ -N(A) \end{pmatrix} \quad B_2 = \begin{pmatrix} -\min(|\Delta\mu_i^{\max}|, |\mu_i^{\max}| + \mu_{0i}) \\ -\min(|\Delta\mu_i^{\max}|, |\mu_i^{\max}| - \mu_{0i}) \end{pmatrix} \quad (7.105)$$

Since there are no equality constraints A_1 and b_1 are empty.

Example # 11

Using the parameters of the previous problem at time $t=0$, the initial dipole solution was

$$\vec{\mu}^A = \begin{pmatrix} 4587.8 \\ 0 \\ 0 \end{pmatrix} \text{Am}^2 \quad \vec{\mu}^B = \begin{pmatrix} 2462.80 \\ -669.915 \\ 1840.58 \end{pmatrix} \text{Am}^2 \quad (7.106)$$

Recall that dipole A was chosen randomly. This produced a torque of

$$\vec{\tau}^A = \begin{pmatrix} 0 \\ 111.397 \\ 0.243 \end{pmatrix} \text{mN-m} \quad \vec{\tau}^B = \begin{pmatrix} 16.169 \\ 78.981 \\ 7.112 \end{pmatrix} \text{mN-m} \quad (7.107)$$

The following constraints are selected.

$$\begin{aligned} |\mu_i^{\max}| &\equiv 10,000 \text{Am}^2 \\ |\Delta\mu_i^{\max}| &\equiv 1,000 \text{Am}^2 \end{aligned} \quad (7.108)$$

After the first iteration, the active set method produces the following change in dipole strength.

$$\Delta\vec{\mu}^A = \begin{pmatrix} -1000 \\ -167.709 \\ -1000 \end{pmatrix} \text{Am}^2 \quad \Delta\vec{\mu}^B = \begin{pmatrix} 342.871 \\ -45.6861 \\ 997.887 \end{pmatrix} \text{Am}^2 \quad (7.109)$$

The x and y component of satellite A's dipole was bounded by the maximum change of the dipole. Since neither dipole was within 1,000Am of the overall maximum limit, the maximum

limit on the dipole component didn't constrain the solution in this iteration step. Letting the minimization routine run, the following dipole solution that produced the minimum torque distribution was found after 13 steps.

$$\vec{\mu}_{\min}^A = \begin{pmatrix} 3906.10 \\ 44.8729 \\ -10000 \end{pmatrix} \text{Am}^2 \quad \vec{\mu}_{\min}^B = \begin{pmatrix} -260.940 \\ -741.019 \\ 2391.60 \end{pmatrix} \text{Am}^2 \quad (7.110)$$

This produced the minimum torque distribution is

$$\vec{\tau}_{\min}^A = \begin{pmatrix} 0.277 \\ 1.179 \\ 0.113 \end{pmatrix} \text{mN-m} \quad \vec{\tau}_{\min}^B = \begin{pmatrix} 16.525 \\ 18.349 \\ 7.488 \end{pmatrix} \text{mN-m} \quad (7.111)$$

This reduced the magnitude of the torques applied to each satellite.

$$\begin{aligned} |\vec{\tau}^A| &= 111.397 \rightarrow 1.216 \text{ mN-m} \\ |\vec{\tau}^B| &= 80.932 \rightarrow 25.804 \text{ mN-m} \end{aligned} \quad (7.112)$$

Recall that this method only finds local minimum. In fact there are four minimal solutions (shown as columns in the matrix). These were found by using different initial conditions.

$$\begin{aligned} \vec{\mu}_{\min}^A &= \left(\begin{array}{c|ccc} 3906.10 & 228.806 & -4042.60 & -260.940 \\ 44.8729 & 701.054 & 65.7673 & -741.018 \\ -10000 & -238.98 & 10000 & 2391.60 \end{array} \right) \text{Am}^2 \\ \vec{\mu}_{\min}^B &= \left(\begin{array}{c|ccc} -260.940 & -4042.60 & 228.806 & 3906.10 \\ -741.018 & 65.7673 & 701.054 & 44.8729 \\ 2391.60 & 10000 & -238.98 & -10000 \end{array} \right) \text{Am}^2 \end{aligned} \quad (7.113)$$

The minimum torque solutions are

$$\vec{\tau}_{\min}^A = \begin{pmatrix} 0.277 & -18.246 & -0.2618 & 16.525 \\ 1.179 & -14.564 & -3.064 & 18.350 \\ 0.113 & -6.039 & -0.086 & 7.488 \end{pmatrix} \text{Nm}$$

$$\vec{\tau}_{\min}^B = \begin{pmatrix} 16.525 & -0.2618 & -18.246 & 0.277 \\ 18.350 & -3.064 & -14.564 & 1.179 \\ 7.488 & -0.086 & -6.039 & 0.113 \end{pmatrix} \text{Nm}$$
(7.114)

Section 7.8.1.2 Implementing into the Algorithm

During the normal mode, the above code is inserted to minimize the torque applied on the satellite formation at each time step. The dipole solution from the previous time step is used to as the initial conditions for the algorithm. The goal will be to reduce the amount of time that the algorithm is in the Angular Momentum Reduction mode.

Example # 12 – Implementing the New Normal Mode that Minimizes the Torque

Running the same example as Example # 9, but using the new Normal mode, Figure 7-35 shows the resulting angular momentum on each satellite.

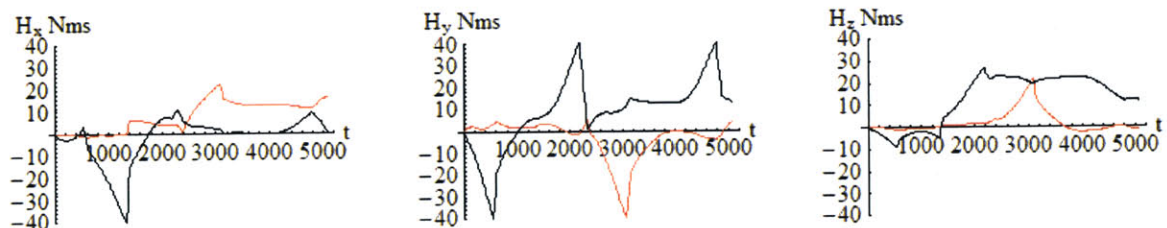


Figure 7-35: Satellite Angular Momentum – Minimize Torque in the Normal Mode

The angular momentum is much better behaved when using this new Normal mode algorithm. This is to be expected. When the algorithm is not removing angular momentum from a satellite, the torques applied are minimized. Thus the angular momentum buildup is kept to a minimum. The following plot shows which mode the algorithm is in over the course of one orbit.

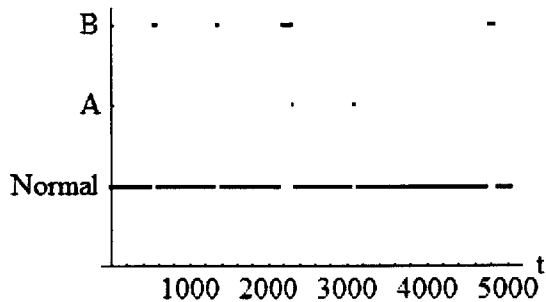


Figure 7-36: Mode Duty Cycle – Minimize Torque in the Normal Mode

Comparing Figure 7-29 to Figure 7-36, it can be seen that the algorithm is in the Normal mode for a larger percentage of time. (91% vs. 78%).

Section 7.8.1.3 Conclusions

By actively attempting to minimize the torque applied to the satellites during the normal state, the angular momentum buildup was much better behaved. Since the normal mode just minimized the torques and did not attempt to adjust the angular momentum, the momentum did build up after a period of time, but at a much lower rate than when the dipole is just chosen arbitrarily.

Section 7.8.2 Specifying the Torque to Minimize the Angular Momentum

The above section minimized the torques on each satellite. Essentially trying to drive the torque vector towards zero. The same method can be used to drive the torque on each satellite to a desired value. Recall, that there are only enough degrees of freedom to directly specify the torque on one satellite, but the method of Chapter 5 allow us to minimize the difference between the desired torque on each satellite and the available torques.

Ideally, the torques applied to each satellite would be in the direction opposite to the angular momentum stored on the satellite.

$$\vec{\tau}_{des} = \frac{-\vec{H}_{des}}{\Delta t} \quad (7.115)$$

However, the torque can only be specified for one satellite at a time. Another possible algorithm is to minimize the difference between the desired torque and the obtainable torque. From equation (7.97), and using the method in the previous section, our new goal is to find the alpha's that minimize the following function.

$$\min_{\vec{\alpha}} |\vec{\tau}_{des} - (C \bullet \vec{\alpha} + \vec{\tau}_0)| \quad (7.116)$$

Section 7.8.2.1 Incorporation in to the Algorithm

This method would replace the Angular Momentum Reduction mode of the algorithm. Instead of just minimizing the angular momentum stored on the one satellite, the angular momentum is minimized across the formation. Because the algorithm minimizes the sum of the squares of the torque components, then the satellite with the large angular momentum, and thus the large desired torque will be preferentially selected.

As the algorithm enters into the Angular Momentum Reduction mode, it must find the best torque distribution. Since there are local minima, it is beneficial to seed the method multiple times to attempt to find the best solution. However, once the best solution has been found, the dipole solution can typically be used to seed the method for each successive time step until the algorithm returns to the normal mode. At the same time, if the torque distribution changes significantly, or the maneuver takes a long time, and the Earth's magnetic field changes, then it may be beneficial to periodically re-seed the method and attempt to find the global minimum.

Example # 13 : Attempt to Specify the Torque Distribution to Minimize the Angular Momentum.

Using the same parameters as the previous example, the following plot shows the satellites' angular momentum over the course of an orbit. Using the same parameters as the previous examples, the following is a plot of the angular momentum gained by the satellites.

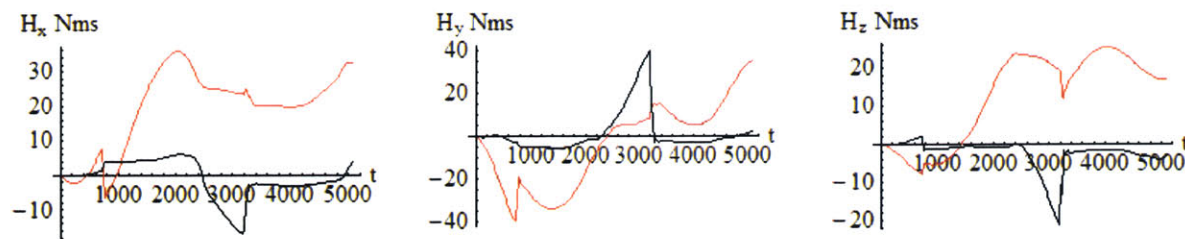


Figure 7-37: Satellite Angular Momentum – Finding the Torque Distribution

The algorithm was also successful in managing the angular momentum buildup in the satellites. The angular momentum buildup is very well behaved compared to the initial version of the algorithm.

Section 7.9 Conclusions

This chapter discussed the implications of satellite formations in the Earth's magnetic field, and provides methods for successfully operating in the Earth's magnetic field.

The forces generated by the Earth's magnetic field are very small and typically neglected. However, a method of incorporating the relative disturbance forces into the equations of motion without using the free dipole was provided. The torques from the Earth's magnetic field, due to their relative size, could not be neglected. In some cases the torque from the Earth's magnetic field was as large if not larger than the inter-satellite torques.

These torques are a mixed blessing. Because of their presence, they must be addressed; otherwise, they will cause reaction wheels to saturate quickly. At the same time, they allow for maneuvers that are not possible without the presence of the Earth's magnetic field. One example is the ability to directly specify the torque on a satellite. When that torque is set to zero, then it is possible to have a satellite with small or no reaction wheels.

Finally an algorithm was presented to manage the angular momentum of the satellites in the formation. This algorithm had two parts, a Normal mode and an Angular Momentum Reduction mode. In the Normal mode the free dipole was initially chosen arbitrarily, but later on in the chapter, the torques applied to each satellite were reduced. Eventually the satellites in the

formation gained enough angular momentum to the point where it became necessary to reduce the amount of angular momentum stored on the vehicle's reaction wheels. The second mode of the algorithm was used to reduce the angular momentum of the satellite. This was done in a variety of ways including specifying the satellites' dipole to minimizing the angular momentum of the formation as a whole.

Examples of satellite formations flying in LEO in the presence of the Earth's magnetic field were presented. The examples validated the algorithms and demonstrated the ability of EMFF to provide the desired relative forces in LEO and to be able to manage the angular momentum stored on each vehicle.

Chapter 8

CONCLUSIONS

Section 8.1 Summary and Key Contributions of the Thesis

This thesis starts with just an idea. This idea came from a need of being able to fly satellites in formation without having to expend large amounts of propellant. This idea was to have electromagnets provide the relative position control of satellites flying in formation. The rest of the thesis, starting with first principles, works through the steps necessary to prove that electromagnetic formation flight (EMFF) is more than just an idea, but a capable way of providing the relative position control for satellites flying in formation.

- Chapters 1 & 2: In these chapters the EMFF concept is introduced to the reader, and a synopsis of the previous work on EMFF systems is provided.
- Chapter 3: In this chapter the electromagnets used on the satellites are modeled in three different ways. Using the exact model for the rings of current, a near-field model is developed that theoretically produces the exact forces and torques at any distance or orientation of the electromagnets. However, because there is no analytic solution, a linearized model, or far-field model, is introduced. This model, while having the benefit of being linear, suffers from the limitation that the satellites must be a minimum distance apart for the model to become valid. To strike a compromise between the far-field and near-field (exact) model, a mid-field model is developed. This model incorporates higher order terms on the expansions of the near-field, yet can still be written in vector form.
- Chapter 4: In this chapter, the equations of motion relating the relative forces and torques are examined, and methods for solving the equations are presented. These equations are identified as being a system of polynomial equations. Polynomial equations have properties that can be examined and exploited. The number of solutions, singular

solutions, infinite solutions and multiplicity are all aspects of polynomial equations and are explored in the chapter.

The equations are determined to be dependent on each other due to Newton's 3rd law. Because the equations of motion are dependant, one equation can be removed and thus there are fewer equations than variables. This allows for the concept of the free dipole. One satellite can arbitrarily set its magnetic field, and the equations of motion can still be satisfied. The discovery of the free dipole is an enabling aspect of the EMFF system. If there was no free dipole, then the EMFF system could not manage its torque and angular momentum.

For the remainder of the chapter, the free dipole is assumed to be defined, and methods for solving the remaining equations of motion are produced. For simple formations, the equations of motion are directly solved for the desired magnetic dipole strength on each satellite. Examples using these formations and equations are presented.

Formations with more satellites are examined next. Due to the complexity of the EOM, the magnetic dipole solutions cannot be solved for analytically, so other numerical methods must be used. Newton's method is briefly presented, and is hailed as a good method when the goal is to find any viable dipole solution. If all of solutions are needed, or the best solution needs to be found, then the continuation method (Homotopy) is used. This method, while more time consuming than Newton's method, systematically finds all the solutions to a polynomial equation. In support of this method, sub-routines that reduce and scale the equations of motion are presented along with working algorithms of the continuation method. Throughout this section example problems are given.

- Chapter 5: In this chapter the angular momentum build-up on the satellites flying in formation is addressed. Specifically the free dipole is exploited to achieve this task. Using the nullspace of the linearized force equations, changes to the dipole solution that still satisfy the force equations of motion are found. Change that also produced a
-

desirable change in the distribution of the torques applied to the formation are found. Typically these changes are chosen so that a metric is minimized.

Due to the linear constraints from the nullspace and the quadratic cost functions, this type of problem is described as a quadratic programming problem. Several methods, including the active set and the gradient projection method are investigated. The algorithms needed to implement these routines are presented and example problems are provided.

- Chapter 6: In this chapter, the operational difficulties of working within the Earth's gravitational field are presented. Formations that lie in free orbit ellipses do not require any control forces to maintain their formation shape. However, many missions have fixed pointing requirements. This places the satellites in non-Keplerian orbits, and thus they require control forces. These control forces, depending on the formation desired, can produce angular momentum build-up that has both periodic and secular components. The forces and torques are presented along with some examples. Finally the effects of the J_2 geopotential are presented along with the forces and torques needed to counteract the effect of formation separation.
- Chapter 7: In this chapter, the effects of operating within the Earth's magnetic field are investigated. Because the Earth is very far away from the satellite formation, the forces produced from operating in the Earth's magnetic field are negligible. However, a method is given that allows for the incorporation of the relative forces produced by the Earth's magnetic field into the equations of motion without loss of the free dipole.

The torques produced by the Earth on the satellite formation are not negligible. In fact, depending on the satellite mission, these torques can be larger than the inter-satellite torques. These disturbance torques are a mixed blessing, because the Earth's field can be exploited to dump angular momentum back into the Earth. Also, because of the presence of the Earth's magnetic field, a desired torque can be explicitly set on one satellite. The ability to arbitrarily set the torque on one satellite leads to a method of

angular momentum management in the Earth's magnetic field. As one satellite's angular momentum begins to build up, it is selected for angular momentum dumping. This process is repeated for any satellite that needs to remove angular momentum from the system. Finally, the methods of Chapter 5 are implemented to manage disturbance torque in the Earth's magnetic field.

Section 8.2 Future Work

The purpose of this thesis is to prove the validity of EMFF and to provide nominal dipole solutions for the satellite formation over time. These nominal dipole solutions are designed to prevent angular momentum from building up on the reaction wheels, both in free space and in low Earth orbit. However, they are by design nominal trajectories. They provide dipole solutions while incorporating the known external forces.

For the unknown external forces, feedback controllers must be designed. These controllers could linearize about the nominal trajectory given by this thesis. The controllers would return the satellites to their nominal position. Work on these controllers is currently proceeding in the MIT SSL and will be implemented on the EMFF testbed.

Also, the algorithms presented in this thesis are somewhat computer intensive. Satellite formation missions may need to re-plan and find a new dipole solution on the fly. Real-time path planning and dipole solution may become necessary. Implementing or modifying the algorithms herein to work on these real-time systems is another research opportunity.

Finally, expansion of the algorithms to many satellite formations is another research opportunity. The EOM become increasingly complex as more satellites are placed in the formation. This thesis provided examples for 2,3 and 5 satellites, but if a formation has 10, 50 or 100 satellites, the EOM may become too unwieldy. Methods for handling these large formations still need to be developed.

Section 8.3 Final Comments

The goal of this thesis is to prove that EMFF works. And works in a variety of environments. This thesis accomplishes that goal. Dipole solutions can be found for two, three, or more satellites. These formations can rotate, spin-up, spin-down, precess, or perform any maneuver that is necessary to accomplish a mission goal. They can do this in free-space, in a gravity well, or in the presence of an external magnetic force. This research provides the basis and starting point to launch EMFF off the ground (pun intended).

Q.E.D.

REFERENCES

- 1) John E. Prussing, Bruce A. Conway, *Orbital Mechanics*, Oxford University Press, New York, 1993.
- 2) Richard H. Battin, *An Introduction to the Mathematics and Methods of Astrodynamics, Revised Edition*; AIAA Education Series, Reston, Virginia, 1999.
- 3) Alexander Morgan, *Solving Polynomial Systems Using Continuation for Engineering and Scientific Problems*, Prentice-Hall, Inc., Englewood Cliffs, New Jersey, 1987.
- 4) Jorge Nocedal, Stephan J. Wright, *Numerical Optimization*, Springer Series in Operations Research, 1999.
- 5) Steven J. Leon, *Linear Algebra with Application*, 4th Edition, MacMillan Publishing Company, New York, 1994.
- 6) Paul A. Tipler, *Physics for Scientists and Engineers*, 3rd Edition, Worth Publishers, New York, NY, 1991.
- 7) Samuel A. Schweighart, *Development and Analysis of a High Fidelity Linearized J2 Model for Satellite Formation Flying*, Masters Thesis, Massachusetts Institute of Technology, June, 1999.
- 8) Edmund M.C. Kong, *Spacecraft Formation Flight Exploiting Potential Fields*, Ph.D. Thesis, Massachusetts Institute of Technology, February 2002.
- 9) Laila M. Elias, *Dynamics of Multi-Body Space Interferometers Including Reaction Wheel Gyroscopic Stiffening Effects: Structurally Connected and Electromagnetic Formation Flying Architectures*, Ph.D. Thesis, Massachusetts Institute of Technology, March, 2004.
- 10) Daniel W. Kwon, *Electromagnetic Formation Flight of Satellite Arrays*, Masters Thesis, Massachusetts Institute of Technology, February, 2005.
- 11) Jeffery G. Reichbach, *Micropropulsion System Selection for Precision Formation Flying Satellites*, Masters Thesis, Massachusetts Institute of Technology, January 2001.
- 12) David W. Miller, Raymond J. Sedwick, et al, *NIAC Phase I Final Report: Electromagnetic Formation Flight*, Massachusetts Institute of Technology, December, 2002.
- 13) Edmund M. C. Kong, D. W. Kwon, Samuel A. Schweighart, Laila. M. Elias, Raymond J. Sedwick, David. W. Miller, "Electromagnetic Formation Flight for Multisatellite Arrays", *Journal of Spacecraft and Rockets 41-4*, AIAA, pp 659-666, July-August, 2004.
- 14) Samuel A. Schweighart, Raymond J. Sedwick, "High Fidelity Linearized J₂ Model for Satellite Formation Flight", *Journal of Guidance, Control, and Dynamics 25-6*, AIAA, pp 1073-1080, November-December, 2002.
- 15) Laila M. Elias, Edmund M. Kong, David W. Miller, "An Investigation of Electromagnetic Control for Formation Flight Applications", *Proceedings of the SPIE Astronomical Telescopes and Instrumentation Conference*, Waikoloa, Hawaii, August 2002.

- 16) David W. Miller, Raymond J. Sedwick, Edmund M. C. Kong, Samuel A. Schweighart, "Electromagnetic Formation Flight for Sparse Aperture Telescopes", *Proceedings of the 2002 IEEE Aerospace Conference*, Big Sky, Montana, March 9-16, 2002.
 - 17) Raymond J. Sedwick, Samuel A. Schweighart, "Propellantless Spin-Up and Reorientation of Tethered or Electromagnetically Coupled Spacecraft", *SPIE 4849-26*, SPIE Highly Innovative Space Telescope Concepts Conference, Waikoloa, HA, August 22-28, 2002.
 - 18) Tatsuaki Hashimoto, Sinichiro Sakai, Keiken Ninomiya, Ken Maeda, Tetsu Saitoh, "Formation Flight using Super-Conducting Magnets", *International Symposium of Formation Flying Missions and Technologies*, Toulouse, France, 2002.
 - 19) Ryosuke Kaneda, Fumito Yazaki, Shin-ichiro Sakai, Tatsuaki Hashimoto, Hirobumi Saito, "The Relative Position Control in Formation Flying Satellites using Super-Conducting Magnets", *2nd International Symposium on Formation Flying Missions and Technologies*, Washington, DC, 2004.
 - 20) E. Kong, M. Tollefson, J. Skinner, J. Rosenstock, "TechSat 21 Cluster Design Using AI Approaches and the Cornwell Metric," AIAA 99-4365.
 - 21) Raymond J. Sedwick, Edmund M. C. Kong, David W. Miller, "Exploiting Orbital Dynamics and Micropropulsion for Aperture Synthesis Using Distributed Satellite Systems: Applications to Techsat 21" AIAA 5289, 1998.
 - 22) R.J. Sedwick, R.J., D.W. Miller, and E.M.C. Kong, "Mitigation of Differential Perturbations in Clusters of Formation Flying Satellites," AAS 99-124, 1999.
 - 23) Challis, J.H. "A Procedure for Determining Rigid Body Transformation Parameters", *Journal of Biomechanics* **28**, pp. 733-737, 1995.
 - 24) Young-Hoo Kwon, "Computation of the Rotation Matrix", *Theories and Practices of Motion Analysis*, <http://kwon3d.com/theory/jkinem/rotmat.html>, 1998.
 - 25) Uri M. Ascher, "Numerical Optimization", *CPSC 542 Class Notes*, University of British Columbia, <http://www.cs.ubc.ca/spider/ascher/542.html>, 2003.
 - 26) Victor M. Becerra, "Nonlinear Programming", *CY4A2 Lecture Notes*, Department of Cybernetics, Univ. of Reading, <http://www.personal.rdg.ac.uk/~shs99vmb/notes/>, 2003.
 - 27) Anthony Padua, "Introduction to Sequential Quadratic Programming, Part 1", *Control and Software Engineering Seminar*, Rice University, <http://www.caam.rice.edu/~adpadu/talks/sqp1.pdf>, 2002.
 - 28) Maria M. Seron, "The Geometry of Quadratic Programming", *Centre for Complex Dynamic Systems and Control*, The University of Newcastle, Australia, <http://murray.newcastle.edu.au/cce/Slides/Geometry.pdf>, 2004.
 - 29) MathWorks, Inc. "Optimization Toolbox", *The Mathworks Helpdesk*, MatLab, 2005.
-

-
- 30) Mathematica, "Mathematica Help File", *Mathematica Ver 5*, 2005.
 - 31) Sharad Bhartiya, "Quadratic Programming Using the Active Set Method", Class Notes CL 603, *Department of Chemical Engineering*, IIT Bombay, http://www.che.iitb.ac.in/faculty/sb/quad_prog2.pdf, 2004.
 - 32) American Superconductor, "HTS Wire", *American Superconductor Datasheets*, <http://www.amsuper.com>, 2005.
 - 33) Jet Propulsion Laboratory, *The TPF Book*, NASA Jet Propulsion Laboratory, 99-003, 1999.
 - 34) National Radio Astronomy Observatory, "Very Large Array", NARO <http://www.vla.nrao.edu/>, 2005.
 - 35) MIT CDIO Class, "EMFFORCE Design Document", MIT Space Systems Lab, Massachusetts Institute of Technology, May 2003.
 - 36) Benjamin L. Schweighart, "EMFF Non-Mission Specific Animation", *4D Artist*, Created for the MIT SSL, <http://www.4dartist.com>, 2004.
 - 37) Samuel A. Schweighart, Raymond J. Sedwick, "Cross-Track Motion of Satellite Formations in the Presence of J_2 Geopotential", *Journal of Guidance, Control, and Dynamics* 28-3, AIAA, May-June, 2005 (Tenative).
 - 38) Samuel A. Schweighart, "Applying Arbitrary Forcing Functions upon Satellites Formations in the Presence of the J_2 Geopotential", Internal Paper, MIT SSL, 2005.
 - 39) Gerald L. Pollack, Daniel R. Stump, *Electromagnetism*, Addison Wesley, San Francisco, 2002.
 - 40) Eric Dennison, "Off-Axis Field Due to a Current Loop", *Netdenizen* <http://www.netdenizen.com/emagnet/offaxis/ilooopoffaxis.htm>, 2005